KfK 4935
IWGFR/84
Dezember 1991

Properties of Structural Materials in Liquid Metal Environment

Proceedings of an International Atomic Energy Agency Specialists' Meeting International Working Group on Fast Reactors Karlsruhe, Federal Republic of Germany, June 18 – 20, 1991

Editor: H. U. Borgstedt
Institut für Materialforschung

Kernforschungszentrum Karlsruhe

KERNFORSCHUNGSZENTRUM KARLSRUHE
INSTITUT FÜR MATERIALFORSCHUNG

KfK 4935
IWGFR/84

PROPERTIES OF STRUCTURAL MATERIALS IN LIQUID METAL ENVIRONMENT

Proceedings of an
International Atomic Energy Agency Specialists' Meeting
International Working Group on Fast Reactors
Karlsruhe, Federal Republic of Germany, June 18-20, 1991

Editor: H.U. Borgstedt

Kernforschungszentrum Karlsruhe GmbH, Karlsruhe

Kernforschungszentrum Karlsruhe GmbH
Postfach 3640, 7500 Karlsruhe 1

ISSN 0303-4003

Meeting Chairman:	**H.U. Borgstedt** **Kernforschungszentrum Karlsruhe, Institut für Materialforschung III**
Co-Chairmen:	**H. Huthmann** **Interatom GmbH., Bergisch Gladbach 1**
	H. Plitz **Kernforschungszentrum Karlsruhe, Projekt Nukleare Sicherheitsforschung**
Scientific Secretary of IWGFR:	**V. Arkhipov** **International Atomic Energy Agency, Vienna**

Contents

Agenda

Tuesday, 18 June 1991

09:00 **Welcome Address**
Prof. K. Kummerer

Session I **Chairman H. Huthmann**
Creep-Rupture Behaviour of Structural Materials in Liquid Metal Environment

09:15	Y. Wada	Sodium Influence on Creep-Rupture Strength of SUS 304
09:55	V.M. Trojanov	The Effect of Decarburization and Carburization in Sodium on the Mechanical Properties of Austenitic and Ferritic Steels
10:40	Yu.M. Trapeznikov	Structural Materials for Sodium Cooled Fast Breeder Reactors
11:20		Coffee Break
11:40	C.G. Escaravage	Design Data for Austenitic Stainless Steel in Sodium Environment
12:00		Lunch Break
13:15	A.N. Ryshkov	The Corrosion and Mechanical Properties of Structural Materials in Sodium
14:00	M.P. Mishra	Salient Features and a few Results from the Sodium Loop Designed at IGCAR for Metallurgical Investigations
14:45	H.U. Borgstedt	The Influence of Decarburizing Sodium on the Creep-Rupture Behaviour of Type 304 Stainless Steel
15:30	H. Huthmann	The Influence of Flowing Sodium on the Creep-Rupture Behaviour of Type 316 L(N) Stainless Steel
16:15	H.U. Borgstedt	The Behaviour of Notched Weldments in Liquid Sodium under Creep Stress
17:30		Buffet in the KfK Casino

Wednesday, 19 June 1991

Session II **Chairman C.G. Escaravage**
Behaviour of Materials in Liquid Metal Environments under Off-Normal Conditions

09:00	G. Menken	Stress Corrosion of Type 304 Steel in Molten NaOH/Na Mixtures
09:45	H.U. Borgstedt	Tensile Tests of Low Alloy Steel 15Mo3 in Sodium
10:30		Coffee Break

Session III **Chairman Y. Wada**
Fatigue and Creep-Fatigue of Structural Materials in Liquid Metal Environment

10:50	Y. Wada	Creep-Fatigue Life Evaluation of SUS 304 in Liquid Sodium
11:30	Yu.M. Trapeznikov	Cyclic Lifetime Change of Various Types of Steels by the Exposure in Alkali Metal Melts
12:15		Lunch Break
13:30	H. Huthmann	Creep-Fatigue Behaviour of Type 304 and 316 L(N) in Flowing Sodium

Session IV **Chairman P.Skeldon**
Crack Propagation in Liquid Sodium

14:15	H.U. Borgstedt	The Measurement of Crack Propagation in CT Specimens in a Sodium Environment
14:50	H. Huthmann	Measurement of Crack Initiation (J-ΔaCurves) in Liquid Sodium on Type 304 Stainless Steel after Previous Creep Damage (Short Contribution)
16:00		Dinner Tour: Annweiler and Burrweiler, Palatina

Thursday, 20 June 1991

Session V **Chairman H.U. Borgstedt**
Conclusions and Recommendations

09:00 -12:00 Elaboration of the conclusions and recommendations

12:15 Lunch Break

13:15 Visit of Laboratories (Sodium Loops CREVONA and FARINA, Creep-Rupture Tests)

16:00 End of the Specialists' Meeting

List of Delegates

V. Arkhipov	IAEA	International Working Group Fast Reactors, International Atomic Energy Agency, P.O. Box 100, A-1400 Vienna, Austria
H.U. Borgstedt	D	Kernforschungszentrum Karlsruhe GmbH, Institut für Materialforschung III, P.O. Box 3640, D-7500 Karlsruhe 1, Germany
C. Escaravage	F	Novatome, 10, rue Juliette Recamier, F-69398 Lyon CEDEX 03, France
H. Huthmann	D	Interatom GmbH., Friedrich-Ebert-Str., D-5060 Bergisch Gladbach 1, Germany
M.P. Mishra	India	Metallurgy Programme, Indira Gandhi Centre for Atomic Research, Kalpakkam 603 102, Tamil Nadu, India
H. Plitz	D	Kernforschungszentrum Karlsruhe GmbH, Projekt Nukleare Sicherheitsforschung, P.O. Box 3640, D-7500 Karlsruhe 1, Germany
A.N. Ryshkov	USSR	Institute of Physics and Power engineering, Bondarenko sq. 1, Kaluga reg., 249020, USSR
P. Skeldon	GB	AEA Technology, NRL Risley, Warrington WA3 6AT, Cheshire, U.K.
Yu.M. Trapeznikov	USSR	The Central Research Institute for Structural Materials "PROMETEY",193167 Leningrad, USSR
V.M. Trojanov	USSR	Institute of Physics and Power engineering, Bondarenko sq. 1, Kaluga reg., 249020, USSR
Y. Wada	J	Materials Development Section, Systems and Components Division, O-arai Engineering Center, Power Reactor and Nuclear Fuel Development Corp., Tokyo 107, Japan

Introduction

The IWGFR Specialists Meeting on Properties of Structural Materials in Liquid Metal Environment was held during June 18 to June 20 1991, at the Nuclear Research Centre (Kernforschungszentrum) in Karlsruhe, Germany. Ten specialists from France, Germany, India, Japan, the USSR, and the United Kingdom attended the meeting. No representatives from countries having observers status at the IWGFR were present. The Specialists Meeting was divided into five technical sessions (see detailed agenda on pages).

The participants were welcomed by Prof. Dr. K. Kummerer, head of the Institute of Materials Research (IMF III) at the Kernforschungszentrum Karlsruhe (KfK).

The meeting was opened by Dr. H.U. Borgstedt, head of the Liquid Metals Laboratory of the IMF III at KfK, who was the general chairman. He was assisted by Dr. H. Huthmann from INTERATOM, Germany, acting as scientific chairman, and Mr. H. Plitz, member of the management of the Nuclear Safety Project (PSF) of KfK, as technical chairman.

IAEA was represented by Mr. V. Arkhipov, who presented a review on the IAEA activities and the current status of nuclear power exploitation in the various countries.

Conclusions

The five sessions were summarized by the chairmen, and the conclusions drawn by them were discussed by the delegates in the final session.

Session I (Part 1 & 2)

Creep-Rupture Behaviour of Structural Materials in Liquid Metal Environment

Part 1:
Chairman: H. Huthmann, Interatom GmbH., Bergisch Gladbach, Germany

Part 2:
Chairman: V.M. Trojanov, Inst. of Physics and Power Engineering, USSR

The work on the creep - rupture properties of austenitic stainless steels in liquid sodium environment of high purity was reported by the Japanese and the two German delegates. The creep - rupture strength of the austenitic stainless steels of the composition of Type 304 and 316 was influenced by the sodium environment in different manners. The influence of sodium however, was more in Type 304 than that in Type 316 stainless steel. Among other factors, carbon potential of the sodium environment was shown to be of importance.

Liquid sodium effects on stainless steel of Type 304 occurred in all tests. In sodium of high carbon content (activity of carbon in Na larger than in steel) the steel showed the effect of TERTIARY CREEP EMBRITTLEMENT, which caused a shorter life time due to the reduction of the duration and the strain in the tertiary creep regime. This effect was, however, not very large. The tertiary creep embrittlement was more pronounced at higher testing temperature.

An additional sodium effect was observed in test environments in which the carbon activity of sodium was below the carbon activity in the steel. This situation caused decarburization of surface layers of the steel. The decarburizing sodium corroded the surface layers of the steel and leached out metallic elements (Ni, Cr and Mn) of the grain boundaries. Grain boundary cracks were formed along the corroded grain boundaries and the cross sections of the specimen were reduced. Thus, enhanced creep rates and earlier onset of tertiary creep resulted in a shortened rupture time. These sodium effects on the properties of structural materials could not be tolerated under normal operating conditions of LMFBR's.

The effects of decarburizing Na were based on surface reactions. The extent of the Na effect depends, therefore, on the surface to volume ratio. It was indeed shown that specimens with a larger diameter were nearly unaffected by sodium.

The carbon potential in LMFBR coolant circuit system depends on the composition of the structural materials, effectiveness of the carbon sinks (cold trap temperature) and probably also on the presence of carbon sources such as ingress of CO_2 and hydrides from the atmosphere and hydrocarbon from the system itself (oil leak from the bearings etc). The effect of decarburizing sodium on steel Type 304 reported by the delegate from KfK is therefore, not a phenomenon which should necessarily occur in a fast reactor.

The mechanical properties of Type 316 and 316 L(N) steels were not sensitive to these two effects of liquid sodium. A limited sodium effect on previously sensitized material of Type 316 L(N) was observed in a creep - rupture test conducted in France. The evaluation is still in progress.

It was pointed out by the Japanese delegate that the grain boundaries of this material were more ductile than those of Type 304 stainless steel under carburizing Na environment. There was no effect of sodium on the steel 316 L(N) under decarburizing conditions, as well.

The work reported by the USSR delegates in three presentations indicated that the effects of carburization and decarburization on the mechanical properties of austenitic stainless steel in contact with sodium of a given carbon potential can be calculated and the design rules for fast reactor components can be based on the results of such calculations. The limited in-sodium tests data available on new austenitic stainless steel Type 316 L(N) revealed that the mechanical properties of this steel are not influenced by the sodium environment

Limited information is available on the creep - rupture behaviour of steam generator materials in liquid sodium environment and mechanical properties data are rather scanty. However, results obtained so far from the limited tests conducted in sodium environment indicate minor effects on the mechanical properties of ferritic and perlitic steel.

It was emphasized that particular attention has to be paid to the weld metals. Tests results however, have not shown any significant influence of the liquid sodium on the mechanical properties of the weld metals of Type 304 and 316 stainless steels. As far as the reported failures of weldments in contact with liquid sodium are concerned, the mechanism of the sodium effects are not yet fully understood. In order to understand the failure mechanism and also to suggest the ways for improving the weld metal mechanical properties for applications in contact with sodium, further studies have to be conducted on weldments in liquid sodium environment.

Session II

Behaviour of Materials in Liquid Metal Environments under Off-Normal Conditions.

Chairman: P. Skeldon, AEA Technology, Risley, UK

In addition to the two contributions from Germany, information on the influence of impure sodium (sodium containing alkali impurities viz. moisture, hydroxide, rust etc.) on the mechanical properties of structural materials was given in one of the contributions from the USSR.

The introduction of moisture into the cover gas can leads to the formation of sodium hydroxide at lower temperatures. However, at higher temperatures > 450 °C sodium hydroxide formed in the cover gas region having moisture content up to 50 vpm is not stable and it is removed either by evaporation or by surface reaction. Exact composition of the oxides that influence mechanical properties of Type 304 after exposure to impure cover gas and sodium at temperatures 350, 450 and 560° C have been identified. The steel did not crack using C-ring specimens, but there was some intergranular attack. The use of C-ring specimens for high temperature stress corrosion tests (> 500 °C) was validated (against stress corrosion).

The causes of failure of low alloy steel 15Mo3 weldments in contact with sodium at moderate temperatures are not fully understood. The failures are associated with hydrogen but cracking has proved difficult to reproduce in laboratory. Measurements of hydrogen partial pressures by means of an electrochemical hydrogen meter showed release of hydrogen at low temperatures, after the addition of FeOOH. Tensile tests of rusted steel in sodium showed ductile behaviour. There were differences in observations due to drawing of scales and wetting of specimens while performing the tests.

Tensile tests and argon containing 5% hydrogen and in sodium / sodium hydride have not produced cracking. Further tests in sodium / sodium hydroxide and in sodium with freshly rusted samples are in progress.

The paper from USSR reported that the austenitic steel Type 304 is most sensitive to alkalinity in sodium. The test results for the creep-rupture and fatigue strength of different materials in contact with impure sodium were obtained.

Session III

Fatigue and Creep-Fatigue of Structural Materials in Liquid Metal Environment.

Chairman: Y. Wada, Power Reactor and Nuclear Fuel Development Corp., Japan

Contributions to this topic were given from Japan, USSR and Germany. Creep - fatigue interaction was shown to be the realistic approach to study the material behaviour in contact with sodium. The austenitic steel Types 304 and 316 L(N) were studied in a wide range of parameters. The failure mode changes from transcrystalline to intercrystalline fracture by increasing the hold time. Tests up-to one year duration have not yet revealed any significant effect of sodium on the steel Type 316 L(N).

The sodium effect on the creep-fatigue behaviour of Type 304 steel was insignificant at low strain ranges even under carburizing conditions. The modified Type 316 L(N) steel is still under long-term tests. The effect of sodium on the grain boundary region (where sodium effect was more than that in the matrix) of this very low carbon steel is still under evaluation by the Japanese group.

Various types of steel were studied in connection with their creep-fatigue behaviour in contact with liquid sodium in USSR. The cyclic time in alkali metals was found to be depended on the composition of the materials and the depth of surface corrosion.

Session IV

Crack Propagation in Liquid Sodium

Chairman: C.G. Escaravage, Framatome / Novatome, France

Two German contributions dealt with the fracture mechanics of the structural materials of Type 304 and 316 L(N) stainless steels in liquid sodium. The threshold fatigue crack growth rates measured in liquid sodium by means of in-sodium crack opening displacement gages were somewhat lower than that in air environment. The experimental results are in agreement with model which predicts that sodium corrosion effects (including carburization / decarburization) are restricted to a crack depth of three times the crack width. This is due the fact that the larger gettering surface is available at the crack face than that at the crack tip.

It was shown in J-Δa tests at 550° C that crack initiation is not enhanced in liquid sodium environment, particularly in materials with previous creep damage.

Session V

Conclusions and recommendations

Chairman: H.U. Borgstedt, Kernforschungszentrum Karlsruhe GmbH, Germany

The first IAEA specialists meeting on mechanical properties of structural materials including environmental effects was held in Chester, UK in 1983. Since then significant progress has been made in the mechanical properties evaluation techniques in liquid sodium environment. Many new materials such as Type 316 L(N) stainless steel and 9Cr-1Mo ferritic steel etc. are being considered as candidate structural materials for LMFBR's applications. Furthermore, many new in-sodium testing facilities have been commissioned and substantially more operating experience has been acquired. These developments have been accompanied and supported by a broader and deeper understanding of mechanical behaviour of structural materials in liquid metal environment.

This IAEA specialists meeting on properties of structural materials in liquid metal environment at Karlsruhe provided an opportunity for an international exchange of information on these developments. In this regards the IAEA and the KfK provided an invaluable help in making the Meet a truly international undertaking. A broad perspective of properties of structural materials of interest to LMFBR was provided by our invited speakers, session chairmen, which made the specialists meeting in all respects an unqualified success. We look forward to the next Meet with the hope of continuing our association.

I also take this opportunity to put forward the statistics of the presently on-going programmes on in-sodium testing in the participating countries as follows:

(a) India

Facilities for materials testing in sodium (INSOT) for creep-rupture, low cycle fatigue, fracture mechanics and corrosion will be available from mid 1993. Preliminary tests are under way in some simple facilities.

(b) EFR

Seven facilities for creep-rupture, low cycle fatigue and corrosion were available in the past. Since 1991, two loops for creep-rupture, low cycle fatigue and fracture mechanics are in operation in Germany. Corrosion loops are still in operation one in France and four in United Kingdom.

(c) USSR

About ten facilities for creep-rupture and low cycle fatigue in liquid sodium are in continued operation.

(d) Japan

Three sodium loops for creep-rupture, two for low cycle fatigue and one for corrosion tests are in continued operation.

Recommendations

1. The delegates agreed with the EFR recommendation that the mechanical properties data generated in air for 316 L(N) steel and 9Cr1Mo (mod.) steel base metal could be safely applied for the design of components operating in reactor quality sodium for components with wall thickness larger than 2 mm.

2. The influence of corrosion, carburization, decarburization, formation of ferritic sub-surface layers and sensitization, however, have to be considered for thin-walled components (thickness < 2mm).

3. The effect of decarburizing sodium on the creep-rupture behaviour of Type 304 stainless steel can be ignored for thick-walled components. However, it has to be taken into account for thin walled components. The carbon potential of the sodium should be evaluated for this case.

4. Control of environment in reactor to highest standard of purity is a key element in preventing environmental assisted cracking and must always be a very high priority to reactor operators. For this reason, standards of, for instance, cover gas purity must be strictly maintained.

5. Further data are needed on environmental assisted cracking of "new" materials e.g. steels 316 L(N) and 9Cr1Mo (mod.) to define the boundaries of stress, and microstructure. Environmental conditions (particularly upper limits of impurities in sodium such as NaOH, Na_2O, etc.) which give rise to environmental assisted cracking have to be defined. Particular attention should be given to weldments.

6. Since cracking in service is often associated with weldments, high standard of welding practice must be adopted. Wherever possible stress relief heat treatments should be used and hard microstructures avoided.

7. There is a need to understand the reason for cracking and also to generate further in-sodium data on the weldments of carbon-manganese steel 15Mo3 to gain confidence in the use of this steel in low temperature sodium environments. This may be relevant to EFR where the reactor roof has to be made from such material in welded segments.

Papers

General Remarks:

The papers are reproduced as received from the authors. Two papers were retyped by the office of Mr. Arkhipov.

The assistance of Messrs. G. Frees and M.P. Mishra in the production of these proceedings is gratefully acknowledged.

Influence of Sodium Exposure on Creep Rupture Strength of Type 304 and 316 Steels

Y. Wada, E. Yoshida, M. Aoki, S. Kato and T. Ito
Materials Development Section, Systems and Components Division,
O-arai Engineering Center, Power Reactor and Nuclear Fuel Development Corp.

ABSTRACT

Creep rupture tests in sodium for one heat of as-received Type 304 steel hot rolled plate were carried out at 500, 550, 600 and 650℃ in carburizing atmosphere using cylindrical specimens of 6mm diameter. Creep rupture strength in sodium was almost same as that in air, though tertiary creep embrittlement was observed. Creep rupture tests in air on another heat of Type 304 steel pre-exposed for 20,000hrs at 500, 550 and 600 ℃ to carburizing sodium were also examined using same type specimens to compare the sodium-exposure effect under stress loading with that under no loading. Creep rupture strength on the pre-exposed material was not different from that of the as-received one. Tertiary creep embrittlement was also observed in this test.

On-set times of tertiary creep and steady creep rates of both tests; in-sodium and post sodium-exposure tests, were almost same as those of in-air tests for as-received materials.

It was supposed that tertiary creep embrittlement should be caused by carburization. Grain boundaries with coagulation of precipitated carbides might crack by large distortion of grains in tertiary creep stage. Tertiary creep embrittlement is related to behavior of grain boundaries near the surface of metal exposed to sodium.

Creep rupture tests in sodium for one heat of as-received Type 316 steel hot rolled plate were carried out at 550 ℃ using thin plate specimens of 3mm thickness. As the results tertiary creep embrittlement was not observed and creep rupture strength in sodium was slightly longer than that in air. It was presumed that grain boundaries of Type 316 steel were more ductile than those of Type 304 steel under carburizing sodium environment. Grain boundaries of low carbon(about 0.01%) and nitrogen controlled(0.06-0.10%) modified Type 316 steel, which is similar to European type 316L(N), were more stable than those of Type 316 steel by the result from the sodium exposure test for 5,000hrs. It was expected that tertiary creep embrittlement of modified Type 316 steel could not occur. Long-time creep rupture test(target life:20,000hrs) for this material is continued now to justify the anticipation.

1. INTRODUCTION

Tertiary creep embrittlement of Type 304 steel has been investigated to evaluate the influence to material integrity. Huthmann reviewed thier activities for ten years and noticed the decarburizing atmosphere[1]. Under non-decarburizing sodium conditions minimum creep rate and time to onset of tertiary creep are not influenced, though tertiary creep embrittlement occurs. But under decarburizing conditions an additional reduction of creep rupture strength with higher creep rates and earlier onset of tertiary creep occurs. This additional effect seems to be related to sodium corrosion of surface layers. Horton comfirmed the observation of tertiary creep embrittlement by Huthmann[2]. Natesan examined creep properties of Type 304 steel that had been pre-exposed to sodium[3]. Under carburizing conditions creep rupture strength was reduced with higher creep rates at 550 ℃. Tertiary creep embrittlement was indicated and the depth of surface intergranular cracks corresponded to the depth of carbon penetration.

Usually decarburizing conditions for Type 304 steel are not expected in the sodium of LMFBRs, because main structural components in large LMFBR system are exposed to sodium with the range of probable carbon concentrations at temperatures between 400 and 550℃. It is supposed that tertiary creep embrittlement should be caused by carburization. Carbide particles precipitate along grain boundaries near the surface by carburizing sodium-exposure, and grain-boundaries with coagulation of precipitated carbides may crack by large distortion of grains in tertiary creep stage. Tertiary creep embrittlement is related to behavior of grain boundaries near the surface of metal exposed to sodium.

So in the present study, two types of creep rupture tests on Type 304 steel hot rolled plates were carried out and the influence to material integrity by tertiary creep embrittlement in carburizing sodium was evaluated. One type is in-sodium test on an as-received material, and the other type is in-air test on a pre-exposed one for 20,000hrs. These test data were examined to compare the sodium-exposure effect under stress loading with that under no loading.

For Type 316 steel, Horton studied creep rupture strength in flowing sodium, and tertiary creep embrittlement was not observed[2),4)]. This phenomenon was also observed in creep rupture tests on pre-exposed materials by Natesan[3], though creep rupture strength was reduced with higher creep rates. In the present study creep rupture tests in sodium for one heat of as-received Type 316 steel hot rolled plate were carried out using thin plate specimens of 3mm thickness to confirm whether tertiary creep embrittlement occurs or not.

2. TEST MATERIALS

Table 1 and 2 list the chemical compositions and mechanical properties of test materials at room temperature. The heat No. A-1 was Type 304 steel for in-sodium test, the heat No.A-2 was also Type 304 steel for in-air test on pre-exposure to sodium and the heat No.B-1 was Type 316 steel for in-sodium test. A-1, A-2 and B-1 are hot rolled plates of 40mm, 40mm and 25mm for thickness, respectively.

3. TEST CONDITIONS

3.1 TEST SPECIMENS

The configurations of creep rupture test specimens are shown in Fig. 1. The surface-to-volume ratios of in-sodium tests are 2/3(mm^{-1}) for 6mm diameter and also 2/3(mm^{-1}) for 3mm thickness. Creep rupture tests in air on as-received

materials were carried out as the reference.

3.2 SODIUM TEST CONDITIONS

The outline of creep test section in flowing sodium, which was used for in-sodium creep rupture test, is shown in Fig. 2. Flow rate of sodium was about 0.5ℓ/min and temperature of cold trap was controlled at 120℃.
The schematic view of specimen holder for pre-exposure to sodium is shown in Fig. 3. Flow rate of sodium was 1m/sec at specimen surfaces.
The test conditions are shown in Table 3.

4. TEST RESULTS

4.1 IN-SODIUM CREEP RUPTURE BEHAVIOR OF AS-RECEIVED TYPE 304 STEEL

The test results on creep rupture behavior in sodium for as-received Type 304 steel are shown in Fig. 4 comparing with those in air. Any reduction of times to rupture was not observed. Steady creep rates of in-sodium test were slightly lower than those of in-air one as shown in Fig. 5. On-set of tertiary creep of both tests of in-sodium and in-air was not different. Examination of correlation between times to tertiary creep and times to rupture is shown in Fig. 6. And a ductility within the tertiary creep range was reduced in intergranular failure conditions as shown in Fig. 7, though the degree of reduction was not distinguished. Deep intergranular cracks starting from the surface was confirmed by optical micrographs of Fig. 8. Number of surface cracks for the specimens tested in sodium was higher than that in air. Tertiary creep embrittlement was recognized in the test.

4.2 CREEP RUPTURE BEHAVIOR OF PRE-EXPOSED TYPE 304 STEEL TO SODIUM

Creep rupture strength was not influenced by the pre-exposure to sodium for 20,000hrs as shown in Fig. 9. But tertiary creep embrittlement was also observed. Fig. 10 shows typical tertiary creep embrittlement. The tendency of rupture elongation given in Fig. 11 was similar as in-sodium test.
It was considered that tertiary creep embrittlement should not be caused by dynamic interaction of flowing sodium and stress. Fig. 12 shows carbon concentration and hardness near the serface of specimen for the exposure condition of 550 ℃ and 20,000hrs. The depth of surface intergranular cracks corresponded to the depth of carbon penetration in the test, as already indicated by Natesan[3] . Under carburizing condition, which is expected in large LMFBR system with the range of probable carbon concentrations at temperatures between 400 and 550℃, carburized surface layers affected earlier initiation of cracks and reduction of ductility.

4.3 IN-SODIUM CREEP RUPTURE BEHAVIOR OF AS-RECEIVED TYPE 316 STEEL

The creep rupture test results obtained for Type 316 steel are shown in Fig. 13. There are also no significant difference between creep rurture strengths in sodium and air, and tertiary creep embrittlement was not found.
From typical creep stain behavior given in Fig. 14, onset of tertiary creep in sodium was slightly later than that in air. Rupture elongations in sodium and air were not different as shown in Fig. 15. Fig. 16 shows micrographs near the surface of specimen, and microcrack were observed not only at the surface and also inside of specimen.

5. DISCUSSION

It is supposed that tertiary creep embrittlement of Type 304 steel should be caused by carburization in sodium. The carbon concentration at the surface of specimen was about 0.3% in the present study. Carbide particles precipitated along grain boundaries near the surface by sodium-exposure for 20,000hrs, and the cracking of grain boundaries with coagulation of precipitated carbide particles may occur by large distortion of grains within tertiary creep range. Tertiary creep embrittlement is related to behavior of grain boundaries near the surface of metal exposed to sodium. Fig. 17 shows the concept of this process.

In structural design on large LMFBR components, primary stresses are usually very low and creep rupture phenomenon by primary stresses is not an actual failure mode. Total strain caused by primary stresses is limited to less than 1.0% using St values by the rules in structural design codes/standards. It is expected that tertiary creep embrittlement should be tolerable for ductile failure like creep rupture, as already indicated by Huthmann[1]. But if carburizing sodium environment is sensitive to cracking of grain boundaries near the surface under large plastic deformation, the acceleration of reduction of creep-fatigue life might occur. For LMFBR components cyclic secondary stresses caused by themal transient are usually dominant, and higher stresses are distributed at the surface of metals. The interaction of sodium environment and cyclic strain loading with hold time is the actual problem for LMFBR structural design. The investigation of tertiary creep embrittlement should be performed as the evaluation of sodium environmental effect on creep-fatigue strength, and the mechanism is discussed in another paper[5].

Comparing the test results on Type 304 steel with those on Type 316 steel, it was presumed that grain boundaries of Type 316 steel were more ductile under carburizing sodium environment. Grain-boundaries near the surface of Type 304 steel cracked early under large plasic deformation within the tertiary creep range, though this phenomenon was not recognized for Type 316 steel. When the grain-boudaries of the surface cracked, microcracks were also initiated in the bulk of metal for Type 316 steel. It is considered that the difference in sodium behaviors of Type 304 and Type 316 steels is caused by molybdenum considering the two steels have similar chemical compositions except molybdenum. It was indicated by Horton[4] that intergranular cracking might be associated with the formation of relatively brittle sodium chromite along the boundaries, and this process might be aided by the formation of an almost continuous network of chromium rich carbide particles along grain boundaries. For the explanation about sodium chromite it is difficult to interpret tertiary creep embritlement of in-air test for Type 304 steel pre-exposed to sodium.

Fig. 18 shows transmission electron micrograph of Type 316 steel exposed to sodium for 5,000hrs at 600℃. Chromium rich metal carbide particles $M_{23}C_6$ were observed for sodium-exposed Type 316 steel along grain boundaries, but embrittlement by carburization and/or sodium chromite does not occur. It is well known that molybdenum has a control effect on precipitation of chromium carbide particles. Relatively fine precipitations are dispersed along the boundaries and coagulation of precipitations does not form continuous network of carbide particles as discussed by Horton[4]. It is same mechanism as the above phenomenon that molybdenum is a controlling element to prevent the formation of chromium poor layers, and effective for stress corrosion cracking of weldments of stainless steels. Grain boundaries with discontinuous distribution of carbides near the surface can deform as well as inside grain boundaries. As the results earlier cracking might not occur by large distortion of grains within the tertiary creep range for Type 316 steel. But for a long time exposure to sodium as long as the in-service time of LMFBR components, the formation of continuous distribution of carbides by coagulation of precipitations might occur. Grain boundaries of low carbon(about 0.01%) and nitrogen controlled(0.06-0.10%) modified Type 316 steel, which is similar to European

type 316L(N), were more stable under carburizing sodium by the result from sodium exposure test for 5,000hrs at 600 ℃ as shown in Fig. 18 and Fig. 19. It was expected that tertiary creep embrittlement of modified Type 316 steel could not occur. Long-time creep rupture test(target life:20,000hrs at 550 & 600℃) data to justify the anticipation for such type materials are not introduced in the present study, because this test is not finished now. Test temperatures are slightly higher to accelate paticipation and coagulation.

6. CONCLUSIONS

(1) Tertiary creep embrittlement on Type 304 steel was observed in the both cases;in sodium and post sodium-exposure tests. It was supposed that earlier cracking of grain boundaries with coagulation of precipitated carbide particles under carburizing conditions might occur by large distortion of grains within tertiary creep range.
(2) In structural design for large LMFBR components, primary stresses are usually very low and creep rupture caused by primary stresses does not occur, while cyclic secondary stresses caused by themal transient are usually dominant in the loading conditions for LMFBR components. Sodium environmental effects on creep-fatigue life under cyclic strain loading with hold time are important for LMFBR structural design considering the tertiary creep embrittlement.
(3) Comparing the test results on Type 304 steel with those on Type 316 steel, it was presumed that grain boundaries of Type 316 steel were more ductile under carburizing sodium environment. Grain boundaries near the surface of Type 304 steel cracked in the early stage of the tertiary creep range, though this phenomenon was not recognized for Type 316 steel.
(4) It is considered that the difference between tertiary creep behaviors of Type 304 and Type 316 steels is caused by molybdenum. Chromium rich metal carbide particles $M_{23}C_6$ were observed for sodium-exposed Type 316 steel along grain boundaries, but embrittlement by carburization did not occur. Grain boundaries with precipitate free zone near the surfase could deform as well as inside grain-boudaries. As the results earlier cracking might not occur by large distortion of grains within the tertiary creep range for Type 316 steel.
(5) For a long time exposure to sodium as long as the in-service time of LMFBR components, the formation of continuous network of carbide particles by coagulation of precipitations might occur. Grain boundaries of modified Type 316 steel were more stable under carburizing sodium. It was expected that tertiary creep embrittlement of modified Type 316 steel could not occur.

REFERENCES

1)H. Huthmann and H. U. Borgstedt, 'Influence of sodium on the creep-rupture behavior of type 304 stainless steel', paper No.511, Vol.2, 4th Int. Conf. of LIMET, 1988
2)C. A. P. Horton and B. H. Targett, 'The creep rupture behavior of fast reactor steels, welds and transition joints in flowing sodium ; a review of CEGB results', paper No.513, ibid.
3)K. Natesan, O. K. Chopra and T. F. Kassner, 'Creep-rupture and low-cycle fatigue behavior of types 304 and 316 stainless steel exposed to a sodium environment', paper No. XIX-6, 2nd Int. Conf. on LM Tech. in Energy, 1980
4)C. A. P. Horton, R. S. Filder and B. H. Targett, 'Creep-rupture studies of fast reactor materials in flowing sodium', paper No. 196, Vol.2, 3rd Int. Conf. on LM Tech. in Energy, 1984
5)Y. Wada, T. Asayama and R. Komine, 'Influence of carburizing sodium on creep-fatigue behavior of SUS304', IAEA IWGFR special document, 1991(to be published)

Table 1 Chemical Compositions (wt%)

Material	C	Si	Mn	P	S	Ni	Cr	Mo	N
A-1	0.07	0.51	0.95	0.029	0.007	9.09	18.56	–	0.015
A-2	0.05	0.58	1.00	0.028	0.007	9.10	18.45	–	0.023
B-1	0.06	0.56	0.85	0.028	0.003	12.50	16.85	2.18	–

Table 2 Mechanical properties at room temperature

Material	0.2% off-set stress(kgf/mm²)	Ultimate tensile strength(kgf/mm²)	Fracture elongation(%)	Grain size ASTM No.
A-1	21.5	67.5	59.7	4.0
A-2	23.0	62.0	61.0	5.0
B-1	25	58	62	5.5

Table 3 Specimen histories and test conditions

Material	Pre-history of specimen	Test environment	Test temperature (℃)
A-1	as-received	in sodium	500, 550, 600 & 650
		in air	
A-2	pre-exposed to sodium for 20,000hrs	in air	500, 550 & 600
	thermal aged for 20,000hrs		
	as-received		
B-1	as-received	in sodium	550
		in air	

NOTE: In-air tests on the pre-exposed specimen were carried out at same temperatures as exposure conditions.

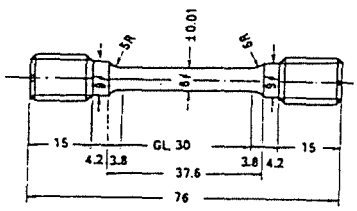

(a)In-sodium test specimen of SUS304

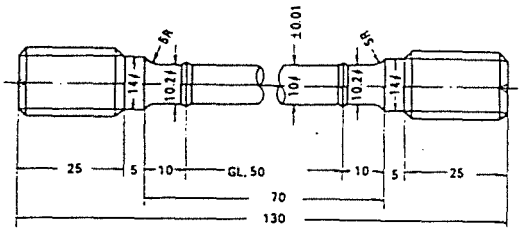

(b)In-air test specimen of SUS304

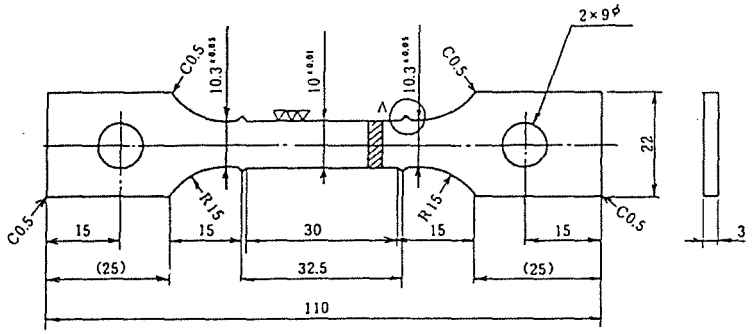

(c)In-sodium and In-air test specimen of SUS316 (unit : mm)

Fig. 1 Configurations of creep rupture test specimens

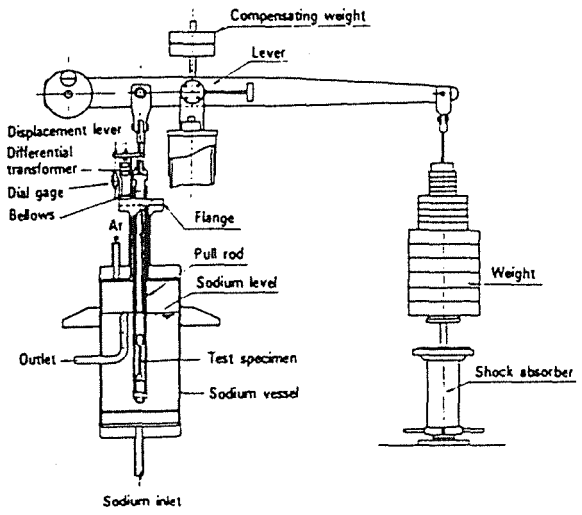

Fig. 2 Outline of creep test section in flowing sodium

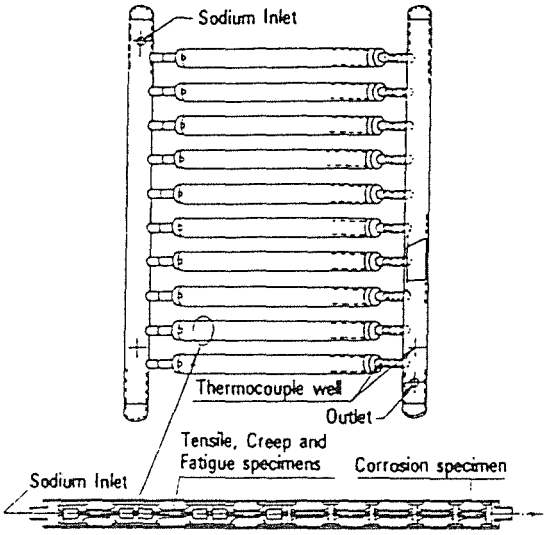

Fig. 3 Schematic view of specimen holder for pre-exposure to flowing sodium

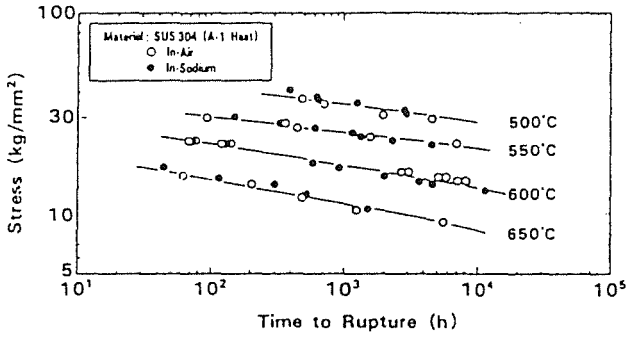

Fig. 4 Creep rupture behavior of SUS304 in sodium and air

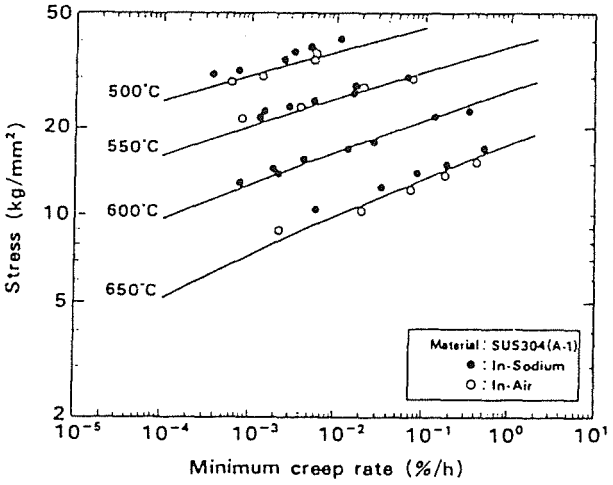

Fig. 5 Minimum creep rates of SUS304 in sodium and air

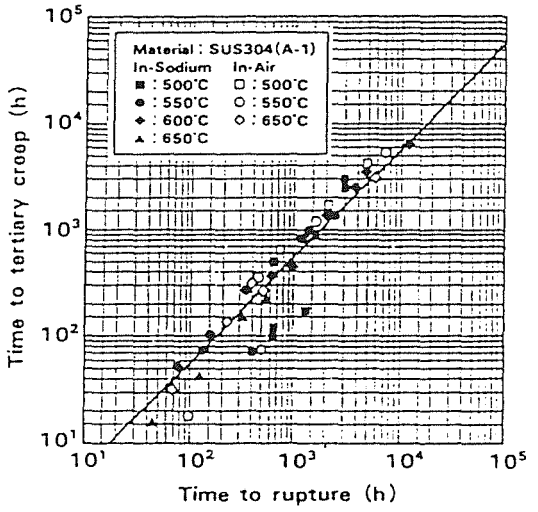

Fig. 6 Time to tertiary creep of SUS304 in sodium and air

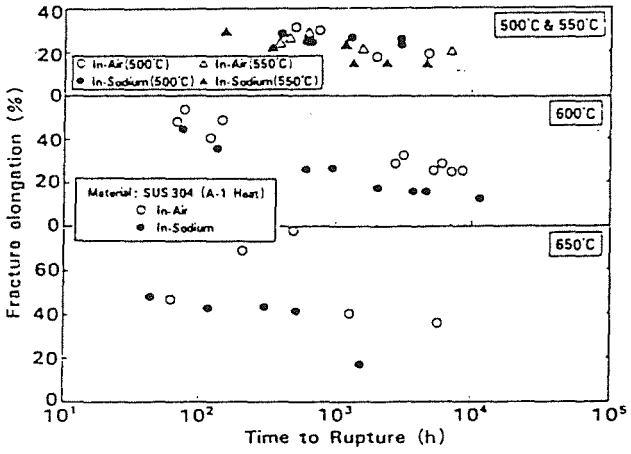

Fig. 7 Fracture elongation of SUS304 in sodium and air

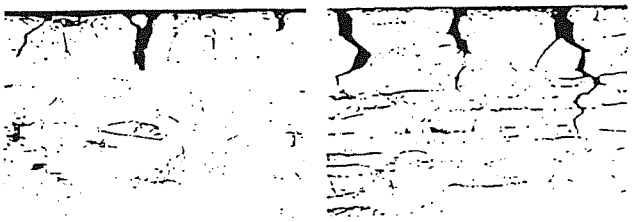

Fig. 8 Micrograph of surface cracks tested in sodium for SUS304 at 600℃

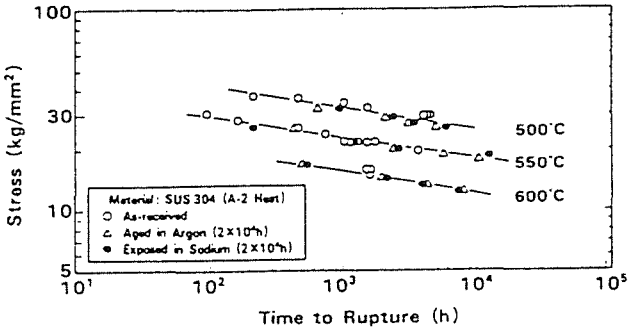

Fig. 9 Creep rupture behavior of as-received, thermal aged and pre-exposed SUS304 for 20,000hrs

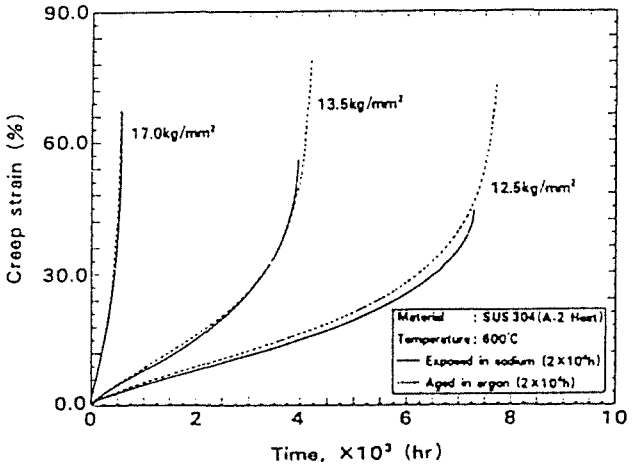

Fig. 10 Creep strain behavior at 600℃ of thermal aged and pre-exposed SUS304 for 20,000hrs

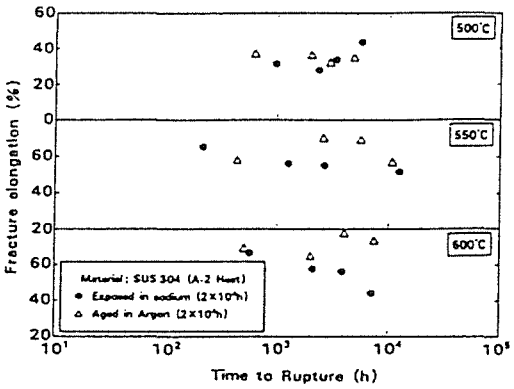

Fig. 11 Fracture elongation of thermal aged and pre-exposed SUS304 for 20,000hrs

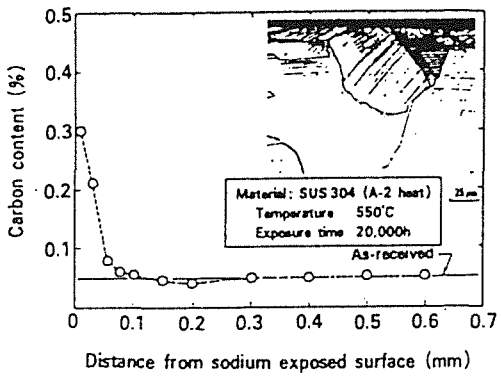

Fig. 12 Distibution of carbon concentration of pre-exposed SUS304 for 20,000hrs

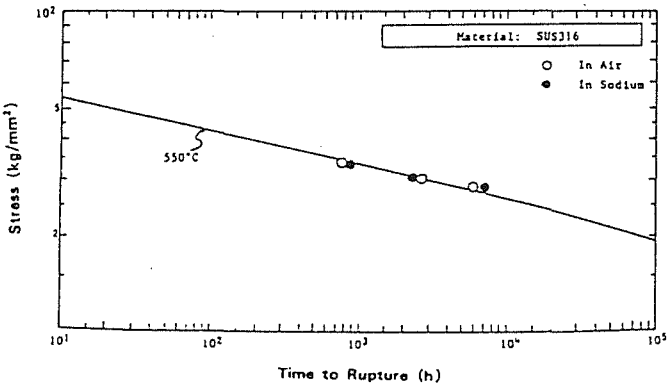

Fig. 13 Time to rupture of SUS316 in sodium and air

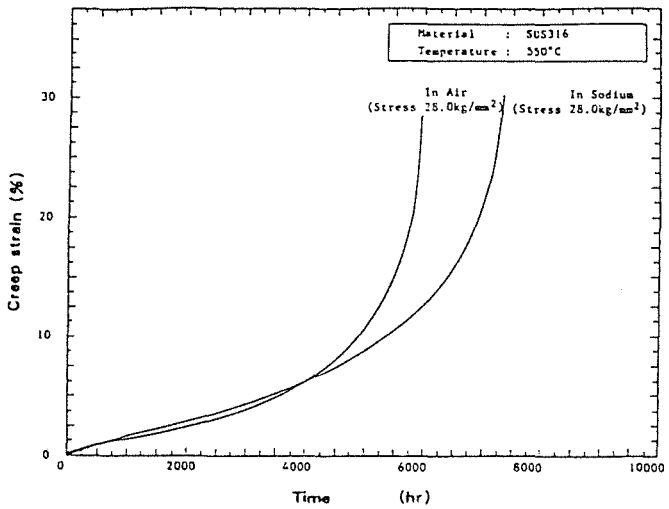

Fig. 14 Creep strain behavior at 550°C of SUS316 in sodium and air

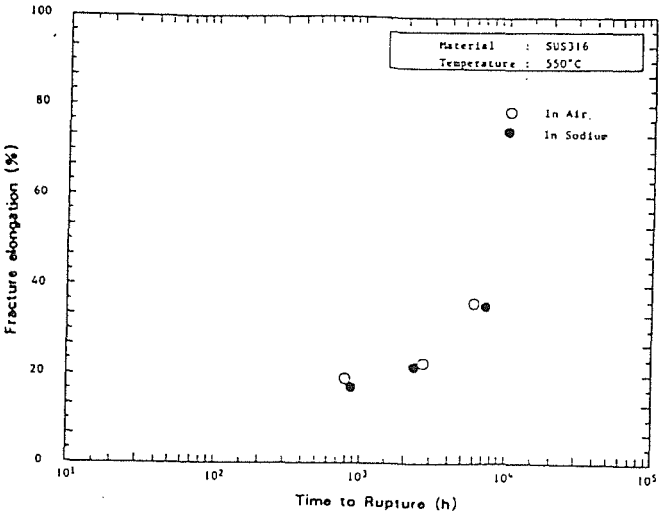

Fig. 15 Fracture elongation of SUS316 in sodium and air

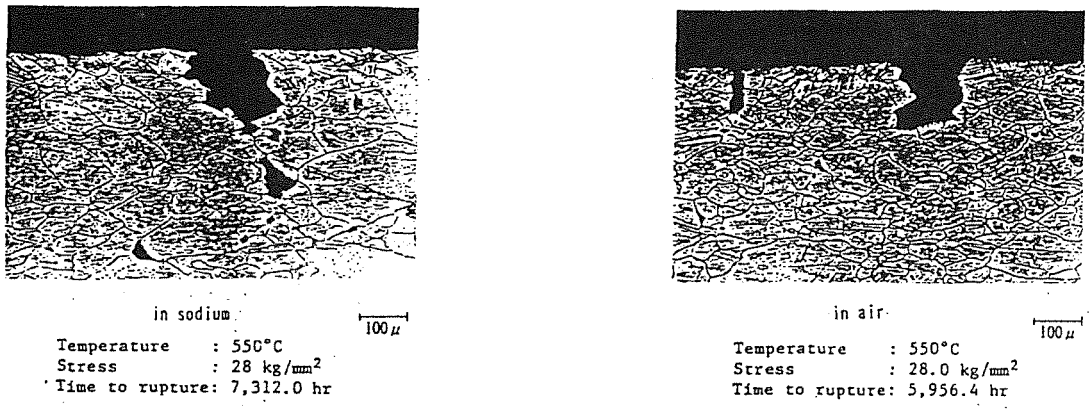

Fig. 16 Micrograph of surface cracks tested in sodium for SUS316 at 550°C

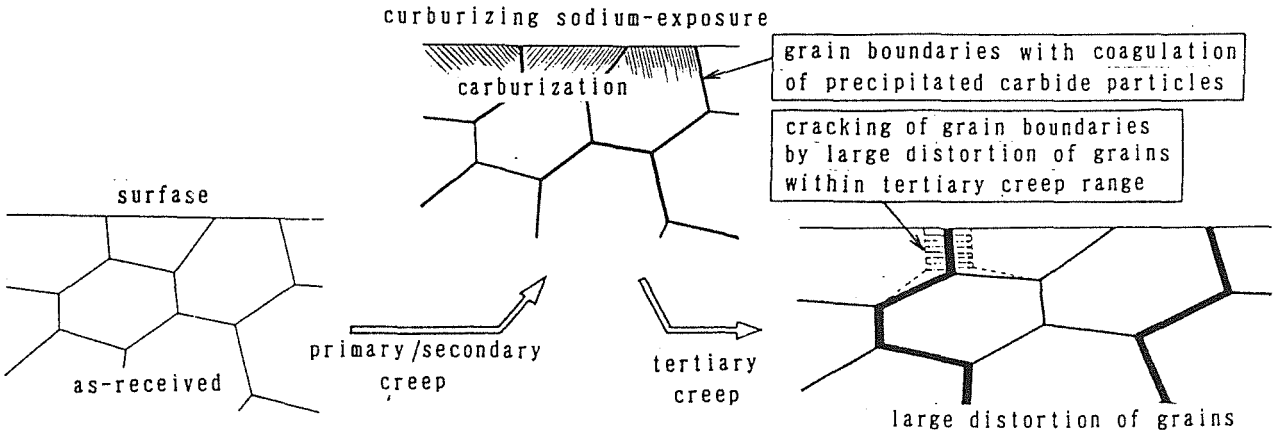

Fig. 17 Concept on process of tertiary creep embrittlement

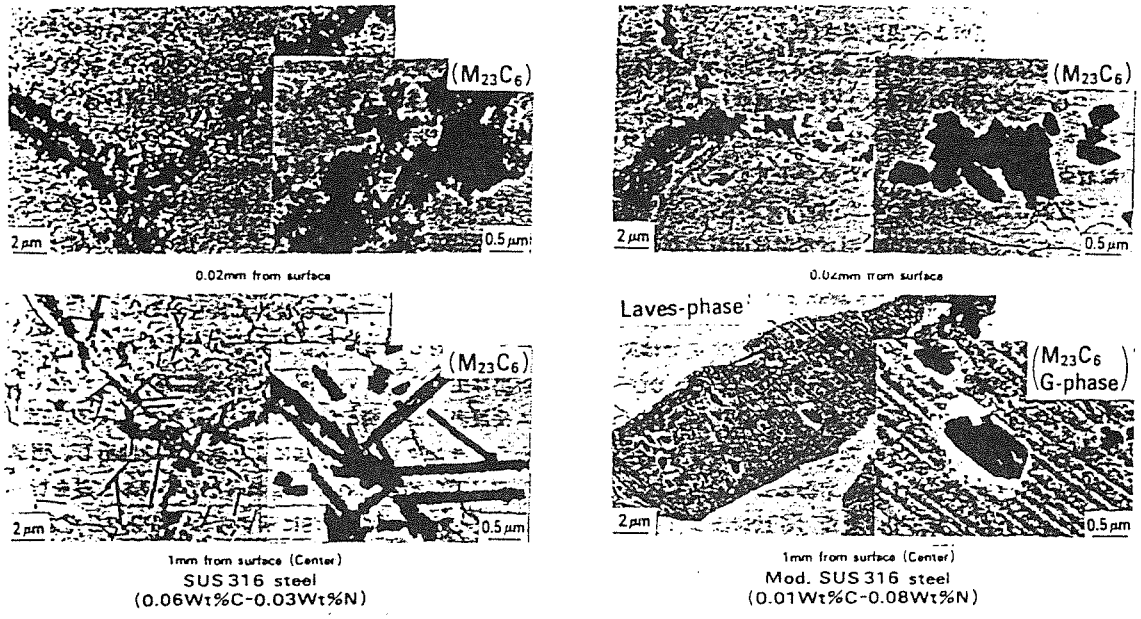

Fig. 18 Transmission electron micrographs of SUS316 and modified SUS316 exposed to sodium for 5,000hrs at 600℃

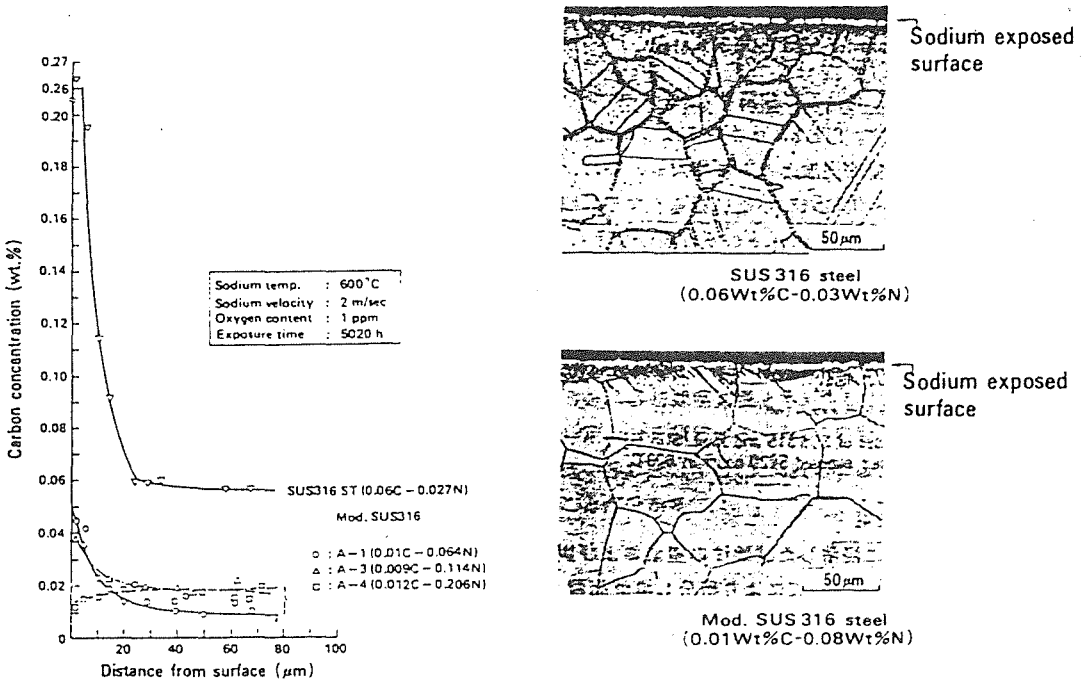

Fig. 19 Carbon profiles and cross sectional microstructures of SUS316 and modified SUS316 exposed to sodium for 5,000hrs at 600℃

The Effect of Decarburization and Carburization in Sodium on the Mechanical Properties of Austenitic and Ferritic Steels

Trapeznikov Ju.M., Trojanov V.M.
The Central Research Institute of Structural Materials, Prometey, USSR
Institute of Physics and Power Engineering, USSR

Abstract

The dependence of the degree and depth of ferritic steel decarburization and austenitic steel carburization in sodium at various temperatures is considered. The calculation of changed layer depths versus time at operating temperatures is given.

The mechanical properties and their dependence on carbon content were studied on various types of austenitic and ferritic steels.

The decrease of ferritic steels yield stress and creep rupture, and the decrease of austenitic steels ductility (σ and δ) is shown. These changes should be taken into consideration for the evaluation of service life of heat exchanger components contacting with sodium.

Introduction

The type X18H9, X16H11M3, X18H10T austenitic steels, Table 1, have been widely used in sodium-cooled fast reactors for the construction of "sodium-sodium" heat exchangers for reactor case and tubings for BOR-60, BN-600 plants /1/.

The type 10X2M steel has been used as a structural material for "sodium-water" steam generators. By the application of 10X2M and X18H9 or X16H11M3 steels it is necessary to estimate the effect of carbon transfer process.

Ferritic steels are decarburized by operation in contact with sodium, austenitic steels - are carburized. The decarburizing process is characterized by strength decrease, and carburizing results in ductility decrease. In this connection it is necessary to find out, how long, at what temperature and under what conditions the reliable operation of components manufactured from austenitic and ferritic steels may be provided with steels combined operation in loops with sodium coolant.

Carbon transfer estimation

This investigation considers the qualitative effect of carbon transfer from one steel to another on mechanical properties.

The process of carbon transfer from ferritic to austenitic steel occurs on account of difference in carbon thermodynamic activity a_c.

At the temperature range of 400-600°C carbon thermodynamic activity for ferritic 10X2M steel is 10-20 times higher than for austenitic steel /3/. The carbon transfer velocity is determined by the following system characteristics: carbon solubility in steel, carbon diffusion mobility, correlation of perlitic and austenitic steel surfaces and system hydrodynamic parameters. In simplified form the total quantity of carbon diffused in metal volume or out of it may be expressed as

$$m = C_o \sqrt{D\tau} \qquad (1)$$

where
C_o - carbon solubility at given temperature
τ - operation time
D - carbon diffusion coefficient at given temperature

As a first approximation, the estimation in accordance with Eq. 1 indicates that carbon flow in α - iron (ferritic steel base) is commensurable with carbon flow in γ - iron (austenitic steel base) when the austenitic steel temperature is 50-100°C higher. However, the process of carbon absorption by austenitic steel is complicated with the formation of carbides in it. Therefore, the investigations of the system "ferritic steel - sodium - austenitic steel" have been performed to estimate the carbon transfer velocity /1,2,5,6,7/.

The experiments with radioactive carbon C^{14} have been carried out for more precise determination of depth and degree of decarburizing and carburizing processes in sodium. The types 10X2M and 10X2MФБ ferritic steels were melted with additions of isotope C^{14}. Long-term tests in sodium in contact with austenitic steel were conducted to evaluate the integration and intensity of carbon isotope C^{14} emission by specimen grinding layer-by-layer. The graphs of the type 10X2M steel decarburization and the types X18H10T and X18H9 steels carburization have been constructed (Fig. 1). Analogous relationships were obtained after various exposure time. The relations of decarburizing and carburizing depth and degree versus exposure time were obtained and it was shown that they are diffusion processes. The depth of 10X2M steel decarburization and X18H9 steel carburization may be calculated with the formula:

$$X = K\sqrt{\tau} \qquad (2)$$

On the basis of experimental results the depth of 10X2M and 10X2MФБ steels decarburization was calculated at various operation time and temperatures (Table 2).

The depth and degree of the type 10XMФБ steel decarburizing is 3-5 times less than that of 10X2M steel. Table 1 indicates that tubes manufactured from 10X2M steel during the exposure time of 10^5 hours at 450°C are decarburized to the depth of 0,6 mm which is comparable with tubes thickness (2-3 mm).

Table 3 gives the carburizing depths of X18H10T steel in contact with 10X2M steel, and it is seen that at 600°C, for the exposure time of 10^5 hours these values are comparible with heat exchanger tubes thickness (0,86 and 1,6-2,0 mm, respectively). The calculations made on the basis of carburizing curves, constructed with the use of radioactive isotope C^{14} reveal that the maximal carbon content in surface layer does not exceed 0,17-0,23% at the temperature range of 550-600°C. Consequently, after long-term oepration (10^5 hours) the "sodium-sodium" heat exchanger tubes will be carburized to the maximal depth of 0,45 mm, and in this case the carbon content value will be decreased (in the direction from the surface to the depth) from 0,20% to 0,08% - an initial value.

The estimation of mechanical properties

To answer the question, how calculated material characteristics would be changed, the metal was melted, differing from 10X2M and X18H9 steels by carbon content /8/. In 10X2M steel the carbon content varied from 0,04 to 0,12%, in X18H9 steel - from 0,08 to 1%. After a standard heat treatment, a short-term aging was done at the temperature range of 500-600°C and properties change versus carbon content was determined
for the type 10X2M steel

$$\sigma_{0.2}^{20} = 170 + 1700(\%C), \qquad \sigma_{b}^{20} = 350 + 1600\ (\%C)$$

$$\sigma^{550} = 120 + 1200(\%C), \qquad \sigma_{10}^{550}4 = 50 + 550\ (\%C)$$

for the type 10X2МФБ steel

$$\sigma_{0.2}^{550} = 120 + 1400(\%C), \qquad \sigma_{b}^{550} = 220 + 1300\ (\%C)$$

As it is expected, by temperature and exposure time increasing, carbon influence on materials strength was decreased.

The effect of absorbed carbon on austenitic steel mechanical properties may be expressed as follows:

$$\sigma_{b}^{650} = 365 + 65(\%C), \qquad \delta^{20} = 54 - 96(\%C) + 40(\%C)^2$$

$$\delta^{650} = 30.5 - 71(\%C) + 39(\%C)^2$$

Even by permissible carbon content of 0,2% and temperature value of 650°C a sufficient margin of ductility in the type X18H9 steel surface layer will be retained ($\delta > 13\%$). Investigations /4/ demonstrate the increase of yield strength, creep rupture and thermal fatigue resistance. The carburizing of austenitic steel decreases short-term and long-term ductility, but does not result in brittle fracture and in decrease of time to failure.

The results of metal investigation after operation

The investigation of tube metals of heat exchangers, steam generators, armature, operated in BOR-60, BN-600 and BN-350 during 10000 - 60000 hours confirm a good agreement of experimentally calculated results with the results, obtained by operation. Thus, the depth of decarburization on BN-600 steam generator tubes after 10000 hours of operation was less by 10% than the calculated value, and on BN-600 steam generator tubes is 0,3 mm less, than the value, indicated in Table 2. Decarburization values for BN-600 steam generator tubes after 37000 hours are close to calculated ones.

The obtained test results with hold times of 61000 hours indicate that decarburization depth was 0,05 mm less, than calculated one. The type X18H10T steel carburizing for 61000 hours at 520°C was equal to 0,3 mm, and the maximal carbon content in surface layer did not exceed 0,20%.

Hardness and carburizing depth measurements of 10X2M steel were performed on tubes, cut from steam generator of BN-350 reactor after 61000 hours of operation (Fig. 2) and strictly correspond to calculated values (Table 2).

Conclusion

By the estimation of heat exchanging equipment service life it is necessary to consider the mechanical properties change as the result of carbon transfer process.

References:

1. Balandin Ju.,F. et al. Structural materials of nuclear power plants. M. 1984.

2. Trapeznikov Ju., M. Atomnaja energija, N 2, 1971, p.71.

3. Mogutnov B.I. et al. The thermodynamics of Fe-C alloys, Metallurgija 1972.

4. Frank-Kamenetskij D.A. Diffusion and heat transfer in chemical kinetics. Nauka, 1967.

5. Trapeznikov Ju.M. Metallovedenie. Sb. N 12, Sudostroenie, 1968.

6. Trapeznikov Ju.M. et al. Voprosji sudostroenija. Ser,7 Metallovedenie, bjip. 1(16) izd. Sudostroenie, 1972.

7. Starkov O.V., Lukjanova I.N. Zashchita metallov, 1974, N 1.

8. Trapeznikov Ju.M. Metallovedenie. Sb. N 12, Izdatelstvo Sudostroenie, 1968.

9. Trapeznikov Ju.M., Shurakov S.S. Metallovedenie, Sb. N 14, Izdatelstvo Sudostroenie, 1970.

10. Maljigin A.F., Trapeznikov Ju.M. Metallovedenie, Sb. N 15, Izdatelstvo Sudostroenie. 1971.

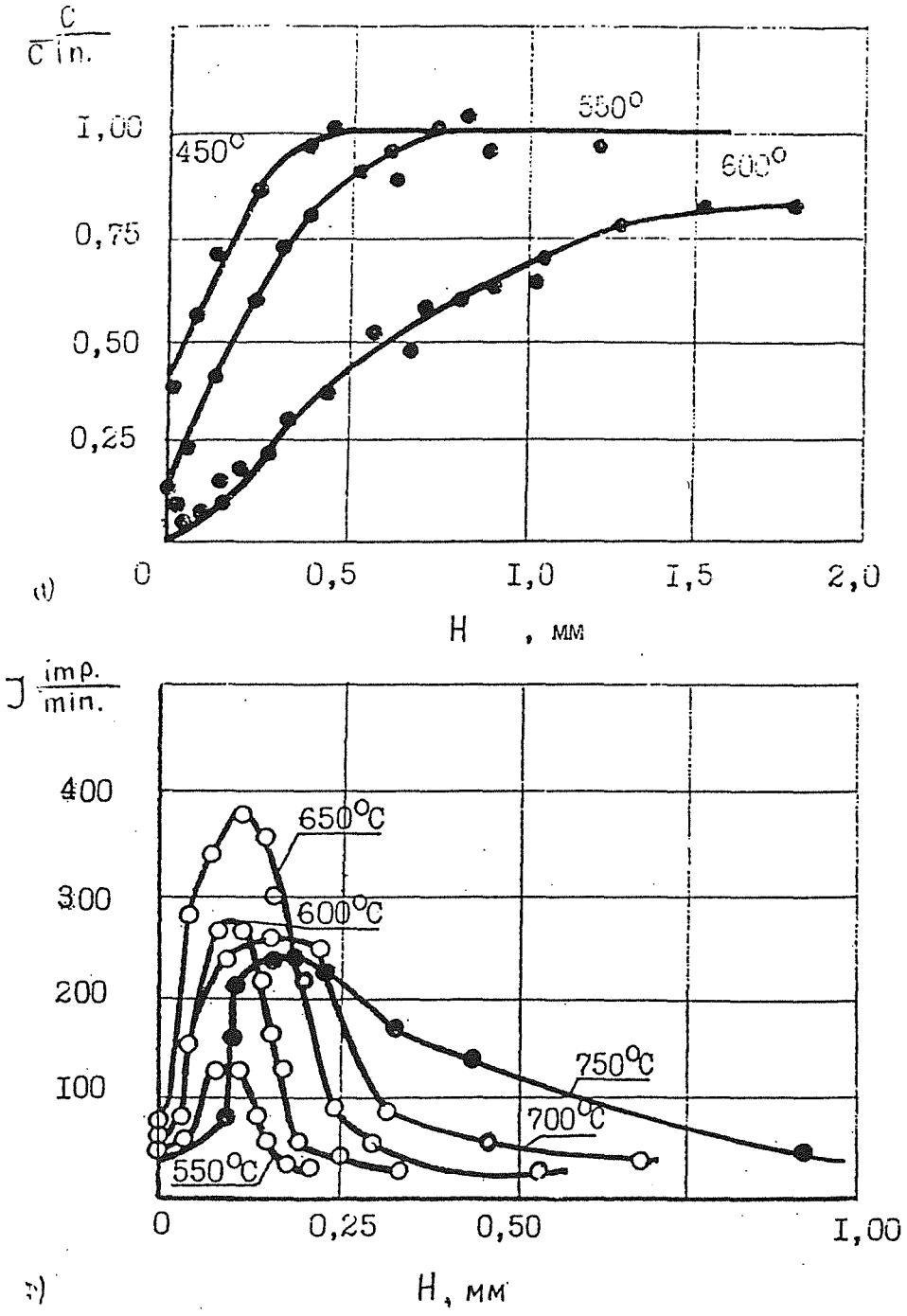

Fig. 1. The depth and degree of carbon content variation in 10X2M and X18H10T steel after exposure in sodium for 4000 hours.

Table 2. 10X2M and 10X2MФБ steel decarburization versus time and temperature

Time, h	Layer depth*, mm				
	Steel 10X2M	Steel 10X2MФБ	Steel 10X2M	Steel 10X2MФБ	Steel 10X2M
	600°C		550°C		450°C
2000	0.60	0.11	-	-	-
4000	0.80	0.19	0.30	0.09	0.10
10000	1.34	0.30	0.48	0.14	0.18
30000	2.32	0.52	0.83	0.25	0.32
100000	4.24	0.95	1.50	0.45	0.61
200000	6.00	1.34	2.13	0.64	0.87

* A layer, which contains 70% of initial carbon

Table 3. X18H10T Steel Decarburization in Contact with 10X2MФБ Steel

Temp., C	Carburized layer thickness, mm				
	4.10^3h	1.10^4h	3.10^4h	1.10^5h	2.10^5h
550	0.09	0.14	0.25	0.45	0.64
600	0.17	0.27	0.47	0.86	1.20
650	0.24	0.38	0.66	1.20	1.70
700	0.30	0.47	0.82	1.50	2.12
750	0.54	0.85	1.48	2.70	3.82

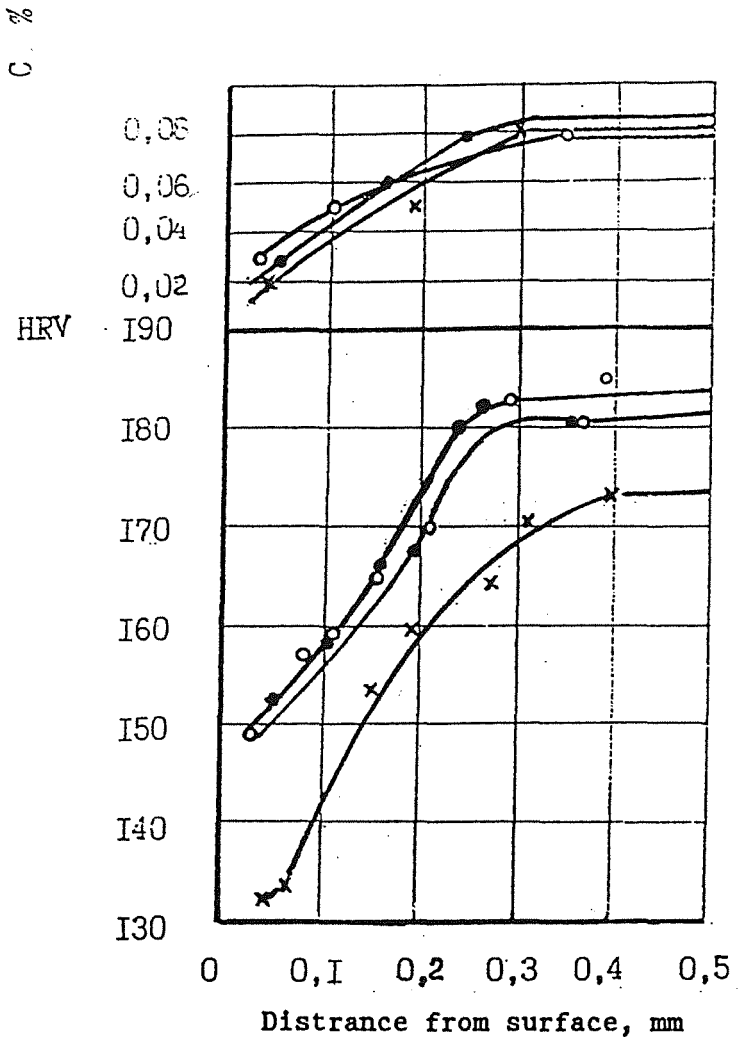

Fig. 2 Carbon content and microhardness variation in tube metal surface of steam generator "Nadjezhnost" after 61000 hours

● - tube 1

● - tube 8

x - tube 17

MATERIALS FOR FAST SODIUM COOLED REACTORS

Trapeznikov Ju.M., Grishmanovskaja R.N.,
Groynin I.V., Trojanov V.M., Malygin A.F.
Central Research Institute of Structural Materials, Prometey

Abstract

This paper describes the problems of materials production and application for nuclear power stations with fast reactors. The results of steels selection for reactor equipment and steels operation characteristics are given. The main criteria for the evaluation of reactor, heat exchanger, steam generator case materials service life are discussed. The resulting characteristics of selected materials service life at various temperatures, under cyclic and thermal loading, corrosion behaviour in sodium with different carbon and oxygen content are considered. The materials investigation after some hold periods in BN-600, BOR-60 and BN-350 plants show that the selected materials may reliably operate during the prescribed lifetime. The main problems concerning materials selection are put forward.

Introduction

The nuclear power plants safety is in considerable degree determined by the performance of structural materials and their weldments used to manufacture the main reactor components. The development and selection of base and weld metals for the equipment of fast reactors (BOR-60, BN-350, BN-600, BN-800, which is now in the construction stage) were performed with the regard for the complex operation conditions and impossibility to repair a series of reactor parts. By the selection of structural materials for case and tubing structures of fast reactors with sodium coolant one should take into consideration such characteristics of steel as short-term and long-term mechanical properties (strength and ductility) in as-produced condition and by the prolonged attack of temperature and irradiation, corrosion resistance in sodium, resistance to thermal-cyclic fracture, resistance to local fracture of welded joints, production processes of high degree.

1. Materials for reactor

After a complex investigation had been performed, types 10X18H9 and 08X16H11M3 unstabilized stainless steels were recommended as candidate materials for reactor main equipment production. Type 10X18H9 steel differs from the widely used in the USSR standard steel by the decrease of carbon content ($\lesssim$ 0,1%), titanium content ($\lesssim$ 0,1%) and phosphorus content ($\lesssim$ o,02%) which results in weldments local fracture resistance increase and the rise of high temperature ductility of irradiated metal. Type 08X16H11M3 steel is applied for the production of more loaded components and the parts operating at higher temperatures. The guaranteed strength values are given in Table 1. Both types of steels retain sufficiently high ductility at prolonged thermal exposure in the temperature range of 500-650°C including long-term creep rupture tests. Thus, the guaranteed long-term ductility (up to 200 000 hours) at 500-600°C is not more than 10%.

Investigations /1/ showed that the mechanical properties change of austenitic steels after irradiation at neutron fluence up to $10^{21} ncm^{-2}$ was practically absent. After irradiation at fluences as high as 10^{22} and even $10^{23} ncm^{-2}$ ductility is reduced up to 2-3 and 10% for 10X18H9 and 08X16H11M3 steels, respectively.

1.1 In-sodium corrosion

Austenitic steels, used in fast reactors, possess high corrosion resistance in dynamic sodium of reactor purity. With the use of numerous experimental results, obtained by testing in loops with forced sodium circulation, a correlation of corrosion depth dependence on temperature and operation time was constructed

$$h = 0.8\tau \quad 10^{-\frac{5400}{T}}$$

This relation is applicable for the range of operating temperatures of 250-650°C, by sodium velocities up to 5 m/s and oxygen content in sodium up to 0,005%. By the evaluation with this formula a component wall is appeared to become thinner to 0,04 mm after operation in sodium at 550°C for 30 years. At temperature up to 650°C and limited oxygen content of 0,005% such steels corrosion in sodium is negligible and for case structures may not be taken into consideration. By the application of austenitic steels in contact with sodium the chemical composition of metal surface layers is appeared to change. A selective solution of chromium, nickel and molybdenum in sodium takes place. It seems evident that the dominant stage of solution is diffusion process of elements supply to the surface contacting with sodium.

It is known that diffusion coefficient of Cr, Ni and Mo in iron is 2-3 orders less than carbon. The depth calculations of elements selective solution at 600-650°C for 30 years showed that the impoverishment in Cr, Mo, and Ni would not exceed the value of 0,15-0,20 mm. Such thickness of changed layer for thin-walled structures cannot reduce the mechanical properties.

The process of carburization may effect mostly on austenitic steels mechanical properties, if there is a source of carbon in sodium loop (ferritic steel or oil catching). It was established in /1,2/ that the maximal carbon content in surface layer did not exceed 0,2 - 0,5% depending on carbon source volume. If it is ferritic 10X2M steel, then carbon content does not exceed 0,25%. The carburization depth was determined at various temperatures, for high temperature components (tubes, heat exchangers) the carburization depth for 30 years will be equal to 0,7 mm.

The investigation of absorbed carbon effect on mechanical properties /2,3/, performed on melts with various carbon content, permitted to estimate such characteristics as short-term and long-term strength and ductility, thermal-cyclic strength resistance. With the increasing of carbon content strength properties increase and ductility decreases. By carbon content 0,2% the long-term ductility reduces in two times and does not exceed the value of 20%.

1.2 Thermal fatigue

Cyclic thermal stresses are most dangerous in fast reactors. The investigation of thermal fatigue resistance of X18H9 and X16H11M3 steels permitted to define:

- permissible number of cycles (N),
- deformation by one cycle ($\Delta\varepsilon$),
- cycle duration (τ)

with the regard for the effect of sodium and irradiation at the fluence $10^{21} ncm^{-2}$.

The estimation showed that allowable values of cyclic deformation ($\Delta\varepsilon$) for the equipment made from these steels at 550°C for 30 years by 1000 stop cycles are equal $\leq$ 0,30% /3/. To increase this characteristic a steel having minimal contamination in non-metallic impurities should be used.

1.3 Local fracture resistance of near the weld zone metal

Near the weld zone metal investigation after high temperature operation of X18H10T steel showed that this type of steel connot be used at temperatures above 450°C due to the formation of cracks of intergranular type. Residual stresses can have a marked effect on local fracture appearance in near the weld zone metal. In this respect the investigation of 10X18H9 and 08X16H11M3 steels has been performed. It was shown that these steels possessed a higher resistance to local fracture of near the weld zone metal as compared with stabilized steels. Thus, time before cracks formation in welded joints, produced from 08X18H10T, 10X18H9 and 08X16H11M3 steels at 550°C is equal to 10^3, 4.10^3 and 3.10^5 hours, respectively.

After weldments solution treatment (stress relieved condition) time before cracks formation was increased by 10 times and more. The temperature for solution treatment is the following: 450°C and 10X18H10T steel; 500°C for X18H9 steel and 560°C for 08X16H11M3 steel.

The complex estimation of 10X18H9 and 08H16H11M3 steels used for fast reactors with sodium coolant shows that these structural materials provide service reliability by the operation temperature of 550°C during 30 years, fig. 1.

2. Materials for steam generator

Type 10X2M steel is recommended for the construction of steam generators of BOR-60, BN-350, BN-600 reactors. Steel mechanical properties permit to use it at high temperatures (Table 1). The investigations with thermal exposures 5.10^4 hours at the temperature range of 300-550°C showed that mechanical properties were practically not changed. The depth of overall corrosion of 10X2M steel in sodium versus time and temperature is expressed as

$$h = 0{,}006.\tau.10^{-\frac{3700}{T}}$$

At 400-500°C and by oxygen content in sodium not more than 0,005 w.% corrosion velocity was in the limits of 0,2-7 mkm/year and practically did not effect on mechanical properties. With oxygen content increasing up to 0,05 w.%, corrosion depth is increased by 3-4 times.

Decarburization in sodium sufficiently influences on mechanical properties variation. The obtained correlations permit to predict the depth of decarburization.

The carbon reduction by 30% results in calculated characteristics decrease by 10-15%. The safety criterium of decarburization depth for 2 mm tube thickness is 0,3 mm, of 2 mm tube thickness - 0,6 mm. In this case structure strength estimation may be performed without mechanical properties consideration, because the summarized effect of the total section strength reduction does not exceed 3-5%.

The corrosion resistance of perlitic steels in water vapour and in water is practically the same, but lower than in sodium. Investigations in experimental loops during 500-1000 h showed that the maximal 10X2M steel corrosion velocity was increased from 0,01 mm/year at 300-350°C to 0,03 and 0,08 mm/year by temperature rise up to 450 and 550°C, respectively. By operation temperature of 500°C the corrosion depth of perlitic steel for 10 years may be ~0,8 mm.

The investigations of tubes of BOR-60 plant after 10000 and 18000 hours revealed that 10X2M steel corrosion resistance in sodium and vapour was even somewhat lower than obtained on experimental models.

The lower decarburization depth (h=0,16 mm) as compared with calculated (h=0,22 mm) is explained by the fact that tube temperature of 450°C was only after 6000 hours, afterwards the temperature was lower.

The short-term mechanical properties of tubes agreed with the requirement of specifications.

10X2M steel tubes operated at BN-350 plant in the periods of 500, 5000, 10000 and 55000 hours at the temperature range of 350-380°C.

The investigations showed that short-term mechanical properties were not changed, the velocities of decarburization and corrosion were low, fig. 2.

The steam generator constructed from 10X2M steel successfully operate at Beloyarskaya nuclear power plant. The study of tubes after 11, 26, 37, 45 and 61 thousands of hours indicated that mechanical properties corresponded to the requirements.

Type 10X18H9 steel is used as a structural material for steam generators of BN-600 plant. It demonstrates high corrosion resistance in sodium, water and vapour, it's technology is of high quality, but it is susceptible to intercrystalline corrosion and corrosion cracing in water.

The new types 05X12H2M and 03X21H32M3Б steels possess higher corrosion resistance in water and vapour; 1%Mo, 1,5%Ni were added to 05X12H2M steel, and carbon content was reduced up to 0,05%; the nickel content in 03X21H32M3Б steel is not more than 30%. The mechanical properties of these steels are given in Table 1. 05X12H2M steel surpasses 10X2M in strength at 400°C and slightly differs from it at higher temperatures. The type 03X21H32M3Б steel is stronger at 500°C. Both steels show the high stability of mechanical properties by temperature - time operation conditions of steam generators.

Type 05X12H2M steel is more weldable than 12%Cr steels, it may be welded without preheating /9/.

The long-term test results (up to 3000 hours) showed that heat treated 05X12H2M and 02X21H32M3Б steels and their weldments are not susceptible to corrosion cracking (in 3% NaCl solution at 300°C, in contact with vapour H_2O + 3%NaCl at 200°C, by 3%NaCl solution supply on the specimen, heated up to 200°C).

They have the advantage over 10X2M steel in vapour-water medium at 400°C by T=50+150°C, frequency 2,5 Hz.

Thus, 05X12H2M and 03X21H32M3 steel comply more fully with the steam generator operation conditions than 10X2M and X18H9 steels and they provide the necessary service life of reactor equipment.

The main problems to solve are the following:

1. The properties estimation and prediction of steels reliability at nuclear power plants.

2. Further investigation of perspective materials for steam generator by models construction, operating up to 10000-150000 hours.

3. The materials mechanical properties change by irradiation.

4. Development and recommendation of new materials for reactor inner components.

References:

1. Balandin Yu.F., Gorynin I.V., Zvezdin Yu.I., Markov V.G. Structural Materials of nuclear power plants. - M, Energoizdat, 1984.

2. Voprosi sudostroeniya, Ser.Metallovedenie, - 1974, vyip.19, p.55-60.

3. The experience of NPP operation and the ways of further atomic energetics development, - M, Atomizdat, 1974.

4. Svarochnoe proizvodstvo - 1982, v.3, p.25-28.

Table 1. The guaranteed steel strength characteristics after heat treatment

Steel tipe	σ_u, MPa at 20°C	$\sigma_{0.2}$, MPa					σ_{10^5}, MPa			
		Temperature, °C								
		20	450	500	550	600	450	500	550	600
10X18H9	490	196	108	98	98	98	–	143	99,8	63,8
08X16H11M3	510	206	137	128	118	118	220	165	124	80
10X2M	343	196	167	142*	–	–	157	94	86*	–
05X12H2M	539	372	304	265	245	–	176	108	73	–
03X21H32M3Б	539	216	167	147	147	–	–	384	216	–

* – at 510°C

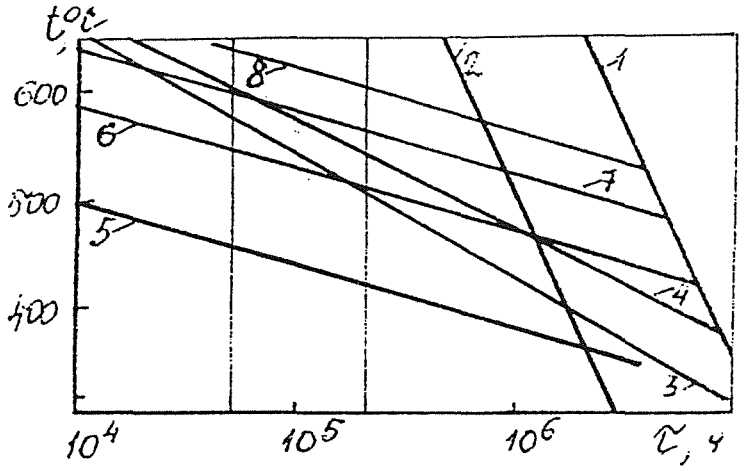

Nomogram of allowable 10X18H9(1-4,6,8), 08X18H10T(5), 08X16H11M3(7) steels properties variation.

1- corrosion in sodium of reactor purity (0,3mm depth)

2- corrosion in sodium with 0.01% O_2

3- carburization in sodium with 0.01% C

4- character variables of cyclic operation by 0,45% deformation

5,6,7,8- local fracture of near the weld zone.

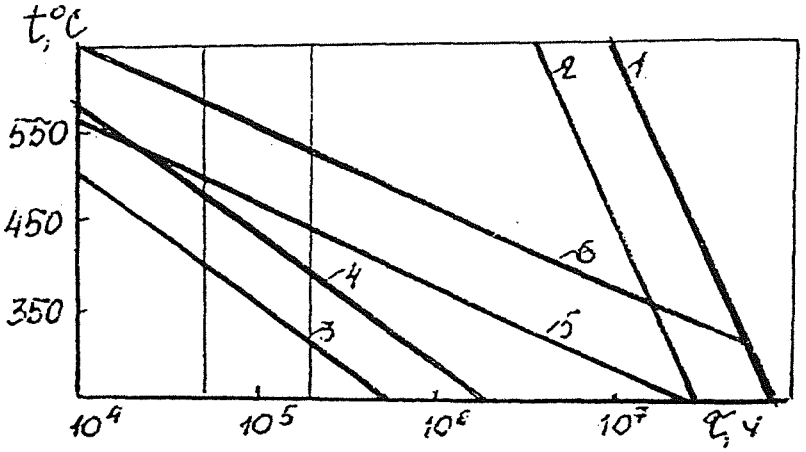

Nomogram of allowable 10X2M steel properties variation

1- corrosion in sodium of reactor purity (0,3mm depth)

2- corrosion in sodium with 0.01% O_2

3,4- decarburization in sodium, 0,3 and 0,6mm depth, respectively

5,6- corrosion in water vapour, 0,3 and 0,6mm, respectively

DESIGN DATA FOR STAINLESS AND HIGH CHROMIUM STEELS IN SODIUM ENVIRONMENT

-:-:-

M. ESCARAVAGE (FRAMATOME / NOVATOME)
M. WARD (NNC)
M. DIETZ (INTERATOM)
M. CAPURRO (ANSALDO)

SUMMARY

The recommended design data to be used for the European Fast Reactor (EFR) project is one of the tasks of the Design and Construction Rule Committee (DCRC), formed within EFR Associates the Design Companies associated for the EFR project. This Committee has reviewed the data on mechanical properties in sodium provided by the AGT9A which is the common Research and Development Working Group on material properties for EFR and which is working in particular on sodium environment effects (subgroup 2A). The DCRC has issued recommendations for the cases where data based on tests in air can be used :

* thick wall components ($\geq$ 2 mm) in 316L (N) stainless steel,

* thick wall components in modified 9Cr1Mo steel if a behaviour similar to that of the standard 9Cr1Mo is confirmed.

The DCRC has still to produce recommendations for :

* thin wall components in 316L (N) steel,

* the case of modified 9Cr1Mo tubes of the Steam Generator bundles (extra thickness covering sodium and water side corrosion).

1 - INTRODUCTION

For the European Fast Reactor (EFR) project, it has been decided to base the design works on the French code RCC-MR supplemented or modified by the recommendations endorsed by the Design and Construction Rule Committee (DCRC). This Committee has also to provide the material data required for the design works. These data are indicated in table 1 and require the analysis of tensile creep, continuous fatigue and fatigue with hold time tests provided by the Working Group AGT9A of the Research and Development organizations involved in EFR project (subgroup 2B of this working group is particulary concerned by sodium effects). Tests in air were only used in a first step and the DCRC has reviewed the possible use of these design data for components required to operate in reactor quality sodium, this quality being defined by the plugging temperature or maximum impurity contents (carbon, oxygen) following the different national practices.

2 - DESIGN DATA FOR 316L (N) AUSTENITIC STAINLESS STEEL

2.1 - Creep properties

2.1.1 - Stress to rupture

As most of the in sodium data are covered by the scatterbands of the in air tests, it is difficult to detect a significant effect of the sodium environment on the stress to rupture. Some shorter rupture times have been observed (with specimens of 4 mm in diameter for rupture times below 10 000 h) but the trend was not confirmed for long running tests and with 6 mm specimens (reference 1).

After discussions within the DCRC and within the AGT9A, it was concluded that the stress to rupture data in air (S_r) were also to be used for components in sodium with a wall thickness not less than 2 mm.

2.1.1 - Stress for the onset of tertiary creep

The comparison of the conditions for the onset of tertiary creep in sodium and in air was difficult. A complication arises in the evaluation of the creep curves from the fact the material develops two stages of secondary creep in air as well as in sodium. When the analysis is concentrated on the transition to tertiary creep, neglecting the transition between stage 1 to stage 2 of secondary creep, the in sodium and in air data are within the same scatterband (reference 1).

The time dependent allowable stress limit S_t for design at elevated temperature is governed by the stress to rupture, the stress for the onset of tertiary creep and the stress $\sigma_{1\%}$ to obtain 1 % of total strain. Considering that the tensile curve and the creep strain behaviour are not affected by the sodium environment for low strains (< 1 %), the DCRC has concluded that the in air values for $\sigma_{1\%}$ and S_t can be used in sodium environment for components with a wall thickness not less than 2 mm.

2.1.3 - Creep strain rate

For the material tested in the as received condition the minimum creep rate data from in sodium and in air tests fall in the same broad scatterband (reference 1).

For the creep strain behaviour, the DCRC has also concluded that the in air data are applicable to sodium environment.

The effect of sensitization on the creep behaviour was studied in France and in Germany using presensitized materials, the results confirmed that the transition in the secondary creep rate and the sensitization are linked. There are recommendations in the RCC-MR to avoid sensitization for the as fabricated components (in the welded joints as well as in the parent materials) and the combined effects of sensitization and sodium environment. The DCRC has concluded that these recommendations could be clarified for thin walled components (< 2 mm).

2.2 - Low cycle fatigue, strain controlled high cycle fatigue

On the 316L steel, the cyclic stress-strain curve appears to be unaffected by sodium environment.

On the standard 316L steel, fatigue lives at 450 °C and 600 °C were found to be longer in sodium than in air but no proposals were made to take credit for this beneficial effect. Also in the UK no difference in endurance was found between high purity sodium and air for strain controlled high cycle fatigue (UK type 316 SS). (reference 2)

2.3 - Elevated temperature low cycle creep fatigue

The UK has carried out fatigue and creep-fatigue tests in high purity sodium. It was concluded, taking also published data into account, that for temperatures in the range 450 °C-625 °C and average strain rate in the cycle $< 1.10^{-4}$ Hz, the behaviour in sodium may be taken to be the same as that in air. A similar conclusion was drawn for the low cycle continuous cycling conditions. (reference 2)

The DCRC has concluded that the same fatigue and creep-fatigue design curves as those in air are to be applied for components in reactor quality sodium.

2.4 - Fracture mechanics data

The fatigue crack growth data in sodium can be taken the same as that in air. From UK evaluations the threshold value in high purity sodium is likely to be greater than that in air, and hence the data sheet values are likely to be conservative when applied to high purity sodium situations, but at present there are insufficient data to specify a value other than the in air values.

For the type 316 steel, one test was performed in the UK in flowing sodium which indirectly shows that the crack growth rate was similar to that in air. Furthermore, since the stress to rupture behaviour was also unaffected by high purity sodium it was concluded that the creep crack growth rate in high purity sodium was the same as that in air.

3 - OTHER EFR MATERIALS

There is only a very limited amount of data on the effect of high purity sodium on the properties of other structural materials and weldments. Some information is available on the wrought normalised and tempered UK 9Cr1Mo steel :

* rupture stress (UK up to 11 785 h exist, no influence of sodium),
* minimum creep rates (UK results up to 11 785 h exist, no influence of sodium),
* low cycle continuous fatigue (no influence of sodium).

For EFR steam generator unit, a modified 9Cr1Mo grade with vanadium and niobium is used due to its improved creep strenghth and toughness. From results on standard 9Cr1Mo steel, no significant effect of sodium environment is expected on the modified 9Cr1Mo grade for thick components. The DCRC shall issue recommendations for the modified 9Cr1Mo later on the basis of on going work within R and D organisations

4 - THIN WALLED COMPONENTS

The DCRC has made provisionnal reservation for the case of thin walled components (tubes and sheets $\leq$ 2 mm). In these cases, several effects are to be considered :

* decarburizing sodium effect,
* effect of sodium on sensitized surfaces,
* corrosion and formation of ferritic sub-surface layer.

If provisions are made to prevent sensitization in the as-fabricated condition, these effects can be covered for design by extra thickness recommendations.

Values for extra thickness will be recommended by the DCRC for each particular case :

* intermediate heat exchanger,
* Na-air heat exchanger,
* steam generator tubes.

It should be noted that for the second and third cases, the major part of the extra thickness will be provided for oxidation on the out of sodium surfaces.

5 - CONCLUSION

The effects of sodium environment on design properties have been reviewed by the Design and Construction Rules Committee within the EFR project.

This committee has issued a recommendation to use the same material design data in reactor quality sodium than those in air, for the 316L (N) stainless stell thick wall components ($\geq$ 2 mm).

The DCRC has still to produce recommendations for parts of thin walled component.

* prevention of sensitization and extra thickness for 316L (N) steel,
* extra thickness for tubes of the steam generator or heat exchanger bundles.

REFERENCES

(1) H. HUTHMANN. The influence of flowing sodium on the creep rupture behaviour of 316L (N) stainless steel (present meeting)

(2) D.S. WOOD, A.B. Baldwin : Creep / fatigue behaviour of type 316 steel in sodium IAEA - IWGFR Conference Chester - October 1983.

TABLE 1. Material properties required for design work following the RCC-MR

A3.1S.1 INTRODUCTION

A3.1S.2 PHYSICAL PROPERTIES

- A3.1S.2.1 Coefficient of thermal expansion
- A3.1S.2.2 Young's modulus
- A3.1S.2.3 Poisson's ratio

A3.1S.3 TENSILE STRENGTH PROPERTIES

- A3.1S.3.1 Minimum and average conventional yield strength at 0,2% offset
- A3.1S.3.2 Minimum and average tensile strength

A3.1S.4 NEGLIGIBLE CREEP CURVE

A3.1S.5 ANALYSIS DATA

- A3.1S.5.1 Values of S_m and S
- A3.1S.5.2 Values of S_t
- A3.1S.5.3 Creep rupture stress: S_r
- A3.1S.5.4 Saturation fatigue curves
- A3.1S.5.5 Isochronous curves, creep strain
- A3.1S.5.6 Stresses S_{Rh} and S_{Rc}
- A3.1S.5.7 Symmetrization coefficient K_s
- A3.1S.5.8 Fatigue-creep interaction diagram
- A3.1S.5.9 Cyclic curves, values of $K\varepsilon$ and $K\nu$
  - A3.1S.5.9.1 Cyclic curves
  - A3.1S.5.9.2 Coefficient $K\varepsilon$
  - A3.1S.5.9.3 Coefficient $K\nu$

A3.1S.6 ANALYSIS DATA (Continued)

- A3.1S.6.1 Average and minimum tensile hardening rule
  - A3.1S.6.1.1 For plastic strain limited to 1%
  - A3.1S.6.1.2 For total strain attaining distributed elongation
- A3.1S.6.2 Bilinear curves
- A3.1S.6.3 Creep-strain rule
  - A3.1S.6.3.1 Primary creep
  - A3.1S.6.3.2 Secondary creep
- A3.1S.6.4 Fatigue curves
- A3.1S.6.5 Maximum allowable strain: D_{max}

CORROSION - MECHANICAL PROPERTIES OF STRUCTURAL MATERIALS IN SODIUM

Ryzhkov A.N., Kononyuk M.Kh., Zhelnin V.D., Liforov G.V.

The Institute of Physics and Power Engineering, Obninsk, USSR

Abstract.

The paper presents the results of research into long-term strength, creep and low cycle fatique properties of steam generator steels in pure sodium and with sodium hydroxide admixture at 500 and 550 °C. The highest sensitivity to alkali effect is manifested by steel 10X18H9. The presence of 5% hydroxide in sodium at 500 °C results in the 5% reduction of the long-term strength as compared to pure sodium tests, 45% rise in creep rate. The most appreciable effect of sodium hydroxide is on low-cycle fatique strength of this steel. When testing in pure sodium and in sodium with 5% hydroxide, with the strain amplitude 0.2% the difference in the number of cycles prior to failure is 2438×10^2 cycles.

1. Corrosion resistance of steels in pure sodium and hydroxidized sodium.

The corrosion rate in austenitic and ferritic steels used in steam-generator construction industry and the advanced ones (table 1) is low in pure sodium (cold trap temperature is 120-140 °C) (table 2).

With an account of tube wall thinning the steel corrosion rate (table 1) will be less than 0.5 μ/year for the temperatures below 530 °C.

As a result of steam generator leakage NaOH hydroxide enters the secondary circuit sodium. Following the steam generator leak the leak-tight modules operate in the nominal temperature regime with an increased NaOH content in sodium. Table 3 shows the results of the analysis for less corrosion-resistant steel 10X2M in the convective sodium flow (sodium rate ≈ 1 sm/s) containing NaOH and in the NaOH melt.

A film of compound sodium oxides was observed on steel samples, which was loosely bonded with the ground metal and can be washed away with a sodium flow.

That is why the mass of samples after the tests was measured

before (mg_τ) and after (mg^*_τ) removing the film with ammonium oxalate solute. The corrosion rates K and K^* given in table 3 are calculated via specimen mass change before (m_0) and after (mg_τ, mg^*_τ) tests:

$$K\ (K^*) = \frac{m_0 - m_\tau (m^*_\tau)}{S\,\tau} \qquad (1)$$

where S - is the area of specimen

τ - time

The 10X2M steel corrosion rate in sodium with hydroxide is two order higher than that for pure sodium (see tables 2,3). However, the increased content of NaOH in the secondary circuit cleaned-up by cold traps occurs during a time period less than 1000 h.

With the corrosion rate K^* of 10X2M steel in NaOH-melt at 500 °C the calculation of the thickness reduction for construction elements made of this steel gives <50 μ. In fact, the thickness reduction will be much less because the concentration of NaOH in sodium will decrease, especially at initial hours of cold traps operation. Thus, short-term sodium contamination with hydroxide will not essentially affect unstressed construction elements performance $\simeq$ 1000 μ in thickness and more.

2. Steel resistance in sodium with hydroxide admixture in the stressed state.

The real construction are loaded with stresses of various levels, therefore, the investigation of stressed material properties is of inter.

2.1. Study of the long-term strength of steels in sodium with hydroxide content.

The long-term strength and creep of steels in sodium containing hydroxide was measured by tested the slab specimens of 4 mm in width, 1 mm in thickness and with gauge length of 17.5 mm at applied constant tensile stress in a specially designed hermetic device. The process of filling and pressurization was accomplished in a glove cell in the argon medium.

Reference specimens were tested in pure sodium in a similar device (fig.1).

The effect of hydroxide on the time to rupture for the steels was also investigated using tubular specimens of various thickness Specimens were loaded by internal pressure of argon. The explored medium (pure sodium and hydroxidized sodium) resided inside the tubular specimen (fig.2).

2.1.1 Effect of NaOH concentration on long-term strength of steels.

The effect of in-sodium NaOH concentration on time to failure in steels was estimated for tubular specimens (21.2x1 mm), made of steel Х9МФБ at 650 and 700 °C for OH-concentrations up to 50%. The experiments feature significant scattering the experimental data. The dependance of time to failure for the steel specimens will be traced only up to the in-sodium NaOH solubility limit, (fig. 3) /1/. Hence, the study of long-term strength and creep of steels seems to be expedient at a saturation concentration level of NaOH for testing temperatures.

2.1.2 Long-term strength of low-alloyed steel 10Х2М in sodium with NaOH admixture at 500 °C.

The results of flat 10Х2М specimen tests for long-term strength at 500 °C yield the following dependences :

$$\lg \sigma = - 0.0771 \lg \tau + 1.7264 \qquad (2)$$

for the tests in sodium containing 5% NaOH and

$$\lg \sigma = - 0.0735 \lg \tau + 1.7287 \qquad (3)$$

for the tests in sodium contaning $< 2 \times 10^{-2}$% oxygen mass.

The resulting dependences show, that the presence of NaOH in sodium causes no significant reductionin 10Х2М steel creep resistance. E.g. if the stedy-state creep rate at a stress 304 MPa in pure sodium is 1×10^{-2} %/h, in sodium with NaOH it this rate is 2.5×10^{-2}%/h.

The dependence of the stedy-state creep rate on σ in NaOH-containing sodium and that in pure sodium is corresponding described by following equations:

$$\lg \sigma \text{ /MPa/} = 0.0995 \lg \dot{\varepsilon} \text{ /\%/hr/} + 1.6588 \quad (4)$$

$$\lg \sigma \text{ /MPa/} = 0.1050 \lg \dot{\varepsilon} + 1.7042 \quad (5)$$

The NaOH addition somehow reduces the elongation of test specimens (approximately by 1.5 - 5%), as a rule with uniform deformation over the gauge length.

For the test time of ≃830 h in the region of the maximum plastic deformation the grain boundary etching was observed at a depth up to 12 μ, the microhardness decreased up to 1050-1500 MPa at depth 30-45 μ. No corrosion was detected after test in pure sodium.

Thus, the presence of NaOH up to 5% wt. in sodium (this is the saturation concentration at 500 °C) causes no essential reduction in long-term strength, plasticity and creep acceleration of 10X2M steel at 500 °C.

2.1.3 Long-term strength of 10X18H9 steel in sodium with hydroxide impurity at 500 °C.

The similar technique was employed for the 10X18H9 steel refractory resistance investigations. The averaged time-to-failure dependences on stress have the form

$$\lg \sigma = - 0.1300 \lg \tau + 1.7066 \quad (6)$$

for the tests in pure sodium and

$$\lg \sigma = - 0.1293 \lg \tau + 1.6842 \quad (7)$$

for the tests in sodium at 500 °C with 5% wt. hydroxide.

The coefficients in Eq.(6) and (7) indicate that the presence of 5% wt. NaOH in sodium does't load to a noticeable reduction in long-term strength.

The presence of hydroxide increases markedly the creep rate of10X18H9 steel (fig. 4).

The coefficients in the equations describing the relationship between the established creep rate and stress differ essentially. For the tests in pure sodium one has

$$\lg \sigma = 0.1492 \lg \dot{\varepsilon} + 1.5536 \quad (8)$$

and for the tests in sodium with 5% NaOH

$$\lg \sigma = 0.1870 \lg \dot{\varepsilon} + 1.5564 \quad (9)$$

The plasticity degradation was observed in specimens due to the presence of 10 - 14 % hydroxide in sodium, with uniform deformation of the total working area of specimens normally observed.

A complex corrosion zone was found at the surface of specimens after the in - NaOH sodium tests, which comprised an outer frontal layer and an intergranular interaction layer with numerous microcracks. With longer test times (with the reduction of stress) the corrosion region thickness increases, and after 600 h. it reaches 90 μ (the front layer - 30 μ, the intergranular one - 60 μ). The microhardness of corrosion region reduces from 2.6×10^3 MPa to 1.5×10^3 MPa.

The steel failure has both intragranular and intergranular character.

The thickness of corrosion layer in control specimens tested in the 5% NaOH sodium medium is 10-15 μ. The post-creep-test steel specimens in pure sodium suffered no corrosive penalties. In this case the failure made is intragranular.

Thus, the tests on 10X18H9 flat specimens (1mm in thickness) at 500 $^{\circ}$C show the concentration of sodium with 5% NaOH to cause unsignificant reduction in long-term strength ($\approx$5%) and to noticeably ($\approx$45%) increase the creep rate.

The laboratory tests on thin-wall (0.25 - 0.30 mm) tubular specimens under the internal argon pressure indicate an essential inpact of NaOH impurity on long-term strength as well: the "time-to-failure" for tubular specimens in sodium with 5% NaOH (T=500°C, P=158 MPa) 370 h., in the pure sodium exeeds 6000 hours.

Equation (1) enables the stress levels causing flat and tubular specimen failure for the same time to be compared (table 4).

As can be observed from table 4, the failure of flat specimens for the same time intervals requires considerably higher stresses,

with the correlation existing between the stresses that result in flat and tubular specimen failure for the same time period (fig. 5). Here, the slope for the straight lines (fig. 5) with a fair agreement equals the ratio of specimens thickness 0.31 (the actual value is0.3 mm/mm) and 0.2 (the actual value is 0.25 mm/mm). In the latter case the composition of flat and tubular specimens somehow differs in chromium (18.36% and 17.96%), nickel (10.4 and 8.84%), carbon (0.06 and 0.08%).

Such a correlation and the straight line slopes allow to assume that the sensitivity of steel specimens to NaOH inpact is determined by the ratio of corrosion zone depth (L) and the specimen thickness (d).

Assuming the linear relationship between the ultimate tensile stress and the L/d value to be

$$\sigma = b_o + b_1 \frac{L}{d} \qquad (10)$$

and the dependence L on temperature and medium inpact time only, the linear correlation of ultimate tensile stresses will be obtained for specimens with thicknesses d_1 (σ_{fl}) and d_2 (σ_{tub}) (see fig. 5)

$$\sigma_{fl} = \frac{d_2}{d_1} \sigma_{tub} + \text{const} \qquad (11)$$

i.e. the straight lines' slope (fig. 5) equals to the ratio of specimens' thicknesses.

Assumption (10) is indirectly confirmed also by the effect of NaOH on long-term strength of thick-walled (1mm) tubular specimens of Х9МФБ(see fig. 3) at elevated temperatures.

Thus, the degree of in-sodium NaOH impurity inpact on refractory resistance of steels is a function of chemical composition, steel microstructure, thickness of specimen.

The presenceof NaOH will not significantly affect the long-term strength of structural components made of 10Х18Н9 steel 1mm in thickness and more, bearing in mind a limited-in-time period of potential NaOH content in sodium as well.

2.1.4 Low-cycle fatigue properties of stainless steel 10X18H9 in sodium with hydroxide impurity at 500 °C.

Materials of steem generators operate under the conditions of static and dynamic loads. The simultenious inpact of pure sodium and dynamic load on 10X18H9 steel at the temperature up to 650 °C results not in reduction but in an increase of cyclic strength [2,3].

Low-cycle fatigue tests of 10X18H9 steel in sodium which contains in the initial state 5 % wt. hydroxide and in pure sodium (check-tests) were conducted with cylindrical specimens (fig. 6) 12 mm in diameter and the gauge length of 25 mm using a standard test machine with a grip travel velocity 0.5 mm/min. The tests were conducted via a rigid sign-variable symmetric cycle. The value of displacements under specimens' tests has been estimated by the readings of indicators installed at the test machine grips. To determine a value of true deformation the check tests of control specimen were carried out at the temperature 500 °C without the medium with the measurement of specimen gauge length diameter variation using a special strain gauge with an accuracy of 1mm.

The results of 10X18H9 steel low-cycle fatigue strength tests are shown in fig. 7. The figure implies that the inpact of 5% wt. NaOH sodium on 10X18H9 steel under sign-variable load stresses causes an significant reduction in cyclic strength, with the effect of this medium inpact on 10X18H9 steel cyclic strength reduction at 500 °C enhanced as the specimen deformation amplitude diminishes, i.e. as the test time becames longer. Thus, e.g. with the difference in the number of steel cycles-to-failure when tested in pure sodium and hydroxidized sodium with the specimen deformation amplitude 0.3% amounting to 99.2×10^2 cycles, under the tests with the deformation amplitude 0.2 % the difference will be 2438×10^2 cycles. With the steel deformation amplitude 0.3 % the cyclic strength in hydroxidized sodium is approximately 2 times lower than in pure sodium. With the deformation 0.2 % the cyclic strength of this steel in hydroxidized sodium is 7 times lower than in pure sodium.

The following relation was identified between the deformation (ε_a) and the number of cycles (N)-to-failure for the steel 10X18H9 at 500 °C:

$$\lg \varepsilon_a = - 0.1484 \lg N + 0.1101 \quad (12)$$

for sodium with a content of 2×10^{-3} % wt. oxyden and

$$\lg \varepsilon_a = - 0.2704 \lg N + 0.5406 \quad (13)$$

for sodium with 5 % NaOH.

The simultaneous effect of hydroxidized sodium medium and sing-variable load at 500 248 °C results in the formation of the region on the specimen surface where this medium interact with grain boundaries with a depth up to 425 μ. Microhardness in the corrosion region is slightly lower (160 - 190 kg/mm^2) than in the metal matrix (260-280 kg/mm^2) . The failure of steel occurs basically over the grain boundaries.

The reference specimens tested in pure sodium demonstrate no corrosion region. The increased etching region is observed on the specimen surface.

Thus, the impact of sodium containing 5% wt. hydroxide results in an essential reduction in cyclic strength at 500 °C. A less number of cycles-to-failure is due to increased corrosiveness of the medium with respect to the main components of steel during a tensile part of cycle. The corrosion products formed in the tensile phase are compound oxides, which act as a wedge at a compression stage. High concentrations of stresses emerge at the point of crack that causes its subsequent propagation and exposure of new surfaces subjected to corrosion.

Table 1

Chemical composition of steels, % wt.

	C	Cr	Mo	Mn	Nb	Ni	V	Si
10X9M	0.10	9.8	0.64	0.4	0.15	0.71	0.1	0.34
10X2M	0.10	2.25	0.70	0.62	-	0.09	-	0.37
10X18H9	0.08	18.3	-	1.3	0.2	8.9	-	0.38

Table 2

Steel corrosion rate in sodium flow, 10^{-5} mg/cm^{2}h

(cold trap temperature is 130 °C)

Temperature, °C	Time, hr	310X9MФБ	10X2M	08X18H9
510	4680		- 4.32	- 0.058
520	4324	- 0.58	- 4.64	
530	4590			-1.30

Table 3

10X2M steel corrosion rate in sodium with NaOH admixture and in NaOH melt.

Temperature °C	Content NaOH, %	K, 10_2 mg/cm^2h	K, 10_2 mg/cm^2h
400	100	- 5.5	-15.0
500	100	-19.1	- 38.6
520	2.6		- 0.21

Table 4

Stresses (MPa) causing failures in plane and tubular specimens of 10X18H9 steel in 5 % NaOH sodium medium at 500 °C for equal time periods.

Form of specimen	Thickness of specimen, mm	Time - to - failure, h					
		105	205	340	370	500	640
Tubular	0.25			190	201	160.8	115
	0.30	206	198		158		
Flat +	1.0	-	1.3	0.2	8.9	-	0.38

+ Calculated data on dependence (7)

References

1. F.A. Kozlov, Yu. I. Zagorulko et al.
Solubility of individual substances in sodium. IPPE - 510.
Obninsk, 1974.

2. Balandin Yu.F., Malygin A.F.
Cyclic strength of 0X18H9 steel in sodium at 550 xC. Phys.-chem.
mechanics of materials, 1979, v.8 N5.

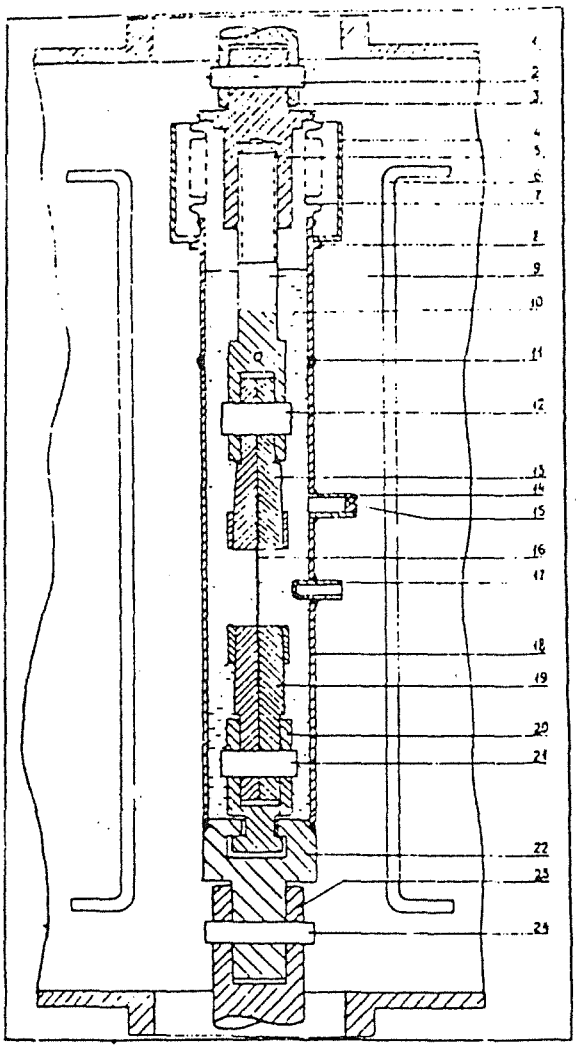

Fig. 1. System for long-term strength tests of materials in sodium containing impurities at 500 °C:

1 - vacuum furnace of the system; 2 - stud; 3 - prism adapter; 4 - screen; 5 - top sleeve of bellow; 6 - heater; 7 - bellow HC-52-17-0.16; 8 - lower sleeve of bellow; 9 - top grip adapter; 10 - sodium; 11 - compensating ring; 12 - studs; 13 - top grip; 14 - tube; 15 - plug; 16 - specimen; 17 - thermocouple jacket; 18 - functional housing; 19 - bottom grip; 20 - bottom grip adapter; 21 - stud; 22 - bottom of housing; 23 - adapter forB-3012M loading mashine mechanism bar; 24 - stud.

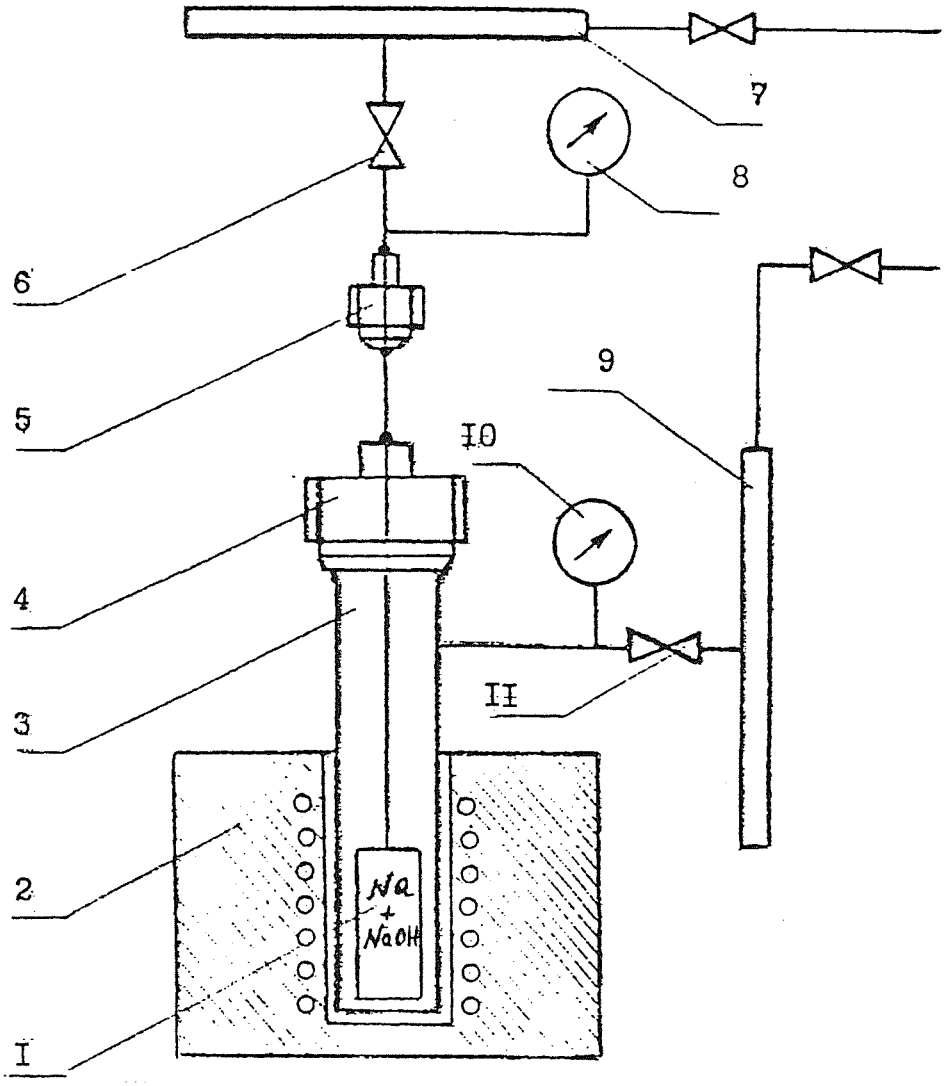

1. Рабочий образец.
2. Электрическая печь.
3. Металлический стакан.
4. Разъёмное соединение шар по конусу.
5. Разъёмное соединение с прокладкой.
6. Газовый вентиль.
7. Газовакуумная линия высокого давления.
8. Манометр.
9. Газовакуумная линия низкого давления.
10. Манометр.
11. Газовый вентиль.

Рис.2. Схема установки для испытаний сталей под напряжением.

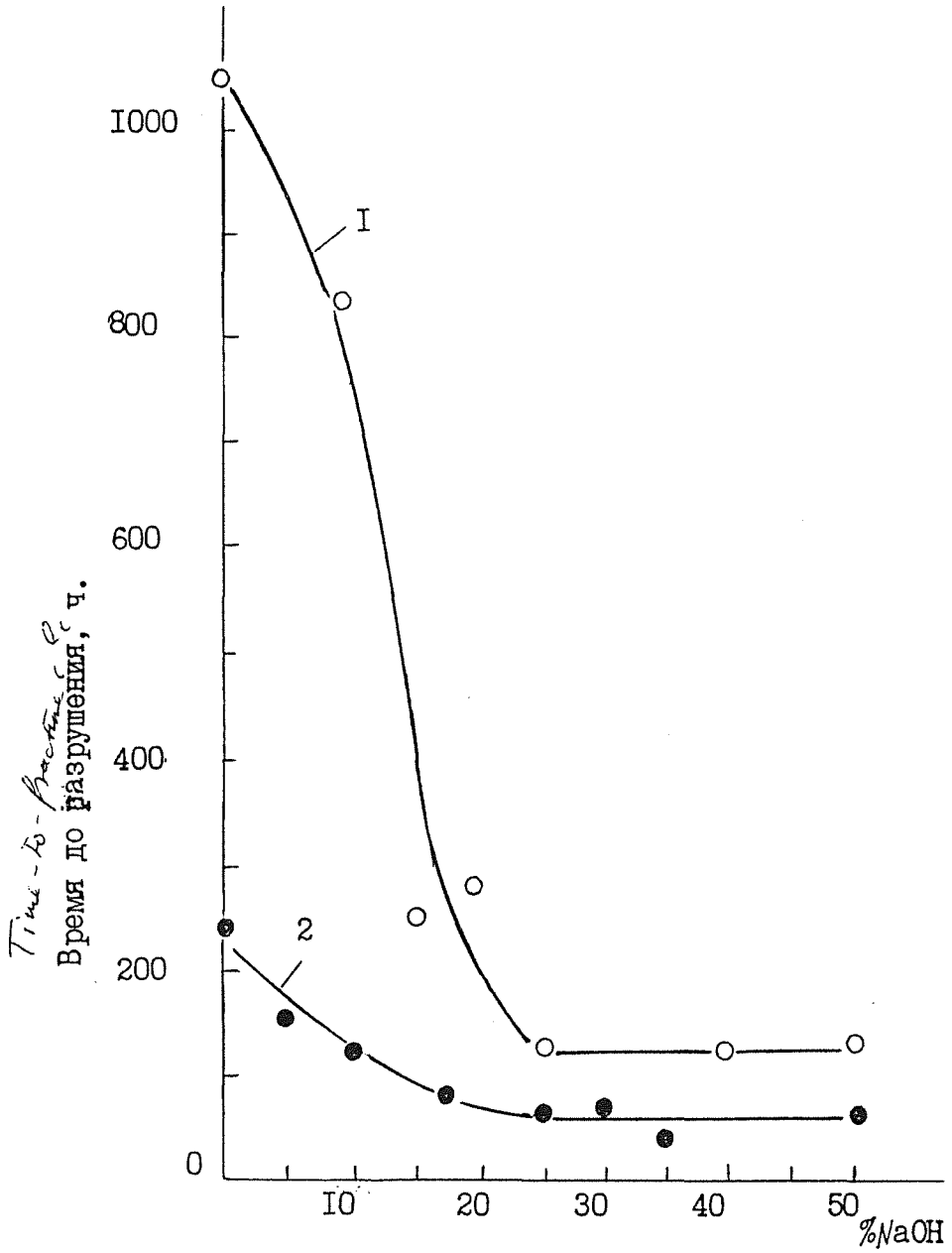

Fig. 3. Dependence of X9M steel tubular specimen time-to-failure on NaOH concentration in sodium at 650 °C, σ = 105 MPa (1) and 700 °C, σ = 57.5 MPa (2)

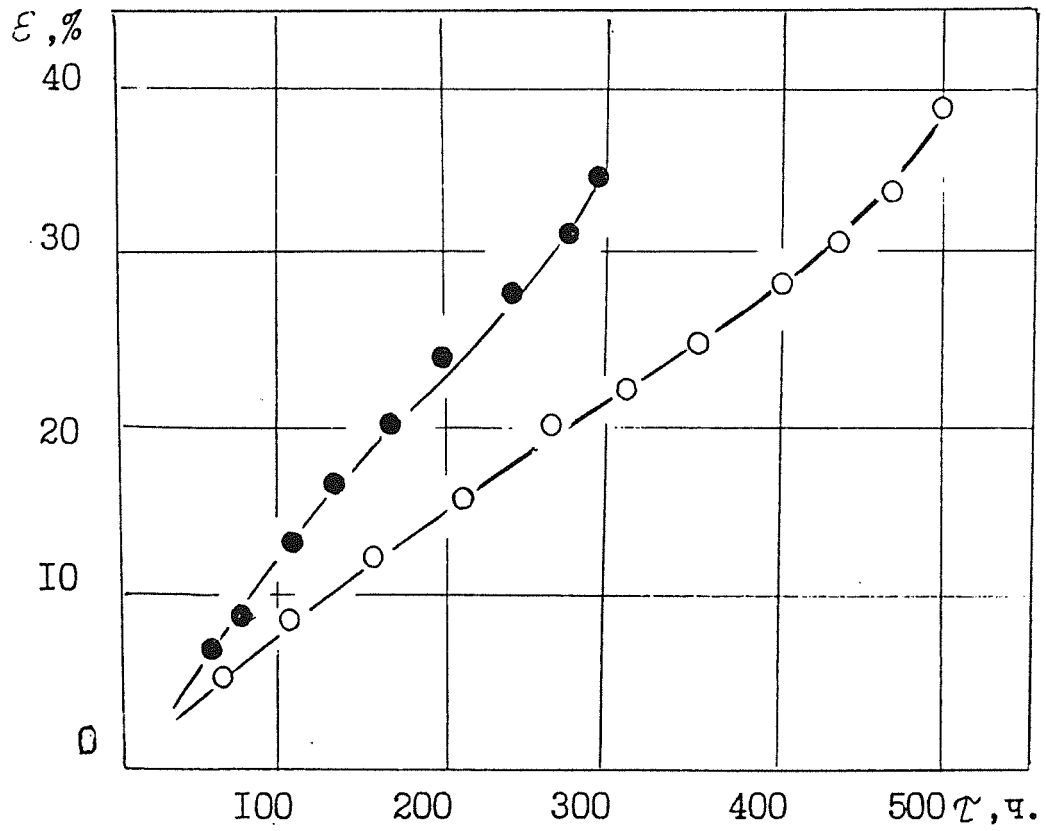

Fig. 4. Curves of 10X18H9 steel creepage at 500 °C in pure sodium (∘) and sodium with 5 % NaOH (•) at σ = 230 MPa.

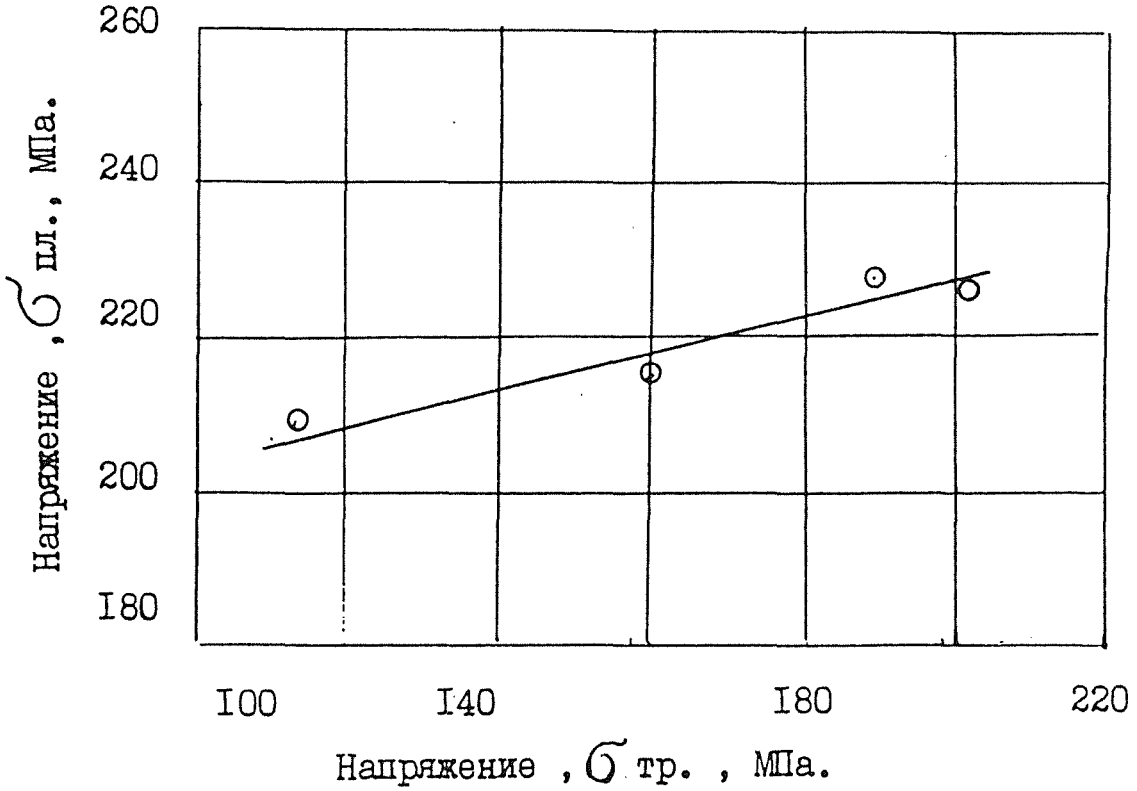

Fig.5. Correlation of stresses causing plane (σ_{pl}) and tubular (σ_{tub}) specimen failure for the same periods of times when tested in sodium with 5 % NaOH at 500 240 °C.

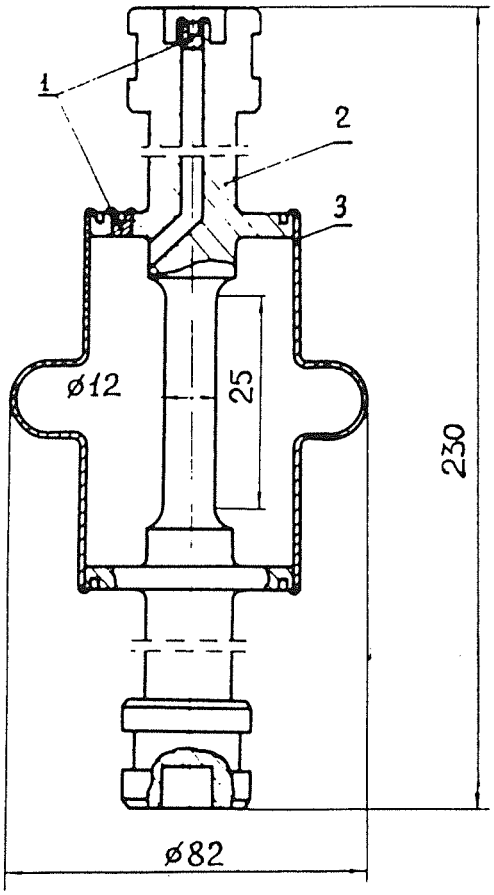

Fig.6. Diagram for material cyclic strength test in sodium containing hydroxide:

1 - plug; 2 - specimen; 3 - shround.

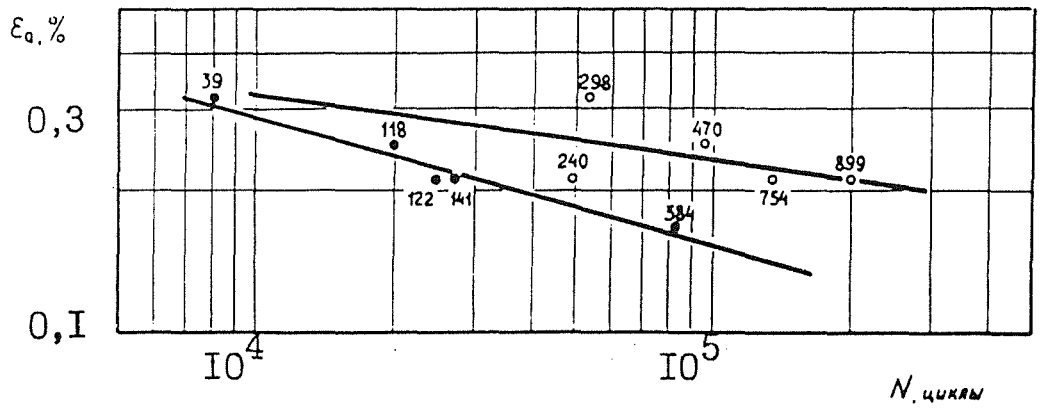

Fig.7. Dependence of the number of cycles-to failure (N) on the values of deformation amplitude (εa) for 10X18H9 steel at 773 °K for test in pure sodium (∘) and sodium with 5 mass % hydroxide (•). The digits at points stand for test time in hours.

Salient Features and a few Results from the Sodium Loops Designed at Indira Gandhi Centre for Atomic Research for Metallurgical Investigations

S. Venugopal, H.S. Khatak, S. Gopal, M.P. Mishra, S.L. Mannan and J.B. Gnanamoorthy

Metallurgy Programme
Indira Gandhi Centre for Atomic Research
Kalpakkam, 603103, India

ABSTRACT

Sodium loops have been designed and built at Indira Gandhi Centre for Atomic Research, Kalpakkam for metallurgical investigations. The design features and the details of the various components of the loops are discussed in this paper. The results of in-sodium tests carried out on austenitic stainless steels have also been discussed.

1.0. INTRODUCTION

Liquid sodium is preferred as a coolant in fast reactors because of its good heat transfer properties. Although it possesses many favourable properties, its use as a coolant introduces a number of problems of material integrity associated with corrosion and mass transport of alloying elements. The transfer of interstitial alloying elements such as C, N, B, etc., poses problems in both primary and secondary sodium circuits of breeder reactors. Transfer of these elements occurs due to activity gradient in the system. In a system built up of stainless steel of one type, carbon is known to be transported from the high to the low temperature regions. In a circuit composed of a ferritic steel and an austenitic stainless steel, transfer of carbon may occur from the former to the latter. Resultant carburisation or decarburization affects the mechanical properties of the materials drastically.

The mechanical behaviour and the mechanical properties of common reactor materials have been studied by many researchers [1 - 23]. A review of the available data by Mannan and Sandya [24] indicate that :

1. Reactor materials such as stainless steel type AISI 316 and 9Cr-1Mo steel do not exhibit inferior creep, fatigue and creep - fatigue interaction behaviour when tested in a high purity sodium environment.

2. Materials such as stainless steel type AISI 304 and 2.25Cr-1Mo are reported to exhibit inferior creep rupture behaviour due to the phenomenon of tertiary creep embrittlement.

3. The purity of sodium, material of construction of the loop and various other factors such as operating temperature, oxygen content, sodium velocity, etc., determine the mass transfer in sodium circuits and thus have a significant effect on the long term mechanical properties.

Since the purity of the flowing sodium and the sodium circuit materials determine the mass transfer and the degradation of the materials, the data generated in one laboratory differ from those of the other. Hence, there is need to generate information on specific materials chosen for the proposed Prototype Fast Breeder Reactor (PFBR) in anticipated sodium chemistry. To wards this goal, the following facilities are being built/operated in the Metallurgy and Materials Programme of the Indira Gandhi Centre for Atomic Research (IGCAR), Kalpakkam :

1. Facilities for Materials Testing in Flowing Sodium (INSOT Project).
2. Mass Transfer Loop (MTL).
3. Trimetallic Sodium Loop (TRIM).
4. Thermal Convection Loop (TCL).
5. Dummy Fuel Pin Test Rig (DFPR).

The salient features of the above loops and the results obtained in the Thermal Convection and Dummy Fuel Pin Rig loops will be discussed in this paper.

2.0. FACILITIES FOR MATERIALS TESTING IN SODIUM

Two sodium loops have been planned to be built for creep, fatigue and creep - fatigue interaction studies in flowing sodium. The facility would help in screening candidate materials for applications in the Prototype Fast Breeder Reactor for deciding on the choice of the heat treatments on chosen materials and their welds and for providing the much needed information to the designer in the areas where sufficient data are not available.

2.1. Salient Features of the Facility

The facility consists of two loops. One of the loops has six test sections for creep testing machines and the other three test sections for low cycle fatigue testing machines. Additionally, an experimental set-up for thermal stripping studies will be housed in the fatigue test loop. Two separate loops for creep and fatigue studies are planned, since the creep rupture tests are long time tests and the fatigue tests are of relatively short durations. Separate loops will ensure efficient running of the tests. Fig. 1 gives the schematic of creep test loop. Each loop would be housed in an area of about 6 m X 6 m and a height of about 12 m. It is planned to install six creep testing machines in creep test loop and three servohydraulic testing machines for fatigue testing in the fatigue test loop.

A centralised computer based control and data logging system will be used in this facility. Mimic diagrams will be installed in the control room for starting, filling, pre-heating and controlling the loop. The loops can be operated automatically after the start-up.

The components and piping of the loop are of nuclear grade stainless steel of AISI type 316 LN similar to the composition proposed for Prototype Fast Breeder Reactor. The sodium will be stored in tanks kept underground. The maximum temperature and velocity of sodium in the test sections will be 923 K and 3 m/s respectively. The maximum temperature in foil equilibration set-up and carbon meter will be 973 K. The design pressure is 6 bars. Argon will be used as cover gas and

the oxygen content of the sodium will be maintained at less than 10 ppm. The main circuit of each loop is branched into two lines, one for purification and the other for test sections and pre-corrosion chamber. The maximum temperature in the purification line will be 623 K. The purification circuit consists of a cold trap for sodium cleaning, a meter for oxygen measurement and a sampler for sodium sampling.

2.2. Important Components

2.2.1. Electromagnetic pumps :

The main pump has a flow capacity of 5 m^3/h capacity at 4.5 bars. Each test section has a booster pump of 2 m^3/h capacity at 2 bars. The pumps for the loops will be designed and built at the Indira Gandhi Centre for Atomic Research.

2.2.2. Heat exchangers :

Each test section consists of one heat exchanger. Economisers will be installed in carbon meter, foil equilibration, cold trap and oxygen meter lines. The heat exchangers and economisers are of single pass counter current shell-and-tube type.

2.2.3. Electrical heaters :

Each test section is provided with a heater chamber equipped with immersion heaters of total heating capacity of 36 kW. The oxygen meter and carbon meter are equipped with heaters of smaller capacities. The pipe lines, dump tank, expansion tank, etc., are wound with surface heater tapes to maintain the temperature of flowing sodium at the desired level.

2.2.4. Degassing chamber :

Degassing chambers are incorporated in between the test section and inlet of the secondary line of the heat exchanger to provide for a head and for the escape of gas bubbles to the expansion tank. The sodium velocity will be sufficiently slow so that gas bubbles can escape to the expansion tank.

2.2.5. Sodium air cooler :

The sodium temperature at the exit of the heat exchanger will be about 643 K. The sodium after leaving the heat exchanger will be cooled in air cooler. The sodium will be flowing inside finned tubes and air blast will be blown on the finned areas of the tubes. The air flow will be regulated to keep the sodium temperature at the desired level.

2.2.6. Sodium dump tank :

At the deepest point of the loop a dump tank is installed in an underground pit of 2 m X 2 m X 2 m size. The volume of the dump tank is 0.5 m^3. The tank will be initially filled with about 450 litres of liquid sodium. Approximately 300 litres of sodium is required to fill up the whole loop and the remaining quantity of 150 litres will be kept in the tank. The temperature of the sodium in the dump tank will be maintained at 473 K.

2.2.7. Expansion tank :

At the highest point of the, a vertically mounted expansion tank with a volume of 300 litres will be provided. During the operation of the loop the expansion tank will be half filled. The temperature of the sodium in the expansion tank will be maintained at 473 K. The lines from the degassing chambers are connected to the bottom of the expansion tank. Dump and expansion tanks are also connected by fill line for maintaining the sodium level.

2.2.8. Pre-corrosion chamber :

The specimens, which are to be tested for low cycle studies will be exposed to sodium in the pre-chamber. The chamber will accommodate 20 test samples at a time.

Foil equilibration chamber and carbon meter are incorporated in the loop to measure the carbon content by two different methods i.e., equilibration and electrochemical. Oxygen meter is also incorporated to measure the oxygen level in sodium. In addition to the above units, sodium filter, cold trap, sodium sampler, level probes are also incorporated in the loops.

2.2.9. Fire and safety systems :

Electrical leak detectors and smoke detectors are provided at the critical points in the loop. The temperature, velocity, level of sodium and argon pressure will be monitored and controlled at set levels. The electrical heating circuits are secured against high earth leakage current with the help of earth leakage circuit breakers. If the fault current of an electrical heater becomes more than 0.5 A the power will be switch off immediately, thus preventing the risk of shocks to the operators.

2.2.10. Current status of the project :

The design of the components has been completed and the fabrication activities have been initiated. The civil and electrical works are nearing completion. The design of electromagnetic pumps has been taken up. The loops are expected to be commissioned by the middle of 1993.

3.0 MASS TRANSFER LOOP

A mass transfer loop has been built to study the transfer of metallic/non-metallic elements from one region to the other within a monometallic dynamic sodium loop and the resulting influence of mass transfer on the tensile and impact properties. The schematic of the loop is given in Fig. 2. The loop consists of two parts : (a) the main loop and (b) the purification loop. The main loop consists of two electromagnetic pumps, three heater units, three air coolers, six sample holders and an expansion tank. The purification loop consists of cold trap economiser, cold trap, plugging indicator economiser, plugging indicator and nickel tube sodium sampler. The sodium has been filled in a loop through microfilter. The total sodium inventory in the loop is about 140 kg. The temperature of sodium at the outlet of heater-1, heater-2 and heater-3 are being maintained at 623 K, 723 K and 823 K respectively and the sodium is being cooled down to 723 K, 623 K and 523 K in cooler-1, cooler-2 and cooler-3 respectively. Six specimen holders with stainless steel specimens are being exposed to hot liquid sodium at the above mentioned temperatures. The material

used for the construction of this loop is stainless steel AISI type 316. The temperature, level and flow rate of sodium are being monitored and controlled in the loop. The loop has been operated for a total period of 5000 hours so far.

4.0 TRIMETALLIC SODIUM LOOP

A trimetallic sodium loop, made up of stainless steel AISI type 316 LN, 9Cr-1Mo and 2.25Cr-1Mo steels will simulate the conditions of the secondary sodium circuit of proposed PFBR with regard to material sequence, temperature gradient, sodium velocities, surface area ratio of the materials, etc.. The main aim of this loop is to study long term carburization/decarburization behaviour and resulting influence on tensile, impact and fatigue properties of the three materials mentioned above. The conceptual design of the loop is given in Fig. 3. The sodium inventory is about 200 litres. Six test sections will be provided in which pre-fabricated samples will be exposed to sodium. The sodium velocity in the test sections is controlled by electromagnetic pumps. The direction of flow of sodium and material sequence are shown in Fig. 3. The inlet and outlet temperature conditions of the secondary sodium side of the intermediate heat exchanger are simulated in the test sections No. 1 and 2 with electrical immersion heaters. The inlet and outlet process conditions of the super heater are simulated in test sections 3 and 4. The process conditions of the evaporator are simulated in the test sections No. 5 and 6. The loop is equipped with purification system and a carbon meter. The loop is provided with instrumentation and control systems for operation and safety. This loop is also expected to be commissioned by the middle of 1993.

5.0 THERMAL CONVECTION LOOP

The schematic of the loop is given in Fig. 4. The hot leg was heated by a resistance heater to a maximum temperature of 723 K. The cold leg is naturally cooled to maintain a temperature gradient of 80 K. The sodium inventory in this loop was 3.5 litres and the calculated flow velocity was 27 cm/s. The samples were exposed to flowing sodium in the sections where the temperatures were 643 K, 683 K and 723 K. The material of construction of the loop was stainless steel AISI type 316.

Flat tensile test samples of solution annealed and 20 % cold worked stainless steel of AISI type 316 were exposed to flowing sodium in this loop. The samples were taken out after 10500 hours of exposure and room temperature tensile tests were conducted. The results of the tests are presented in Figs. 5 and 6 along with the data on unexposed samples. The yield strength (YS) and the ultimate tensile strength (UTS) are higher for the exposed samples than those of unexposed samples. The reduction in area (RA), uniform elongation (UE) and total elongation (TE) are lower than those of unexposed samples and dependent on the temperature of exposure. The fractographic observations on the samples exposed at 723 K revealed that the fractures were intergranular in nature. The samples exposed at lower temperatures showed predominantly ductile dimple fracture. This behaviour could be due to the effects of ageing and carburization. The intergranular mode of fracture observed in the central region of the fractured samples exposed at 723 K indicates that the thermal ageing

has also influenced the properties in addition to the effect of carburization. Chemical analysis of 0.1 mm thick foil exposed at 723 K showed an increase in the carbon content from 0.054 % to 0.08 %. This confirmed that carbon transfer had taken place from sodium to steel.

The results of tensile tests on cold worked material are shown in Fig. 7 and 8. The effect is opposite to that observed for solution annealed material i.e. reduction in YS and UTS and enhancement in UE and TE. However, loss in RA has not been found in sodium exposed cold worked samples. At higher temperatures of exposure loss in YS and UTS and improvement in elongation was minimum whereas decrease in RA was maximum. Fractographic observations showed ductile fracture at all the temperatures of exposure. The observed effects could partly be attributed to stress relief and recovery effects in addition to carburization and ageing. The trend is similar to that observed in the case of solution annealed material. Experimental procedure and results are discussed in detail elsewhere [23].

6.0 DUMMY FUEL PIN TEST RIG

The schematic of the rig is shown in Fig. 9. It has been fabricated from stainless steel AISI type 304. The rig was filled with commercial grade sodium through a 5 μm stainless steel filter at 443 K. The temperature of the sodium was raised to and maintained at 723 $\pm$ 10 K. The flow rate of sodium in the test section is maintained at 2.85 m^3/h which will give a velocity of 4.5 m/s in the test sections. This rig has been built by the Engineering Development Division of IGCAR and used to study the influence of sodium on tensile properties.

Tensile test samples of stainless steel of AISI type 316 in solution annealed and welded conditions were exposed to sodium in this loop for 5,500 hours. The weldments prepared by TIG process had been machined in such a way that the weld was at the centre of the sample. The tensile test results are presented in Table 1. The YS is found to increase by 20 % compared to that of unexposed sample. There is no significant change in UTS and elongation with reference to unexposed sample. The increase in YS is in conformity with increase in hardness near the surface (Fig. 10) which is due to carburization effects of sodium. The influence of sodium on the weld metal is similar to that on the base metal.

7.0 SUMMARY

The degradation of mechanical properties of materials on exposure to sodium is dependent on many parameters such as temperature, purity and velocity of sodium and chemical composition / sequence of loop materials. Hence the properties of the materials should be evaluated under the appropriate conditions envisaged in the reactors. With this in view sodium loops have been / are being designed and built at Indira Gandhi Centre for Atomic Research for metallurgical investigations. The design features and the detail of components are discussed. The inferences from the investigations carried out on the exposed materials have also been indicated.

ACKNOWLEDGEMENTS

The authors are grateful to Dr. Placid Rodriguez, Head, Metallurgy and Materials Programme, Indira Gandhi Centre for Atomic Research, Kalpakkam for his guidance and encouragement. Thanks are also due to Dr. H.U. Borgstedt of KfK, Karlsruhe for useful discussions and comments during various stages of INSOT project as well as some of the loop tests. Contributions from engineers of the Engineering Development Division and Nuclear System Division towards the design, construction and operation of the facilities are also gratefully acknowledged.

REFERENCES

[1] H. Huthmann and H.U. Borgstedt,
Proc. of IV Int. Conf. on Liquid Metal Engineering and Technology, 12-17 October 1988, Avignon, France, Paper 510.

[2] H. Bohm and H. Schneider,
J. Nucl. Materials, 24 (1976) 188.

[3] W.J. Anderson et.al.,
Mechanical Properties of Stainless Steels in Sodium and Application to LMFBR Design, AI-AIC-1300, Atomics International, 1972.

[4] G.P. Dykova and V.I. Nikitin,
Zhidkiye Metally Sbornik Statey, 1963, p. 292.

[5] R.S. Fidler,
Proc. of II Int. Conf. on Liquid Metal Technology in Energy Production, 1980, Paper 19-18.

[6] E. te. Heesen and E.D. Grosser,
Proc. of Int. Conf. on Materials for Nuclear Steam Generators, Gatlinburg, Tenn., 1975.

[7] C.A.P. Horton and B.H. Targett,
Proc. of IV Int. Conf. on Liquid Metal Engineering and Technology, 12-17 October 1988, Avignon, France, Paper 513.

[8] H.U. Borgstedt, G. Frees and G. Drechsler,
Res. Mechanica 25 (1988) 71.

[9] R.S. Fidler and M.J. Collins,
Atomic Energy Review, March 1975, p. 3.

[10] D.S. Wood, D.H.C. Prince and J. Wynm,
Proc. of IWGFR Specialists Meeting on Properties of Primary Circuit Structural Materials Including Environmental Effects, 10-14 October, Chester, England, P. 673.

[11] C.A.P. Horton, R.S. Fidler and B.H. Targett,
Proc. of III Int. Conf. on Liquid Metal Engineering and Technology, 9-13 April, 1984, Oxford, Paper 196.

[12] C. Phaniraj, B. Seith, G. Drechsler and H.U. Borgstedt,
PSB, October, 1987, KfK, FRG.

[13] K. Natesan, O.K. Chopra and T.F. Kassner,
Proc. of II Int. Conf. on Liquid Metal Technology in Energy Production, 1980, Paper 19-41.

[14] H.U. Borgstedt and H. Huthmann,
Proc. of IV Int. Conf. on Liquid Metal Engineering and Technology, 12-17 October 1988, Avignon, France, Paper 509.

[15] T. Aruyama, S. Kato, R. Lomine, M. Hirano, Y. Wada, S. Kano and I. Nihei, ibid., Paper 512.

[16] K. Natesan, O.K. Chopra and T.F. Kassner,
Proc. of II Int. Conf. on Liquid Metal Technology in Energy Production, 1980, Paper 19-41.

[17] D.S. Wood,
PNC/CEA-ENEA-DEBENE Exchange Meeting with UKAEA Participation, Paper E.I.

[18] D.S. Wood and A.B. Waldwin,
Proc. of III Int. Conf. on Liquid Metal Engineering and Technology, 9-13 April, 1984, Oxford, Paper 195.

[19] M. Hirano, K. Kitao, I. Nihei and A. Yoshiteshi,
ibid, Paper 201.

[20] O.K. Chopra, K. Natesan and T.F. Kassner,
Proc. of II Int. Conf. on Liquid Metal Technology in Energy Production, 1980, Paper 19-9.

[21] H.S. Khatak, B. Seith, G. Frees, G. Drechsler and H.U. Borgstedt,
Trans. IIM, Vol. 42 (Supplement), 1989-S235, TPCF9.

[22] H.U. Borgstedt, G. Drechsler, G. Frees, H.S. Khatak, Z. Peric and B. Seith,
Int. J. Fracture, 32, R23-R28 (1986).

[23] H.S. Khatak, H. Shaikh and J.B. Gnanamoorthy,
Proc. of IV Int. Conf. on Liquid Metal Engineering and Technology, Avignon, France, 17-21 October, 1988, Paper No. 514.

[24] S.L. Mannan and R. Sandya,
"An Assessment of the Influence of Sodium on Elevated Temperature Mechanical Properties of FBR Materials", Materials Development Division Report No. MDD/71.4/89/1.

Table I : Tensile properties of stainless steel AISI 316 and its weldments before and after exposure to sodium, tested at a strain rate of 6.6×10^{-4} S^{-1}.

S.No.	Specimen condition	YS (MPa)	UTS (MPa)	UE (%)	TE (%)
1	Base metal (unexposed)	265	633	53	60
2	Base metal (exposed)	313	632	45	57
3	TIG Weldments (unexposed)	281	588	28	33
4	TIG Weldments (exposed)	332	591	26	28

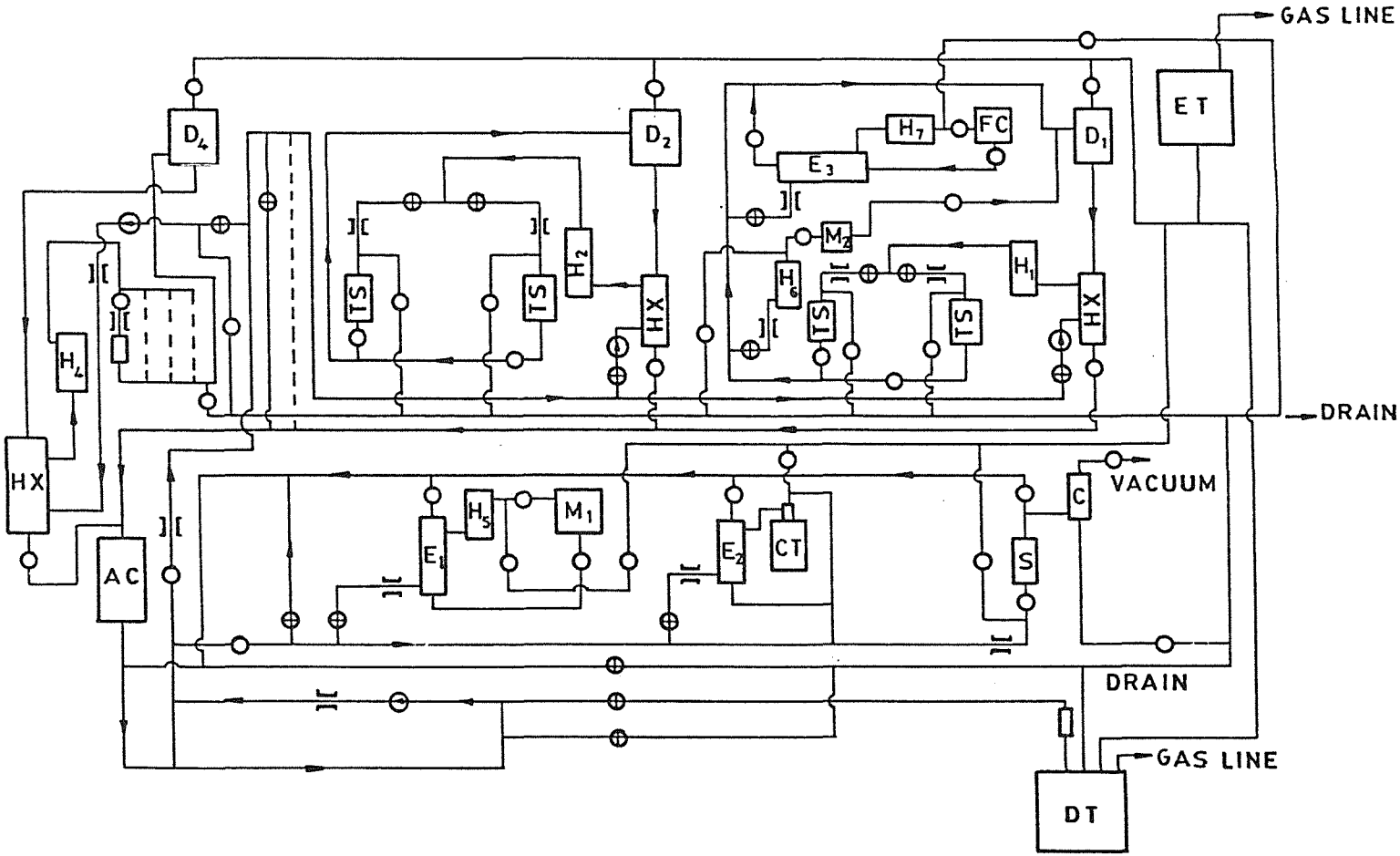

1. DT - DUMP TANK
2. ET - EXPANSION TANK
3. HX - HEAT EXCHANGER
4. AC - AIR COOLER
5. TS - TEST SECTION
6. FC - FOIL CHAMER
7. CT - COLD TRAP
8. H_1-H_7 - HEATERS
9. E_1-E_3 - ECONOMISERS
10. M_1-O_2 METER
11. M_2 - CARBON METER
12. S - SAMPLER

⊕ E.M. PUMP
][FLOWMETER
⊕ MOTORISED VALVE
○ MECHANICAL VALVE

Fig. 1 Creep Loop of INSOT project

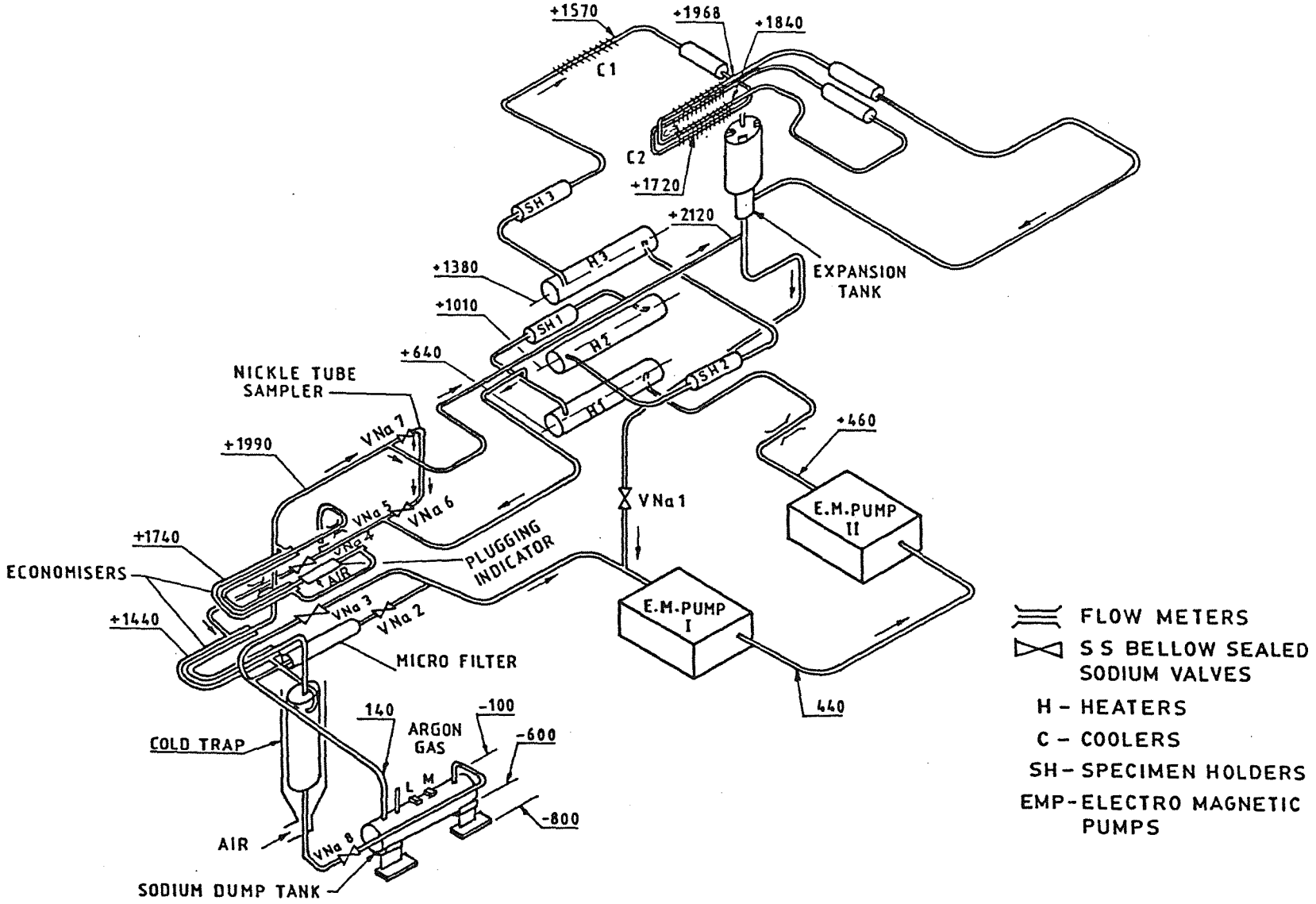

Fig. 2 Mass Transfer Loop layout

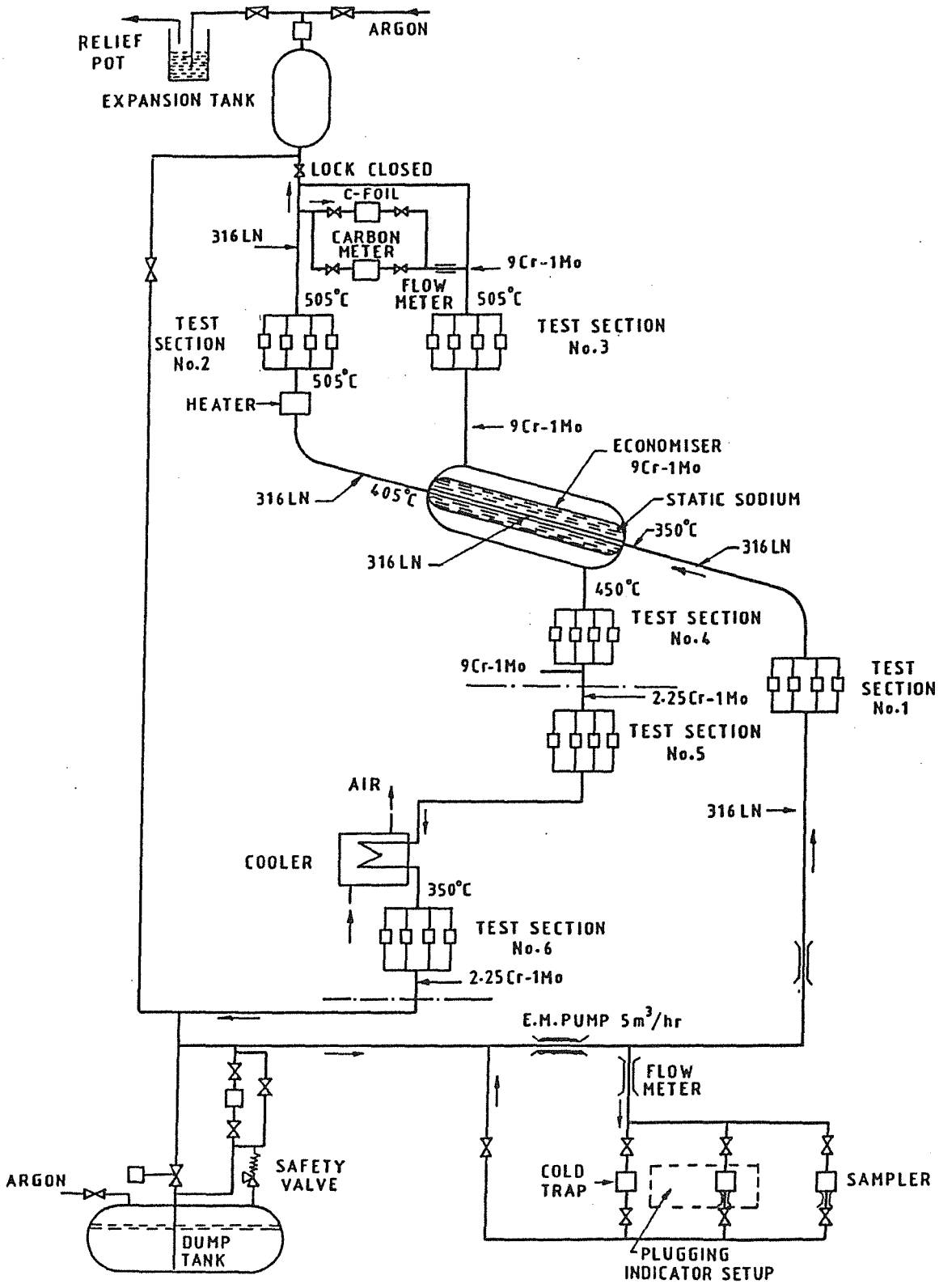

Fig. 3 Trimetallic Sodium Loop (TRIM)

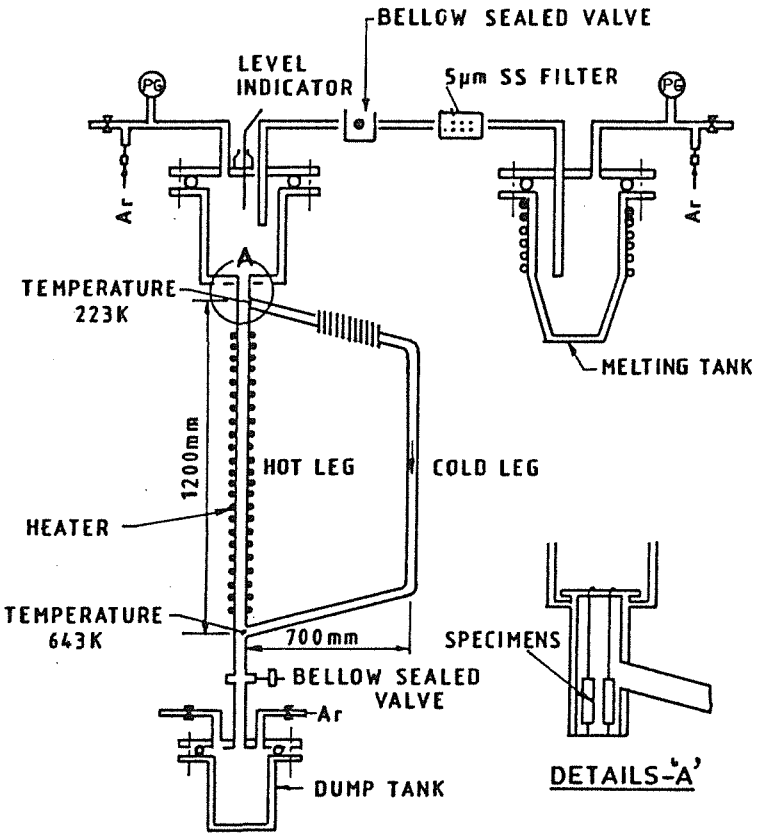

Fig. 4 Thermal Convection Loop (Schematic)

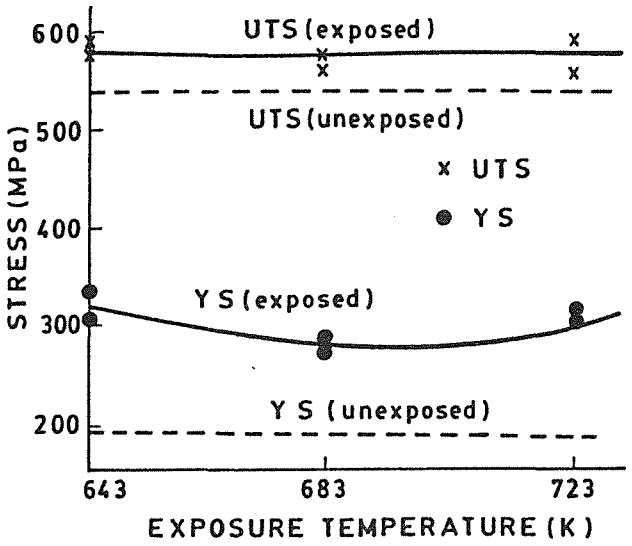

Fig. 5 Influence of sodium exposure (10,500 hours) on room temperature YS and UTS of solution annealed AISI 316 stainless steel with respect to temperature of exposure in thermal convection loop. Strain rate used : 5.5 X 10^{-4} s^{-1}

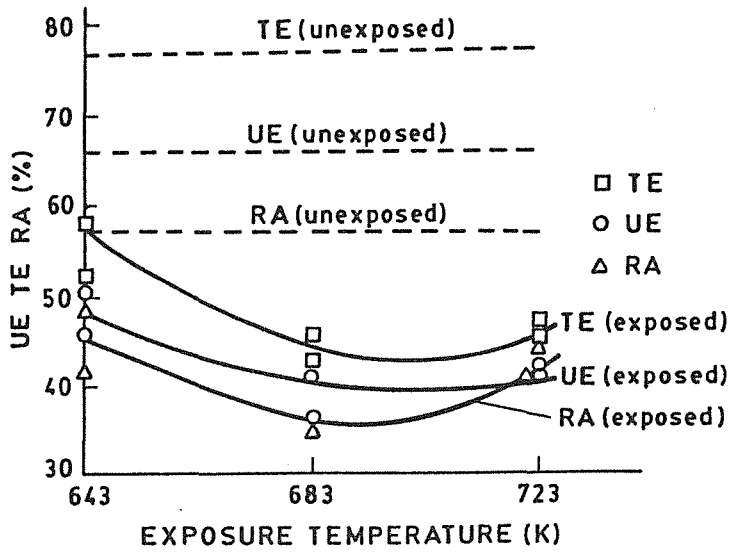

Fig. 6 Influence of sodium exposure (10,500 hours) on room temperature UE, TE and RA of solution annealed AISI 316 stainless steel with respect to temperature of exposure in thermal convection loop. Strain rate used : 5.5 X 10^{-4} s^{-1}

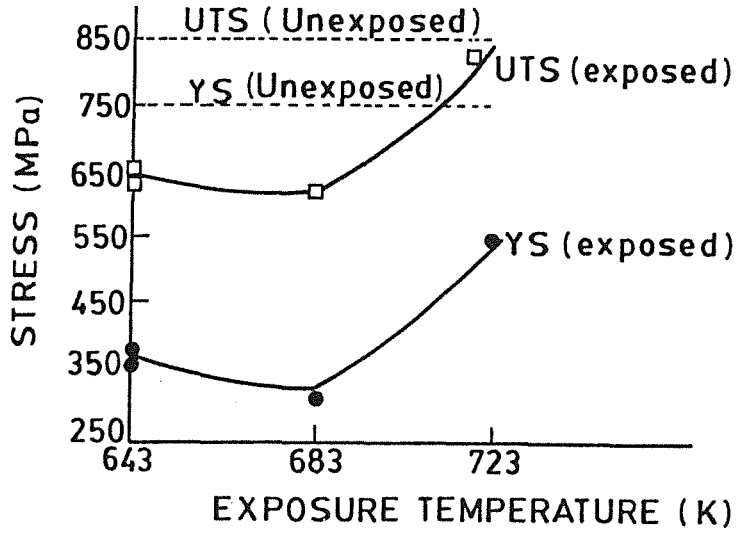

Fig. 7 Influence of sodium exposure (10,500 hours) on room temperature YS and UTS of 20 % cold rolled AISI 316 stainless steel with respect to temperature of exposure in thermal convection loop. Strain rate used : 5.5 X 10^{-4} s^{-1}

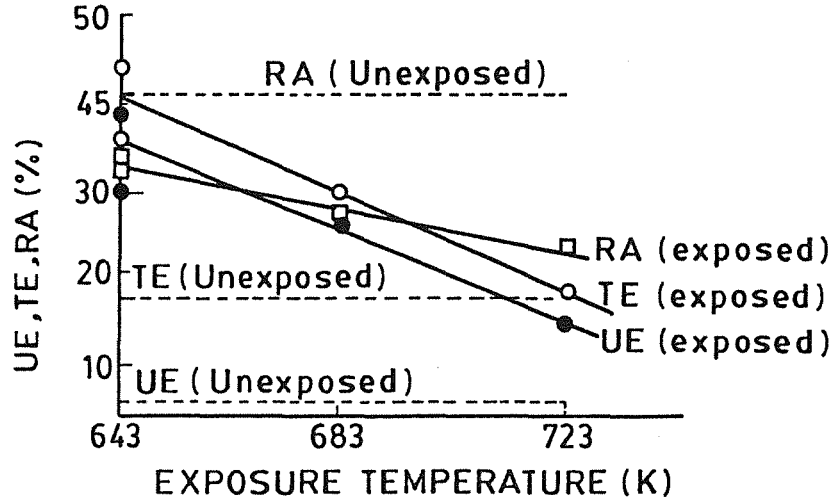

Fig. 8 Influence of sodium exposure (10,500 hours) on room temperature UE, TE and RA of 20 % cold rolled AISI 316 stainless steel with respect to temperature of exposure in thermal convection loop. Strain rate used : 5.5 X 10^{-4} s^{-1}

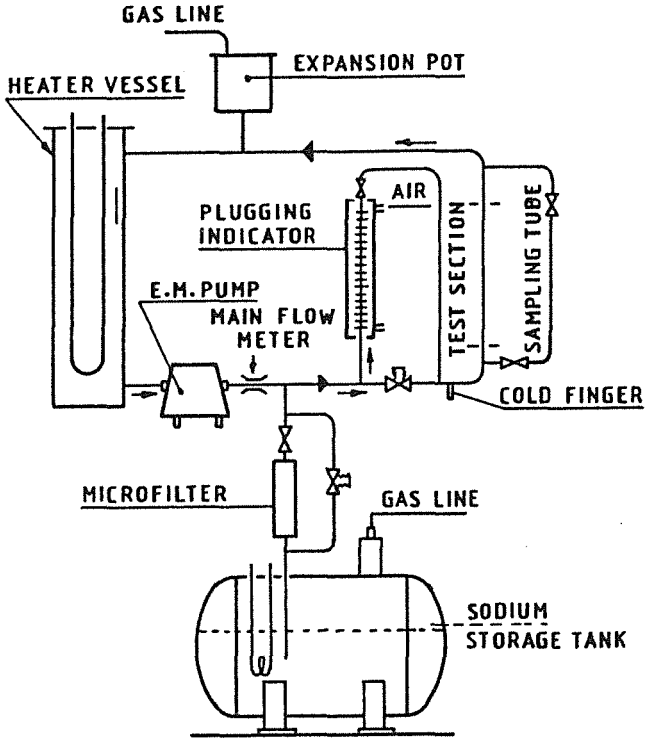

Fig. 9 Dummy Fuel Pin Test Rig (Schematic)

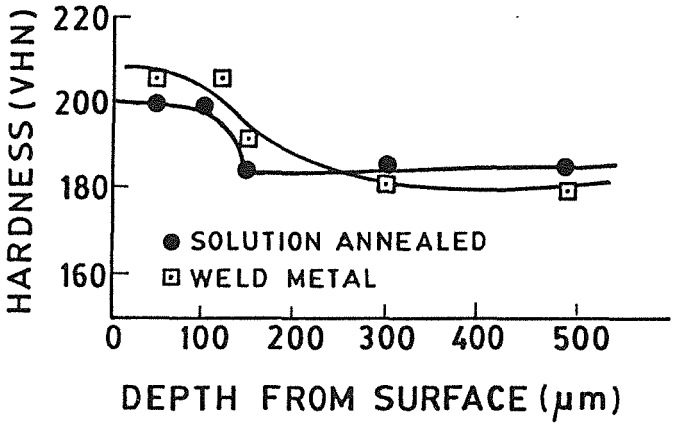

Fig. 10 Hardness depth profile after sodium exposure (5,500 hours) of AISI 316 base metal and its weldments at 773 K

THE INFLUENCE OF DECARBURIZING SODIUM ON THE CREEP-RUPTURE BEHAVIOUR OF TYPE 304 STAINLESS STEEL

H.U. Borgstedt *, G. Frees * and H. Huthmann **

* Kernforschungszentrum Karlsruhe GmbH.
Institut für Material- und Festkörperforschung II
Postfach 3640, D - 7500 Karlsruhe

** INTERATOM GmbH.
Friedrich-Ebert-Str.
D - 5060 Bergisch Gladbach 1

Abstract

The influence of flowing liquid sodium at 550°C on the creep-rupture behaviour of the structural material of the SNR 300 reactor, X6CrNi18 11 (DIN 1.4948, equivalent to Type 304 ss) was studied in two non-isothermal sodium loops. It was shown that the effects of sodium are dependent on the carbon activity of the sodium. Under normal (non-decarburizing) sodium conditions a limited reduction of times-to-rupture occurs. This reduction is due to a reduced ductility within the tertiary creep range. The minimum creep rate and the onset of tertiary creep are not influenced.
Under decarburizing conditions which are not expected to occur in the sodium of LMFBR's, an additional loss of creep strength was observed. The steel showed higher creep rates and an earlier onset of tertiary creep. This additional effect seems to be caused by sodium corrosion of surface near layers reducing the unaffected cross section. It depends on the surface-to-volume ratio, and it was nearly suppressed, when specimens with larger diameter were used.

1. Introduction

The use of liquid sodium as a coolant for fast reactors requires the knowledge of the long - term mechanical properties of structural materials in flowing liquid metal.
The material losses of steels due to sodium corrosion are negligible at temperatures up to 550 °C even in fast flowing sodium, some leaching of austenite stabilizing elements may, however, occur, and the exchange of nonmetallic elements like carbon and nitrogen may cause changes in mechanical properties since these elements are important for the mechanical strength of steel. The sodium environment is a reducing one, in which oxygen partial pressures are below the stability of iron - chromium spinells which form the passivation layers of the steels. All these physico - chemical parameters may influence the long - term behaviour of the structural materials of a fast breeding reactor.

Therefore, uniaxial creep - rupture tests were performed on base material, welded joints and heat - affected - zone (HAZ) material of X6 CrNi 18 11- steel (DIN 1.4948, equivalent to type 304 SS) in air and in the non - isothermal sodium loops at Interatom and KfK, including in - sodium tests up to 18 000 hours.
This paper gives a review of these tests and the results of metallographic post test examinations gained within the program.

2. Experimental Conditions

2.1 Materials and Test Facilities

The creep rupture tests were performed on cylindrical specimens with a diameter of 4 mm, which were fabricated perpendicular to the rolling direction. The specimens were tested in the solution annealed condition. To demonstrate the effect of thickness some specimens with 6 mm diameter were also used. The geometry of the specimens is given in Fig. 1a.
The characteristic data of the tested materials are listed in Table 1. The specimens for the welded joints were taken from the central parts of two 20 mm thick plates, as shown in Fig.1b. The chemical composition of the filler material is given in Table 1.
For testing HAZ - material some specimens were machined from bars with 20 mm diameter which have been heat treated; simulating a welding procedure according to preliminary rules of the Kerntechnischer Ausschuß was simulated.
The creep - rupture tests were conducted under constant load in conventional creep machines, which were connected to the sodium loops at Interatom and KfK. In all facilities the strain was continuously measured outside the test cell at the loading bars [1,2]. The equipment was thermally equilibrated before the starting of tests, strain and stress probes were crosschecked and compared to the equipment working in the normal atmosphere. The temperatures were measured by thermocouples, which were immersed in the sodium close to the specimen.

2.2 Sodium Loops

In order to provide the representative sodium conditions of a LMFBR, the tests were performed in non - isothermal, pumped sodium loops, providing well - characterized sodium conditions as summarized in Table 2. Detailed descriptions of the sodium loops are given in [1] for the AWN at Interatom and in [2] and [3] for the KP1 - and CREVONA - loops at KfK.
The contamination of sodium with non - metallic impurities was controlled by cold traps which were continuously operated at about 125 °C, corresponding to an oxygen concentration less than 2.0 wppm. The carbon and nitrogen contents were measured by means of the equilibration of stainless steel foils. The analyses of the foils reveal carburizing and slightly denitriding conditions in the Interatom loop, whereas the foils of the KP1 - and CREVONA - loop show a loss of carbon and nitrogen. More exact values of the chemical activity of carbon were obtained by means of the diffusion carbon meter (Harwell [4]). The meter indicated a significant difference of the two loops in the carbon potentials, which is demonstrated in Fig.2.

3. Experimental Results

3.1 Results for X6 CrNi 18 11 - Base Material

The results of the creep rupture tests performed on heats No. 325 and 402 of X6 CrNi 18 11 base material in the sodium loops at KfK and Interatom are given in Figures 3 and 4 together with the results of parallel tests performed in air on the same heats and identical specimen geometries.
A comparison of the calculated regression lines in Fig.3 and 4 shows that for both heats rupture time decreases for the tests in sodium. The decrease in time to rupture is higher in the loops of KfK.
The small reduction in time to rupture, measured in the Interatom - loop is caused by a reduced ductility in the tertiary region of the creep curve, whereas the onset of tertiary creep and the minimum creep rates are not influenced by the sodium environment. This is clearly demonstrated e.g. by a comparison of the creep curves measured at 199 MPa with heat No.402 in air and in sodium (Fig.5) and by a comparison of times to onset of tertiary creep, $t_{2/3}$, and minimum creep rates measured in both media for this heat (Fig.7).
In contrast to these results the creep rupture tests performed in the sodium loops at KfK revealed a more severe effect of sodium at 550°C, with an earlier onset of tertiary creep and higher minimum creep rates in sodium compared to those in air. In comparison between the two heats this difference is smaller for the heat No.402 than for heat No. 325.

3.2 Results for X6 CrNi 18 11 - Welded Joints

In sodium tests have been performed on welded joints from heat No.401 and heat No. 206. The comparison of the times to rupture shows that the times to rupture are higher in sodium than in air for the welded joints from heat No.402 at Interatom (Fig.6) and that only a slight decrease in rupture time was measured in the KfK - loop on the welded joints from heat No.206 (Fig.8). In both test series no significant influence of sodium on minimum creep rate and time to onset of tertiary creep occurred.

3.3 Results for X6 CrNi 18 11 - HAZ - Material

Since most of the welded joint - specimens tested in the KfK - loop show the final fracture in the HAZ of the base material additional tests have been performed with specimens prepared from heat treated material (heat No.402) simulating HAZ - conditions. The results given in Fig.7 show that in comparison between air and sodium there is a slight decrease in rupture time in sodium similar to that for the base material, but the values of rupture time are still higher than those measured on the welded joints. This proves that the HAZ is not a weak region with regard to sodium influence.

3.4 Results for X6 CrNi 18 11 - Low Carbon Heat

If the difference in carbon activities between X6 CrNi 18 11 steel ("normal type 304) and the sodium of the KfK - loops is responsible for the strong sodium effect measured in the KfK - loops, then a low carbon version should not reveal this strong effect. This assumption was proved by creep rupture tests in the CREVONA - loop with a low carbon heat of X6 CrNi 18 11 - steel (Interatom No. 170). The results given in Fig.9 show that in comparison to in - air tests only a slight reduction in time to rupture occurred in the sodium of the KfK - loop similar to the effect observed in the Interatom - loop.

3.5 Results for X6 CrNi 18 11 - Heat Treated Specimens

Some specimens of the heat 325 have received a particular heat treatment in order to suppress sensitization during the creep - rupture tests. They were first sensitized by heating to 550 °C for 100 hours and in a final step they were kept for 30 hours at 700 °C; this step was performed to get a rediffusion of chromium into the grain boundary zones. The results of creep - rupture tests in the KfK - loop were nearly identical with those of reference tests in air, the additional sodium effect was suppressed by this heat treatment, only the reduction of the tertiary creep regime was observed.

3.6 Results for X6 CrNi 18 11 - 6 mm Diameter Specimens

Depending on the mechanism of the environmental effect the surface to volume ratio can be an important factor. Therefore in-sodium creep rupture tests have been performed by KfK on specimens of 6 mm gauge diameter with 30 mm gauge length from heat No. 325 of X6 CrNi 18 11. The results, given in Fig.3, show that the rupture lives for the 6 mm specimens tested in the KfK - loop reach that of the 4 mm specimens tested in the Interatom - loop. Detailed analyses reveal that minimum creep rate and onset of tertiary creep is almost the same as for the in-air tests.

3.7 Microstructural Observations

Extensive post test examinations have been performed to clarify the mechanism of sodium effects, especially

- the differences between the results from the Interatom - loop and the KfK - loops and
- the occurrence of tertiary - creep embrittlement.

Following the differences in carbon activity in the sodium loops, carbon profiles have been measured by means of a microprobe. The results given in Fig.10 show a surface carburization up to a depth of 140 μ m, for the specimen tested in the Interatom - loop, whereas the specimen tested in the CREVONA - loop of KfK reveals only a carburized layer of 20μ m. This result was qualitatively confirmed by microscopical observations, which show much more carbide precipitations in the surface of the specimens from the Interatom - loop than for the specimens tested in the KfK - loop.

A statistical evaluation of the cracks showed that the number of deep surface cracks is higher for the specimens tested in the KfK - loop compared to that for the specimens from the Interatom - loop.
Generally, the specimens from both sodium loops developed more deeper intergranular cracks starting from the surface than the air - specimens. This is confirmed by optical micrographs of cross sections of the gauge lengths of the specimens tested in air and in sodium (Fig.11). The specimens exposed to sodium exhibit deep intergranular cracks with sharp crack tips, whereas the specimen exposed to air only exhibits shorter and blunted cracks.
The formation of surface cracks during the creep life of specimens of the heat No. 402 was studied in a series of tests at the same level of stress and the temperature of 550 °C.
The time - to - rupture at the stress σ=215 MPa was t_F = 3236 h, three additional specimens were taken out of the sodium test section after 781 (~ 0,25 t_F), 1498 (~0.5 t_F) and 2210 (~0.75 t_F) hours.
The metallographic examination indicated the early formation of grain boundary cracks at the surfaces of the specimens. We observed cavities at grain boundaries after 0.25 t_F, when the material had just entered the region of secondary creep. Chains of such cavities grew together to forme surface cracks. After 0.5 t_F we found the fully developed surface cracks at grain boundaries which did not significantly grow up to 0.75 t_F, the damaged surface layer was about 0.1 mm thick. The creep rate at minimum weakly scattered around $\dot{\epsilon}$ = 1.5 $\cdot 10^{-5}$ h $^{-1}$, faster than in air environment. The whole secondary creep regime was influenced by the presence of the surface cracks which caused the increase of the secondary creep rate. Analyses of the fracture surface show for the sodium specimens a higher fraction of intercrystalline fracture than for the specimens tested in air.

4. Discussion of the Results

4.1 Effects in Decarburizing Sodium

An outstanding result of this cooperative study is the difference found between the effects in the sodium loops of KfK and Interatom.
In an earlier paper [6] the much more pronounced sodium effect in the KP1 - loop had been attributed to impurities of heavy metals (Pb, Sn and Zn), which were found in higher concentration in this loop and additional enriched at the crack tips of specimens tested in this loop. The results obtained in the CREVONA - loop with high purity sodium [3] show a sodium effect comparable to that in the KP1 - loop. This shows that heavy metal impurities cannot be responsible for the differences in the mechanical properties found between the KfK and the Interatom sodium loops.
From the results of this paper it became obvious that the difference in carbon activity causes the different behaviour. The mechanism of this decarburizing sodium is not fully understood but from the available results it can be accepted that the decarburizing effect acts on the grain boundaries.

The main effect of sodium corrosion is leaching of Cr, Ni and Mn from the regions close to the surface and to the grain boundaries. This leads to further decarburization of these regions and reduces the stability of precipitated carbides which can be dissolved in the decarburizing sodium. Higher carbon activities in sodium stabilize the Cr - content in the steel surface by formation of carbides. In the decarburizing sodium of the KfK - loops the loss of carbide and chromium leads to the formation of initiation sites at the exposed grain boundaries which will form cracks by the presence of mechanical loads or plastic deformations. Because these effects are restricted to the diffusion zone the influence on the creep rupture behaviour is strongly dependent on the surface to volume ratio of the specimens. Therefore, the environment effect is much more pronounced for 4 mm diameter specimens than for the 6 mm diameter specimens.
The described processes are influenced by different parameters:

- Carbon activity
  - in sodium with high carbon activity these effects are suppressed (e.g. Interatom results)
  - a low carbon content of the steel reduces the carbide precipitation on grain boundaries and the formation of cavities (e.g. KfK results on X6 CrNi 18 11 - low carbon version)
- Grain size
  in heats with small grain size the carbide precipitation is distributed over a higher portion of grain boundaries and therefore the effect is less pronounced (e.g. differences between heat 325 and 402)
- Sensitization and diffusion heat treatment
  removal of the impoverishment of Cr near the grain boundaries caused by heat treatment suppressed the sodium effect (e.g.KfK results on heat treatment material)
- Cold work
  cold worked material, where carbides precipitate additionally on slipbands, have lower carbide concentration on grain boundaries and hence only a small effect of sodium (e.g. former results from KfK [6]).
- Alloying additions
  additional content of molybdenum reduces the leaching of chromium and hence stabilizing the carbon content of the matrix (e.g. KfK - results on type 316 SS do not show any sodium effect).

4.2 General Effects of Sodium

Independent from carbon activity the creep tests on type 304 steel show reduced tertiary creep strain and duration. A possible explanation for this tertiary creep embrittlement could be that the discussed dissolution of grain boundary carbides is activated in carburizing sodium too, if a certain amount of plastic deformation has been reached.

A different explanation can be derived from the observed higher number of deep surface cracks, occuring in sodium tests. In the extreme case of only one deep crack the stress concentration at the crack tip is much higher than in a specimen with comparable ligament with a lot of cracks distributed all over the bulk material. This higher stress condition will lead to a faster fracture of the specimen without large plastic deformations.
In air the oxidation causes a blunting of the crack tip and a reduction of stress concentration ahead of the crack tip. Similar observations have been made in creep tests conducted in air and in argon containing 15 ppm oxygen [7]. In sodium no blunting occurs and the crack continue to grow. Such inhibition of crack is believed to be responsible for increasing rupture life where creep rate remains uneffected [8]. The observation of deeper and sharper cracks in sodium can be attributed to restricted oxygen supply. This in turn is considered to be responsible for reduced tertiary creep in sodium leading to reduced rupture life.
It should be mentioned that the crack growth rate itself is not accelerated by the sodium environment, at it was shown in creep crack growth tests in the Interatom - loop [9].

4.3 Relevance for the Design

Thin walled components of X6 CrNi 18 11 - steel subjected to creep conditions in sodium should be designed by taking care of the effect of decarburizing sodium. For LMFBRs these effects are not expected to occur, since the operating experience of large operating reactors and sodium loops do not show a tendency for decarburization at and below 550 °C.
The reduced tertiary creep strain can be tolerated, since the structural materials will not reach the onset of tertiary creep. This is because sufficient safety margins are included in the design rules.

5. Conclusions

From the creep rupture tests performed in sodium on X6 CrNi 18 11 - steel (type 304 SS) with rupture times up to 18.000 hours at 550 °C the following conclusions can be drawn:

1. The influence of sodium on the creep rupture properties of this steel depends on the carbon activity of sodium

2. Under normal (non - decarburizing) sodium conditions a limited reduction of times to rupture occurs which is caused by a reduced ductility within the tertiary range of creep. Minimum creep rate and time to onset of tertiary creep are not influenced by the sodium environment. This is tolerable for the structural material of a LMFBR.

3. Under decarburizing conditions, which are not expected in the sodium of LMFBRs, an additional loss of creep strength with higher creep rates and earlier onset of tertiary creep occurs for the base material.
   This additional effect seems to be related to sodium corrosion of surface near layers, reducing the unaffected cross section. It depends on the surface - to - volume ratio, and it was nearly suppressed by specimens with 6 mm diameter.

4. The welded joints do not show this additional effect of decarburizing sodium, and the HAZ is not a weak region of a welded joint with regard to influence of sodium.

5. Microstructural observations show a more brittle behaviour for all specimens tested in sodium with deeper intergranular cracks starting from the surface of the specimens. This phenomenon is assumed to cause the reduction in ductility of tertiary creep.

Acknowledgements

We gratefully acknowledge the contributions of our colleagues at KfK (Z. Peric, G. Drechsler, B. Seith, G. Wittig and C. Phaniraj) and Interatom (Dr.H. Breitling, O. Gossmann, P.Quintus, H.M. Yun and K.G. Samuel). The work at KfK was generously supported by the Fast Breeder Project of the Kernforschungszentrum Karlsruhe, we want to express our thanks to Dr.W. Marth, Dr.G. Mühling and Mr.H. Plitz. The work at Interatom has been funded by the Bundesminister für Forschung und Technologie in the framework of the reactor safety programme, which is gratefully acknowledged.

References

[1] H. Huthmann, G. Jenner
in: Liquid Metal Engineering and Technology,
The British Nuclear Energy Soc., London 1984, Vol.2, 472

[2] H.U. Borgstedt, G. Drechsler, G. Frees
Z. Werkstofftechnik 12 (1981) 250 - 2256

[3] H.U. Borgstedt, G. Frees
in: Material Behaviour and Physical Chemistry in Liquid Metal Systems,
Ed. H.U. Borgstedt, Plenum Press, New York 1982, 153

[4] H.U. Borgstedt, C.K. Mathews, S.R. Pillai
in: Liquid Metal Engineering and Technology ,
The British Nuclear Energy Soc., London 1984, Vol.1, 75

[5] G. Frees, H.U. Borgstedt, G. Drechsler
DVS - Berichte Band 75 (1982) 272
(Deutscher Verband für Schweißtechnik, Düsseldorf)

[6] H. Huthmann, G. Menken, H.U. Borgstedt, H. Tas
2nd. Int. Conf. on Liquid Metal Technology in Energy Production, 1980, Richland, Washington

[7] C. Phaniraj. K.G. Samuel, S.L. Mannan, P. Rodriguez
in: Proc.Int.Conf. on Creep,
JSME, IMechE, ASME, ASTM, Tokyo, April 14 - 18, 1988, 205

[8] J.K. Tien, J.M. Davidson
Adv. Corros. Sci. Technol.7 (1979) 1

[9] K. Krompholz, H. Huthmann, E.D. Grosser, J.B. Pierick
Eng. Fract. Mech. 16 (1982) 809

Table 1: Characterization of Test materials

Type	X6CrNi18 11 (DIN 1.4948, equivalent Type 304 ss)			
Heat No.	227766	294771	231861	239825
Interatom No.	325	402	206	170
Plate	40 mm	20 mm	20 mm	10 mm
Heat treatment	sol. ann.	sol. ann.	sol. ann.	sol. ann.
Grain Size(ASTM)	3.5	5.5	4	5

Chemical Composition (wt-%)

Mat. No.	C	Si	Mn	P	S	Cr	Mo	Ni	B	N
325	.050	.37	1.37	.010	.005	18.55	<.01	10.89	.0034	.058
402	.060	.47	1.67	.015	.004	17.82	.03	10.72	.0028	.034
206	.055	.44	1.82	.023	.012	17.78	.04	11.15	-	.041
170	.027	.36	1.35	.030	.012	17.52	.46	10.14	-	.030
402-WM	.045	.21	1.16	.013	.007	19.15	.03	10.30	-	-
206-WM	.042	.67	1.38	.020	.010	19.03	-	10.42	-	-

WM: Weld metal used for welded joints of 402- or 206- material

Table 2: Sodium Loops Used for Creep Rupture Tests

Facility/Location	KP1 / KfK	CREVONA / KfK	AWN / Interatom
Status	dismantled	operational	operational
Material of pipes	X5CrNi18 9*	X5CrNi18 9	X6CrNi18 11
Inventory of Na	100 kg	500 kg	600 kg
Flow of Na	0,3 $m^3 \cdot h^{-1}$	0.38/0.55 $m^3 \cdot h^{-1}$	0.08/0.18 $m^3\ h^{-1}$
Flow rate at specimens	3 $m \cdot s^{-1}$	3 $m \cdot s^{-1}$	4.3 $m \cdot s^{-1}$
Temperatures/°C			
Test section Main loop Cold leg Cold trap	550 500 380 140 - 145	550 500 400 125 ± 5	500 / 550 520 380 125 - 130
Chemistry Foil equilibration for C and N	decarburizing slight denitriding	decarburizing slight denitriding	carburizing slight denitriding
Carbon activity (Harwell- Meter)	-	2· 10^{-3}	6 · 10^{-3}

*) Hot leg of the loop

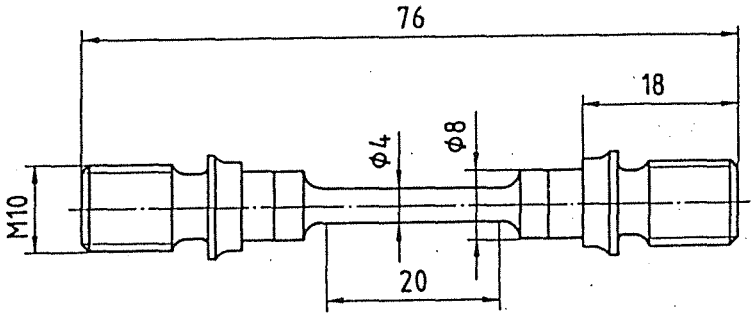

1 a) Dimension in mm

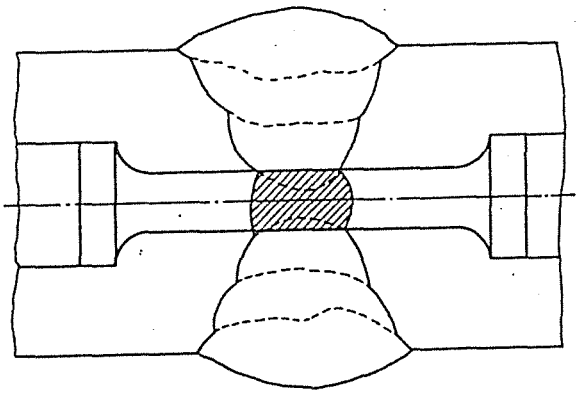

1 b)

Fig. 1: Specimen for creep rupture tests in sodium and position of weld metal in gauge length

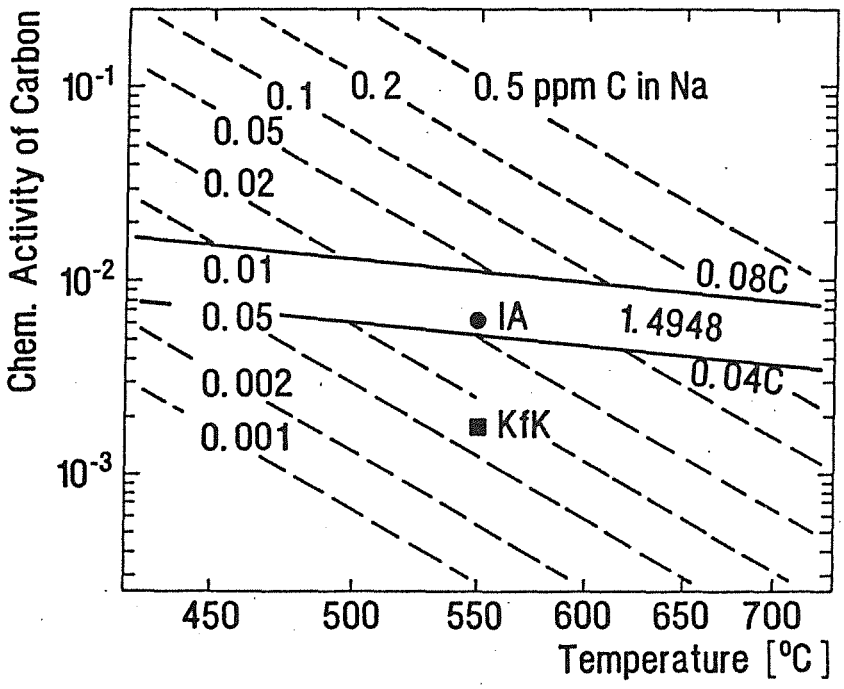

Fig. 2: Carbon activities in sodium loops of KfK and Interatom in comparison with equilibrium diagram for Type 304 steel and liquid sodium

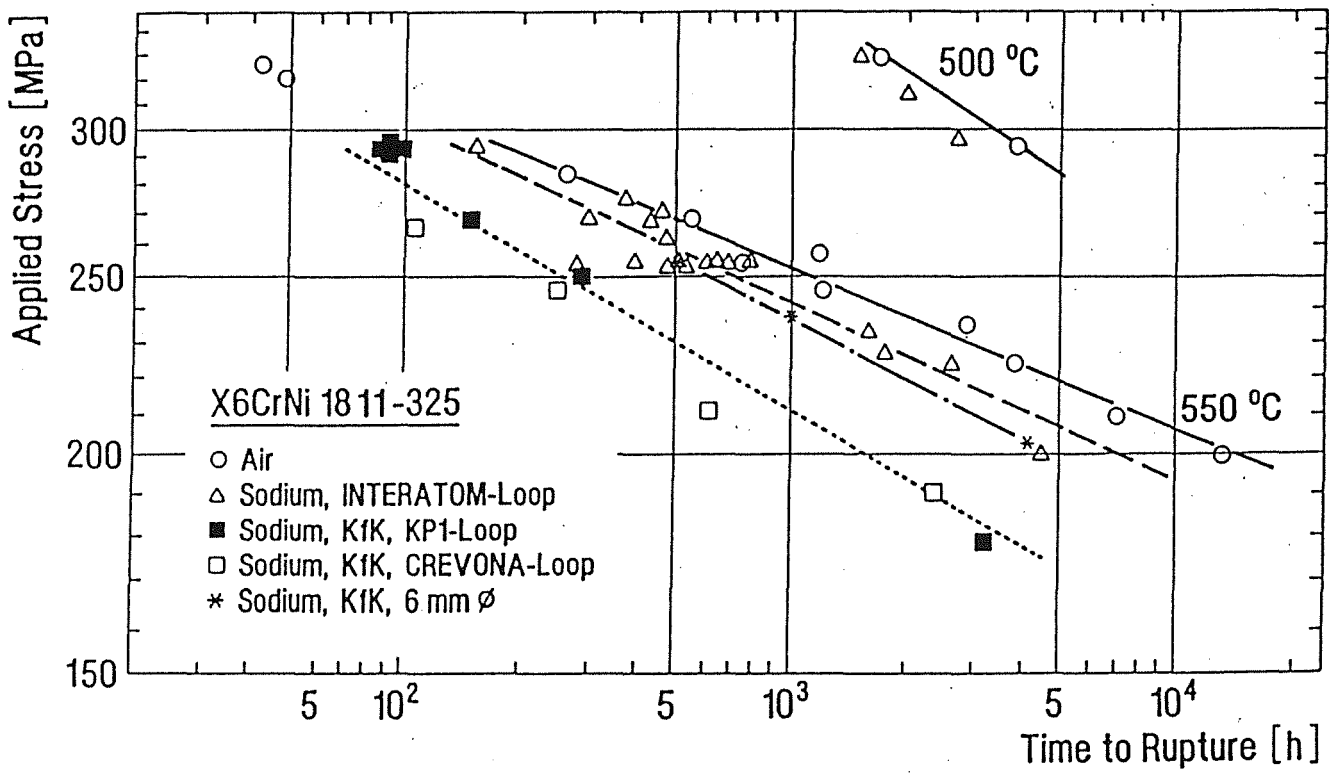

Fig. 3: Time to rupture of Type 304 ss (coarse grained heat) measured at 500 and 550 °C in air and in the sodium loops at KfK and Interatom

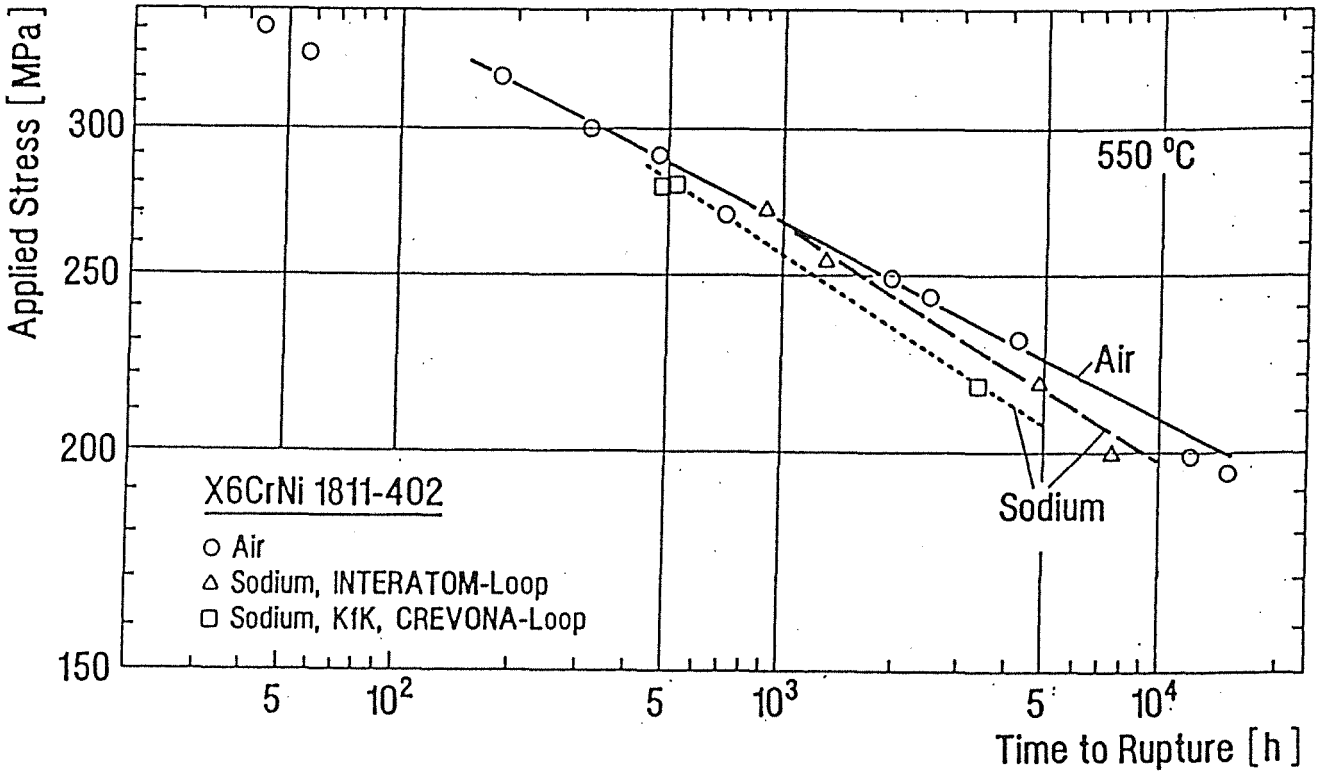

Fig. 4: Time to rupture of Type 304 ss (fine grained heat) measured at 550 °C in air and flowing sodium at KfK and Interatom

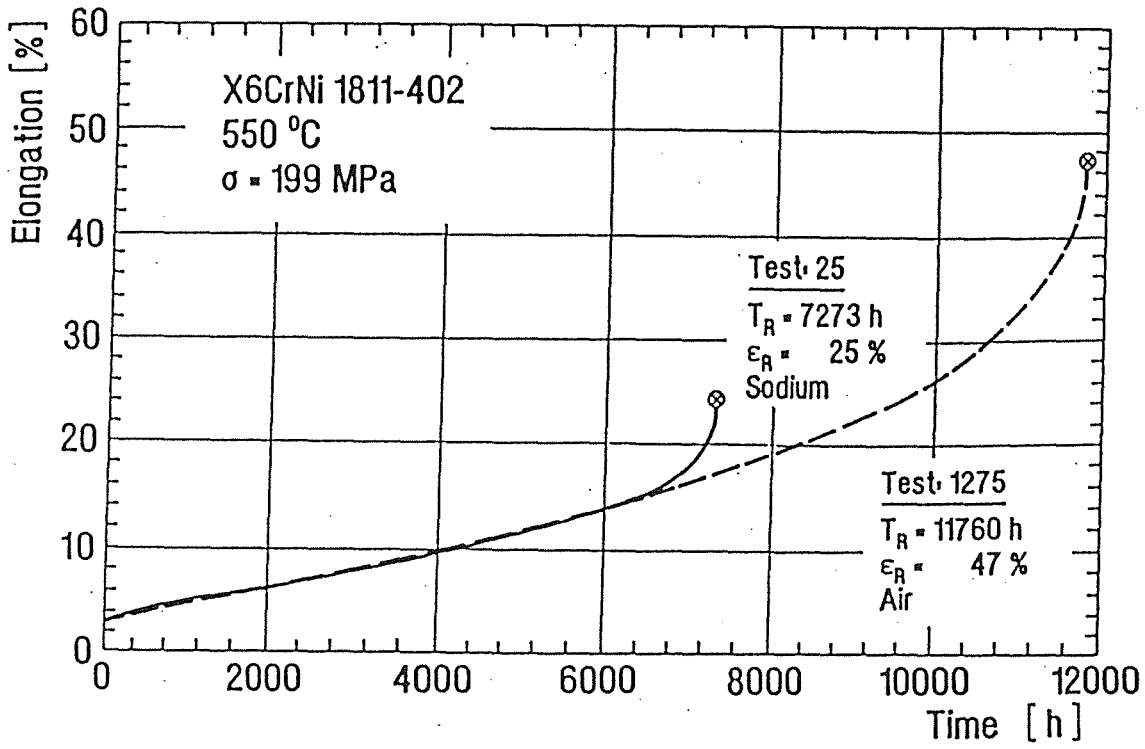

Fig. 5: Comparison of creep curves measured on Type 304 - steel at 550 °C in air and in flowing sodium at Interatom

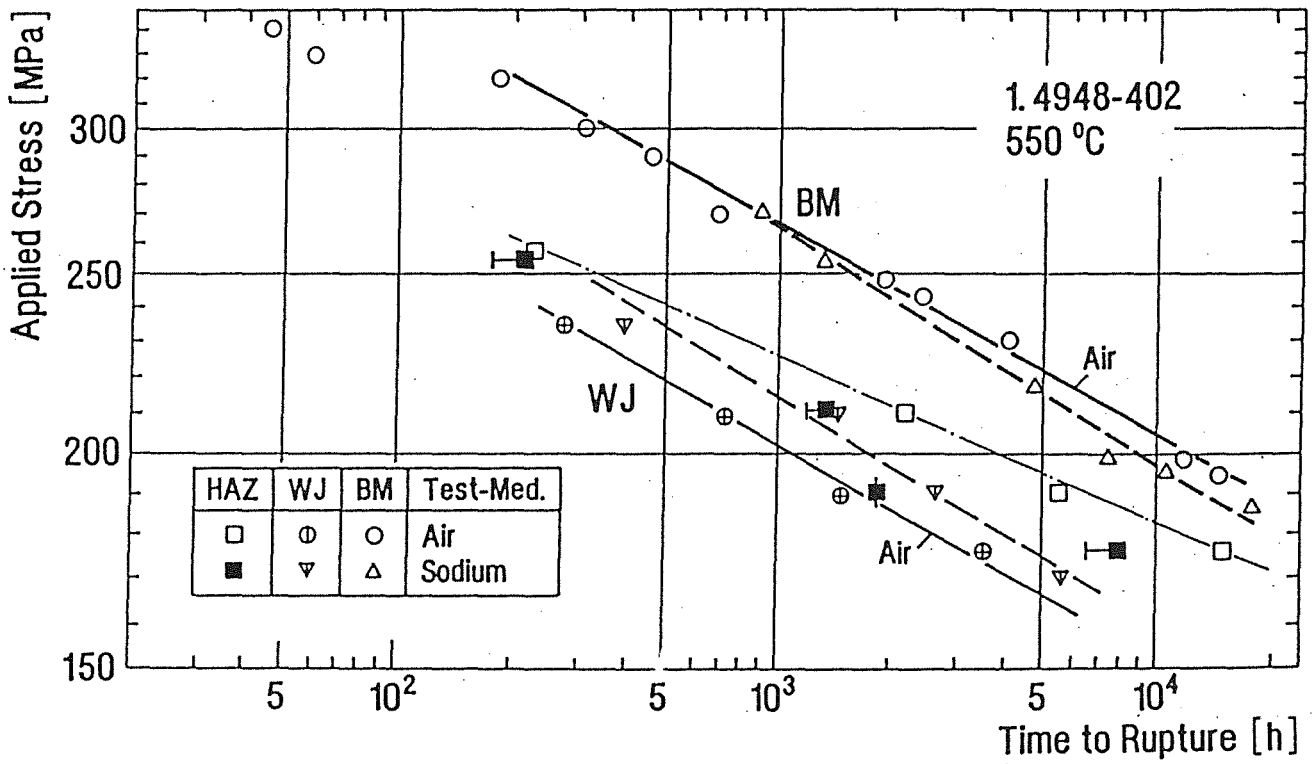

Fig. 6: Time to rupture of Type 304 ss, base material (BM), welded joints (WJ) and heat affected zone material (HAZ) measured in air and flowing sodium (Interatom - loop)

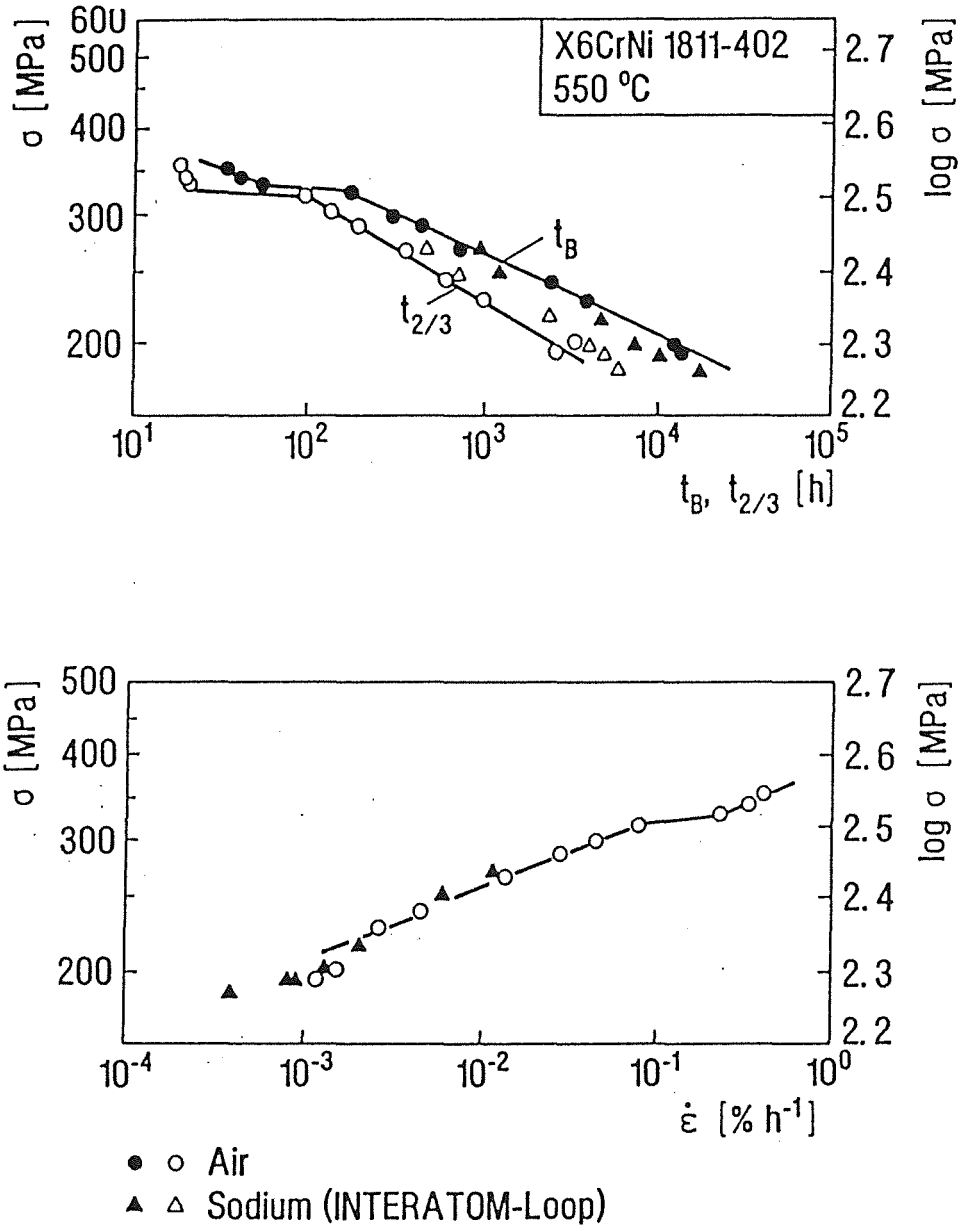

Fig. 7: Time to rupture, t_B, onset of tertiary creep $t_{2/3}$ (above), and minimum creep rate, $\dot{\varepsilon}$, measured on Type 304ss at 550 °C in air and in flowing sodium

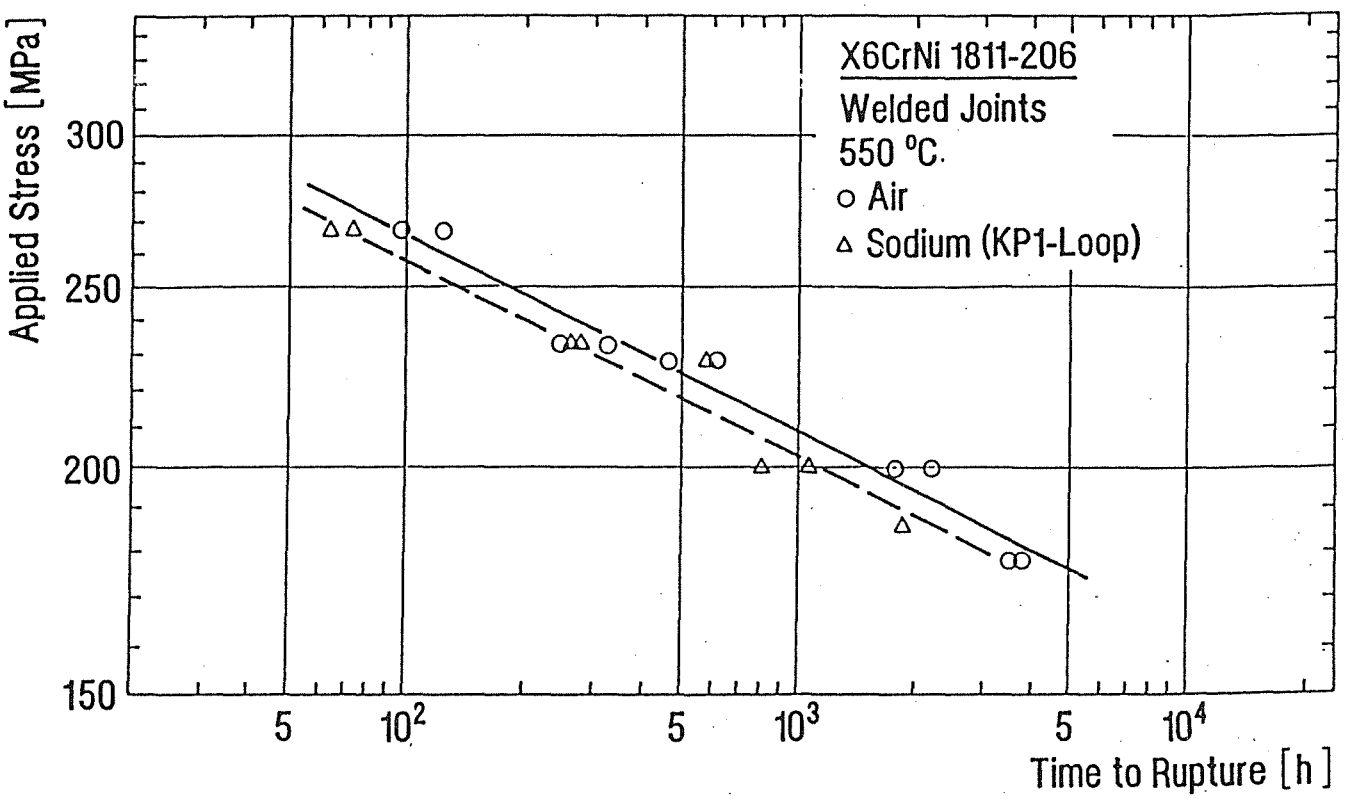

Fig. 8: Time to rupture of Type 304 ss welded joints measured in air and flowing sodium by KfK (KP1 - loop)

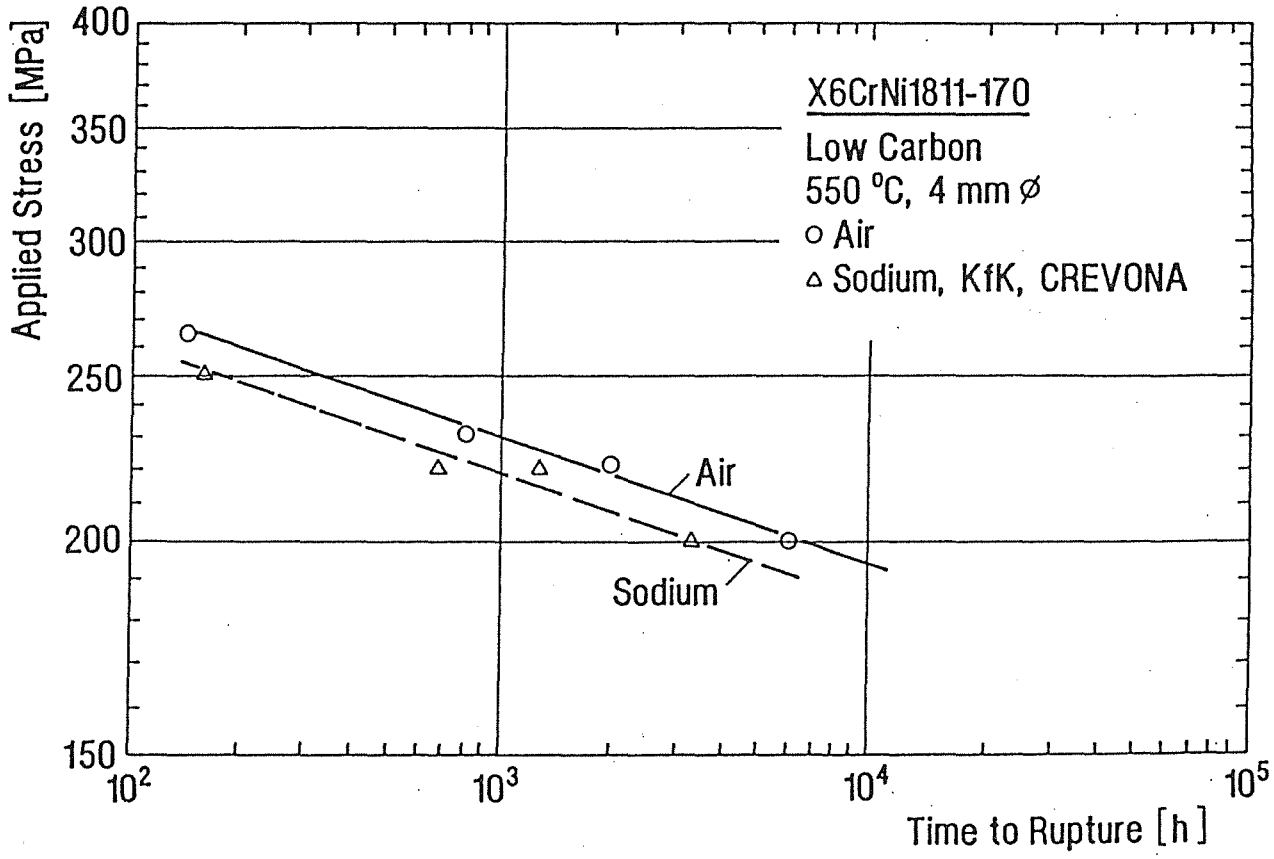

Fig. 9: Time to rupture of Type 304 ss (low carbon heat) measured in air and flowing sodium by KfK (CREVONA - loop)

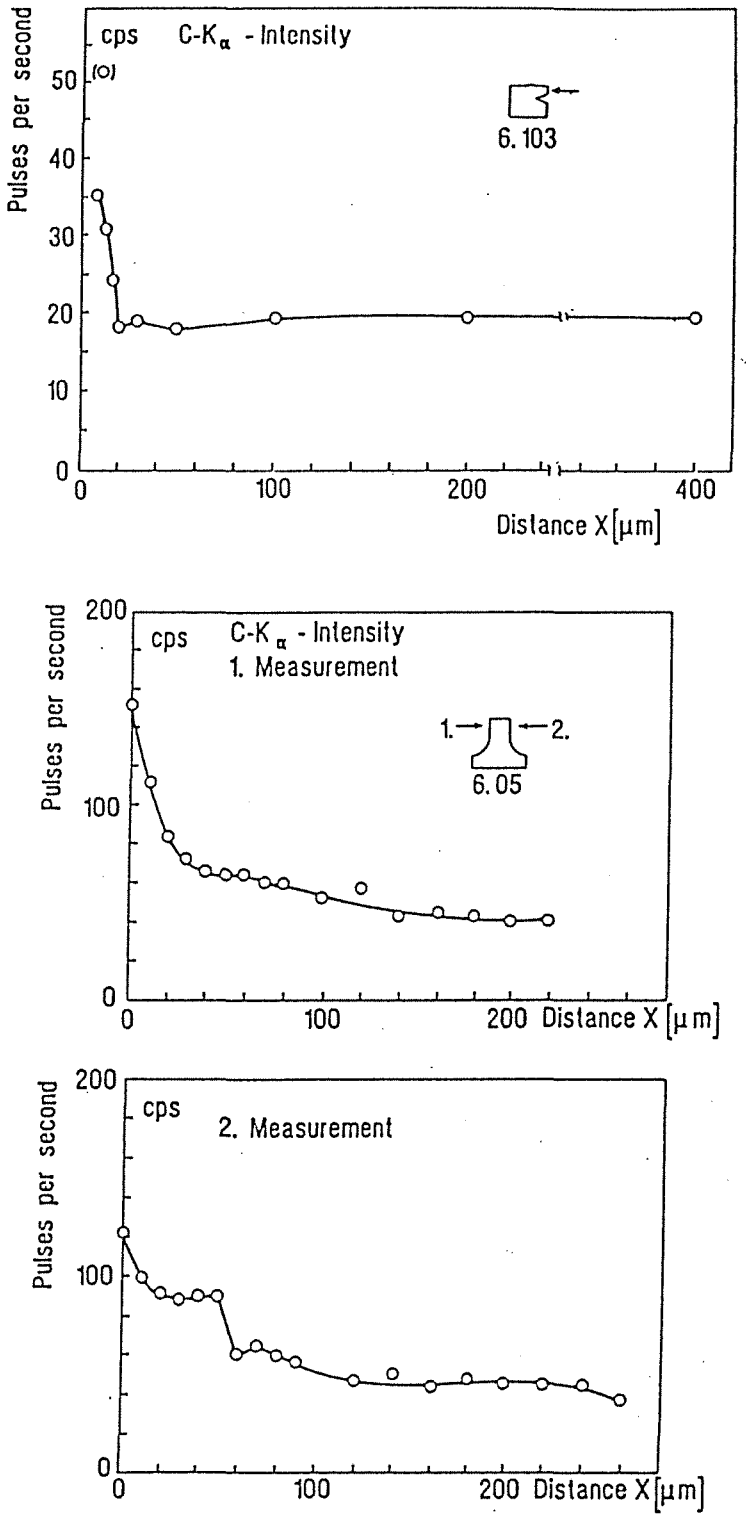

Fig.10: Carbon profiles of specimens after creep rupture tests in flowing sodium measured by microprobe from GfE - TH. Aachen; Specimen from CREVONA (190 MPa, 2371 h) (on top); AWN Specimen (199 Mpa, 44605 h) (bottom)

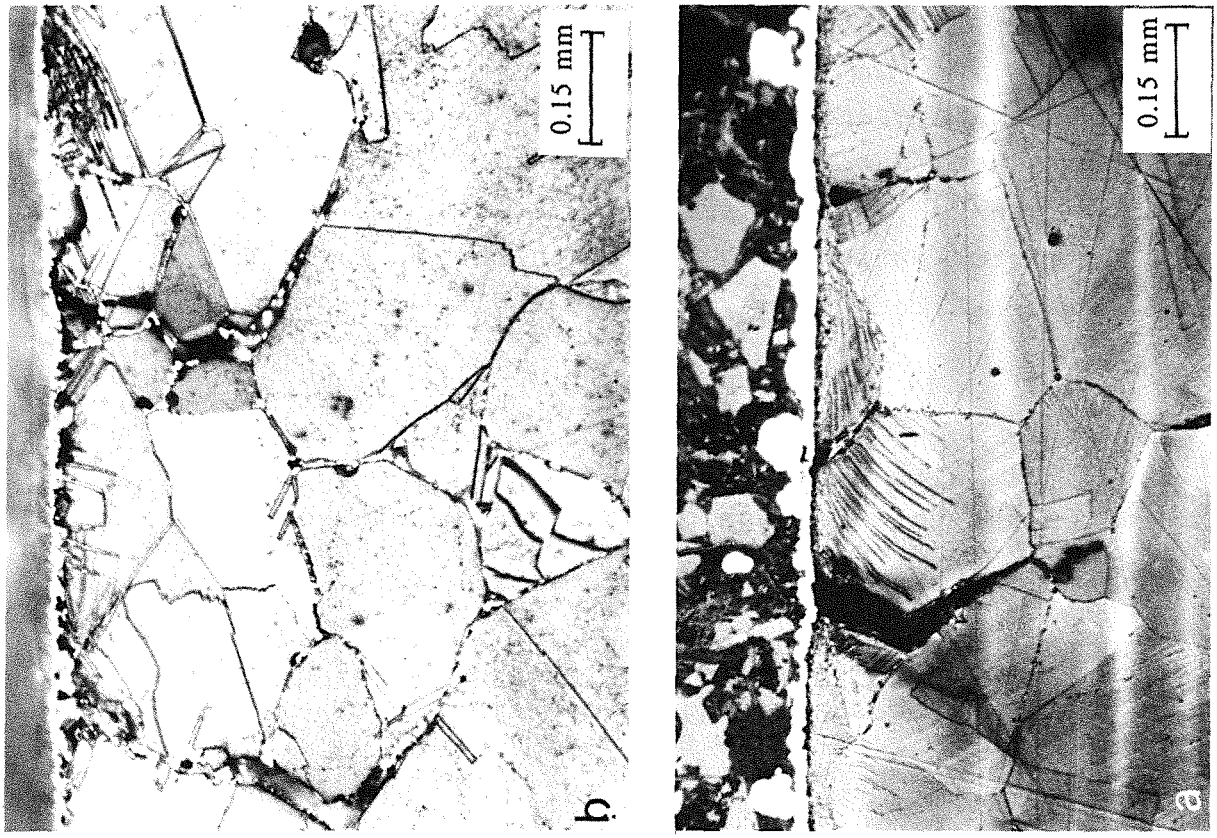

Air, 550 °C
224 MPa, t_R = 3848 h

Sodium, 550 °C
215 MPa, t_R = 3236 h

Fig.11: Optical photographies of Type 304 ss specimens after creep rupture tests in air and sodium at 550 °C (200 x)

THE INFLUENCE OF FLOWING SODIUM ON THE CREEP-RUPTURE BEHAVIOUR OF TYPE 316L(N) STAINLESS STEEL

H. Huthmann/Interatom GmbH, Bergisch Gladbach, Germany
H.U. Borgstedt/Nuclear Research Center, Karlsruhe, Germany
Ph. Debergh/EdF, Les Renardières, France
C.A.P. Horton/National Power, Leatherhead, England
D.S. Wood/AEA Technology, Risley, England

ABSTRACT

In liquid sodium some leaching of austenite stabilizing elements and the exchange of nonmetallic elements like carbon and nitrogen may occur and cause changes in the long-term mechanical properties of structural material.

To determine the influence of sodium on the creep rupture properties of 316L(N) steel, which will be used in the European Fast Reactor (EFR), two heats of this material have been tested in five different sodium loops at 550 °C. In total 42 uniaxial creep rupture tests in sodium with running times up to 27.00 h and 36 parallel tests in air are available. In addition to the as-received condition one heat has been tested in a pre-sensitized (600 °C, 1000 h) condition.

For the as-received condition no significant effect of sodium was found and it can be concluded that the design of components starting operation in as-received condition in high purity sodium can be based on in-air data of

- stress rupture strength
- stress rupture ductility
  (elongation and reduction of area)
- conditions for onset of tertiary creep and
- minimum creep rate.

Provisional reservations should be made in recommendations for sensitized material, because for the pre-sensitized material the times to rupture and onset of tertiary creep are somewhat shorter in sodium than in air. The measurements performed on 4 mm diameter specimens of the pre-sensitized material indicate a reduction in strength of about 10 %. Metallographic post test examinations on these specimens and a CEC study contract will lead to final recommendations.

1 INTRODUCTION

The use of liquid sodium as a coolant for fast reactors requires the knowledge of the long-term mechanical properties of structural materials in this flowing medium. The material losses of steels due to sodium corrosion are negligible at temperatures up to 550 °C even in fast flowing sodium; some leaching of austenitic stabilizing elements may, however, occur, and the exchange of nonmetallic elements like carbon and nitrogen may cause changes in mechanical properties. This was shown in a previous study on Type 304 stainless steel [1, 2].

To determine the influence of sodium on the creep-rupture properties of 316L(N) steel, which will be used in the EFR (European Fast Reactor), two heats of this material have been tested in the sodium loops of AEA-Risley, CEGB-Marchwood, EdF-Les Renardières, KfK-Karlsruhe and Interatom-Bergisch Gladbach.

In this paper a common evaluation of these creep-rupture tests performed in sodium at 550 °C and parallel tests in air is given.

2 MATERIAL, SPECIMENS AND TESTS

A characterization of the two heats of 316L(N) steel is given in Table I. Concerning the maximum values of the nonmetallic inclusions the Krupp heat appears to have a very high purity, whereas Tole SQ has more impurities, specially long oxides. Special aspects due to these impurities, which might have an influence on thin-walled components, are not regarded.

Cylindrical specimens with different diameters (4 to 9 mm) taken perpendicular to the rolling direction have been used. An overview of the tests performed on the two heats of 316L(N) steel is given in Tables II, III and IV. The specimens have been tested in the as-received condition and additionally after a previous sensitation (1000 h at 600 °C, EdF-tests).

In addition to the time of rupture (t_R) the rupture elongation (A) and the reduction of area (Z), a common evaluation of the creep curves to determine the minimum creep rates ($\dot{\varepsilon}_{min}$) and the times to onset of tertiary creep (t2/3) has been performed. Because the determination of these parameters are dependent on the selection of the area of secondary creep from the creep curves, all creep curves have been evaluated by one person.

3 DEVELOPMENT OF TWO STAGES OF SECONDARY CREEP

In the evaluation of the creep curves a complication arises from the fact that the 316L(N) material develops two stages of secondary creep in long running tests where sensitation takes place during the test. This is demonstrated in the creep curves measured at 265 MPa (Fig. 1). The second stage of secondary creep occurs only on the as-received material,

whereas the material with a previous sensitation shows only one stage of secondary creep rates.

4 DETERMINATION OF TIMES TO ONSET OF TERTIARY CREEP T(2/3) AND SECONDARY CREEP RATES

The characteristic transition times, t(2/3), have been determined by the 0.2 % offset method as indicated in Fig. 1. If two stages of secondary creep occurred the first transition time, $t_1(2/3)$, is related to the onset of the second stage of secondary creep and only the second transition time, $t_2(2/3)$, is due to the onset of tertiary creep.

Accordingly two values for the two regions of secondary creep have been determined for the tests with running times larger than about 6000 h.

5 RESULTS AND DISCUSSION

5.1 TIMES TO RUPTURE

The times to rupture measured on both heats in the as-received condition are given in Figs. 2 and 3.

Most of the in-sodium data are covered by the scatterbands of the in-air tests. Deviations to shorter rupture times occur for the in-sodium tests of Interatom and EdF on Tole SQ (Fig. 2) for rupture times below 10,000 h with specimens of 4 mm diameter, but this trend is not confirmed in the long running tests at 240 MPa, where the test in the Interatom loop, terminated after 27,001 h, has a running time which is about 10,000 h longer than could be expected from the extrapolation from the Interatom tests at higher stress levels.

The same behaviour has been measured on the Krupp-cast 528 (Fig. 3). The reduction in time to rupture measured in sodium at 260 MPa in the Interatom loop does not occur at the lower stress level of 220 MPa, where the tests in sodium and in air have been terminated after about 19,000 h.

The creep curves measured on both heats in sodium and in air do not show significant differences.

Additionally it was shown at 275 MPa on Tole SQ (Fig. 2) that the specimen with 6 mm diameter tested in sodium does not show the reduction in time to rupture as the specimen with 4 mm diameter.

From that it can be concluded that for components with more than 4 mm thickness starting operation in the as-received condition and load levels which lead to operating times more than 10,000 h no effect of sodium will occur for the times to rupture.

The times to rupture measured in sodium and in air on Tole SQ (4 mm specimens) in a sensitized (1000 h, 600 °C) condition are given in Fig. 4. The rupture times measured in sodium are reduced in comparison to the in-air data which correspond to a

reduction of strength of 10 % for the 100,000 h value. This effect measured on specimens with 4 mm diameter is expected to be of no significance for components with larger thickness, but no proof is available.

5.2 ELONGATION AND REDUCTION OF AREA

The stress rupture ductility can be described by the creep strain (= total elongation after fracture - elongation after loading) and the reduction of area measured on the fractured specimens.

Figs. 5 and 6 show that the creep strain and the reduction of area measured on Tole SQ are not influenced by the sodium environment. The same conclusion can be drawn for the Krupp cast (Figs. 7 and 8). The low strain of the in-sodium test KfK 10 (Fig. 5) can be due to the comparable high value of initial strain after loading. No explanation is available for the comparable low creep strain for the in-air test UK/NS4 (Fig. 8).

For Tole SQ, tested in the sensitized condition, a small reduction in creep strain seems to occur in sodium (Fig. 9) but this is not confirmed by the measured reductions of area (Fig. 10).

5.3 TRANSITION TIMES AND ONSET OF TERTIARY CREEP

Figures 11 and 12 show the times to onset of tertiary creep determined on Tole SQ and the Krupp cast (Interatom-No. 528) of the 316L(N) material. In these figures $t_1(2/3)$ is only regarded, if it is due to the onset of tertiary creep, transition times between the first and second phase of secondary creep are neglected.

Fig. 13 gives the times to onset of tertiary creep for the SQ-cast tested in a sensitized condition (1000 h, 600 °C).

In the as-received condition (Fig. 11 and 12) the sodium and the air-data are within one scatterband. In the sensitized condition (Fig. 13) the times to onset of tertiary creep measured in sodium are all somewhat shorter than measured in air, which corresponds to a reduction in strength of 15 MPa, extrapolated to 100,000 h.

5.4 SECONDARY CREEP RATES

Figs. 14 and 15 show the minimum creep rates determined from the tests on Tole SQ in the first and in the second phase of secondary creep. In Fig. 16 the minimum creep rates measured on the Krupp cast are given. Transitions from the first to the second phase of secondary creep are indicated by arrows.

The min. creep rates for Tole SQ in the sensitized condition (Fig. 17) fall together in one scatterband.

5.5 DISCUSSION OF THE RESULTS ON SENSITIZED MATERIAL

From Figs. 4 and 13 it appears that the strength of the pre-sensitized material is reduced by a sodium environment. A comparison with the times to rupture tested in the as-received condition (Fig. 19) shows that even the in-air data of the sensitized condition are lower for high load levels but below about 240 MPa (corresponding to rupture times >20,000 h) the rupture times of the pre-sensitized material will reach the scatterband of the material tested in the originally as received condition.

A curved scatterband or even a knee in the scatterband for the as-received material is justified because sensitization takes place during the tests at about 4,000 h to 8,000 h.

The extrapolated in-sodium data of the sensitized material will reach the in-air scatterband of the as-received material too, but at a somewhat lower load level at about 10^5 h.

Without understanding of the mechanism, why the strength of the sensitized material is reduced in sodium, it is difficult to give a recommendation for the design. Provisional reservations should be made for components starting operation in the sensitized condition in sodium. It is expected that this is restricted to comparably thin-walled components ($d < 4$ mm) when it has been shown that this is due to a surface effect.

Post-test examinations on the tested specimens will be done and a final conclusion should be drawn including the results of the metallographic investigations.

6 SUMMARY AND CONCLUSIONS

Uniaxial creep rupture test have been performed on the base material of two heats of 316L(N) at 550 °C in flowing sodium and in air. Totally 42 tests in sodium with running times up to 27,000 h and 36 parallel in air tests are available. Additionally to the as-received condition 1 heat has been tested in a previously sensitized (600 °C, 1000 h) condition.

Additionally to the evaluation of the creep rupture data an evaluation of the creep curves measured by all partners has performed. It was found that in the long term tests (>6000 h) two stages of secondary creep developed, which can be due to sensitation occurring during the tests.

For the as-received condition no significant effect of sodium was found and it can be concluded that the design of components starting operation in as-received condition in high purity sodium can be based on in-air data of

- stress rupture strength
- stress rupture ductility (elongation and reduction of area)
- conditions for onset of tertiary creep and
- minimum creep rate.

Provisional reservations should be made in recommendations for sensitized material, because for the material tested in the pre-sensitized conditions the times to rupture and onset of tertiary creep are somewhat shorter in sodium than in air. The measurements performed on this specimens with 4 mm diameter indicate a reduction in strength of about 10 %. Metallographic post test examinations on these specimens will lead to final recommendations.

REFERENCES

[1] BORGSTEDT, H.U., HUTHMANN, H., Influence of sodium on the creep-rupture behaviour of Type 304 stainless steel, Journal of Nuclear Materials 183 (1991)

[2] BORGSTEDT, H.U., HUTHMANN, H., The influence of decarburizing ssodium on the creep-rupture behaviour of Type 304 stainless steel, this IWGFR Specialists' Meeting

	Tole SQ	Krupp-528
Type	ICL 167 SPH	316L mod
Supplier	Creusot-Loire	Krupp SW
Heat No	T9075	013824 (Interatom-528)
Plate No	T81/Tole SQ	5
Plate Dimensions	30 x 2000 x 5000 mm	30 x 1000 x 1000 mm
Melting Process	Electro furnace + A.S.V.	ESR
Solution Annealing	90 min 1100 °C/H_2O	30 min 1080 °C/H_2O
Grain Size (ASTM)	2 - 4	2 - 4
Delta Ferrite (Fischer)	0 - 0.4 %	0
Nonmetallic *) Inclusions acc. to DIN 50602, maximum values	SS: 1 OA: 3 OS: 8 OG: 2	SS: 0 OA: 0 OS: 0 OG: 2 - 3

*) SS: long sulphides, OA: dissolved oxides, OS: long oxides, OG: globular oxides

Chemical Composition (wt %)

Element	C	S	P	Si	Mn	Ni	Cr	Mo	N	Co	Cu	B (ppm)
Tole SQ	0.030	0.001	0.021	0.44	1.84	12.3	17.5	2.47	0.075	0.15	0.17	11
Krupp 528	0.024	<0.003	0.015	0.13	2.01	12.54	17.44	2.40	0.061	0.04	0.05	7

Tensile Properties at Room Temperature (transverse)

	$R_{p0.2}$/MPA	R_m/MPa	A(5d)/%	Z/%
Tole SQ	277 - 280	567 - 578	58 - 57	82 - 80
Krupp 528	273 - 280	592 - 598	46 - 47	58 - 59

Characterization of 316L(N) Heats **Tab. I**

	Test No.	Diam.	Med.	Load	Rupture Time	EPS(0)	Elongation	Red.of Area	t1(2/3)	t2(2/3)	creep-rate 1	creep-rate 2
1	KFK/01	4,0	Na	380	570	17,9	27,5		350		3,65e-8	
2	KFK/07	4,0	Na	380	824	13,7	26,3	27,5	456		1,34e-8	
3	KFK/10	4,0	Na	360	1328	18,3	22,2	28,0				
4	KFK/06	4,0	Na	360	1107	15,4	25,5		518		6,94e-9	
5	KFK/03	4,0	Na	330	2875	12,9	21,3	23,0	1947		1,28e-9	
6	KFK/05	4,0	Na	330	2487	10,7	18,4	22,5	1695		2,74e-9	
7	KFK/08	4,0	Na	330	2273	13,0	18,4	21,5	1282		2,22e-9	
8	KFK/04	4,0	Na	320	3547	11,5	20,2	18,5	2130		1,80e-9	
9	KFK/09	4,0	Na	320	3755	11,8	17,4	19,0				
10												
11	KFK/2789	4,0	Air	380	353	14,4	32,0	43,5				
12	KFK/2747	4,0	Air	360	779	14,3	24,5	30,9				
13	KFK/2761	4,0	Air	330	2204	11,4	20,0	23,0				
14	KFK/2716	4,0	Air	320	2158	13,0	19,0	23,0				
15												
16	IA/8.25	4,0	Na	380	726	15,2	26,5	37,0	415		3,08e-8	
17	IA/8.28	4,0	Na	340	1748	10,3	18,7	26,2	1494		6,65e-9	
18	IA/8.29	4,0	Na	300	3412	5,3	15,5	18,3	2500		3,58e-9	
19	IA/8.36	4,0	Na	275	6329	5,4	13,3	12,9	5850		6,89e-10	1,6e-9
20	IA/8.35	4,0	Na	275	13820	5,6			4070		3,82e-10	1,1e-9
21	IA/8.37	4,0	Na	240								
22	IA/8.39	4,0	Na	240	> 27165	4,4			5373	>27165	2,17e-10	1,9e-10
23												
24	IA/6.02	6,0	Na	360	1150	15,7	26,3	30,0	756		5,73e-9	
25	IA/6.04	6,0	Na	275	12801	7,0			6000	10400	3,80e-10	6,5e-10
26	IA/6.09	6,0	Na	240	>14258	4,1			8150	>14258	8,30e-11	
27												
28	IA/8.27	4,0	Air	380	392	17,2	23,8	38,9	272		3,40e-9	
29	IA/8.30	4,0	Air	340	1142	13,4	17,0	29,1	820		8,00e-10	
30	IA/8.31	4,0	Air	300	6704	8,0	11,1	22,4	4550	6125	1,00e-9	3,0e-9
31	IA/8.32	4,0	Air	275	12107	6,0	10,7	17,8	4000	9627	2,65e-10	1,1e-9
32	IA/8.33	4,0	Air	240	>27001	2,4			7788	>27001	2,78e-10	2,7e-10
33												
34	EDF/0890	5,0	Air	360	811	13,6	25,0	35,0	500		1,27e-8	
35	EDF/0001	5,0	Air	360	1092	13,4	23,0	26,0	527			
36	EDF/0002	5,0	Air	330	1945	10,6	19,0	19,0	1710			
37	EDF/0003	5,0	Air	310	3193	8,4	18,0	21,0	2070			
38	EDF/0004	5,0	Air	290	5959	5,5	14,0	21,0	3800			
39	EDF/0976	5,0	Air	290	5150	8,3	15,0	15,0	2235		7,54e-10	
40	EDF/0005	5,0	Air	275	7745	6,1	14,0	22,0	5400			
41	EDF/0977	5,0	Air	265	13348	6,9	15,5	19,0	4475	10136	3,93e-10	1,0e-9
42	EDF/0006	5,0	Air	260	6300							
43	EDF/0874	5,0	Air	240	20221	4,9			8000		2,85e-10	2,9e-10
44	EDF/0007	5,0	Air	240	18204	3,3	12,0	13,0	16700			
45	EDF/0987	5,0	Air	240	16000	4,9			6000		2,22e-10	4,2e-10
46												
47	EDF/81-8	4,0	Na	360	786	14,7	25,0	38,0	437		1,21e-8	
48	EDF/81-7	4,0	Na	310	2535	7,6	23,0	34,0				
49	EDF/81-6	4,0	Na	265	9410	5,6	13,4	19,0				
50	EDF/81-9	4,0	Na	265	10400	9,0						
51												
52	UK/IA1	5,0	Na	340	2312	13,5			1656		1,62e-9	
53												
54	CEGB/PN50	3,8	Na	320	2697	11,6	19,1	27,6	2000		2,69e-9	
55												
56	CEGB/PA50	3,8	Air	320	2752	11,7	18,9	21,0	2022		2,22e-9	
57	CEGB/PA53	3,8	Air	300	4656	9,7	16,5	18,7	2875		1,34e-9	

Dimensions:

Load in MPa — Red. of Area in %
Rupture Time in h — t1(2/3), t2(2/3) in h
EPS(0) in % — Creep rate in 1/sec
Elongation in % — Diameter of specimens in mm

Creep rupture tests performed on 316L(N) - Tole SQ **Tab. II**
performed in air and flowing sodium at 550 °C

	Test No.	Dim.	Med.	Load	Rupture Time	EPS(0)	Elongation	Red.of Area	t1(2/3)	t2(2/3)	creep-rate1	creep-rate2
1	IA/11.03	4,0	Air	310	758	13,2	29,8	33,6	540		3,00e-8	
2	IA/11.06	4,0	Air	280	2946	11,0	30,1	33,4	1840		8,87e-9	
3	IA/11.04	4,0	Air	260	12002	8,2	35,4	48,3	5800	9100	2,49e-9	3,83e-9
4	IA/11.05	4,0	Air	220	19130	6,6			6800	19130	3,92e-10	2,78e-10
5												
6	IA/11.02	4,0	Na	310	918	13,2	27,5	26,6	500		2,40e-8	
7	IA/11.07	4,0	Na	260	3018		17,8	19,5	2820		2,70e-9	
8	IA/11.08	4,0	Na	220	>18956	5,8			14500	>18956	1,28e-10	4,03e-10
9	IA/11.09	4,0	Na	220	>15976	0,6				>15976	1,04e-10	
10												
11	UK/NS4	5,0	Air	360	417	16,5	18,7	40,1	357		2,02e-8	
12	UK/NQ7	9,0	Air	340	718		31,3	34,6				
13	UK/NQ6	9,0	Air	310	1066		18,6	23,3				
14	UK/NS8	5,0	Air	280	2899	8,2	21,6	23,0	2066		5,12e-9	
15	UK/NS9	5,0	Air	260	>26709		23,0	27,5	15602	23470	5,23e-10	9,37e-10
16												
17	KFK/2	4,0	Na	320	476	19,8	28,5	32,0	220		3,85e-8	
18	KFK/3	4,0	Na	300	1449	15,5	27,5	36,1	960		1,27e-8	
19	KFK/4	4,0	Na	290	1636	11,5	33,0	35,5	1015		1,89e-8	
20	KFK/5	4,0	Na	280	2763	11,3	35,0	39,5	1680		1,03e-8	
21	KFK/1	4,0	Na	270	6313	10,3	35,5	40,5	3320	4010	4,20e-9	5,82e-9
22	KFK/7	4,0	Na	250	15480	8,6	33,0	40,0				

Creep rupture tests performed on 316L(N) - Krupp cast 528 performed in air and flowing sodium at 550 °C — Tab. III

	Test No.	Diam.	Med.	Load	Rupture Time	EPS(0)	Elongation	Red.of Area	t(2/3)	creep-rate
1	EDF/0862	5,0	Air	360	223	14,6	33,0	33,0	131	1,10e-8
2	EDF/0872	5,0	Air	290	1874	8,2			1810	3,24e-9
3	EDF/0861	5,0	Air	265	7605	6,8	17,0	19,0	4400	1,29e-9
4	EDF/0877	5,0	Air	240	>33500	1,5			19051	4,08e-10
5										
6	EDF/81S04	4,0	Na	360	94	13,1	30,2	39,7	76	2,28e-7
7	EDF/81S02	4,0	Na	360	159	13,8	26,6	36,0	119	8,29e-8
8	EDF/81S08	4,0	Na	330	353	11,6	25,8	34,0	230	
9	EDF/81S12	4,0	Na	310	732	9,0	19,0	23,4	575	1,80e-8
10	EDF/81S10	4,0	Na	265	2782	6,0	13,9	21,1	2325	2,40e-9
11	EDF/81S11	4,0	Na	265	3537	6,0	13,8	14,4	3146	1,26e-9
12	EDF/81S07	4,0	Na	240	11447		16,2	23,4		

Dimensions:

Load in MPa	Red. of Area in %
Rupture Time in h	t1(2/3), t2(2/3) in h
EPS(0) in %	Creep rate in 1/sec
Elongation in %	Diameter of specimens in mm

Creep rupture tests performed on 316L(N) - Tole SQ in the sensitized condition (600 °C, 1000 h) in air and flowing sodium at 550 °C — Tab. IV

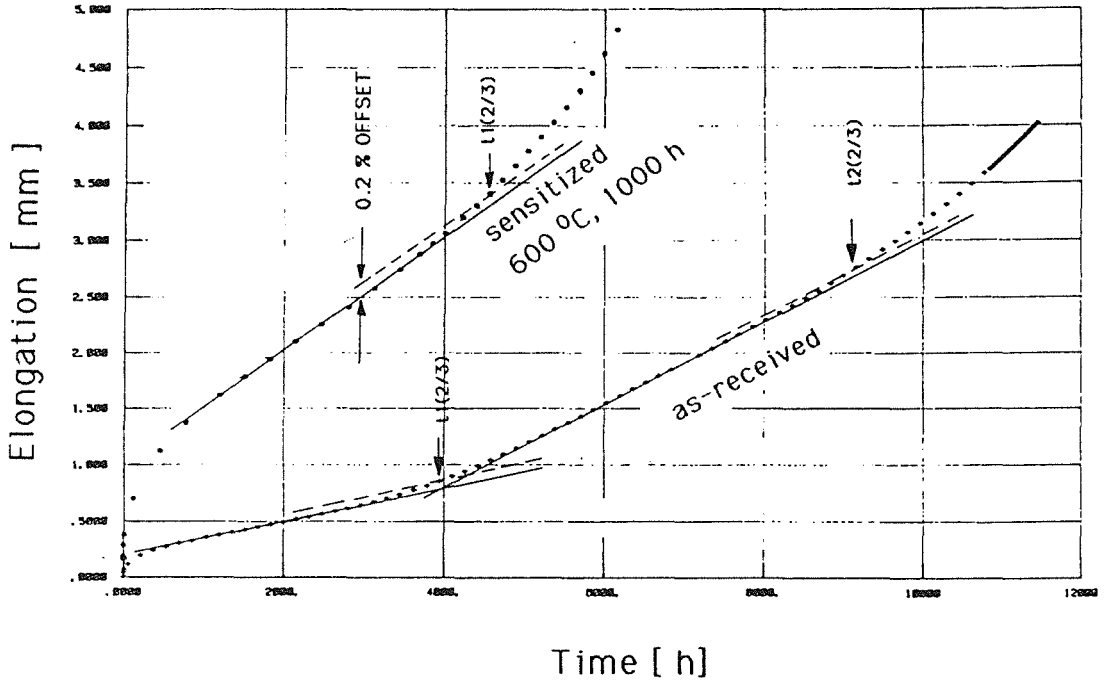

Fig. 1 Creep curves of 316L(N)-Tole SQ, measured in the as-received and sensitized (600 °C, 1000 h) condition at 550 °C in air at 265 MPa (EdF-Data)

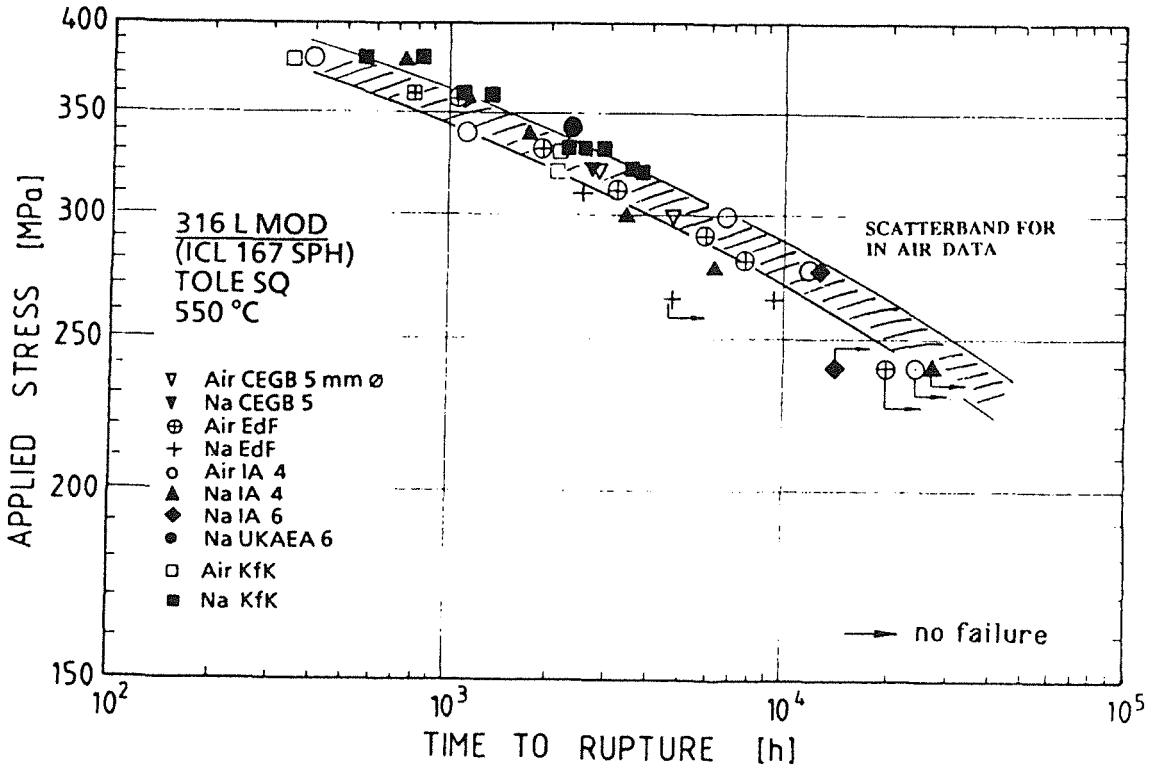

Fig. 2 Time to rupture of 316L(N)-Tole SQ measured in air and flowing sodium at 550 °C

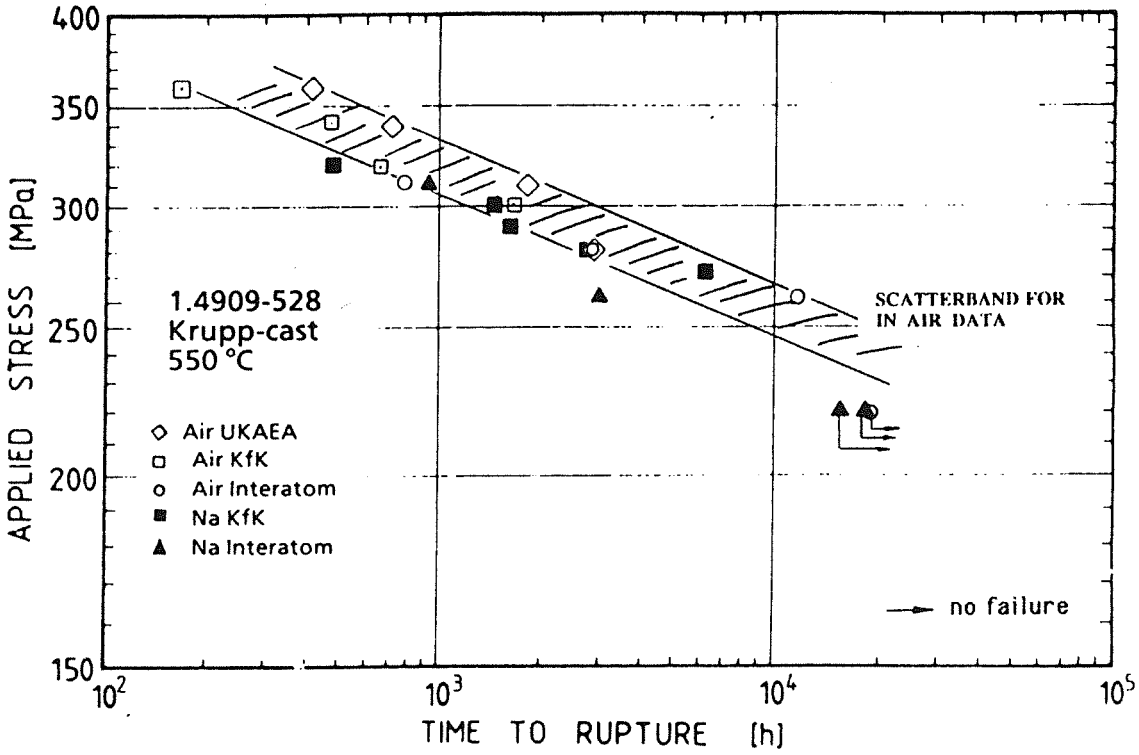

Fig. 3 Time to rupture of 316L(N)-Krupp cast 528 measured in air and flowing sodium at 550 °C

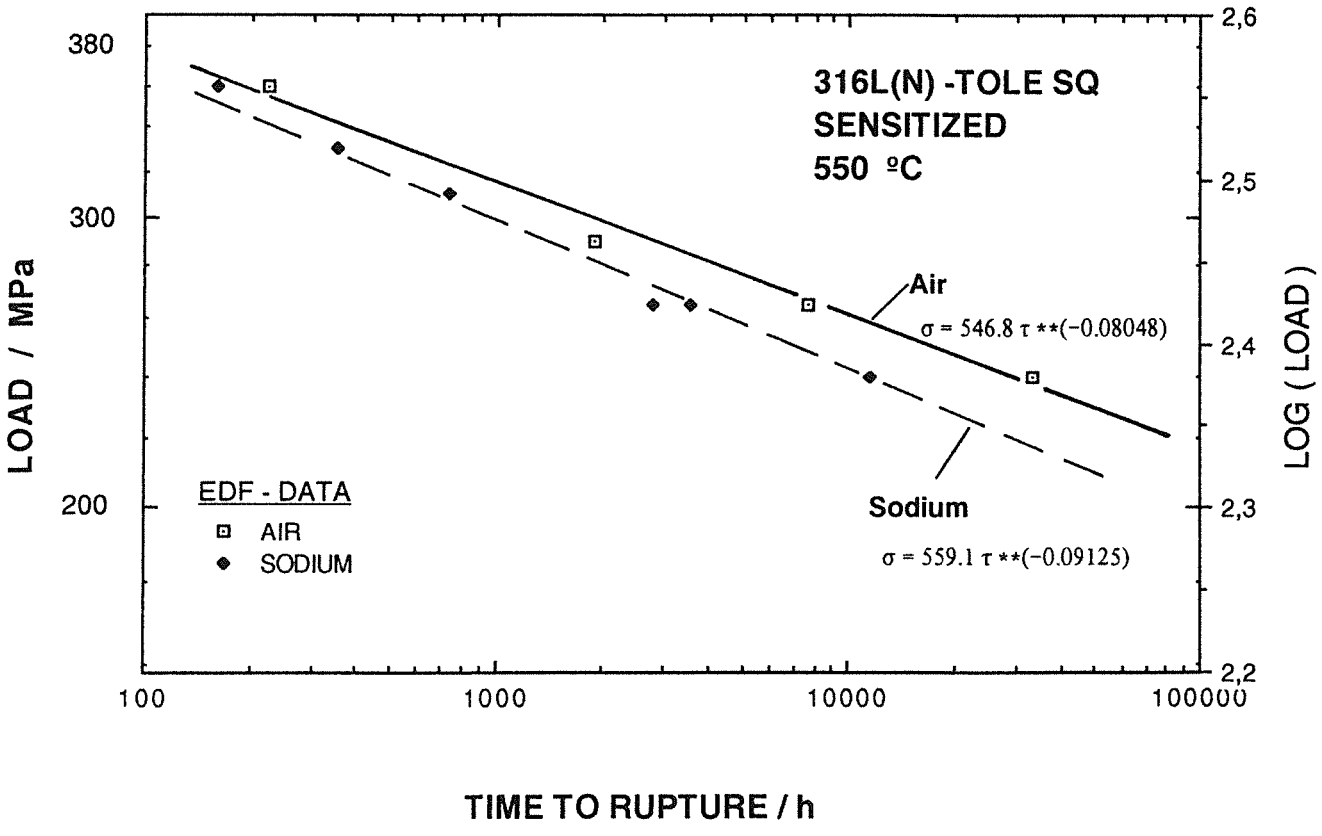

Fig. 4 Time to rupture of 316L(N)-Tole SQ measured in the sensitized (600 °C, 1000 h) condition at 550 °C in air and flowing sodium (EdF data)

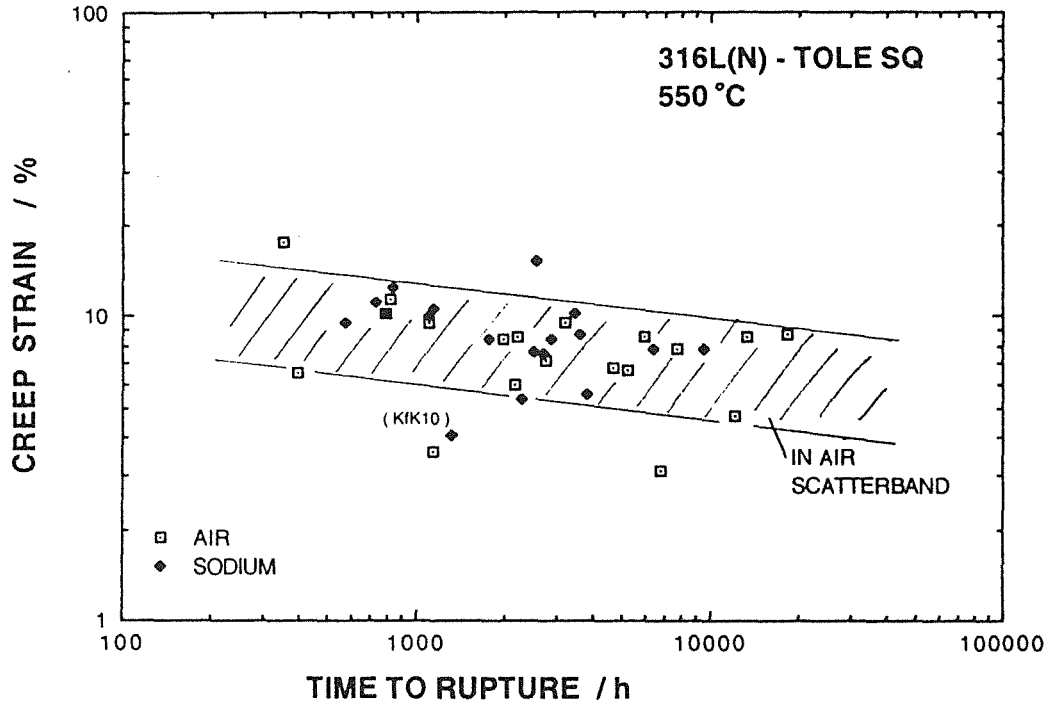

Fig. 5 Creep strain (total elongation - loading strain) for 316L(N)-Tole SQ measured in tests in air and flowing sodium at 550 °C

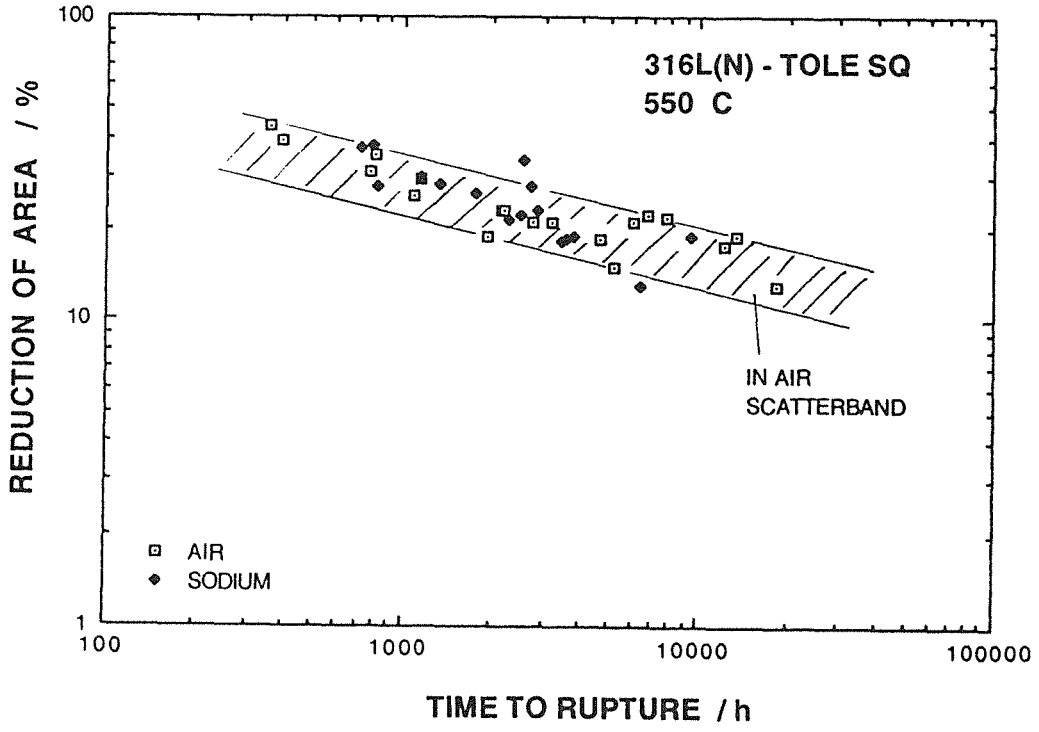

Fig. 6 Reduction of area for 316L(N)-Tole SQ measured in tests in air and flowing sodium at 550 °C

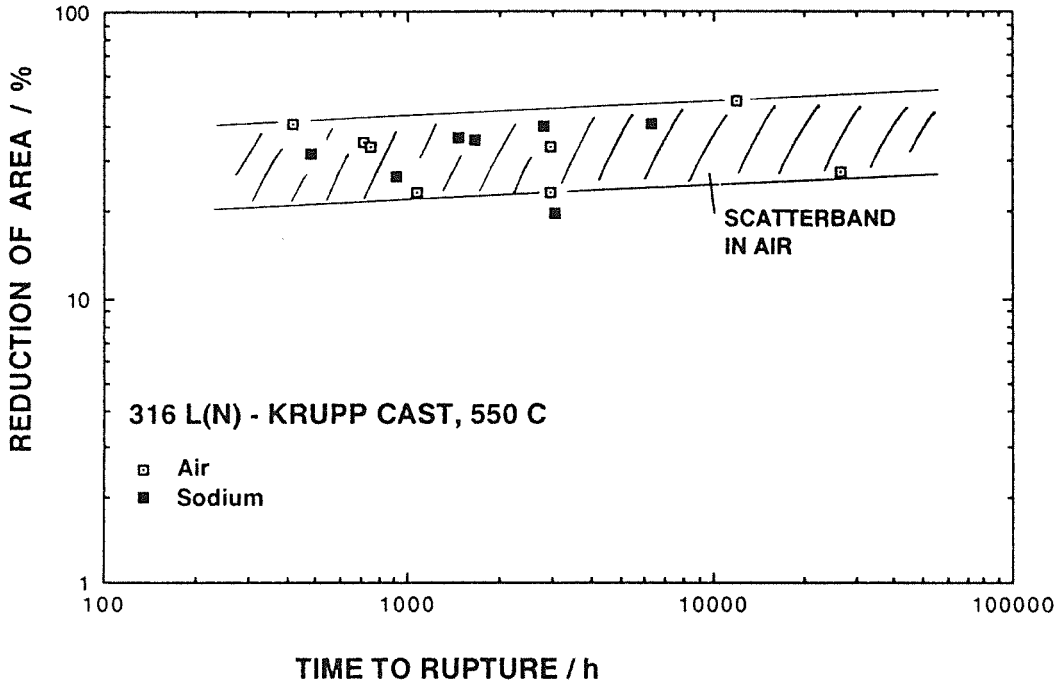

Fig. 7 Reduction of area for 316L(N)-Krupp cast 528 measured in tests in air and flowing sodium at 550 °C

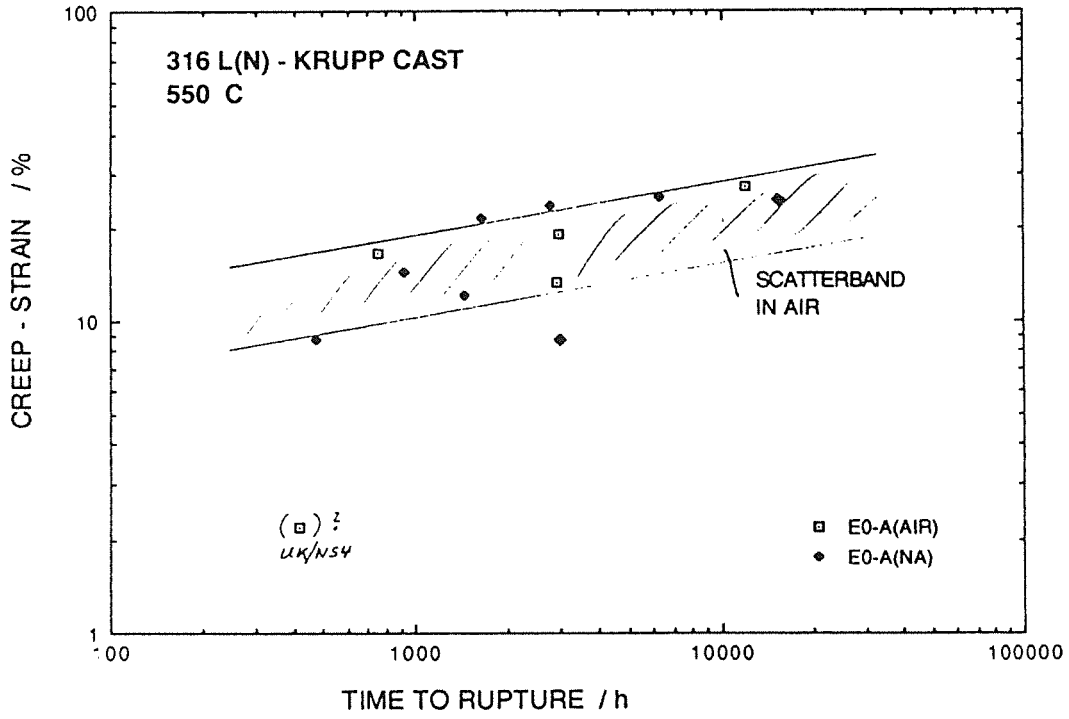

Fig. 8 Creep strain (total elongation - loading strain) for 316L(N)-Krupp cast 528 measured in tests in air and flowing sodium at 550 °C

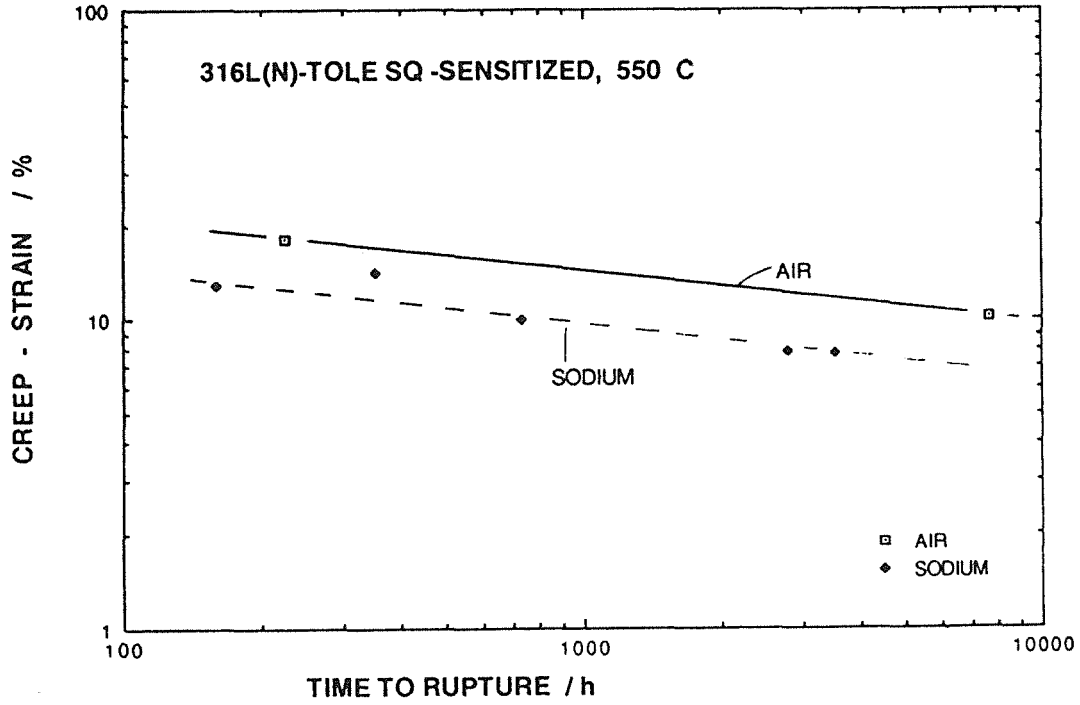

Fig. 9 Creep strain (total elongation - loading strain) for 316L(N)-Tole SQ tested in sensitized condition (600 °C, 1000°) in air and in flowing sodium at 550 °C (EdF-data)

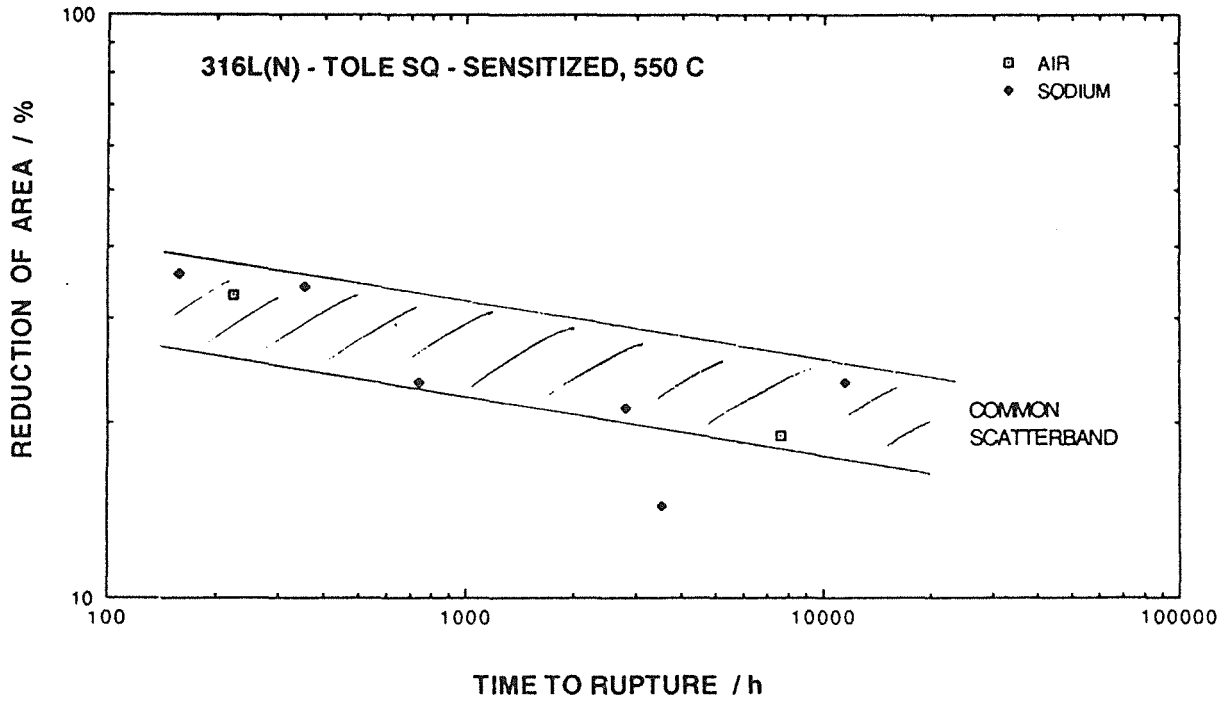

Fig. 10 Reduction of area for 316L(N)-Tole SQ tested in sensitized condition (600 °C, 1000 h) in air and flowing sodium at 550 °C (EdF data)

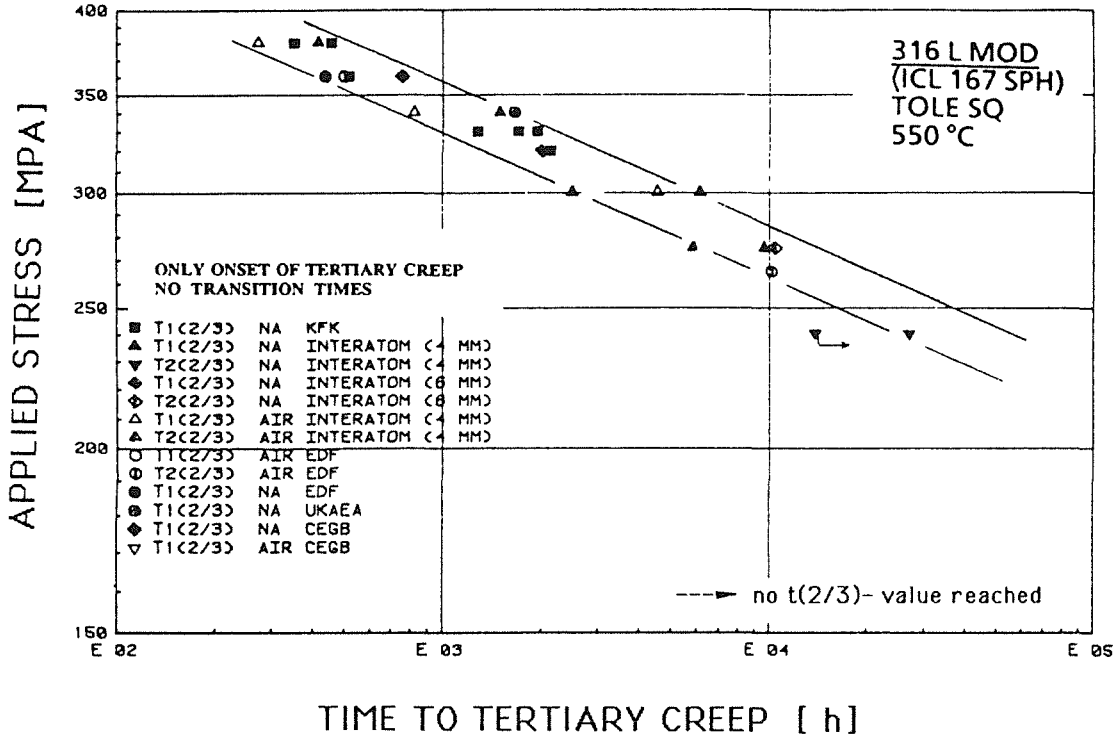

Fig. 11 Time to onset of tertiary creep for 316L(N)-Tole SQ measured in air and flowing sodium at 550 °C

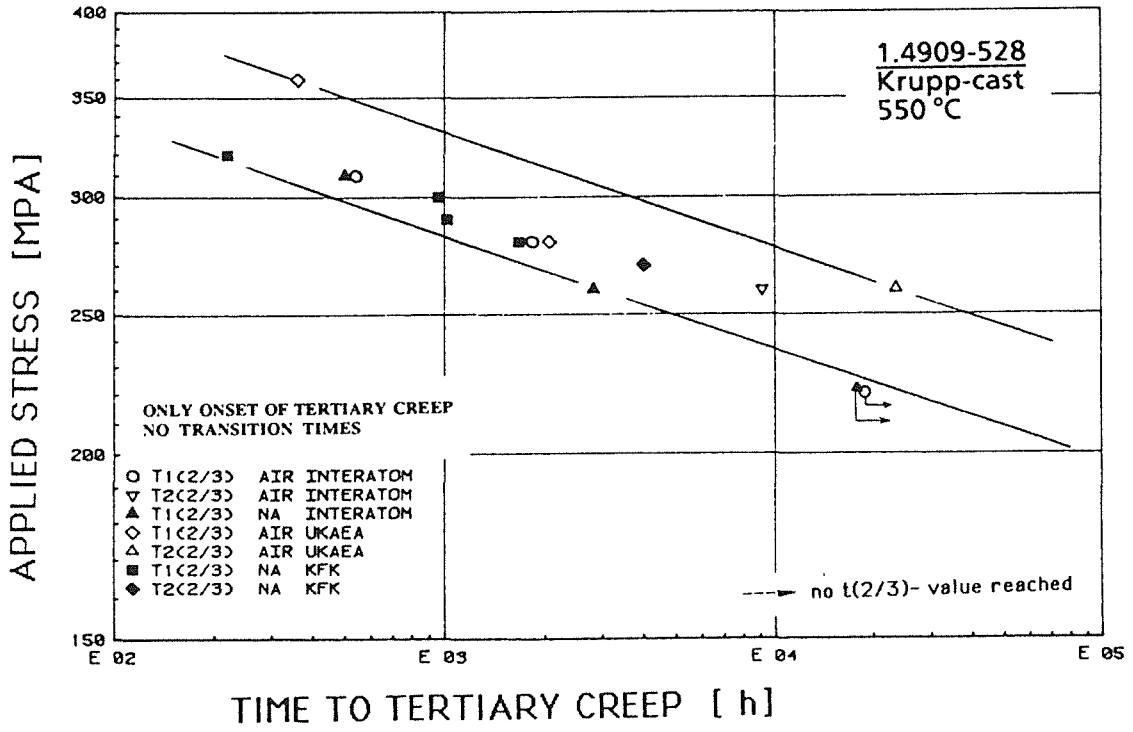

Fig. 12 Time to onset of tertiary creep for 316L(N)-Krupp-cast 528 measured in air and flowing sodium at 550 °C

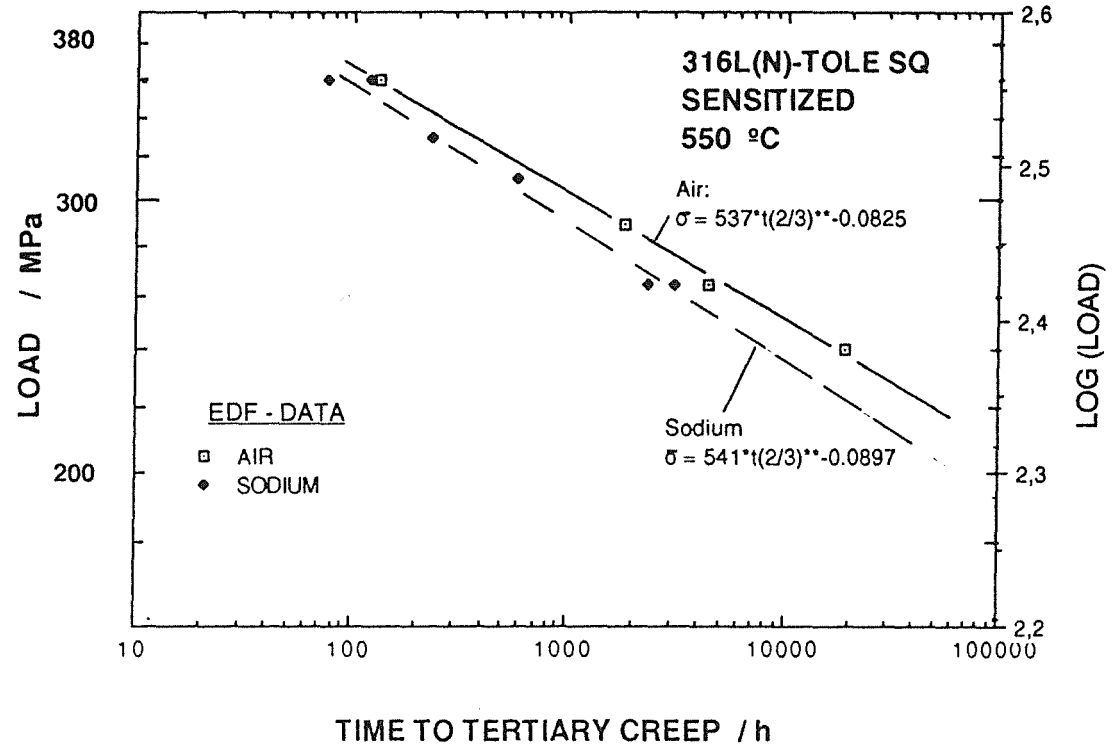

Fig. 13 Time to onset of tertiary creep for 316L(N)-Tole SQ, sensitized (600 °C, 1000 h) condition, measured in air and flowing sodium at 550 °C (EdF data)

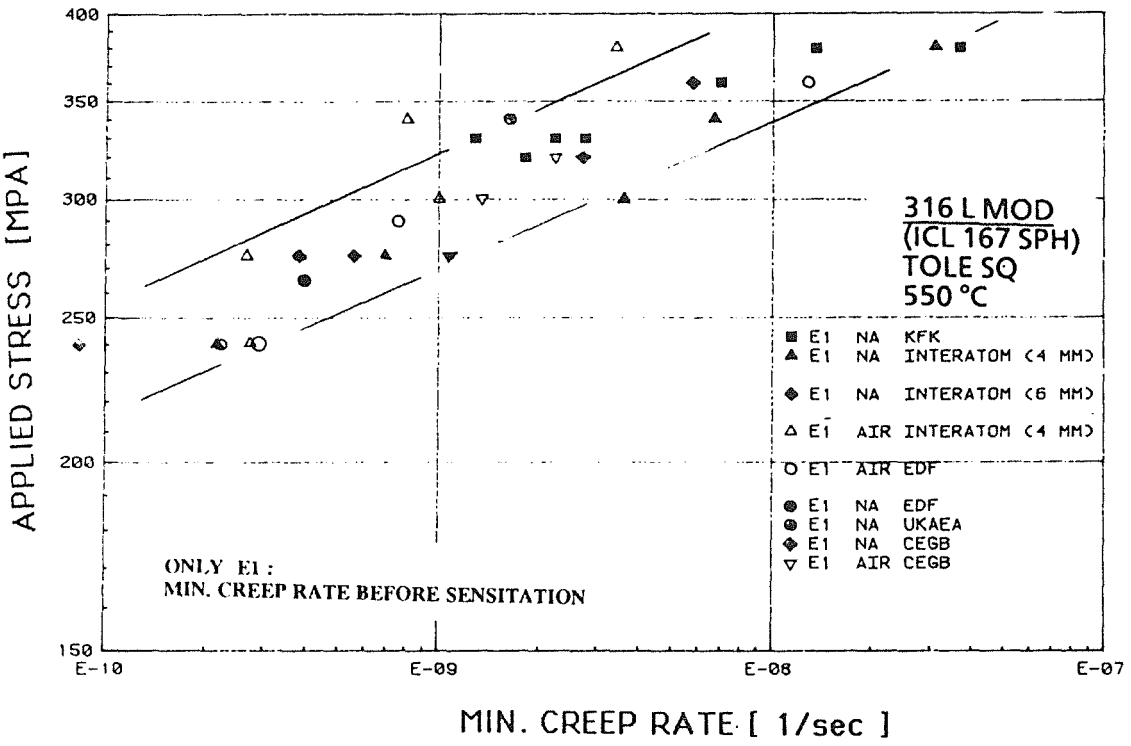

Fig. 14 Minimum creep rate for 316L(N)-Tole SQ measured in the first phase of secondary creep in air and flowing sodium at 550 °C

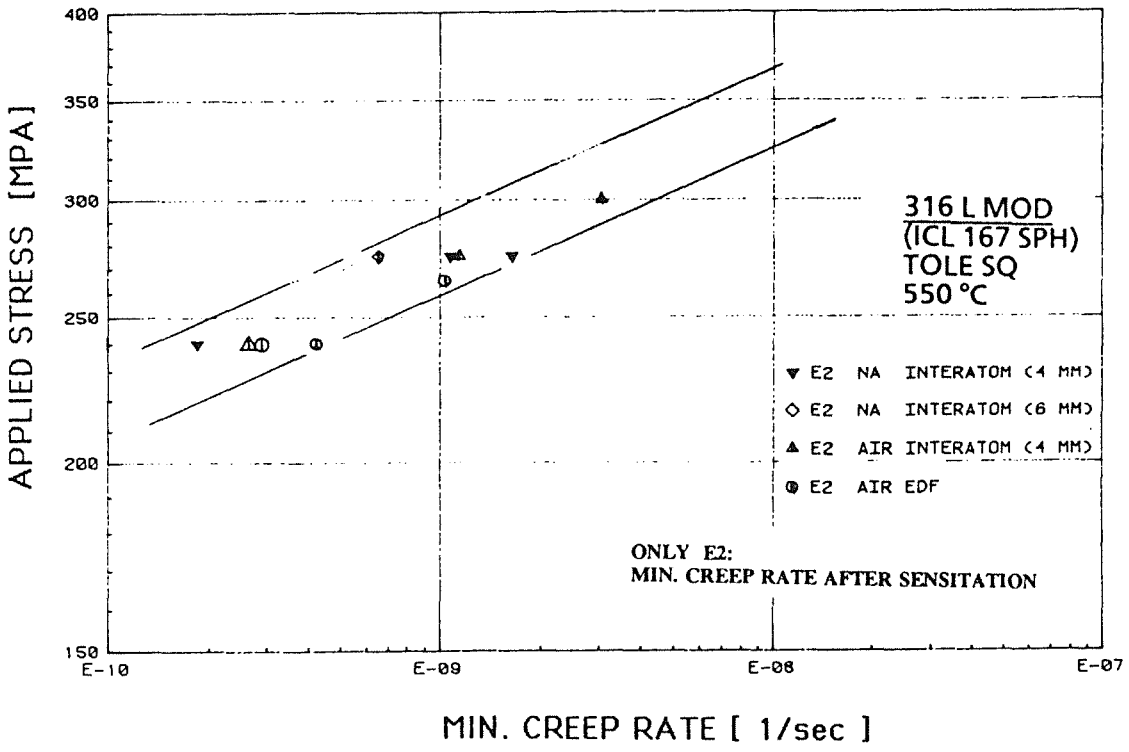

Fig. 15 Minimum creep rate for 316L(N)-Tole SQ measured in the second phase of secondary creep in air and flowing sodium at 550 °C

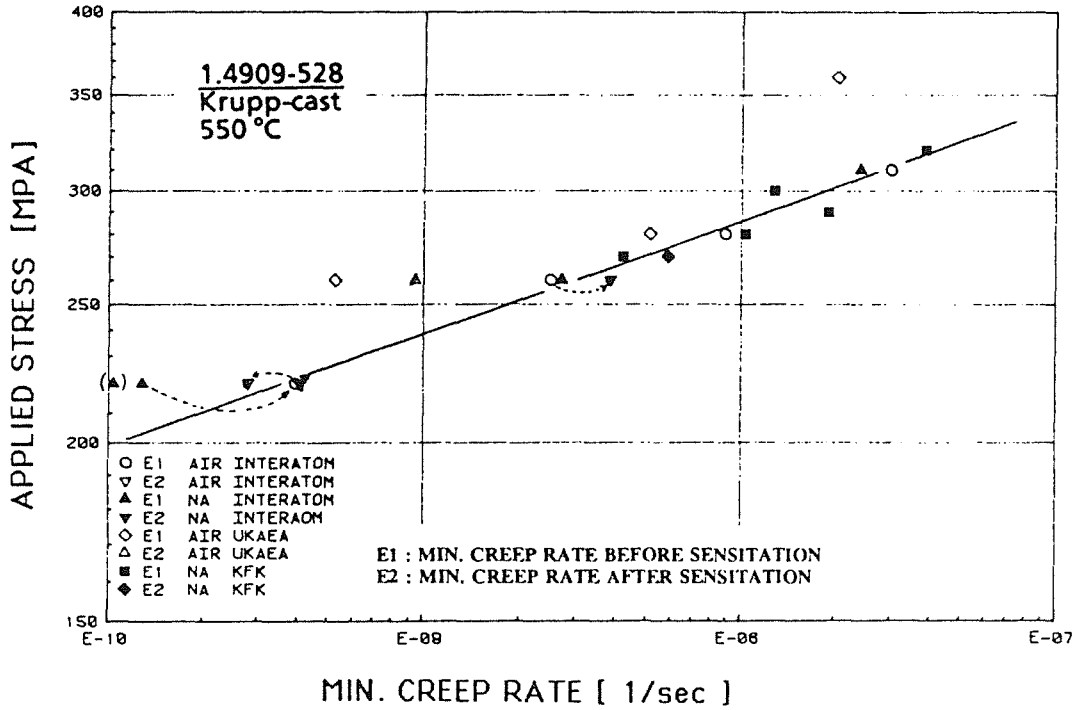

Fig. 16 Minimum creep rate for 316L(N)-Krupp cast 528, measured at 550 °C in air and flowing sodium.
Transitions of min creep rates from the first to the second phase of secondary creep are indicated by arrows

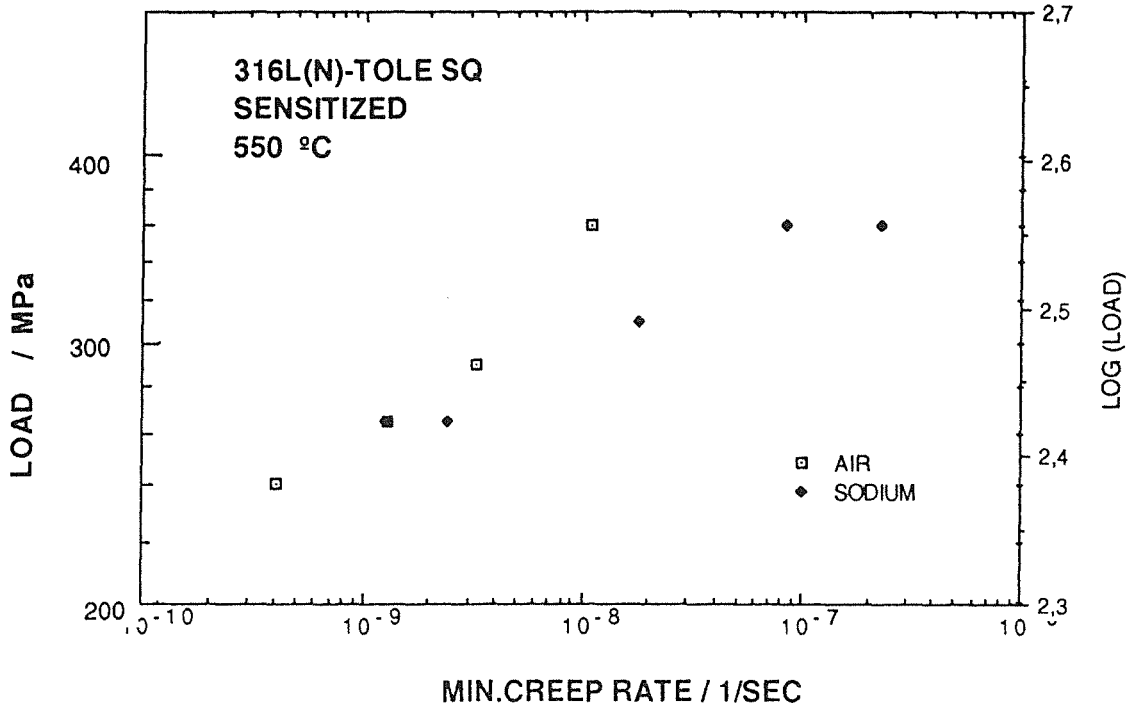

Fig. 17 Minimum creep rate for 316L(N)-Tole SQ, sensitized (600 °C, 1000 h) condition, measured in air and flowing sodium at 550 °C (EdF-data)

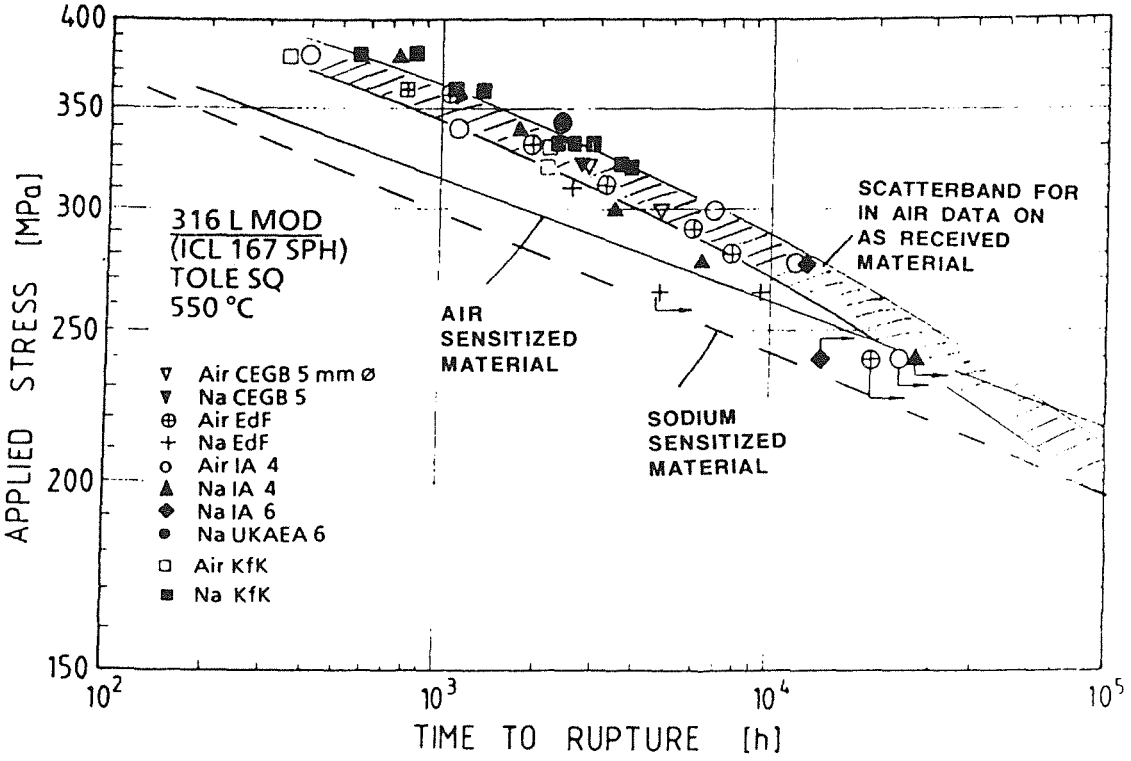

Fig. 18 Comparison of times to rupture measured on 316L(N)-Tole SQ, tested in the as-received and sensitized (600 °C, 1000 h) condition

THE BEHAVIOUR OF NOTCHED WELDMENTS IN LIQUID SODIUM UNDER CREEP STRESS

H.U. Borgstedt and G. Frees

Kernforschungszentrum Karlsruhe
Institute for Material Research III
D-7500 Karlsruhe 1, Postfach 3640, Germany

Abstract

The influence of flowing sodium of 550°C on the creep-rupture behaviour of welded specimens of the austenitic steel AISI 304 (X6 CrNi 18 11) containing a sharp ellipsoidal pre-crack rectangular to the gage length in the welded zone is studied in a sodium loop applying stresses in the range of 140 to 200 MPa.

The life-times of the specimens tested in both media, air and sodium, can be related to the residual stresses in the plane of the pre-crack. The sodium of high purity reduces the time-to-rupture of the welded specimens containing a pre-crack. Strain and fracture are concentrated in the notched weldment. The fracture mode is related to the orientation of the welded layers.

However, the loss of rupture strength (related to the residual stress) is smaller than in preceding in-sodium creep-rupture tests with base material of the same steel, however, from a different batch and in sodium of a lesser degree of purity. A possible mechanism of the influence of sodium and its corrosive action on the crack formation during the creep deformation is discussed.

1. Introduction

An influence of flowing liquid sodium on the creep-rupture behaviour of the structural material of the SNR 300, X6 CrNi 18 11 (AISI 304) at 550°C has been observed in earlier tests [1,2]. In sodium tests, the time to rupture is reduced and the fracture is preceded by the formation of numerous intergranular cracks. Though welded specimens behave differently, there is no particular influence of the flowing sodium on the time to rupture. The fracture occurs in the large grain area at both sides of the weldment, and they seem to be the weak points in the specimens [3]. However, the reduction of the life-time of the specimens is smaller in the case, in which the specimens contain a welding. Defects in the piping of sodium circuits are often located in the surrounding of welded joints. This may be due to the fact that material defects are more often located in the weldings than in the base material. Defected weldings may fail by a faster growing of flaws in the case of superimposure of stress and the action of sodium. To get a more detailed information on the behaviour of defected weldments, a programme was initiated to test the creep-rupture behaviour of welded specimens of the steel X6 CrNi 18 11 in flowing liquid sodium at 550°C. The results of this experimental program will be presented here.

2. Material and fabrication of specimens

The 20 mm thick plate of the austenitic steel X6 CrNi 18 11, the composition of which is shown in the Table 1, was cut into stripes. Two of the stripes were prepared for an X-welding by machining one edge in angles of 30°. They were welded together applying the WIG process. The joint was filled with eleven layers. During the filling, the origins for defects were brought in by drilling a fine hole up to 3.5 mm from the centre of the plate. At the tip of it we placed a grain of zirconia and closed the cavity before the joint was completely filled up. The particles could be located by X-ray techniques. We cut the rough specimens of 8 mm diameter and developed flaws by oscillating them in the atmosphere. The position and size of these pre-cracks we estimated by eddy current methods. Finally, the creep-rupture specimens of 6 mm diameter and 30 mm gage length were fabricated in a way, that the weldments formed the central part of the gage length. The size of the flaws produced in that way, is estimated by measuring the length of the surface crack. The flaws in the 60 specimens of this testing programme were in the order of 10 to 35 % of the cross section, a typical example is shown in Fig.1.

3. Experimental methods

The creep rupture- tests is air were performed in conventional creep machines. The in-sodium programme could be carried in the CREVONA loop, which has four test sections for the exposure of cylindrical creep specimens under static load. Fig.2 shows the design of the in-sodium creep machine and the mode of loading and measuring the strain out of the sodium environment. The load cell and the extensometers are located below the heated test section to avoid their heating up. The sodium temperatures at the input and the outlet and also the flow velocity of the sodium were estimated in each of the four sodium lines connected

to the testing devices. The flow velocity was maintained at 3 m/s. A by-pass line continuously passed a cold trap at 125°C. Oxygen, carbon and metallic element concentrations were estimated by probes or several times analysed after taking out sodium samples. The impurity concentrations are listed in Table 2.

The specimens were degreased and then screwed into the specimen-holder of the test sections, which were closed under flowing argon after removing the remaining atmospheric gases by evacuation. Afterwards the test sections were heated to the temperature of the main loop (about 350°C), and the sodium passed in after opening the valves. The sodium reduced and washed away all traces of oxides, hydroxides and carbonates still present in the test sections. After a purification period of one day the temperature was raised to the desired value of 550°C, and we started the test by loading the creep machine after reaching thermal equilibrium. The load was slowly increased to the value producing the desired stress on the specimen. The single test sections could be emptied or refilled during the loop operation.

The nominal stress applied was 140, 160, 180, and 200 MPa. Taking into account the remaining cross section in the plane of the pre-crack, the effective stress as residual stress was calculated. After rupture the specimens were taken out of the test sections and examined for their metallurgical changes by several techniques.

4. Test results

After measuring the time to rupture of about 60 specimens we compared the values gained in the in-air and in-sodium tests by selecting groups of specimens in which the applied stress and the size of the pre-cracks were fairly agreeing. Within these groups the residual stress values were of the same order. The creep curves of such groups are used to evaluate the differences of the creep-rupture behaviour in both environments. The Fig. 3 compares the creep curves of a typical set of such specimens. The specimens exposed to the flowing sodium crack after a shorter time in all cases. The creep curves are measured over the whole gage lengths of the specimens. They do not correspond to the creep in the area surrounding the pre-cracks, and the apparent differences of the creep curves cannot be used to estimate secondary creep rates of the strained area of the specimens.

The time-to-rupture of specimens tested in both environments can be related to the residual stress in the plane of the pre-cracks. This is demonstrated by Fig. 4. The relationships are different for tests in air (eq. 1) and in sodium (eq. 2), indicating the decrease of the life-time due to the action of the liquid metal. The equations fit best the results of all creep-rupture tests of the programme.

$$\log_{10}\tau_R(MPa) = 2.479 - 0.0353 \cdot \log_{10} t_B(h) \tag{1}$$

$$\log_{10}\tau_R(MPa) = 2.541 - 0.0649 \cdot \log_{10} t_B(h) \tag{2}$$

The time-to-rupture of some specimens without pre-crack in the weldment tested in the sodium loop is only slightly higher than the values deduced from eq. 2.

The values of strain-to-rupture of the specimens in the both environments do not differ, since only a small part of the gage length contributes to the measured strain. Also the reduction of area seems to be independent on the test medium.

The path of the fracture seems to be influenced by the relative situation of the grains and the welded layers in respect to the pre-crack. Cavities and side cracks can be detected in the grain boundaries along the long dimension of the grains crossing the layers, if the grains are in parallel orientation to the plane of the pre-crack. In the same way the boundary between two welding layers can be the path of the crack development. Therefore, the crack surfaces can be of different topographic appearance. In the case of straight parallel orientation of the grains and the pre-crack plane, the fracture develops in this plane, the creep-crack occurs then as the continuation of the pre-crack. On the other hand, pre-crack and fracture are in different planes, if the orientation of grains and layers is not in the plane of the pre-crack. However, all these different fracture modes can be observed in specimens tested in air as well as in sodium.

One of the specimens, removed from the sodium loop before the onset of the tertiary creep, gives a picture of the development of the creep -cracks, which cause finally the fracture. In this specimen the pre-crack is opened to a width of 0.3 mm, and from both ends of it some small cracks are growing into the highly deformed weldment.

The fracture mode of the pre-cracked specimens differs completely from that of some reference specimens, which contain intact weldments without any pre-cracks. Though having the fracture life predicted by eq. 2, they develop small cracks along the whole gage length. The fracture is located in the welding zone. However, also in the base material one can see many cracks. The area around the fracture contains a high concentration of such cracks of intergranular character.

The fracture surfaces can be devided into three parts, the initial pre-crack, the surface formed by the growing of the creep cracks during the exposure to the sodium, and the residual fracture in an area of high deformation. The last part is of transgranular mode. In many cases the second part has the same appearance of the fracture surface as the pre-crack. Also a complete change of the fracture morphology can be observed depending on the orientation of the grains and welding layers as mentioned above.

The metallographic study does not show any phenomena of the sodium corrosion of the steel, though under the parameters in the sodium loop the specimens should lose 0.0005 mm/year of their radius due to the solution of material by the liquid metal. Chemical analyses of foils of the same type of steel indicate a slight depletion of carbon and nitrogen out of the specimens. The appearance of their surfaces reveals that there has been the sodium-steel chemical exchange, the surface seems to be completely reduced.

5. Discussion and results

As indicated by eq. 1 and 2 sodium reduces the time-to-rupture or the creep-rupture strength of welded steel 1.4948 (AISI 304) with pre-cracks. However, the loss of creep-rupture strength observed in these tests is smaller than in the earlier tests with base-material of another batch of the steel [1]. The effect of sodium on the creep-rupture behaviour of the

pre-cracked specimens is evident even in the absence of traces of heavy metals dissolved in the liquid sodium. The presence of up to 20 ppm of lead, tin and zinc in the preceding creep-rupture tests in sodium was claimed to be the reason for the loss of strength. Indeed, the effect was smaller in the very pure sodium, in which the notched specimens were tested. Different batches of the steel show some differences of the creep-rupture strength, and also the sodium influence might be different.

Some of the specimens with more than 30 % part of the cross sections pre-cracked and tested with a relatively low load are at the lower border of the scatter-band of the values, which are taken to calculate the eq. 2. From this we can conclude that the effects are somewhat influenced by the size of the remaining cross section. Sodium influences the mechanical behaviour of the specimens by surface reactions. A region of a small cross section has a high relationship of surface to volume. Therefore, an influence of sodium of the time-to-rupture of such specimens is not surprising. On the other hand, these values are influencing the constants of eq. 2. If we would not include such results into the estimation of the equation, the difference between the eq. 1 and eq. 2 would be much smaller. All the pre-cracks in the specimens in this programme represent a much larger portion of the cross section than the size of the defects that can be safely detected in a component of the fast reactor. We can therefore conclude that the evaluation of our tests leads to conservative relationships.

If we calculate nominal creep rates from the creep curves gained in the tests in air and in sodium, we get different results. It seems that the creep rate in sodium may be somewhat faster than in air. However, we have to consider that the strain is concentrated to a very small area of the gage length. The effects cannot be measured exactly. It seems that a discussion of the creep rates and also the creep strain needs more precise information on the area deformed and its relationship to the whole gage length. The virtual creep rate in the in-sodium tests can be influenced by the development of cracks, which may not be the case in the control tests.

However, there is one effect of sodium on the steel, which can cause a slight loss of strength even in relatively short periods of time. The very pure sodium of our loop causes, as mentioned above, a slight decarburization and denitriding. The intergranular character of the cracks in the tests of base material indicates that the sodium dissolves grain boundary material as precipitated carbides or carbonitrides [2], thus forming germs of cavities between the grains. The cavities formed in that way may be the weak points of the structure, and from here grain boundary cracking starts. Such effects may not be evident, if the sodium does not leach the interstitial elements from the steel. Further investigations have to be done to verify the proposed mechanism of the sodium impact on the high temperature strength of stainless steel. If the action of the liquid metal would take this path, there would be several possibilities to influence the sodium as well as the steel in order to suppress the effect. One can change the precipitates in grain boundaries by changing the thermomechanical treatment of the steel. It is also possible to raise the potentials of carbon and nitrogen in the sodium in order to avoid leaching of the elements and dissolution of grain boundary precipitates.

Acknowledgements

We gratefully acknowledge the contributions of Dr.H. Grützner, Institute for Applied Material Research, Bremen, to this work. We express our thanks to Dr.Ch. Adelhelm, Mrs. Bennek-Kammerichs, and Mrs. Z. Peric for their assistance, and Mr. Drechsler, Mr. Kleiber and Mr. Wollensack for the operational and testing work with the CREVONA loop.

References

[1] H. Huthmann, G. Menken, H.U. Borgstedt, N. Tas,
"Influence of Flowing Sodium on the Creep Rupture and Fatigue Behaviour of Type 304 ss at 550°C",
Second Int. Conf. on Liquid Metal Technology in Energy Production,
Conf.- 800401-P2, p.19-33

[2] H.U. Borgstedt, G. Drechsler, G. Frees,
Z. Werkstofftechnik 12 (1981), 250-256

[3] G. Frees, H.U. Borgstedt, G. Drechsler,
"Natriumeinfluß auf das Zeitstand-und Kriechverhalten von geschweißten Proben des SNR-Strukturwerkstoffes X6 CrNi 18 11 (Werkstoff-Nr. 14948)"
DVS-Bericht Band 75"Schweißen in der Kerntechnik", 1982, p.272-275

Table 1: Composition of the Stainless Steel X6 CrNi 18 11 (batch 326)

Element	C	Si	Mn	P	S	Cr	Ni	Mo	Ti	N
Conc. (w-%)	0.068	0.43	1.89	0.15	0.005	18.92	10.49	0.04	0.01	0.08

Table 2: Concentrations of Impurities in the Sodium during the Loop Operation

Element	O	C	Fe	Cr	Ni	Mn	Ca	Zn	Pb	Si	Sn	Cu
Conc. (w-ppm)	2.5	0.15	4	4	0.4	0.12	3	<1	<4.5	<0.75	<0.9	<0.5

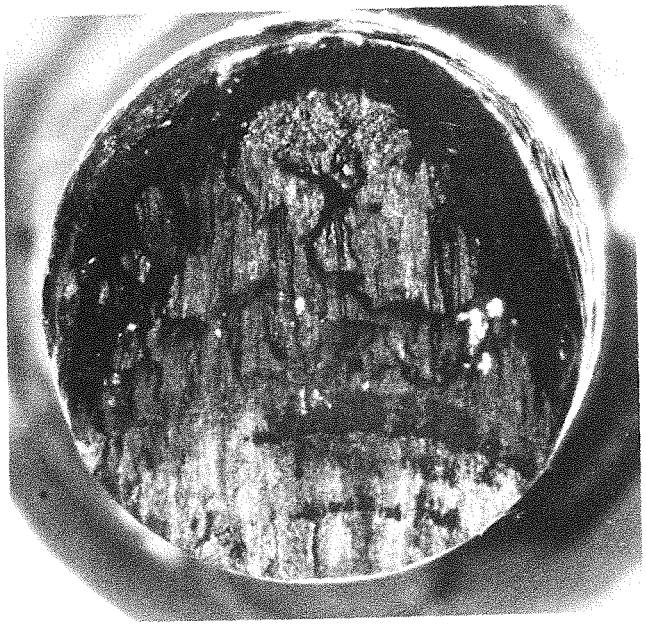

Fig. 1: Crack surface of one of the specimens showing the size of the Pre-crack

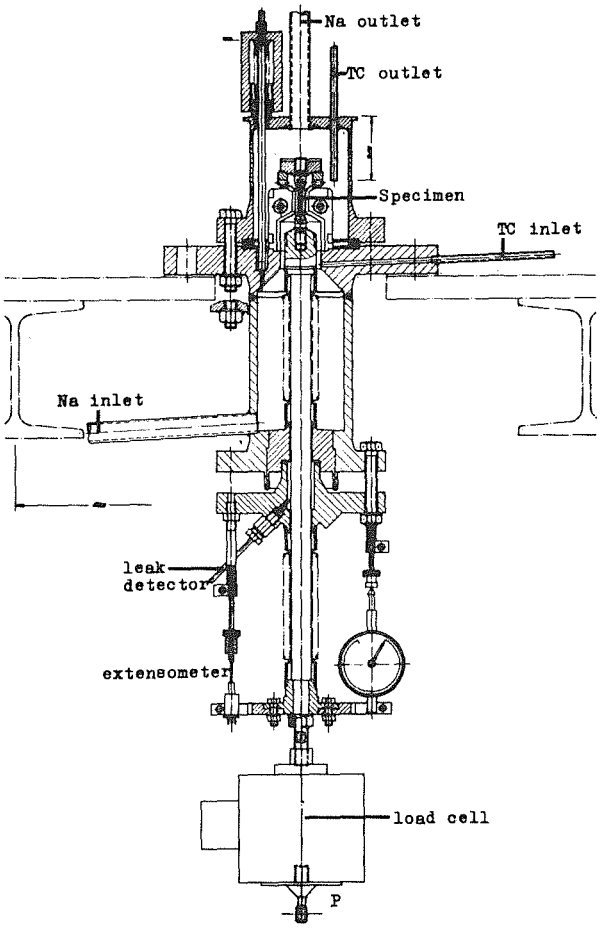

Fig. 2: Creep-rupture test section of the sodium loop CREVONA (sectional view)

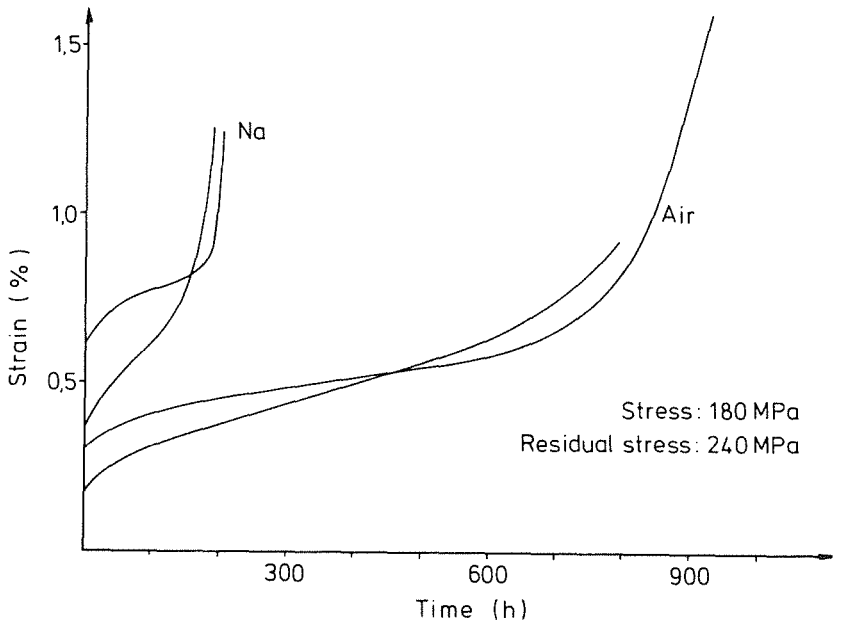

Fig. 3: Comparison of some creep curves or tests in air and in sodium at comparable residual stress (pre-cracked specimens)

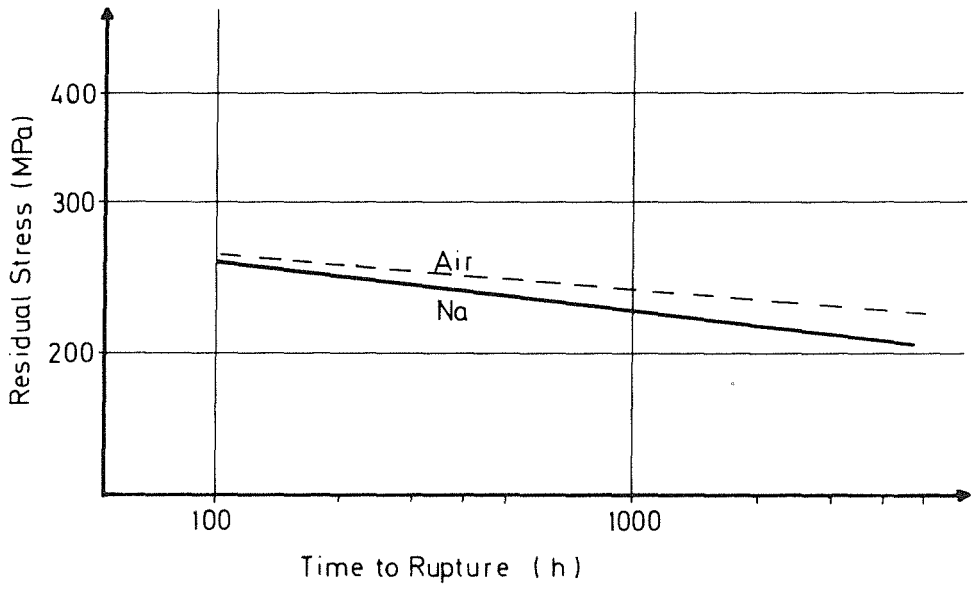

Fig. 4: Time-to-rupture as a function of the residual stress in the pre-cracked specimens

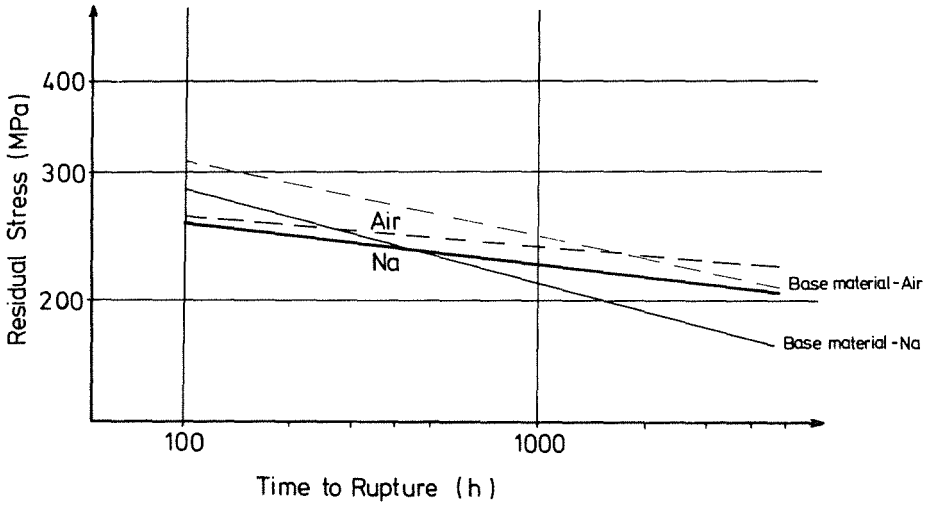

Fig. 5: Comparison of the results with earlier findings (base material)

Stress corrosion of type 304 stainless steel in molten NaOH/Na mixtures

by G.Menken, W.Dietz
INTERATOM
Bergisch Gladbach, Germany

Abstract

NaOH may be formed under special conditions on components during the ingress of water vapour in a sodium system in the cover gas region. Experiments were performed in order to quantify the corrosion effects, which were produced in stressed samples due to the reaction with a limited amount of dry NaOH on the surface during the exposure under sodium vapour conditions in the temperature range between 350°C and 560°C. The experiments showed that the amount of NaOH and the duration of exposure was important for the corrosion effects. The highest effects were found, when the H_2/H_2O containing gas reacts near the sodium level at low temperatures above the melting point of NaOH (ca 320°C), i.e. when a consumption of NaOH either by evaporation or by the reaction with the metal was negligible. If there exist a sodium vapour pressure in equilibrium with 450°C, NaOH surface films are not stable in the presence of 50 vpm H_2O and corrosion reactions are limited. At much higher temperatures of 560°C any NaOH films are removed either by evaporation or by a surface reaction and even at 50 vpm H_2O the formation of new NaOH was not possible if sodium at 560°C was available.

1 Introduction

The occurance of NaOH in LMFBR-systems is normaly avoided by the effort for sealing properly all sodium containing system components against air or water environments. The risk of high corrosion rates or stress corrosion cracking is well known for structural materials under wet NaOH conditions. It was the aim of the following experiments to study the stress corrosion effects under conditions with limited moisture supply in Na/NaOH mixtures, as well as with a limited quantity of this mixture as a surface film on stressed samples.

From metallografic techniques as well as investigations on cover gas components it was known, that NaOH produced a selective attack on the delta ferrite in the steel, especially the weldments. It was therefore needed to investigate the corrosion effect on weldment type specimens.

Different sample geometries had to be tested in order to see if they were able to show stress corrosion effects under such high temperatures (560°C), at which relaxation might reduce the stresses.

2. Qualification of the sample geometry

A specimen type with "realistic" internal stresses of a weldment was of interest for the test programm. U-bent specimen, disk specimen and C-ring specimen were tested in standard $MgCl_2$ solution, ASTM G 36-73, but only C-ring samples showed reproducibly a crack formation. The C-ring sample was then further qualified. The sample was constructed in accordance to ASTM G38, [outer diameter 34 mm, thickness 2.4 mm] as shown in figure 1. The circumferential weld was made in a groove of 2x6 mm of a bar with 34 mm diameter. To generate a C-ring, the outer diameter was reduced to 34 mm and a inner bore was machined into the bar. In the tensile machine the elastic-plastic deformation was investigated and with these data a deformation just above the yield strength was choosen for the deformation in the tests. (After the high temperature exposures there could be measured an elastic deformation in the sample at room temperature, which confirmed that the stresses were near the high temperature yield strength during the experiments). In order to demonstrate, that cracks would occur in the samples, if stress corrosion conditions at high temperature are established, exposures in capsules with pure NaOH without any special dry out procedures were performed at 550°C. It was not possible to produce cracks within 200 hours in 1.4948 material (304 type stainless steel), but in alloys with higher nickel content, as Hastalloy S or Incoloy 800H, it was possible. The list of the materials is given in table 1. One can assume, because the yield strength of Incoloy 800 and type 304 ss have about the same magnitude at room temperature and 550°C, that the higher corrosion rate in 304 stainless steel avoided the crack formation, and that not the different relaxation behaviour was responsible for this result. Examples for the crack formation are given in figure 2.

3. Materials

The characterisation of all materials, is given in table 1. The material 1.4948, which was the material for the C-ring specimen in the experiments, was heat treated before welding at 575°C / 100h, in order to get a sensitized condition.

Table 1: Material characterisation

Material	1.4948	CN 18/11 IG	Inc.800H	Hastalloy S
Heat	4.040/106*	80472098	154237	2635C2320
Supplier	Höver	Böhler	-	-
Thermal Treatment	575°C/100h	-	750°C/30h	750°C/30h
Composition w %				
C	0.04	0.05	0.08	0.005
Si	0.4	0.5	0.47	0.41
Mn	1.1	1.6	0.75	0.49
P	0.029	0.012	0.011	0.007
S	0.01	0.012	0.003	0.002
Cr	18	19	20.21	14.68
Ni	10.8	10	31.46	rest
Mo	0.4		0.02	14.63
Ti.Ta.Nb	0.05		0.36	
Fe	rest		rest	
-			0.26 AL	.3Al,.5Co
RP 0.2,20°C, N/mm²	ca.247	-	240	386
RP 0.2,650°C, N/mm²	ca.126	-	-	-

remark: *) other heats were used for the sample qualification

4. Samples

The geometry of the samples is given in figure 1. The outer surface of the C-rings were smooth grinded after welding. As mentioned above, the C-rings were compressed at room temperature and then hold at a plastic deformation of 0.5 mm.

5. Preparation of the Na/NaOH mixture

Pure NaOH p.a. was used for the experiments. By the addition of 0.3 % weight of pure sodium any traces of moisture were removed (Except test G and H). This procedure as well as the complete sample preparation was performed in a glove box with an atmosphere free of moisture. When the mixture was held for one hour at about 350 °C, the samples were immersed for some minutes and than removed and hold for a short time at temperature, in order to drain the excess NaOH. When about 4 mg NaOH/cm² remained on the samples, they were ready for the exposure.

The exposure to controlled atmosphere was done in capsules with a gas inlet on the bottom and a gas outlet on the top. In order to supply a sodium vapour, the bottom was filled with sodium above which passed the inlet gas stream. Exception: In test G the capsule was complete closed, without connection to the gas loop.

Table 2: Test conditions and main results

Test	Temp. °C	Vapour H_2/H_2O vpm/vpm	Time hrs	Oxide Met.loss µm	Selective corrosion µm	Corrosion Depth tot. µm	NaOH addition mg/sample	Sample
A	350	440/815	3013	2	3	5	200	A1-15
B	350	40/815	1003	8	110	118	60	A1-10
C	350	40/815	2821	5	150	155	300	A2-11
C	350	40/815	2821	3	0	3	198	A2-14
D	450	30/50	3015	2	18	20	130	A1-6
E	560	30/50	1000	2	12	14	92	A2-12
F	560	30/50/*	2925	12	88	100	124	A1-25
G	560	pot closed**	300	8	82	90	197#	A2-5
H	560	40/815/**	300	2	0	2	100#	A2-13

Test	Temp. °C	Selective corrosion µm	Residual alkalinity mg Na	Weight§ change mg/sample	Reaction products on top of the surface	Sample
A	350	3	44	-167	$NaFeO_2$, Na_2CrO_4, Na_2O, NaOH	A1-15
B	350	110	14	+12	$NaFeO_2$, Na_2CrO_4, Na_2O, NaOH, Na_5FeO_4	A1-10
C	350	150	166	+17	n	A2-11
C	350	0	35	-152	n	A2-14
D	450	18	97	+47	Na, Na_2O,	A1-6
E	560	12	n	n	$NaCrO_2$, alfa-Fe	A2-12
F	560	88	0.8	-23	($NaCrO_2$, Ni), Fe_3O_4	A1-25
G	560	90	8	-162	NaCrO2, NaFeO2, alfa-Fe, (Fe3O4)	A2-5
H	560	2	3	-65	NaFeO2, (alfa-Fe), Fe3O4	A2-13

*) In this experiment there was no sodium vapour addition

#) In this test, NaOH was not dried by 0.3 %w Na addition

n) Not determined

§) [Weight+NaOH-film, before test]-[weight after test, with all deposits]

6. Exposure of the samples

As mentioned, the samples were stressed, wetted with NaOH and fixed into capsules with some sodium under conditions of the inert atmosphere of a glove box. Then they were fitted into a Helium gas loop, which supplied a controlled gas atmosphere with respect to impurities as O_2, N_2, H_2O, CO, CH_4 and H_2

The exposure conditions are summarized in table 2.

At the end of the experiments the capsules with the samples were transfered to the glove box and the samples were removed and examined under inert atmosphere.

7. Examination of the samples

The following measurements were performed:

Weight change, residual elastic deformation, composition of surface layers by x-ray diffraction under inert gas atmosphere, amount of residual alkalinity, longitudinal and transverse metallografic cross sections with the determination of oxide layers and selective corrosion effects.

The metallografic results and surface analysis results are given in table 2.

7.1 Metallografic results

The surfaces of all samples were oxidized during the experiments, the coloration was brown at 350°C and it was gray at 450°C. At 560°C it was brown, when $NaFeO_2$ was later analysed otherwise it was gray. The metal loss due to surface oxidation did not exceed 12 µm. Selective oxidation was observed along grain boundaries up to 88 µm. In the experiments at 350°C a selective oxidation and crack formation up to 150 µm was observed along grain boundaries in the base material or, in a smaller depth, along the delta ferrite in the weld. Examples of the corrosion effects ar given in fig. 3, 4.

7.2 Surface composition

The tests started with NaOH-wetted samples with an amount of 60 to 300 mg NaOH. It was found by the weight change measurements, that the sample in experiment A and one sample of experiment C at 350°C lost 167 to 152 mg or 23 mg in experiment F at 560°C . In the other experiments at 350°C and 450°C the sample weight increased by 12 to 47 mg. When the samples were rinsed for some minutes in

demineralized water the "residual alkalinity" could be measured, it is calculated as Na. At 560°C, experiment F, about no Na could be washed away.

In the case of the 450°C experiment, there was a bright sodium film visible on the sample.

By x-ray diffraction under inert atmosphere, $NaFeO_2$ and Na_2CrO_4 were measured together with Na_2O and NaOH at 350°C, while at 450°C, the deposits of Na were too thick to measure corrosion products underneath, and at 560°C traces of $NaCrO_2$ and Ni, and mainly Fe_3O_4 were determined on the surfaces.

8. Discussion of results

The experiments were performed in order to quantify the corrosion effects in stress corrosion samples, which are produced in the samples by the reaction of a limited amount of NaOH on the surface during the exposure under sodium vapour conditions. The NaOH was assumed to be the result of moisture impurities in any cover gas, therefore the cover gas in the experiments was enriched with moisture.

At 350°C three experiments have been performed. In experiment A about no corrosion had been detected, while during experiments B and C, selective corrosion up to 150 μm attacked the grain boundaries. The reaction products and therefore the oxygen and hydrogen potential, which determined the thermodynamic stabilities of the reaction, where about the same. The higher hydrogen content of 440 vpm instead of 40 vpm in the case of the experiment (A) with low corrosion effects could perhaps influence the thermodynamic stability of Na_2O in the $Na-Na_2O-NaH-NaOH$ system, but this compound was found in both cases (A,B). The examination of the samples after the test A, which was not mentioned above, showed that the sample holder between the sample and the sodium level was covered with thick sodium oxides. In experiment C it was found (see figure 5), that the sample just beside the gas inlet (A2-11) had the high corrosion effects, while the sample (A2-14) in position more away from the sodium level and from the gas inlet, had the same small corrosion effects as they were observed in experiment A. The samples with the small corrosion effects lost most of their NaOH amount during the experiment while the samples with higher corrosion at 350°C slightly increased in weight. The supply of the wet gas produced in the case of the higher corrosion effects more and more NaOH because the sodium level, the gas inlet and sample surface were very near together. In the other cases the gas reacted with the sodium before it reached the samples, and a great part of NaOH was evaporated from the sample, either in form of Na or NaOH.

At 450°C metallic sodium had wetted the sample, thick Na_2O crystals had been observed in the sodium film. The vapour pressure of Na was high enough to reduce the NaOH in this experiment, which also had a reduced moisture supply. Nevertheless some intergranular selective corrosion up to a depth of 18 μm had been observed.
At 560°C a general oxidation occured on the samples. The existance of alfa-Fe gives some advise to the reaction chain of the corrosion products. In experiment F, in which 124 mg NaOH were available at the beginning and in which no sodium vapour was added, the greatest part of the reaction products was Fe_3O_4. It can be assumed, that in experiment (E), with sodium, $NaFeO_2$ was the first reaction product and that this compound was decomposed. $NaCrO_2$ was formed in the experiments because it was more stable than $NaFeO_2$. In experiment (F) without sodium, and because of further H_2O supply with the cover gas, Fe_3O_4 was formed. The serie of tests at this temperature with sodium vapour (test E), closed capsules (test G), and the use of NaOH, which was not dried by 0.3 %w Na addition (tests G, H), allows the following interpretation:
Test H: At high oxidation potential with 815 vpm H2O the main constituant of the steel reacted, and no selective corrosion occured.
Test G: In the closed capsule some NaOH diffused away from the sample, the reaction products followed the chain of their thermodynamic stability and selective corrosion occured.
Test F: In this test the material behaved similar to Test G, due to the longer time the selective corrosion ended up with $NaCrO_2$, which was the most stable Cr compound, Ni, which could not be oxidized, and the main element oxidized to Fe_3O_4.
Test E: In this test sodium vapour was available, the NaOH film was quickly decomposed before the end of the first 1000 hrs, the most stable oxide, the NaCrO2 was the main corrosion product. The main constituant of the alloy, iron, was not further attacked, alfa-Fe was found, that means that no NaOH was available at the end of test and therefore the corrosion by NaOH was stopped.

9. Conclusion

Summarizing, the experiments showed that the amount of NaOH and the duration of exposure to NaOH-films was important for the corrosion effects. The highest effects were found, when the H_2/H_2O containing gas reacts near the sodium level at low temperatures above the melting point of NaOH (ca 320°C), i.e. when a consumption of NaOH either by evaporation or by reaction was negligible. If there existed a sodium vapour pressure in equilibrium with 450°C, NaOH layers on the sample were not stable in the presence of 50 vpm H_2O and corrosion reactions were limited. At much higher temperatures of 560°C any NaOH films were removed either by evaporation or by a surface reaction and even at 50 vpm H_2O the formation of new NaOH was not possible if sodium at 560°C was available.

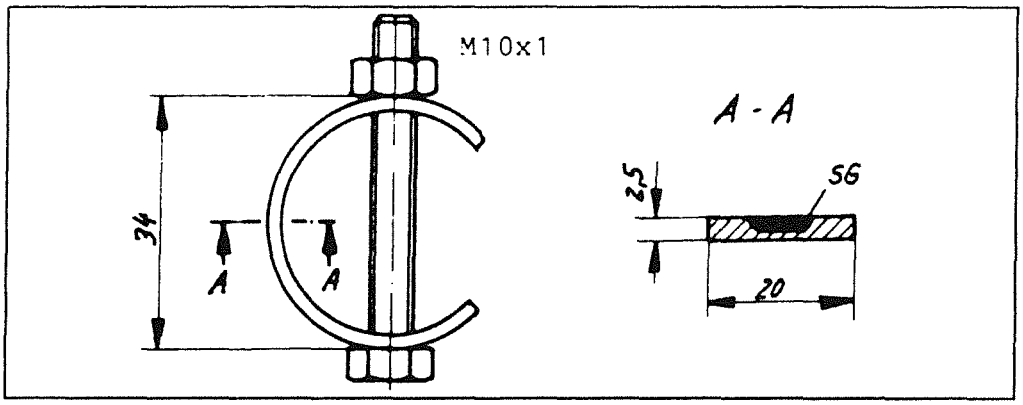

Figure 1: Geometry of the C-ring samples

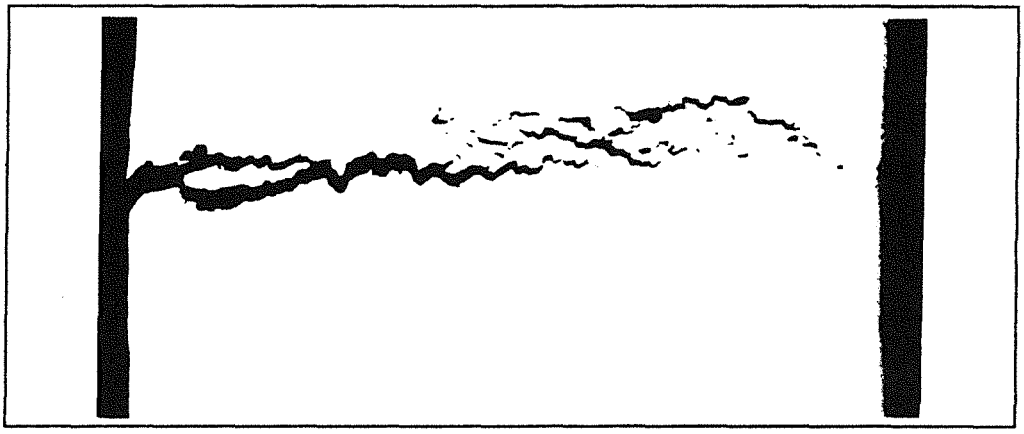

Figure 2: Cracks in Hastalloy S after 200 hrs at 550 °C in pure NaOH

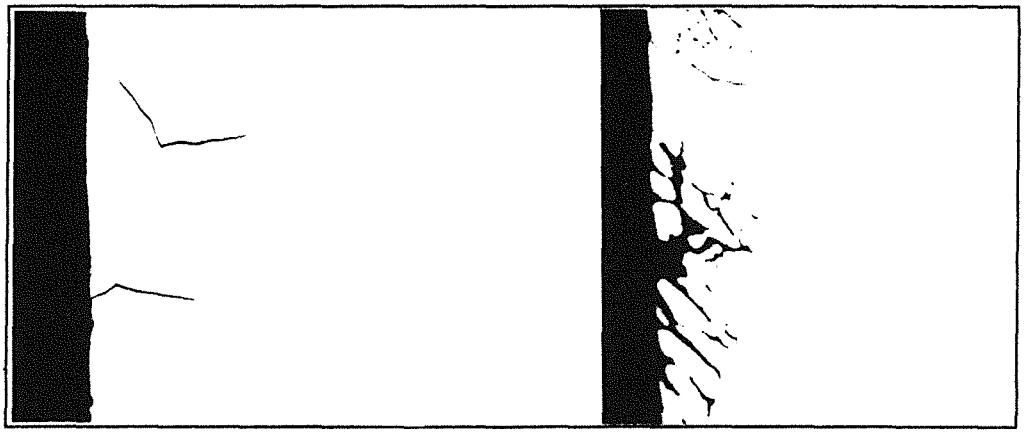

a) Base material 200 X b) Weldment 500 X

Figure 3: Selective corrosion in 1.4948 after 1003 hrs exposure at 350 °C in experiment B, magnification: 200 X

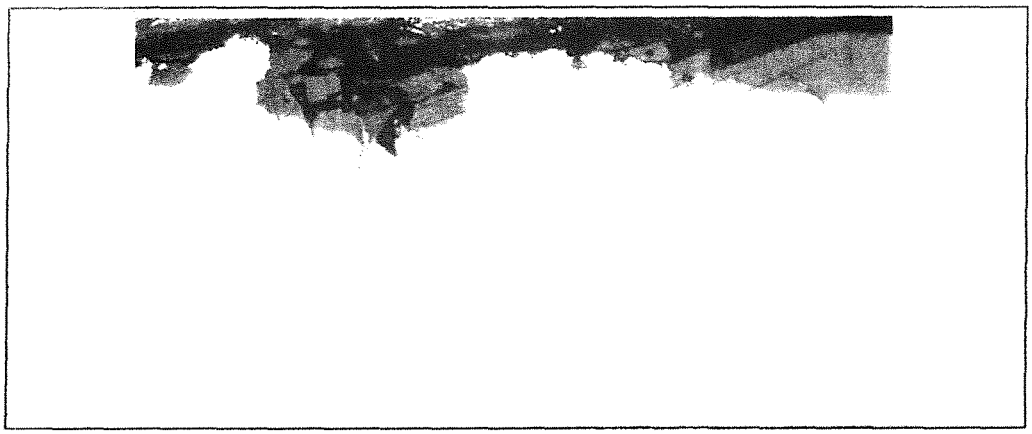

Figure 4: Selective corrosion in 1.4948 after 2925 hrs exposure at 560 °C in experiment F, Base material 500 X

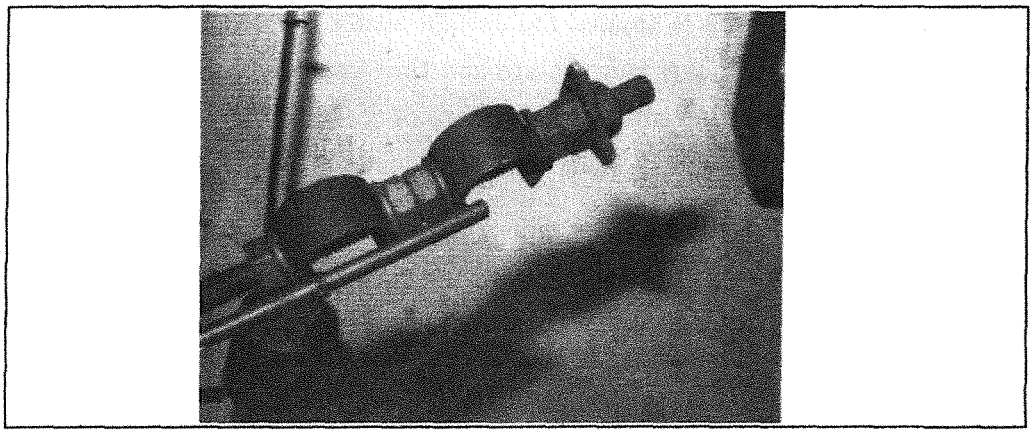

Figure 5: The sample holder with the gas inlet tube of experiment C

Tensile Tests of Low-Alloy Steel 15Mo3 in Sodium

H.U. Borgstedt, Z. Peric

Kernforschungszentrum Karlsruhe GmbH.
Institut für Materialforschung III
P.O. Box 3640, D-7500 Karlsruhe 1

Abstract

The low-alloy steel 15Mo3 is applied for peripherically situated components of fast reactors which are operated under low temperature and flow conditions. In the German fast reactor, SNR 300, the sodium drain tanks are fabricated of this material. The fuel element storage tank of the SUPER PHENIX in France was also made of this steel.

After the filling of these drain tanks with sodium, cracks occurred at weldments, though the temperature was not higher than 150 °C and the stress on the material was not higher than the yield point. The cracks developed without a significant deformation of the component in their neighbourhood.

Tensile tests of welded and rusted samples of the steel 15Mo3 were performed in liquid sodium at 110, 140, 200 and 300 °C in order to get information on the mechanisms of the crack formation under these conditions. All specimens failed in a ductile manner, the tensile curves in air and in Na were nearly identical. The possibility of a liquid metal embrittlement can be excluded from the test results.

The reaction of wet rust with sodium could not yet introduced into the test procedure, a new set-up is prepared in which such reactions may be superimposed to the tensile stress. Final conclusions can be drawn after the finishing of these tests.

1. Introduction

Small sodium leaks were detected at four of ten drain tanks of the SNR 300 fast reactor after their filling with sodium [1]. The drain tanks were fabricated of the low alloy steel 15Mo3. The leaks were caused by cracks at weldments which were trans-crystalline and with low strain. The crack surfaces were not oxidized while the surfaces of the tanks were rusted. Thus, the cracks were formed during or after the procedure of filling with sodium. The very low temperature (about 150 °C) and the short time of contact with sodium exclude any effect of liquid sodium corrosion on the low alloy steel 15Mo3.

Another case of failure of this steel in contact with sodium at 180 °C was reported in the literature [2]. The spent fuel element storage tank of the French fast reactor SUPER PHENIX was constructed of the same material. A sodium leak occurred after a longer period of operation time in the inner wall of the double wall system. The leak was located not so far from the sodium-atmosphere interface, it was also in the surrounding of a weldment.

2. Experimental

2.1 Material and specimens

The composition of the steel 15Mo3 (no. 1.5415) is listed in the Table 1, the analyzed components of the alloy are within the range of the nominal composition.

Table 1: Composition of the steel 15Mo3 (no. 1.5415)

Element	C	Si	Mn	P	S	Cr	Mo
nominal compos.	0.12-0.20	0.10-0.35	0.40-0.80	0.040	0.040	$\leq$0.30	0.25-0.35
melt no. 074495	0.14	0.17	0.55	0.010	0.020	n.a.	0.27

n.a. not analyzed

One group of the specimens were made of weld metal, and they were rusted before the tests. Their cross sections were 6 · 3 mm which were reduced to 4 · 3 mm in the plane of the

notches in the centre of the gage length. The rust was produced by means of exposure to a wet atmosphere at 60 °C for 6 days. A hydrogen content of the rust layers was not determined.

A second group of specimens had a cylindrical geometry of 4 mm diameter and 20 mm length. Some of them had also a notch in the centre of the length. The specimens did not receive a final heat treatment.

A third group of specimens was fabricated of a plate of base metal of the steel 15Mo3. The specimens were also of cylindrical size of the dimensions given above. A sharp notch was brought-in in elliptical size in the centre of the gage length.

2.2 Testing devices

The principle of the test capsule is shown in Fig. 1 [3]. The container is made of Type 304 stainless steel with a provision to fix the specimen holder at its bottom and with a bellow on its closing flange. The load bar is kept movable within a certain limitation, thus, the strain can be brought onto the specimen within a closed volume. The capsules were of a volume of 45 ml only, for some additional tests larger capsules (of 600 ml content) have been fabricated in a similar design.

A trace heater is used to heat the specimen and the environment to the desired test temperature which is measured by means of a thermocouple. An electronic energy supply generator keeps the temperature constant within ± 3 K. The surrounding insulating material supports the efforts to keep the temperature constant. The bottom of the capsule and the load bar are connected to the two grips of the testing machine (Instron, 2.5 t). The machine allowed tensile tests at various levels of strain rates. The capsule was recently equipped with a provision to fill in the liquid metal at the position in the testing machine in order to avoid the drying of the rust during the preparations of tests. The same type of capsule was inserted into a constant-load creep test facility which is described in detail in [4].

The tests were performed at strain rates of $\epsilon = 8 \cdot 10^{-4}\ s^{-1}$ and $3.5 \cdot 10^{-5}\ s^{-1}$, and at temperatures of 110, 140, 200, 240, and 300 °C.

3. Results of tensile tests

The results of the tests with the first series of specimens at 110, 200, and 300 °C with a strain rate of $\epsilon = 8 \cdot 10^{-4}\ s^{-1}$ in Na and in air did not reveal any influence of the test medium on the R_e and R_m values and the ductility as well. This is clearly indicated by the results presented in Table 2 and by the tensile curves in Fig. 2. The elongation and reduction of area demonstrated ductile tensile behaviour of the steel 15Mo3 in both environments, air and sodium. The scatter of the results might be due to the differences of the micro structures in the weld material.

The results showed a still larger scatter in the second series of tests (see Table 3) which were performed with rusted and partly notched specimens at 140 and 240 °C and with $\epsilon = 3.5 \cdot 10^{-5}\ s^{-1}$. The rust which was mainly lost during the contact with sodium of 140 and 240 °C did not significantly influence the tensile behaviour of the specimens. The presence of notches (cross sectional plane of 12.0 mm^2) did not influence the values of R_e and R_m , but the strain-to-rupture appeared to be decreased due to the fact that the strain was concentrated to a small range around the notches. The effect of the temperature on the tensile behaviour of these specimens was negligible.

Table 2: Results of tensile tests of steel 15Mo3 in air and in Na
($\epsilon = 8 \cdot 10^{-4}\ /s^{-1}$)

Environment	Temperature °C	d_0 mm	R_e MPa	R_m MPa	A %	Z %
Na	110	4.028	462	616	12.5	40
Na	110	4.012	481	597	10.5	46
air	110	4.015	480	604	11.8	50
Na	200	4.011	543	714	12.0	38
Na	200	4.25	540	719	10.5	40
air	200	4.008	482	684	5.5	26
Na	300	4.020	462	699	5.75	37
Na	300	4.004	467	732	10.75	38
air	300	4.000	500	718	10.5	34

The results showed a still larger scatter in the second series of tests (see Table 3) which were performed with rusted and partly notched specimens at 140 and 240 °C and with $\epsilon = 3.5 \cdot 10^{-5}\ s^{-1}$. The rust which was mainly lost during the contact with sodium of 140 and 240 °C

did not significantly influence the tensile behaviour of the specimens. The presence of notches (cross sectional plane of 12.0 mm^2) did not influence the values of R_e and R_m , but the strain-to-rupture appeared to be decreased due to the fact that the strain was concentrated to a small range around the notches. The effect of the temperature on the tensile behaviour of these specimens was negligible.

Table 3: Results of tensile tests of steel 15Mo3 in air and in Na
($\epsilon = 3.5 \cdot 10^{-5}$ $/s^{-1}$; specimens partly rusted [r], second group with notch)

Environment	Temperature °C	s_f mm^2	R_e MPa	R_m MPa	A %
Na	140	18.0	635	730	5.2
Na[r]	140	18.0	662	680	5.2
Na[r]	140	18.0	558	750	18.5
Na	240	18.0	590	670	12.6
Na[r]	240	18.0	574	640	5.2
Na	140	12.0	858	1095	18.2
Na[r]	140	12.0	770	840	1.0
Na[r]	140	12.0	851	915	3.2
Na	240	12.0	719	920	11.6
Na[r]	240	12.0	588	670	6.2

Some stress corrosion tests were performed in which the influence of hydrogen on the mechanical properties of the steel 15Mo3 should be studied. Specimens of this steel containing a sharp notch were loaded with $\sigma = 500$ MPa in the residual cross section at the notch and exposed to pure Ar and an Ar 5% H_2 mixture at 150 °C within a capsule which was designed for creep-rupture tests [4]. There was no influence of the hydrogen content in the environment on the mechanical behaviour of the material. A third test was performed in the same apparatus in which the environment was a mixture of 600 cm^3 molten sodium with 0.8 g NaH. The specimen was loaded with $\sigma = 533$ MPa at a temperature of 150 °C. The specimen was not attacked by this environment, there was also no embrittling effect of the hydrogen content in this test.

Further tests are in preparation in which the specimens of steel 15Mo3 should be contacted with the environment after loading and heating to about 150 °C. A new capsule was designed for such tests for which rusted specimens will be prepared as well.

4. Results of metallographic studies

The metallographic examination of welded specimens of steel 15Mo3 after the tensile tests in liquid sodium environment show that cracks form in the heat effected zone outside the weldments. The tensile behaviour of the specimens is indicated by the orientation of the grains in the zone of reduced cross section. This deformation of grains occurred in the tests in both media, air and sodium.

Additional examinations of the fully welded material demonstrate that the formation of cracks is influenced by the structure of the weldment. The cracks in such grains which are vertically orientated to the direction of stress grow under very low degree of deformation, while the deformation is much larger in grains which are orientated in the direction of the stress. In the latter case the reduction of area is also more pronounced.

The influence of the orientation of the grains on the deformation and fracture of the welded material 15Mo3 is confirmed by the fractographic examinations by means of the scanning electron microscope. The morphology of the fracture surface contains ductile regions beside brittle regions with intercrystalline surface structure. Fig. 3 shows an example of a ductile region of the fracture plane in a specimen of the second series. The fracture morphology is related to the tensile behaviour of the specimens.

5. Discussion of results

The tests under various gaseous and liquid environments did not verify the effects which occurred in the drain tanks of the SNR 300 reactor. The addition of hydrogen gas to the corrosive media did not lead to an embrittling reaction of the steel 15Mo3 with the environment. In all tests ductile behaviour of the steel was observed in the whole range of parameters. Effects may only occur, if atomic hydrogen is present in the neighbourhood of a stressed region of the material. In the case of our samples, molecular hydrogen is present in the gaseous system (Ar + 5 % H_2). The surfaces of the samples are covered with oxides which are dried in the presence of sodium. In this form they act as barrier against the ingression of hydrogen into the steel.

It was found that wet rust (FeOOH) evolves hydrogen in contact with sodium [5], and the reaction may be fast enough to supply the sample surface with hydrogen atoms. Thus, it may be concluded that wet oxide may be a source for atomic hydrogen. Test in which specimens covered with wet rust should be contacted with sodium under stress are, therefore, under preparation. Another source for the occurrence atomic hydrogen at the interface between steel and sodium might be sodium hydroxide which under certain conditions forms in reactions of sodium with water vapour. This has still to be approved.

The results of tests of the stressed steel in contact with sodium containing sodium hydride indicate, that atomic hydrogen is necessary but not sufficient to cause hydrogen embrittlement. The Na/NaH mixtures did not influence the tensile tests and the constant stress tests as well which were performed with the steel 15Mo3. This may be explained by the insulating action of the oxide layers which were present in all these tests. It was seen that the dry oxide suppresses the wetting of the specimens. This supports the conclusion that the diffusion of hydrogen into the steel may also be suppressed.

The tests have not yet reproduced the effects which were found in some cases of failure of the steel 15Mo3 in praxis. It was concluded that the failures might have been caused by hydrogen embrittlement. If this would be true, there should be a superimposure of the effect of atomic hydrogen and of locally concentrated stress. It seems questionable that wet rust (FeOOH) might be the source for the atomic hydrogen which acts as the embrittling agent. The local concentration of stresses is indicated by the fact that the failures occurred in weldments or in their neighbourhood. The atomic hydrogen may interact with the stressed region of the steel 15Mo3, if there is the possibility for free exchange of the atoms between sodium and the steel. This is not the case in the presence of oxide layers.

All results can be interpreted in the sense that a liquid metal embrittlement can be excluded as the reason for the failure of the steel 15Mo3 in contact with sodium at moderate temperatures.

Acknowledgements

We gratefully acknowledge the contributions of Dr. M. Grundmann to the early part of this work.

References

[1] Note, Atomwirtschaft 30 (1985) 486.

[2] A. Berjon, R. Dupraz, "La localisation de la fuite de sodium du barillet de super phénix", 4th Internat. Conf. on Liquid Metal Engineering and Technology, French Soc. of Nuclear Energy, Paris 1988, Vol. 3, paper 702.

[3] H.U. Borgstedt, M. Grundmann, "Liquid Metal Embrittlement as a Corrosion Phenomenon",EUROCORR '87, Preprints, DECHEMA, Frankfurt 1987, 141- 146.

[4] M. Grundmann, Report KfK 4703, Kernforschungszentrum Karlsruhe 1990

[5] T. Gnanasekaran, V. Ganesan, G. Periaswami, C.K. Mathews, H.U. Borgstedt, J. Nucl. Mater. 171 (1990) 198-202.

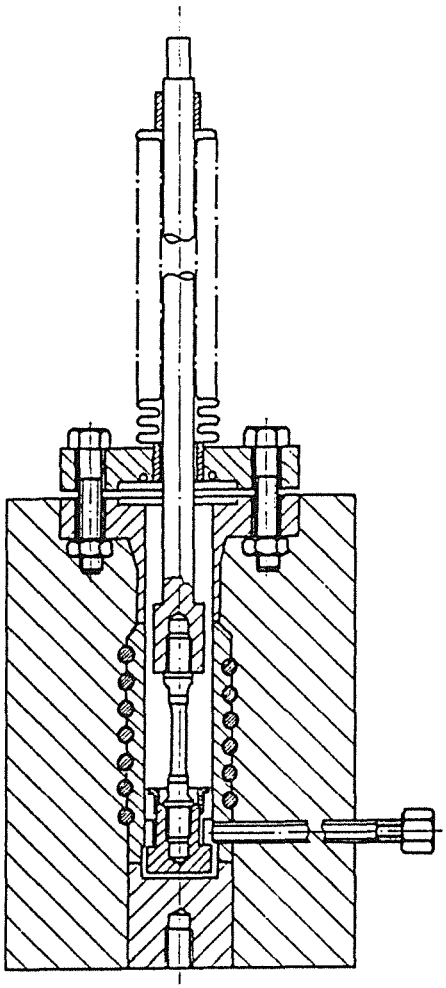

Fig. 1: Test capsule for tensile testing of cylindrical specimens of steel 15Mo3 in the presence of sodium; the capsule may be connected with a tensile testing or creep machine [2,4].

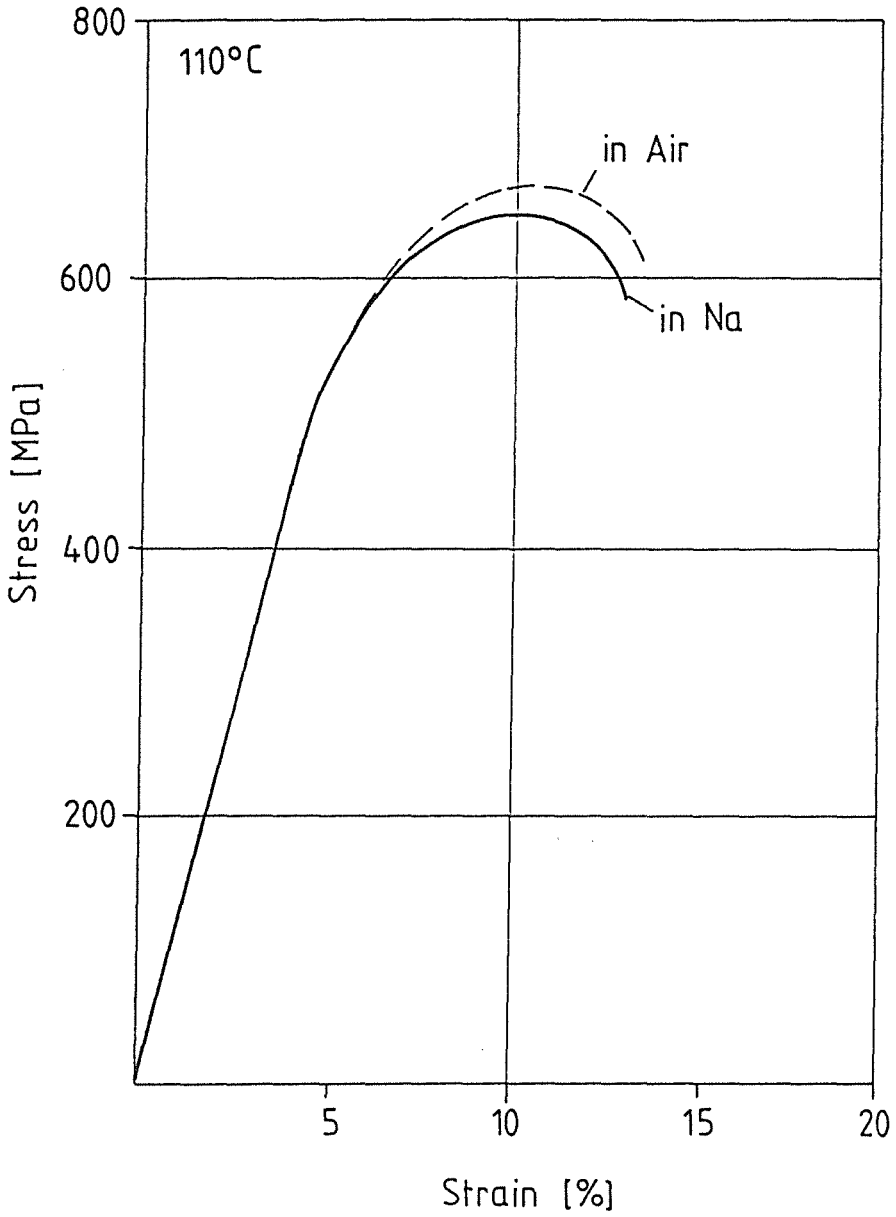

Fig. 2: Results of tensile tests of specimens of steel 15Mo3 in air and in Na environment at 110 °C.

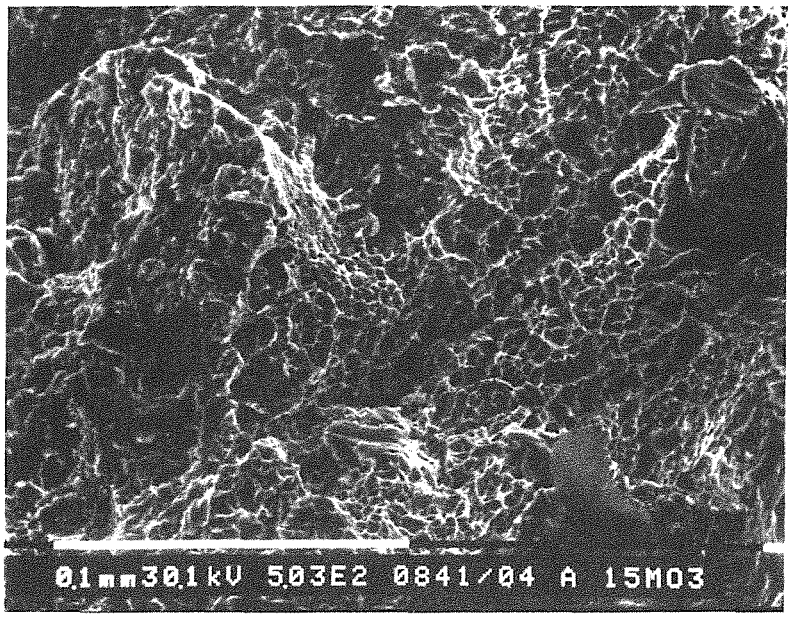

Fig. 3: SEM image of the ductile part of the fracture plane of the first specimen of Table 3.

Influence of Carburizing Sodium on Creep-Fatigue Behavior of Type 304 Steel

Y. Wada, T. Asayama and R. Komine
Materials Development Section, Systems and Components Division,
O-arai Engineering Center, Power Reactor and Nuclear Fuel Development Corp.

A B S T R A C T

In carburizing sodium, grain boudaries with coagulation of precipitated carbides were observed in a sodium affected zone for Type 304 steel. It was considered that grain-boundaries might crack, when a large distortion of grains occurs within the tertiary creep range. Therefore it should be noticed that this phenomenon might affect creep-fatigue strength. In the present study the creep-fatigue test was carried out in strongly carburizing sodium by inserting a carbon source in sodium near the test specimen at 550 ℃ for Type 304 steel hot rolled plate. Test conditions were as follows,

(1) strain range of 0.94%, strain hold time of 1hr
(2) strain range of 0.98%, strain hold time of 10hrs
and (3) strain range of 0.43%, strain hold time of 1hr.

For tests (1) and (2), many surface cracks were observed. In both cases, main cracks were initiated on grain boundaries of the surface of tested specimens. Creep-fatigue lives of tests (1) and (2) were slightly shorter than those of in-air tests. But for test (3), only a few cracks were observed on the surface of tested specimen and many intergranular micro-cracks were observed in the bulk of metal. Creep-fatigue life was almost same as that of in-air test. It was considered that the main crack of test(3) should be initiated inside of test specimen and the sodium environment could not affect the crack initiation. For higher strain ranges(strain range of about 1%), grain boundaries were distorted cyclically by plastic deformation, and might crack near the surface similar to tertiary creep embrittlement in carburizing sodium. For lower strain ranges, grain boundaries near the surface were deformed elastically because of hardening effect by carburizing, and could not crack.

The carbon concentration near the surface of low carbon(about 0.01%) and nitrogen controlled(0.06-0.10%) modified Type 316 steel was much smaller than that of Type 304 or 316 steel in carburizing sodium. For such type materials, it should be noticed that cracks might be initiated on the grain boundaries of the surface for lower strain ranges because of lack of hardening effect by carburization. It is recommended that long-time creep-fatigue test should be performed for lower strain ranges.

1. INTRODUCTION

Tertiary creep embritlement of Type 304 steel is observed in creep rupture test in flowing sodium[1)-4)]. For this phenomenon test specimens were fractured with deep surface cracks along grain boundaries[1)-4)], and in carburizing sodium grain boundaries with coagulation of precipitated carbides were observed in a sodium affected zone[2),4)]. It was considered that grain-boundaries might crack, when a large distortion of grains occurs within the tertiary creep range[4)].

In structural design on large LMFBR components, primary stresses are usually very low and cyclic secondary stresses caused by thermal transient are dominant, and stresses at the surface of metals are higher by distribution of temperatures and bending loads. The interaction of sodium environment and cyclic strain loading with hold time is the actual problem for LMFBR structural design. If the cause of tertiary creep embrittlement is the sensitivity to cracking of carburized grain-boundaries under a large plastic deformation, the acceleration of reduction of creep-fatigue life might occur. Therefore the investigation of tertiary creep embrittlement should be linked to sodium environmental effect on creep-fatigue life.

As the studies on creep-fatigue behavior in sodium, several efforts were already contributed. Borgstedt investigated creep-fatigue behavior of Type 304 steel in sodium[5)] and it was discussed that the creep-fatigue interaction may be influenced by the effects of sodium corrosion particularly under decarburizing conditions as also observed in creep-rupture tests. On the other hand it was expected under carburizing sodium that both creep-fatigue lives in sodium and air were not different. Creep-fatigue behavior of Type 316 steel was examined by Wood[6)] and all the test data were plotted within the scatter band of in-air test. It seems by researches up to the present that the influence of carburizing sodium on creep-fatigue strength for Types 304 and 316 steels is tolerable. But test data for a long duration time were very few and the test environment was too mild for metals to conclude the carburizing sodium-exposure effect on creep-fatigue behavior of LMFBR components.

In the present study creep-fatigue test for a longer duration time was carried out in strongly carburizing sodium by inserting a carbon source in sodium near a test specimen at 550℃ for Type 304 steel hot rolled plate to examine creep-fatigue behavior under severe tertiary creep embrittlement conditions.

2. TEST MATERIAL

Table 1 and 2 list the chemical compositions and mechanical properties at room temperature of Type 304 steel used in the present study. Product form of this material is a hot rolled plate of 40mm thickness.

3. TEST CONDITIONS

3.1 TEST SPECIMENS

The configuration of creep-fatigue test specimen in sodium is shown in Fig. 1. It is consisted of a creep-fatigue specimen section and a bellows which encloses the specimen section. To give a strongly carburizing atmosphere a spacer made of 0.45% carbon steel is placed in the inside of bellows. This spacer is decarburized by sodium-exposure, and the surface of test specimen section is carburized in sodium with high carbon activity. The surface-to-volume ratio of in-sodium tests is $2/5(mm^{-1})$ for 10mm diameter.

3.2 SODIUM TEST CONDITIONS

Grips of test specimens were connected to test machine consisted by an electro-hydraulic servo system. Inlet and outlet of bellows were connected to pipes of sodium loop by flexible joints. Before the mechanical loading, sodium was circulated to purify the contamination of sodium inside of bellows. Oxygen density was controlled by cold trap temperature of 120℃, and flow rate of sodium was about 1 m/sec at specimen surfaces. After sodium circulation, inlet and outlet of bellows were sealed by freezing of sodium. As the results, static sodium with high impurity was put into the bellows.

Strain of parallel section was controlled by the displacement between two projections of shoulders of the specimen. The displacement between two projections was calibrated to the strain of parallel section measured by preliminary test in air. This method was already applied to low-cycle fatigue tests in sodium[7].

Test temperature was 550℃. Controlled strain was the trapezoid waveform with a strain hold time at tensile peak. Test conditions were as follows.

(1) strain range $\Delta \varepsilon_t$ of 0.94%, strain hold time t_H of 1hr
(2) strain range $\Delta \varepsilon_t$ of 0.98%, strain hold time t_H of 10hrs
and (3) strain range $\Delta \varepsilon_t$ of 0.43%, strain hold time t_H of 1hr.

No. (1) is the reference. No. (2) was to examine the longer hold time effect. No. (3) was to clarify the interaction of sodium environment and creep-fatigue loading within the range of low plastic strain for a longer duration time. In all cases, the strain rate was 0.1%/sec.

4. TEST RESULTS

4.1 PROFILE OF CARBON CONCENTRATION OF POST-FAILURE SPECIMENS

Carbon penetration profile of post-failure specimens was measured using five thin foils with a thickness of 0.2mm sliced from the surface of specimen shoulder. Fig. 2 shows the measurement results on all test specimens. The carbon concentration at the surface was much higher and carbon penetration was deeper than those under normal conditions[4]. Carburizing behavior depended on not only the duration time but also the strain range by Fig. 2.

4.2 CREEP-FATIGUE BEHAVIOR IN STRONGLY CARBURIZING SODIUM

Test results on creep-fatigue lives in the present study were shown in Fig. 3 comparing with the test data in air. There were no difference between creep-fatigue lives in sodium and air for the strain hold time of 1hr. As for the case of 10hrs strain hold, creep-fatigue strength in sodium seems slightly lower than that in air.

Fig. 4 shows cyclic strain hardening behavior in strongly carburizing sodium. Stress ranges in air were saturated earlier than those in sodium. But this phenomenon does not depend on carburizing sodium environment, because the ratio of carburized surface layers to total cross section is less than 10%. About 10%up of stress ranges cannot be explained, even if stresses of surface layers become 50%up to the inside of metal. It was an important point that displacement between two shoulders was controlled. Fig. 5 shows cyclic stress-strain relations of Type 304 steel at 550℃ with strain hold time of 1hr. Stress ranges depend on strain control modes, and not on test environment. It was supposed for the shoulder displacement control that dynamic strain ageing might be more effective by the elastic follow-up occuring within the parallel sections.

4.3 MICRO-SCOPIC OBSERVATIONS OF FAILURE MODES

Fig. 6 shows SEM observations of fracture surfaces of all the tested specimens. Intergranular fracture was recognized for each case. Fig. 7 shows crack initiation and propagation modes of each specimen observed by optical microscope. For the cases of $\Delta\varepsilon_t$ =0.94%, t_H = 1hr and $\Delta\varepsilon_t$ = 0.98%, t_H = 10hrs, a number of cracks were initiated on grain boundaries and propagated along them. On the other hand, for the case of $\Delta\varepsilon_t$ = 0.43%, t_H = 1hr only one intergranular crack with the length of about two grain was observed as shown in Fig. 7, though a number of intergranular cracks were found inside of metal near the fracture surface.

5. DISCUSSION

From the present study the influence of carburizing sodim-exposure on creep-fatigue was not unified at 550℃ for SUS304. In the case of $\Delta\varepsilon_t \fallingdotseq 1\%$, which is a relatively high strain range, fracture was dominated by the propagation of intergranular cracks initiated on the surface of specimens, even if the duration time is longer(t_H = 10hrs, total test duration:2,531hrs). In such conditions the cracking might occur in grain boundaries with coagulation of precipitated carbide particles near the surface similar to tertiary creep embrittlement in carburizing sodium, when grain boundaries were distorted cyclically by plastic deformation. But in the case of$\Delta\varepsilon_t \fallingdotseq 0.43\%$, which is a lower strain range, micro-cracks were initiated along grain boundaries in the bulk of metal, and fracture was dominated by the growth and linkage of micro-cracks. For a lower strain range grain boundaries near the surface could deform elastically because of hardening effect of grains by carburizing, and the earlier cracking did not occur. Fig. 8 shows the concept on the process of initiation of micro-cracks.

In structural design of large LMFBR components, primary stresses are usually very low and tertiary creep embrittlement might be no problem for ductile failure like creep rupture, as already indicated by Huthmann[1] . While for LMFBR components, cyclic secondary stresses caused by thermal transient is usually dominant, and stresses at the surface of metals are higher by distribution of temperatures and bending loads. The interaction of sodium environment and cyclic strain loading with hold time is the actual problem for LMFBR structural design. The investigation of tertiary creep embrittlement should be connected to sodium environmental effect on creep-fatigue life. From the present study, when the cause of tertiary creep embrittlement is the sensitivity to cracking of carburized grain-boundaries under large plastic dermation, the acceleration of reduction of creep-fatigue life could occur for relatively high strain ranges. As the fact, in the case of $\Delta\varepsilon_t$ = 0.98%, t_H = 10hrs, the creep-fatigue strength in sodium seems slightly less than that in air. If the extrapolation to the range of duration time for 300,000hrs is required on the basis of the test result on$\Delta\varepsilon_t$ = 0.98%, t_H = 10hrs, the reduction of creep-fatigue strength by carburizing sodium-exposure effect has to be considered. But strain range caused by thermal transient is usually much lower than 0.5%. So the extrapolation to the range of duration time for 300,000hrs should be based on the test result on $\Delta\varepsilon_t$ = 0.43%, t_H = 1h, and it was concluded that the reduction of creep-fatigue strength by carburizing sodium-exposure has not to be evaluated. Though this judgement was done by only three test data on creep-fatigue behavior for a long time in strongly carburizing sodium, it was confident because the mechanisms of tertiary creep embrittlement and reduction of creep-fatigue strength for higher strain ranges in sodium could not work for lower strain ranges.

For low carbon(about 0.01%) and nitrogen controlled(0.06-0.10%) modified

Type 316 steel[5], it should be noticed that cracks might be initiated at the surface for low strain ranges because of lack of hardening effect by carburizing and reduction of creep-fatigue strength on surface layers of metal. Therefore it is recommended that long time creep-fatigue test should be performed in lower strain ranges for such type 316 stainless steels. Bending test using a thin plate, if possible, might be better than push-pull one because of direct superimposition of damages by sodium environmental effect and maximum cyclic strain loading.

6. CONCLUSIONS

(1) The influence of carburizing sodim-exposure on creep-fatigue was not unified at 550℃ for Type 304 steel. In the case of $\Delta \varepsilon_t \fallingdotseq 1\%$, which is a relatively high strain range, fracture mode was dominated by the propagation of intergranular cracks initiated on the surface of specimens. In such conditions the cracking might occur in grain boundaries with coagulation of precipitated carbide particles near the surface like tertiary creep embrittlement in carburizing sodium, when grain boundaries were distorted cyclically by plastic deformation.
(2) In the case of $\Delta \varepsilon_t \fallingdotseq 0.43\%$, which is a lower strain range, micro-cracks were initiated along grain boundaries in the bulk of metal, and fracture mode was dominated by growth and linkage of micro-cracks. For a lower strain range grain boundaries near the surface could deform elastically because of hardening effect of grains by carburizing, and the earlier cracking did not occur.
(3) In structural design on large LMFBR components, cyclic secondary stresses caused by thermal transient is usually dominant, and cyclic strain ranges are much lower than 0.5%. Therefore the extrapolation to the range of duration time for 300,000hrs should be based on the test result on $\Delta \varepsilon_t = 0.43\%$, $t_H = 1h$, and it was concluded that the reduction of creep-fatigue strength by carburizing sodium-exposure effect has not to be evaluated.
(4) For low carbon and nitrogen controlled modified Type 316 steel, cracks might be initiated at the surface for low strain ranges because of lack of hardening effect by carburizing and reduction of creep-fatigue strength on surface layers. It is recommended that long time creep-fatigue test should be performed for lower strain ranges for such type 316 stainless steels.

REFERENCES

1) H. Huthmann and H. U. Borgstedt, 'Influence of sodium on the creep-rupture behavior of type 304 stainless steel', paper No. 511, Vol. 2, 4th Int. Conf. of LIMET, 1988
2) C. A. P. Horton and B. H. Targett, 'The creep rupture behavior of fast reactor steels, welds and transition joints in flowing sodium ; a review of CEGB results', paper No. 513, ibid.
3) K. Natesan, O. K. Chopra and T. F. Kassner, 'Creep-rupture and low-cycle fatigue behavior of types 304 and 316 stainless steel exposed to a sodium environment', paper No. XIX-6, 2nd. Int. Conf. on LM Tech. in Energy, 1980
4) Y. Wada, E. Yoshida, M. Aoki, S. Kato and T. ito, 'Influence of sodium exposure on creep rupture strength of types 304 and 316 steels', IAEA IWGFR special document, 1991(to be published)
5) H. U. Borgstedt and H. Huthmann, 'Low- and high cycle fatigue behavior of type 304 stainless steel in liquid sodium', paper No. 509, ibid.
6) D. S. Wood and A. B. Baldwin, 'Creep/fatigue behavior of type 316 steel in sodium', paper No. 195, ibid.
7) T. Maruyama, S. Kato, R. Komine, M. Hirano, Y. Wada, S. Kano and I. Nihei, 'Low-cycle fatigue properties of SUS304 stainless steel in elevated temperature

Table 1 Chemical Compositions (wt%)

Material	C	Si	Mn	P	S	Ni	Cr	Mo	N
A-3	0.05	0.60	0.87	0.026	0.002	8.94	18.59	—	0.019

Table 2 Mechanical properties at room temperature

Material	0.2% off-set stress(kgf/mm²)	Ultimate tensile strength(kgf/mm²)	Fracture elongation(%)	Grain size ASTM No.
A-3	21.8	63.6	71.9	4.5

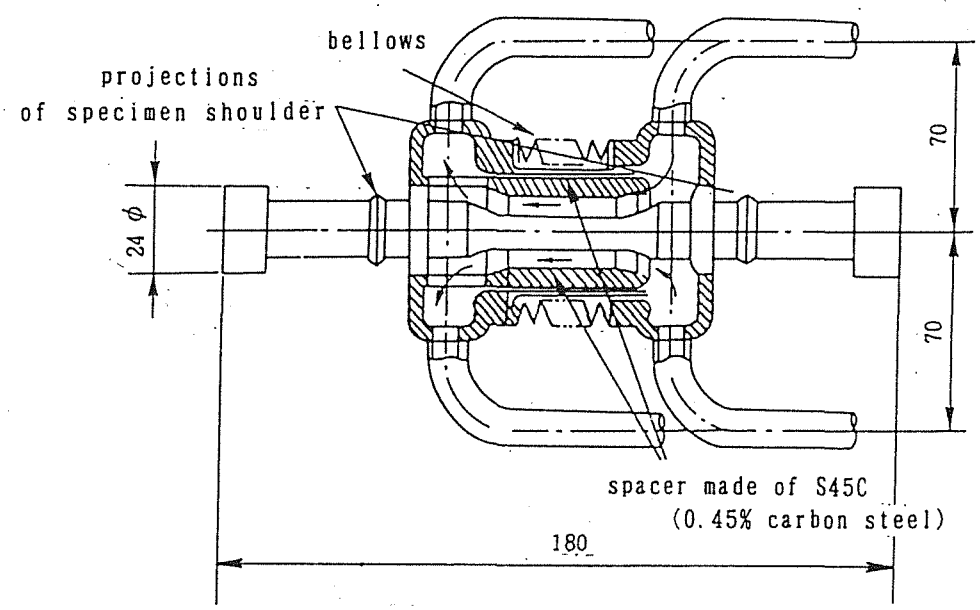

Fig. 1 Configurations of creep-fatigue test specimen in sodium

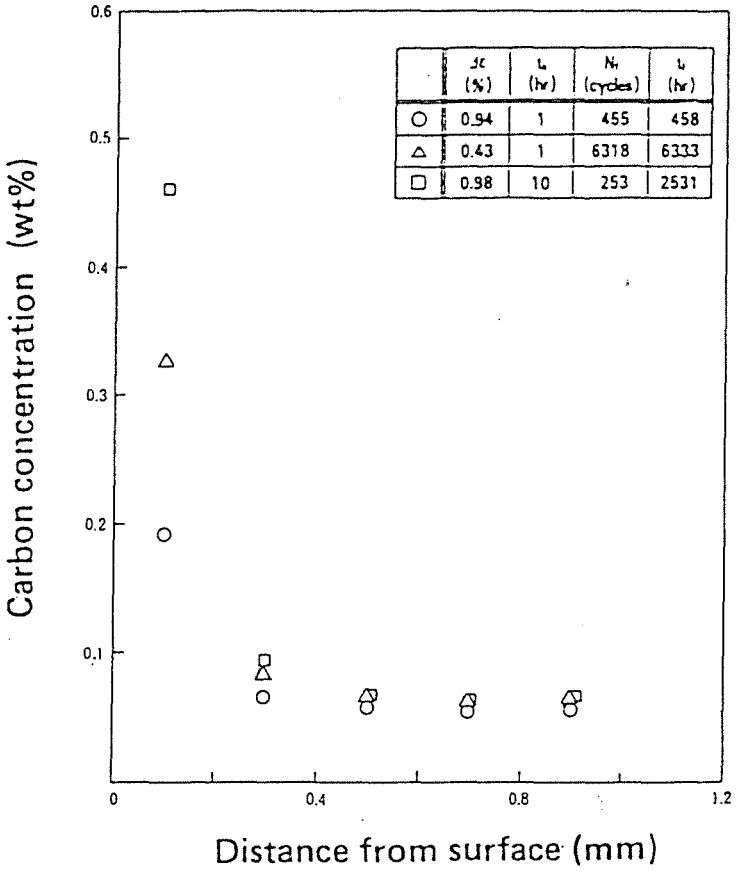

Fig. 2 Carbon penetration profile of tested specimens

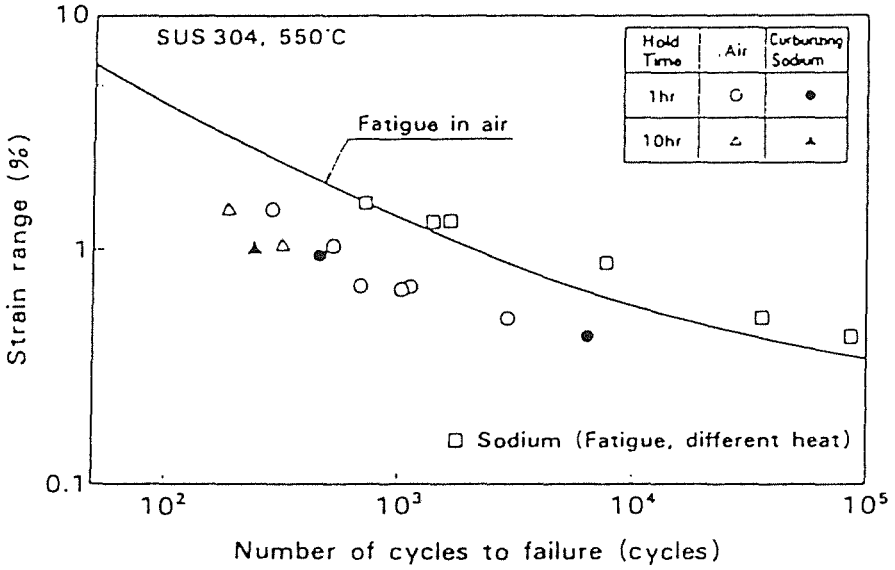

Fig. 3 Creep-fatigue life in carburizing sodium

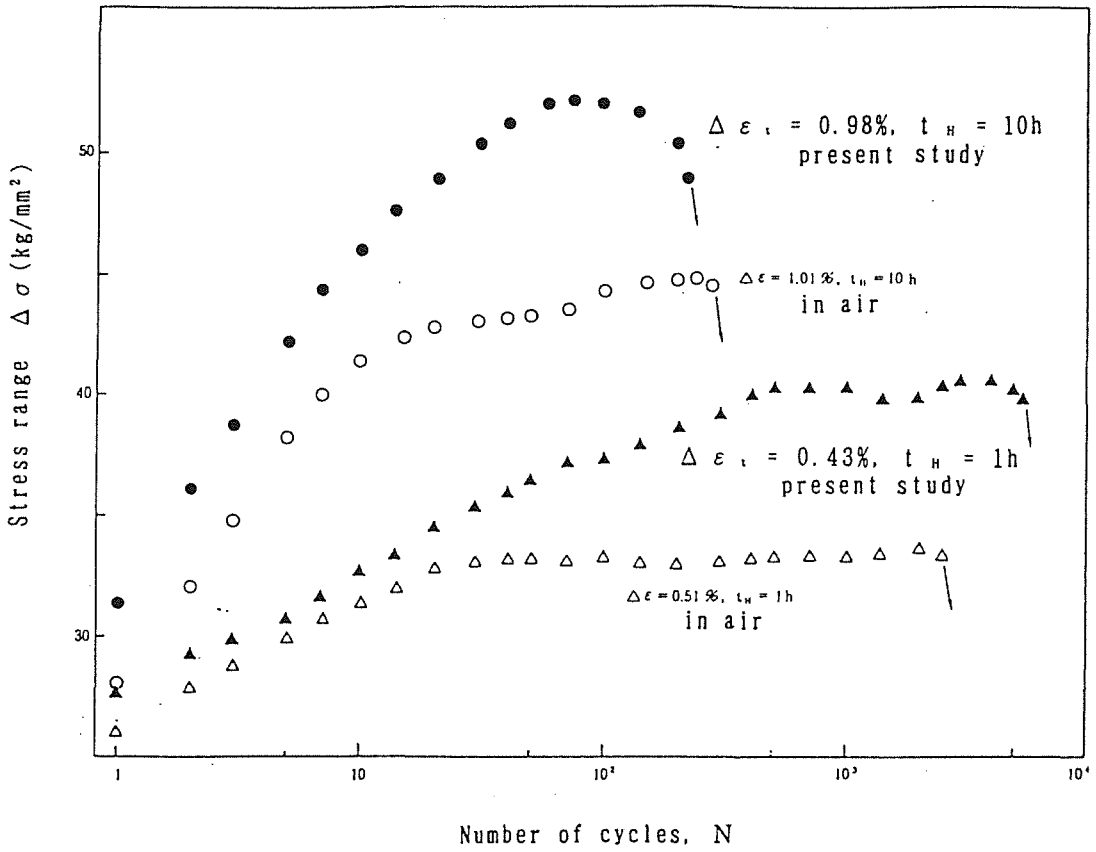

Fig. 4 Cyclic strain hardening behavior in carburizing sodium

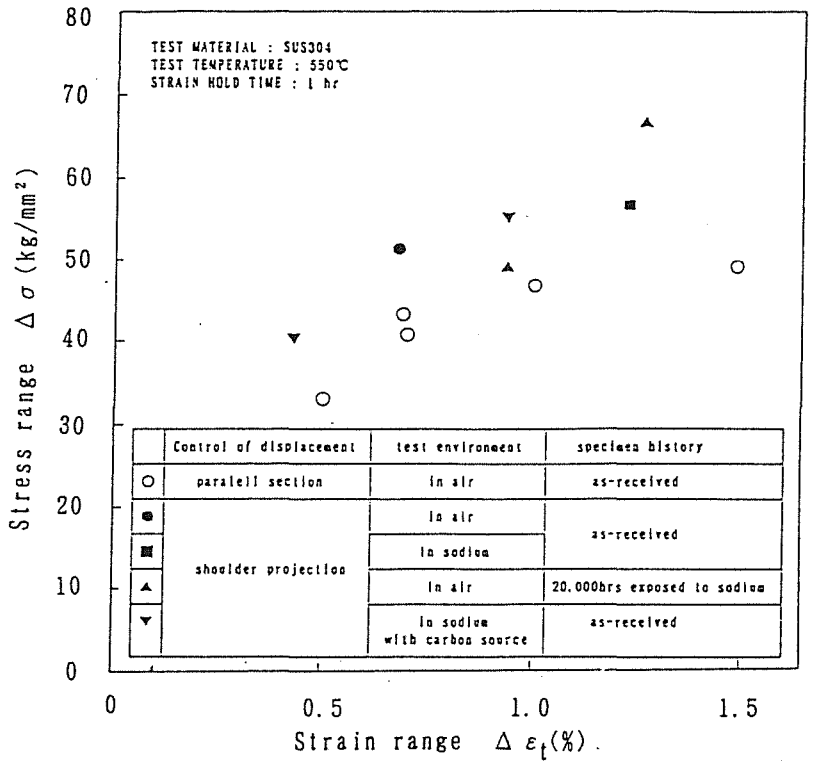

Fig. 5 Comparison between cyclic strain hardening behaviors of two types of strain control methods (shoulder guage & parallel guage)

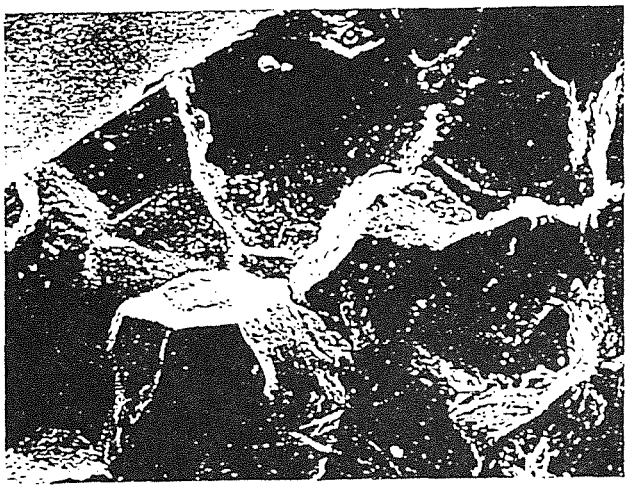

(a) $\Delta \varepsilon_t$ = 0.94% & t_H = 1hr

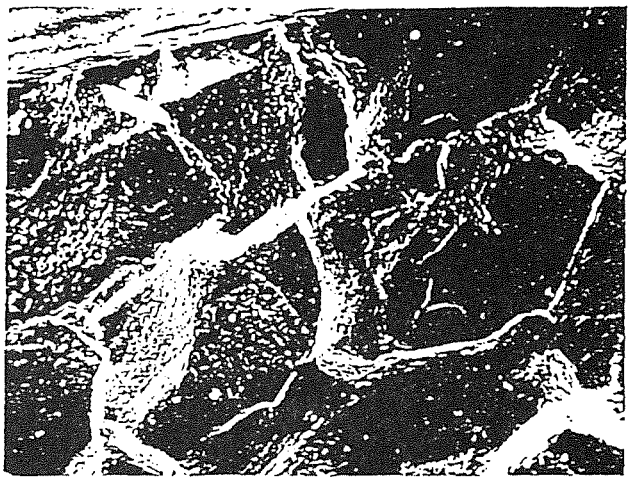

(b) $\Delta \varepsilon_t$ = 0.98% & t_H = 10hrs

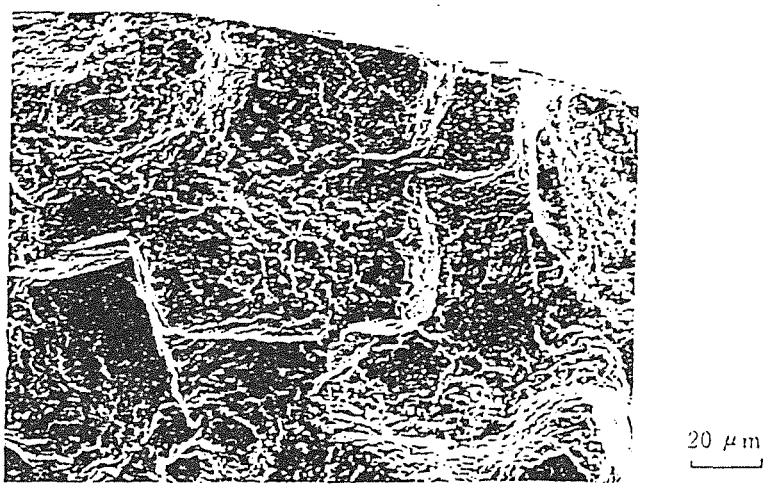

(c) $\Delta \varepsilon_t$ = 0.43% & t_H = 1hr

Fig. 6 Observation of fracture surfaces of creep-fatigue tested specimens

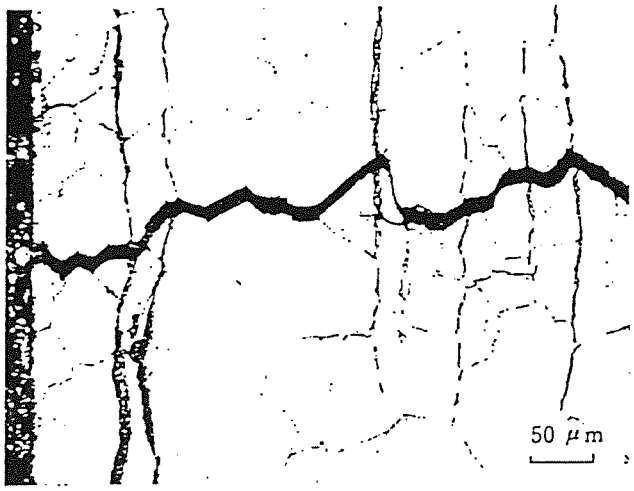

(a) $\Delta \varepsilon_t$ = 0.94% & t_H = 1hr

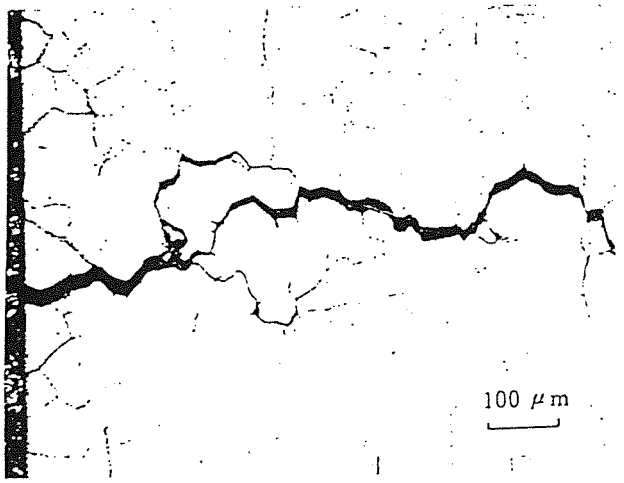

(b) $\Delta \varepsilon_t$ = 0.98% & t_H = 10hrs

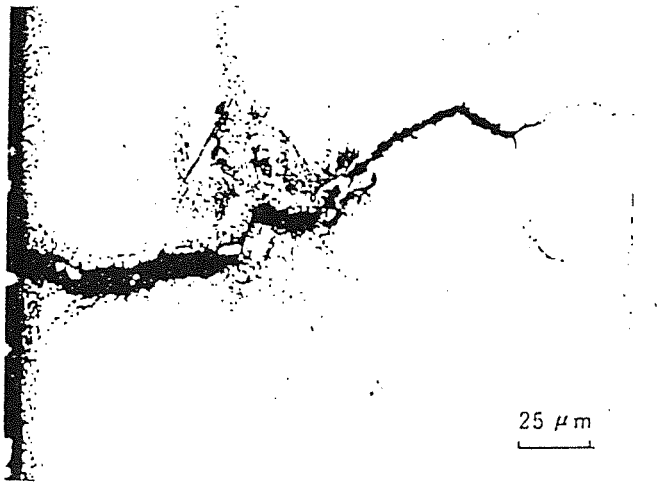

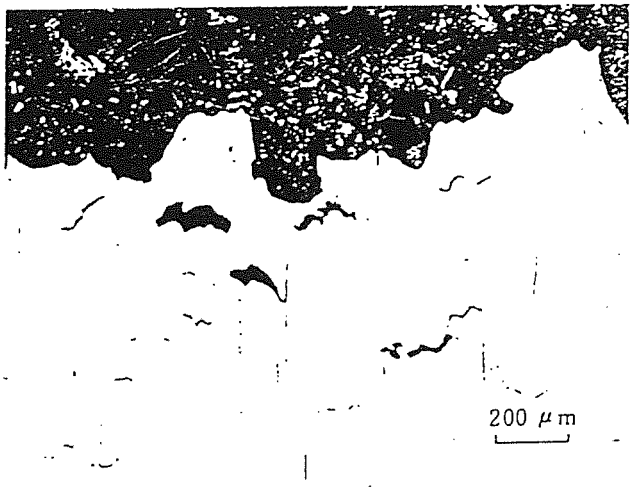

(c) $\Delta \varepsilon_t$ = 0.43% & t_H = 1hr

Fig. 7 Observation of crack initiation modes of creep-fatigue tested specimens

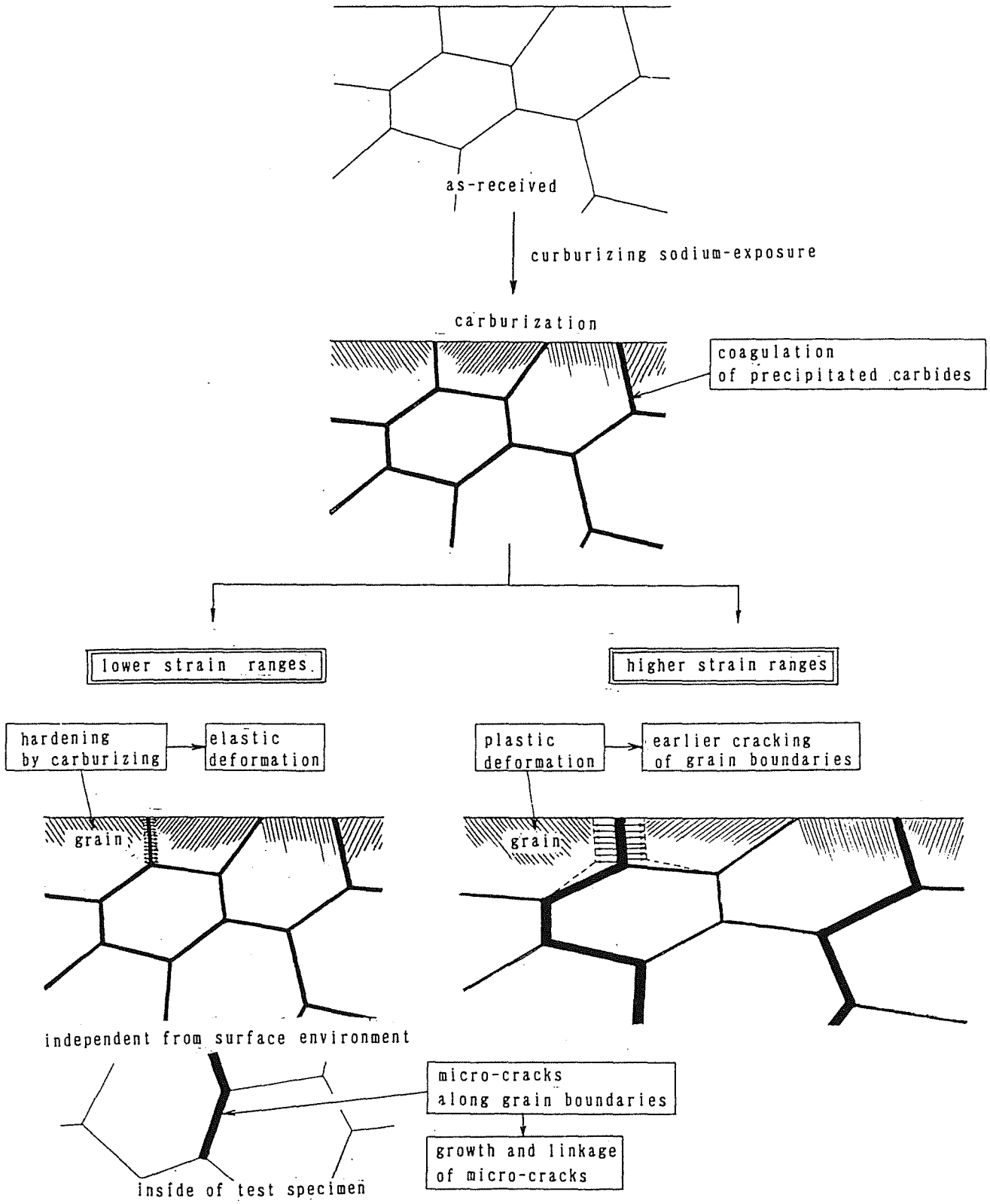

Fig. 8 Concept on process of creep-fatigue crack initiation in carburizing sodium under creep damage dominant

Cyclic Lifetime Change of Various Types of Steels by Exposure in Alkali Metal Melts

Malygin A.F., Goryacheva L.A., Troyanov V.M., Trapeznikov Ju.M.
The Central Research Institute of Structural Materials, Prometey, USSR
Institute of Physics and Power Engineering, USSR

Abstract

The paper considers the generalized mechanisms of cyclic lifetime variation of different steel types by the effect of liquid metal environments at the temperature range of 450-750°C. The investigation of corrosion factor influence on the characteristics of steels cyclic strength was performed on the basis of test results comparison in liquid metal - inert media and in air - inert media.

The generalized regularities of cyclic lifetime change in alkali metal melts and in air in the wide range of temperature-time loadings versus the corrosion damage characteristics are given. The carbon content change in surface year was non found by specimens tests.

The perlitic steels lifetime increase may reach 20 times by frontal corrosion depth and as for austenitic steels-8 times.

Introduction

It is well known that low cycle fatigue resistance of steels contacting with alkali metal melts may be similar or increased with respect to this characteristic obtained in air. This paper considers the generalized mechanisms of cyclic lifetime variation of different steel types by the effect of liquid alkali metal environments (sodium, potassium - sodium eutectics). The type X18H9, X18H10T, X21H32M3Б austenitic steels have been investigated at 450-750°C, the type X19H11M3 ferritic-austenitic steels - at 550-650°C, and the type 10X2M, 10X2МФБ perlitic steels at 550-650°. Steels of these grades are widely used as structural materials for nuclear power plant equipment /1/. The investigation of corrosion factor influence on the characteristics of steels cyclic strength was performed on the basis of test results comparison in liquid metal-inert media and in air-inert media. Thermal fatigue tests of steels were carried out in sodium and potassium-sodium eutectics with oxygen content of 1.10^{-4} - 1.10^{-2} weght percents and carbon content - up to 1.10^{-3} weght percents. The thermal loading was realized by specimens heating in argon up to 450-750°C and sharp cooling in liquid alkali metal up to 50-450°C.

The tests of steels were conducted by heating-cooling process of fixedly attached specimens in air, and by specimens slow heating in air and sharp cooling in vapour-air medium. The fixedly attached specimens were also tested in seale ampules with argon, containing 7.10^{-4} weght percents of oxygen. The steels cyclic lifetime in liquid metal medium and in air (N), and also in inert medium (N_o) was determined by the appearance of cracks of the depth α = 0,5 mm. The cyclic base of test was 10^4 cycles, the maximal exposure time - 10^4 hours.

The corrosion behaviour of perlitic steels in liquid metal media was determined by the uniform iron solution from their surfaces, and by the selective nickel and chromium solution with the respect to austenitic steels. The velocities of these processes are increased with the increasing of test temperature and oxygen concentration in alkali metal. The change of carbon concentration in specimens surface layer by testing in liquid metal environment was not revealed. It is explained by the absence of carbon transfer process.

The perlitic steels corrosion behaviour in air is characterized by the formation of little-protective oxide films at the surface of these less heat resistant steels, and as a result oxidation occurs at the surface, along grain boundaries.

The increased heat resistance of austenitic steels is achieved at the expense of the formation of films of spinel type at the steel surface which protects from intergranular oxidation.

The depth of frontal corrosion "h" was the main characteristics material corrosion damage in liquid metal environment and in air; by its determination the described corrosion process should be taken into consideration. In Figure 1 the generalized regularities of cyclic lifetime change in alkali metal melts and in air in the wide range of temperature-time loadings versus the corrosion damage characteristics are given for various types of steel (h/a). The observed perlitic steel lifetime may reach 20 times increase by frontal corrosion depth $h > 10^{-6}$ mm, (Fig. 1a) and as for austenitic steels by $h > 2.10^{-8}$ mm - approximately 8 times (Fig. 1b) increase.

By relatively low intensity of corrosion process the difference in values of steel cyclic lifetime in alkali metal melts and in inert medium is practically absent (N/N_o), as there is no embrittlement influence of alkali metal melts on steels. The high intensity of corrosion processes prevents the formation of nucleus microcracks and the tips of generating cracks are blunted.

The cyclic lifetime decrease (Fig. 1a) of perlitic steels in air is the result of their grain boundaries oxidation. Austenitic steels do not reveal the cyclic life decrease in air due to protective oxide film formation. By intensive oxidation of austenitic steel surfaces the lifetime increase up to 2,5 times is observed (Fig. 1b).

The comparative steel cyclic lifetime estimation in alkali metals melts may be performed for given temperature-time loading conditions with the use of corresponding frontal corrosion depths in the media.

References

1. Ju.F. Balandin, I.V.Gorynin, Ju.I.Zvezdin, V.G.Markov. Structural materials of nuclear power plants. M. Energoizdat, 1984.

2. C.R.Brinkman, I.P.Strizak, M.K.Booker and C.E. Jaske. - J. of Nuclear Materials, 62 (1976), N 2-3, p.181-204.

3. Ju.F.Balandin, A.F.Malygin, - FHMM, 1972, N 5, p.57-59.

4. H.Atstomo, Bergisch Gladbach, Germany, 17-21 October.

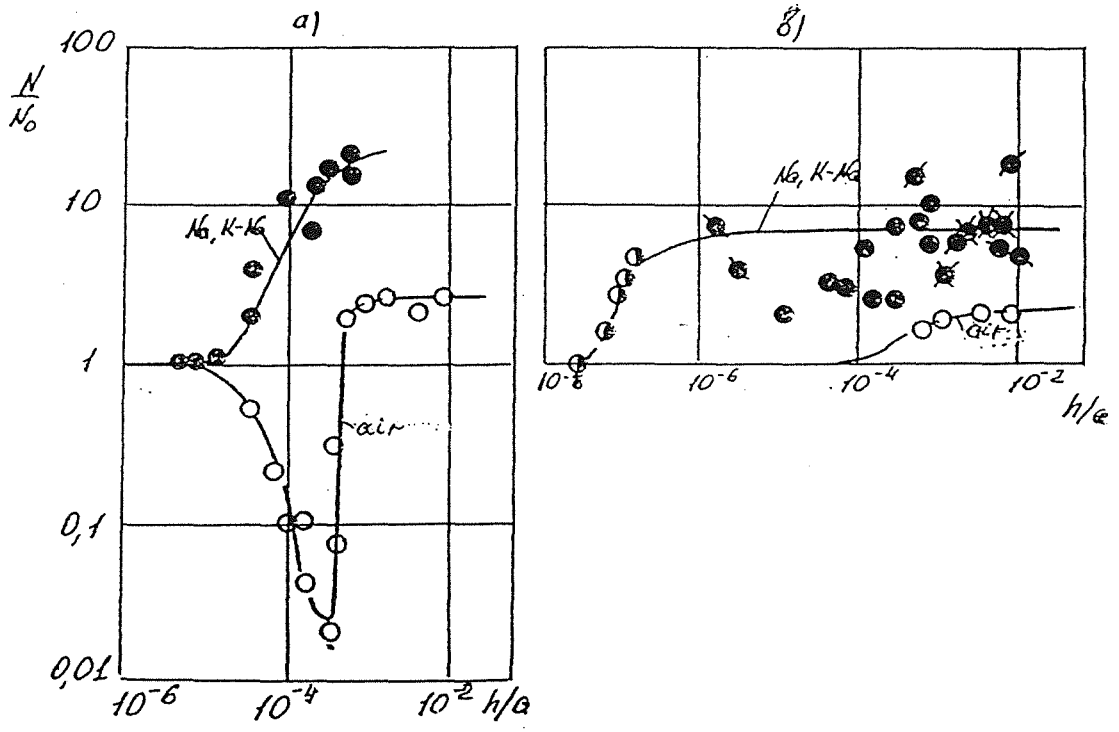

Fig. 1 Cyclic lifetime variation of perlitic steel (a), Cr-Ni austenitic and ferritic-austenitic steel (b) in alkali metal melts (Na, K-Na) in air and in inert medium.

CREEP-FATIGUE BEHAVIOUR OF TYPE 304 AND 316L(N) IN FLOWING SODIUM

H. Huthmann
Interatom GmbH
Bergisch Gladbach 1, Germany

ABSTRACT

Low cycle fatigue tests with hold periods up to 24 h have been performed on types 304 and 316L(N) stainless steel in air and in flowing sodium at 550 °C.

It was shown that the number of cycles to failure decreases with increasing hold times and that the failure mode changes from trans- to intercrystalline fracture. A beneficial effect of sodium occurs under pure cyclic loading and with short hold times. With the longest hold times similar behaviour in both environments has been observed. Tests on long term pre-exposed (sodium, 550 °C, 10,000 h) specimens show that strong carbide precipitation increases the number of cycles to failure in flowing sodium.

1 INTRODUCTION

Important mechanical properties for safe design of fast breeder reactors are the number of cycles to failure in low cycle fatigue (LCF) and rupture time in creep. Low cycle fatigue loadings occur due to the reactor start up and shut down and due to power transients. Operating temperatures are in the range where creep deformation can occur and the interaction between creep and fatigue is an important aspect of the material behaviour in assessing the life time of the component. Creep fatigue interaction is governed by a large number of variables such as loading conditions, hold time, temperature, strain range, environment, microstructure and their mutual interactions.

This investigation was carried out to evaluate the influence of flowing sodium and hold time on the LCF-life and fracture mechanisms of AISI type 304 and 316L(N) stainless steels at 550 °C. A detailed description of the creep-fatigue behaviour of type 304 in air is given in [1].

For type 304 the influence of different microstructural conditions obtained by pre-ageing the specimens in flowing sodium at 550 °C for 10,000 hours simulate the material behaviour under service conditions.

2 EXPERIMENTAL DETAILS

2.1 Materials and Specimens

A characterization of the materials used for the LCF-tests with hold times is given in Table I. Hourglass type specimens with a minimum gauge diameter of 8.8 mm and a gage length of 21 mm were taken perpendicular to the rolling direction. The specimens were welded into bellows, as shown in Fig. 1, for the in-sodium tests. The shrouds inside the bellows permit a sodium velocity of 2.5 m/s within the gauge length of the specimens.

For the tests in sodium the specimens were pre-exposed for 500 h at 550 °C in flowing sodium to remove the chromium-oxide layer from the surfaces of the specimens. Correspondingly, the specimens for the in-air tests were thermally aged in argon at 550 °C for 500 h.

2.2 Sodium Loop

In order to gain representative test results for the corrosive conditions of liquid metal fast breeder systems the tests have been performed in the non-isothermal sodium loop of Interatom. A description of this loop is given elsewhere [2].

2.3 Test Procedure

The tests were performed with servo-hydraulic MTS-systems (short term tests) and electromechanical Schenck-systems (long running tests in sodium and in air). They were conducted in the axial strain-control mode with a strain rate of $4 \cdot 10^{-3} s^{-1}$ with a fully reversed triangular wave form and zero mean strain. Hold times were introduced at the maximum tensile strain since it was found to be the most deleterious type of loading. The strain was measured by extensometers outside the furnace attached to the collars of the embellowed specimens by measuring rods. The load was controlled by a load cell located between the rigid rod and the cross-head of the fatigue machine. No correction was made due to the hourglass type of specimens, therefore the actual strain values in the thin section of the gauge length will be something higher than the measured values.

3 TEST RESULTS

3.1 Results for Type 304

On type 304 low cycle fatigue tests in flowing sodium have been performed at strain ranges of

$\Delta\varepsilon_t$ = 0.6 % with hold times up to 30 min, and
$\Delta\varepsilon_t$ = 1.0 % with hold times up to 24 hours.

The largest running time was about 1 year. The detailed results are given in Table II.

A comparison of the number of cycles to failure reached in sodium and in air is given in Fig. 2. As is known from earlier investigations for the low cycle fatigue behaviour without hold periods [2] a beneficial influence of sodium is observed at 3 minutes hold time, too. But for $\Delta\varepsilon_t$ = 0.6 % degradation of fatigue life is found to be faster with increasing hold time up to 2 hours when compared to the results in air. For tests with hold times longer than 6 hours; no influence of environment is observed. Metallographic examination was undertaken to understand the difference in this behaviour. Specimens for these tests were fabricated from different plates of heat No. 402. Grain size determination from the shoulder region of these tested specimens, where an environmental influence can be excluded, showed that the specimens fall in two distinctive grain sizes. The specimens tested in air and those tested in sodium with hold times of 6 hours and more had an average grain size of 0.018 mm while the specimens tested in sodium with hold times of 2 hours and less had an average grain size of 0.035 mm. The observed difference in fatigue life for hold times less than 2 hrs may therefore be due to the difference in grain size by a factor of two. Hence a direct comparison of the influence of environment is not possible for hold times up to 2 hours.

Figure 3 shows the typical microstructure of the specimens aged for 500 and 10,000 hours in flowing sodium. Considerable amount of carbide precipitation is observed especially at grain boundaries in specimens aged for longer duration.

The number of cycles to failure as a function of total strain range is shown in Fig. 4. The results are compared with the continuous cycle (with zero hold time) behaviour of specimens aged for 10,000 hours at 550 °C in flowing sodium. Two important observations can be made. Fatigue life decreases with increase in hold time and strain range. Carbide precipitation is found to increase the number of cycles to failure at the strain ranges examined.

The surface cracks formed on these specimens are examined by scanning electron microscopy (SEM). Figure 5 shows the typical photographs of the surface cracks formed on the failed specimens. The cracks are formed at an angle of 90 degrees to the tensile axis and they are found to originate at the exposed grain boundaries. Hold time and pre-ageing is found to have an influence on the formation of surface cracks. It is observed that increasing hold time is associated with longer surface cracks while longer ageing time increases their number.

The optical micrographs of the longitudinal section of the samples are shown in Fig. 6 which clearly explains the origin and propagation of the cracks formed at the surface. At short hold times surface cracks initiate intergranularly and propagate in a mixed mode. The initiation and growth behaviour is entirely intergranular in nature at long hold times. This is supplemented by the features observed on the fracture surface as shown in the Fig. 7.

The features around the tip of a growing crack can be understood from the evidence shown in Fig. 8. For short hold times the crack grows in the beginning in a mixed mode. Intergranular cavitation is seen in specimens aged for longer duration or tested with large hold times.

3.2 Results for Type 316L(N)

On type 316L(N) low cycle fatigue tests in flowing sodium have been performed at strain ranges of

$\Delta\varepsilon_t$ = 0.6 % with hold times up to 300 min, and
$\Delta\varepsilon_t$ = 0.4 % with hold times up to 30 min.

The numbers of cycles to failure are given in Table II. Fig. 10 gives the comparison with parallel tests in air. For this material the grain size of the specimens tested in air and in sodium are the same (70 - 80 µm), which allows a valid comparison.

For LCF-tests without hold periods the numbers of cycles to failure are significantly higher in sodium than in air. For both strain ranges (0.4 % and 0.6 %) the numbers of cycles to failure approach the in-air data with increasing hold times. For $\Delta\varepsilon_t$ = 0.6 % the number of cycles to failure in sodium and in air are nearly the same for hold times of 300 minutes. For $\Delta\varepsilon_t$ = 0.4 % the in-sodium test with 30 min hold period was terminated after 8360 cycles, which was already close to the number of cycles reached in air.

Accordingly the development of the maximum stress at maximum strain with cycles is the same in sodium and in air for $\Delta\varepsilon_t$ = 0.6 % and t_h = 300 min. Fig. 11 shows that in both environments a strong cyclic hardening occurs with maximum stress values at about 500 cycles.

The stress values after relaxation (σ_{relax}) are given in Fig. 12 for these tests, likewise no significant difference occurred due to environment.

The metallographic examinations of these specimens with $\Delta\varepsilon_t$ = 0.6 % and t_h = 300 min. indicate a higher plastic deformation of the in-air specimen in the area of the developed crack. This is shown in the SEM-photographs of those specimens in Figs. 13a and 13b. But in both environments the crack starts and grows intergranularly. That is shown in the optical micrographs of Fig. 14. The intergranular character of the creep-fatigue cracks is clearly shown in the SEM-photograph of the fracture surface of the in-sodium test (Fig. 15).

4 DISCUSSION

For both materials a higher number of cycles to failure occurred in sodium than in air for the pure cyclic loading and for cyclic loading with short hold periods. With increasing hold times the cycles to failure are similar.

A possible explanation for this behaviour could be based on the change in fracture mode which occurred when changing from fatigue to increasing creep loading. Under pure fatigue loading crack initiation takes place by shear deformation of the material in the surface area and crack growth is transgranular. This was clearly demonstrated by [2] for type 304 and similar behaviour can be assumed for type 316L(N).

When hold times are introduced, cavities are appearing at the outer surface of the specimens tested in air and in sodium (Figs. 9 and 10). This leads to an intercrystalline fracture mode with increasing hold times.

It can be assumed that the higher number of cycles to failure measured in sodium are due to a beneficial effect of sodium occurring in fatigue when crack initiation takes place by shear deformation (e. g. in sodium no oxide formation hampers sliding processes on fresh metal surfaces as it occurs in air).

When intergranular fracture becomes dominant, as shown for type 316L(N) with $\Delta\varepsilon_t$ = 0.6 % and 300 minutes hold time (Figs. 14 and 15), the beneficial influence of sodium is not effective and the numbers of cycles to failure are the same in air and in sodium.

With this assumption it can be expected that a further increase of hold time will not lead to lower number of cycles to failure in sodium than in air as this could be expected from a linear extrapolation of the in-sodium data in Figs. 2 and 10. Unfortunately this cannot be proved by experiments, because the longest tests performed have already running times of about one year.

Regarding the long term aged specimens of type 304 it was observed that the number of cycles to failure is increased compared to the short term aged material. Influence of carbide precipitation on the creep fatigue life was studied earlier [3] in type 316 stainless steel at 550 °C with a tensile hold time of 30 minutes. It was shown that the life increases with the increasing amount of carbide precipitation at all strain ranges investigated. A significant role played by grain boundary carbide was noted. The beneficial influence of carbide precipitation on fatigue life was also observed by Dean and Plumbridge [4]. Grain boundary precipitates play an important role in grain boundary sliding. Morris and Harris [5] found that the extent of grain boundary sliding was reduced on ageing due to precipitates pinning the boundary. The present results also confirm similar behaviour in sodium in type 304 stainless steel as the number of cycles to failure is higher for specimens aged for 10,000 hours compared to the life of the specimen aged for 500 hours.

5 CONCLUSION

The following conclusions could be derived from the performed low cycle fatigue tests with hold periods in air and in sodium and the microstructural examinations of failed specimens.

1. Types 304 and 316L(N) stainless steel show a beneficial effect of sodium under pure cyclic loading and cyclic loading with short hold times. With increasing hold times similar behaviour in air and sodium has been observed.

2. This behaviour can be explained by an beneficial effect of sodium occurring for transcrystalline fracture. For intercrystalline fracture no effect of sodium occurs. From this no effect of sodium has to be expected for tests with longer hold times than applied.

3. Carbide precipitation is found to have beneficial influence in increasing the number of cycles to failure under creep fatigue conditions in dynamic sodium.

4. Larger grain size of a part of the 304-specimens leads to a reduced number of cycles to failure in sodium.

ACKNOWLEDGEMENT

The present work has been funded by the Bundesminister für Forschung und Technologie in the framework of the reactor safety programme which is gratefully acknowledged. Furthermore the author would like to thank Mr. K.G. Samuel from Materials Development Division, Indira Gandhi Centre for Atomic Research, Kalpakkam, India, for essential contributions to this paper, he made during his stay at Interatom under Indo-German bilateral agreement.

REFERENCES

[1] MEURER, H.P., BREITLING, H., Evaluation of the creep-fatigue behaviour of X6 CrNi 18 11, International Spring Meeting on Fatigue at High Temperatures, Société Française de Metallurgie, Paris 9 - 11 Juin 1986

[2] HUTHMANN, H., JENNER, G., Influence of sodium on the low and high-cycle fatigue behaviour of type 304 stainless steel in "Liquid Metal Engineering and Technology", (Proc. 3rd Int. Conf., Oxford 1984), Vol. 2, BNES, London 1984, 473 - 477

[3] HORAK, J.A., SIKKA, V.K., RASKE, D.T., "Review of Mechanical Properties and Microstructure of Types 304 and 316 Stainless Steel after Long Term Ageing" IAEA-IWGFR-49, Chester, England, 10 - 14 October 1983, paper 90-2

[4] DEAN, M.S., PLUMBRIDGE, W,J., "Mechanical Behaviour and Nuclear Applications of Stainless Steel at Elevated Temperatures", Metal Society, London, Book No. 280 (1982) 13

[5] MORRIS, D.G., HARRIS, D.R., Met. Sci., 12 (1978) 532

Table I: Characterization of Materials

Type/DIN-No.	304SS/1.4948	316L(N)/1.4909
Manufacturer:	Südwestfalen AG	Krupp SW
Basic Heat No.:	2947771	013824
Plate thickness:	20 mm	30 mm
Interatom-No.:	IA-402	IA-528
Heat treatment:	1020 °C sol. ann./ Water quenched	1020 °C sol. ann./ Water quenched
Grain size:	18 µm, 35 µm	76 µm

Chemical Composition (wt%)

Material	C	Si	Mn	P	S	Cr	Mo	Ni	B	N
IA-402	0.0600	0.47	1.67	0.015	0.004	17.82	0.03	10.72	0.0028	0.034
IA-528	0.0240	0.13	2.01	0.015	<0.003	17.44	2.40	12.54	0.0007	0.061

Material	V	Al	Zn	Cu	Co	Nb	Ta	Ti	O	As
IA-402	0.091	0.015	0.002	0.025		<0.01	<0.01		0.0012	0.29
IA-528				0.05	0.04	<0.01	<0.005	<0.01		

Mechanical Properties

Material	Temp./°C	$R_{p0.2}$/MPa	R_m/MPa	A/%	Z/%
IA-402	20	258	604	70	79
	550	132	406	41	72
IA-528	20	265	571	55	80
	550	119	392	42	76

Table II: LCF-Tests with Hold Periods in Tension Performed in Flowing Sodium at 550 °C

Material	Pre-exposure	Strain Range [%]	Hold Period [min]	No. of Cycles to Failure
Type 304 (IA-402)	500 h, Na, 550 °C	1.0	0	
			3	1750, 1871
			360	502
			1440	362
		0.6	0	
			3	6214
	10^4 h, Na, 550 °C	1.0	0	7744
			3	2177
			30	1063
			120	611
		0.6	0	37946
			3	6514
			30	3895
Type 316L(N) (IA-528)	500 h, Na, 550 °C	0.6	0	50275
			10	5809
			30	3851
			90	2726
			300	1544
		0.4	0	327839
			3	32750
			30	>8360

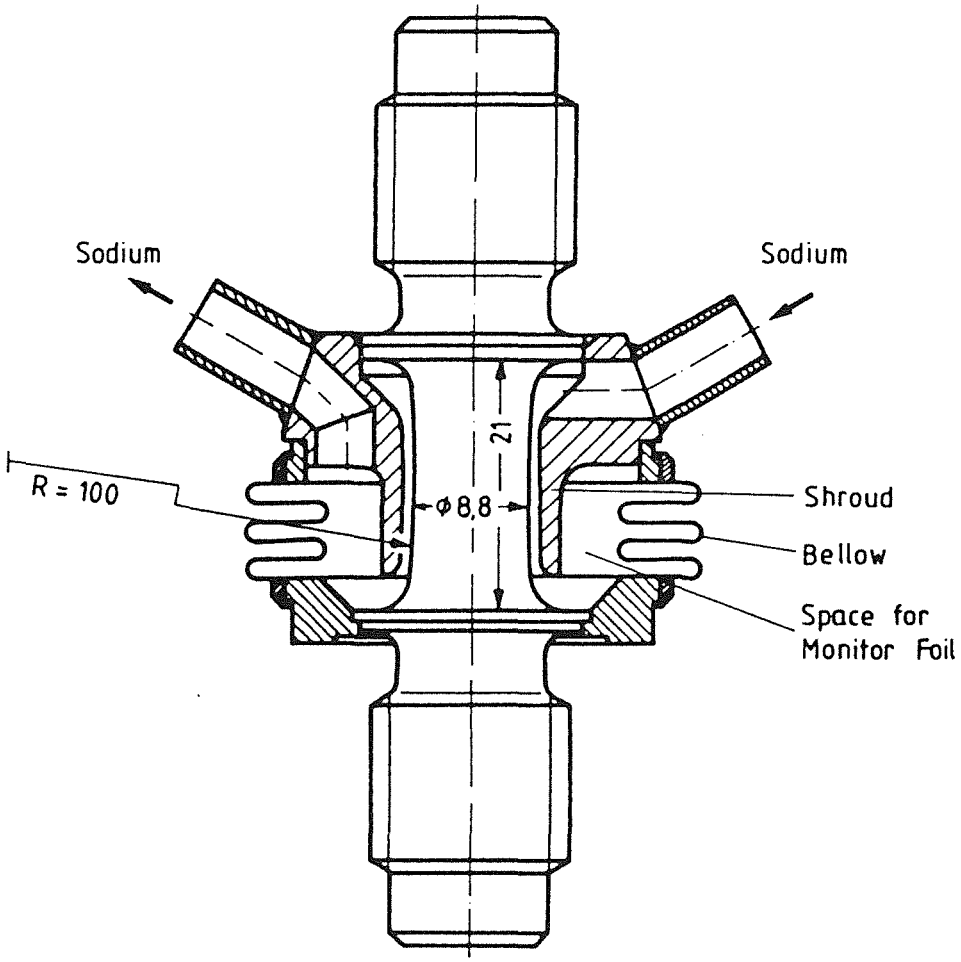

Fig. 1 LCF specimen for testing in flowing sodium

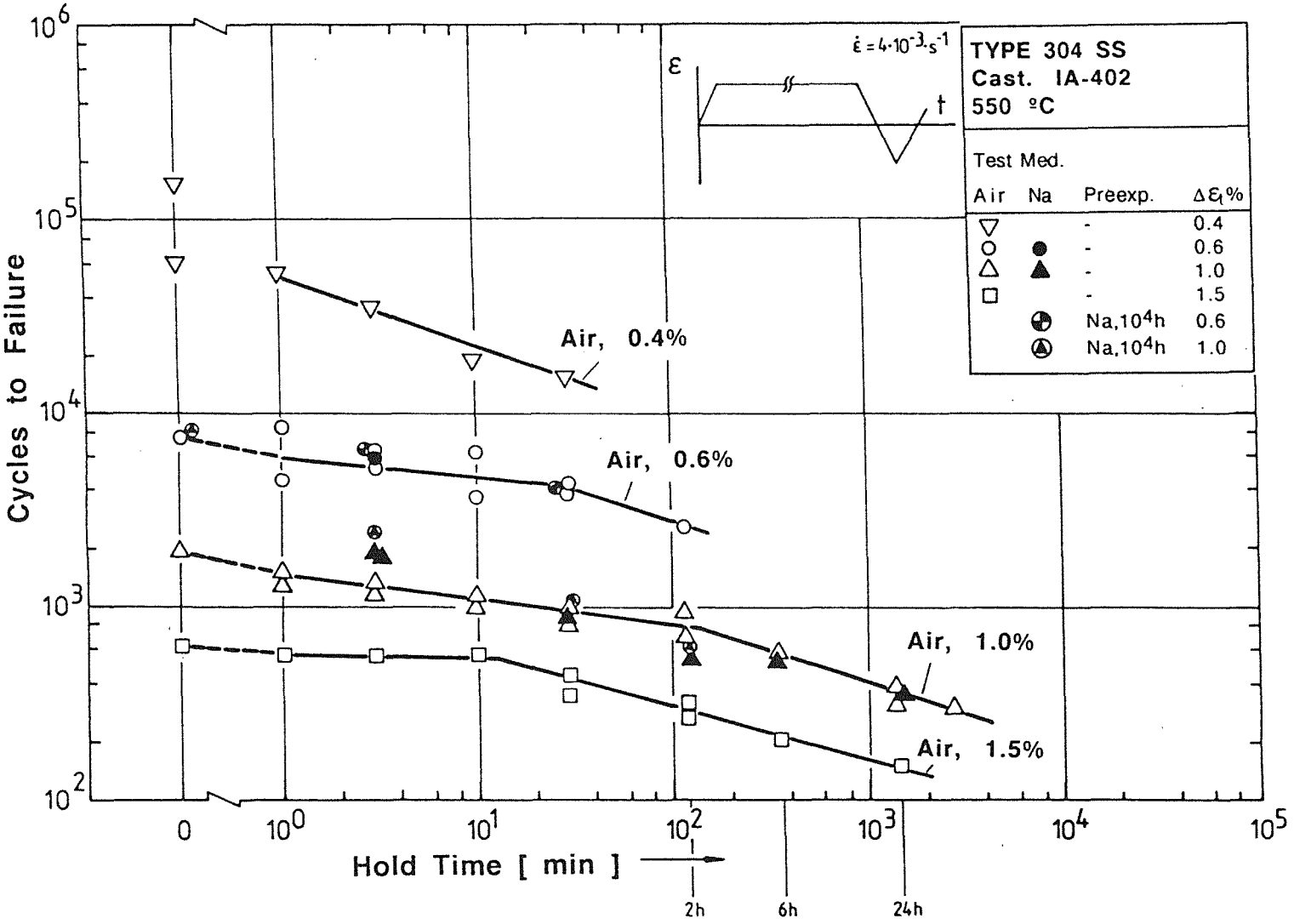

Fig. 2 Influence of hold times on the LCF-behaviour of 304 ss at at 550 °C in air and flowing sodium

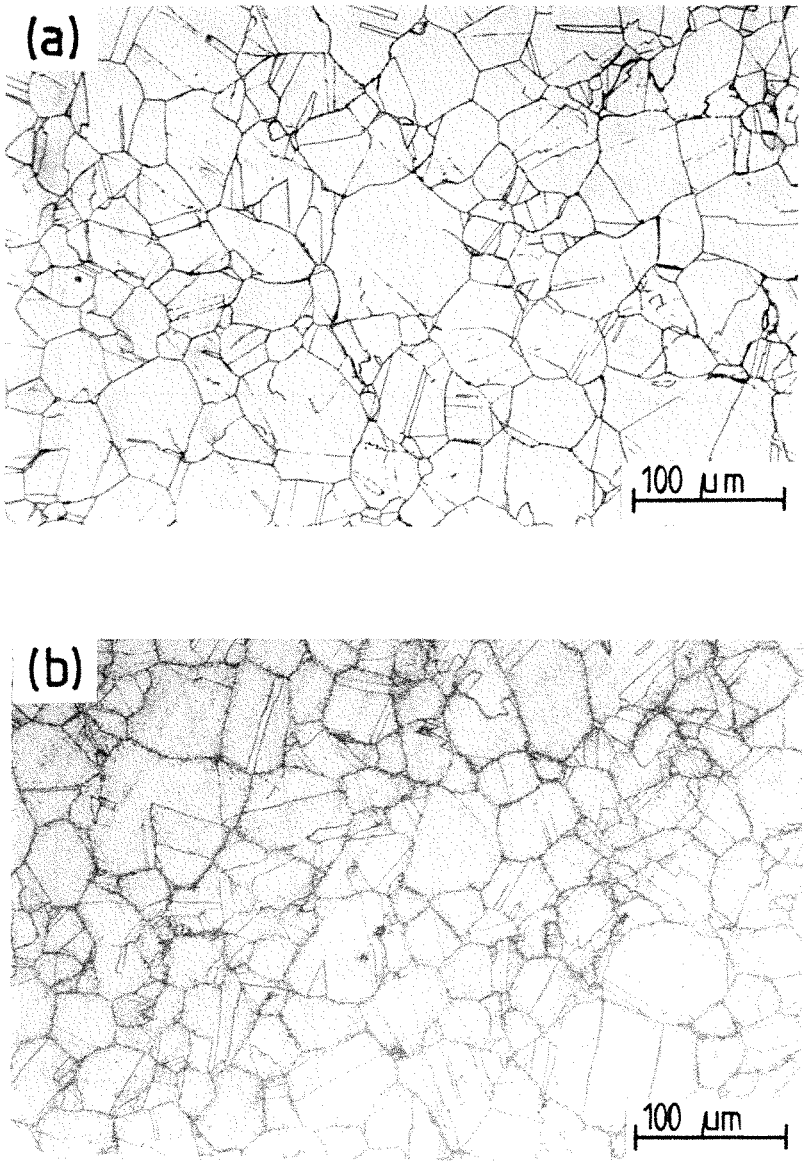

Fig. 3 Microstructure after ageing in flowing sodium a) after 500 h, b) after 10.000 h

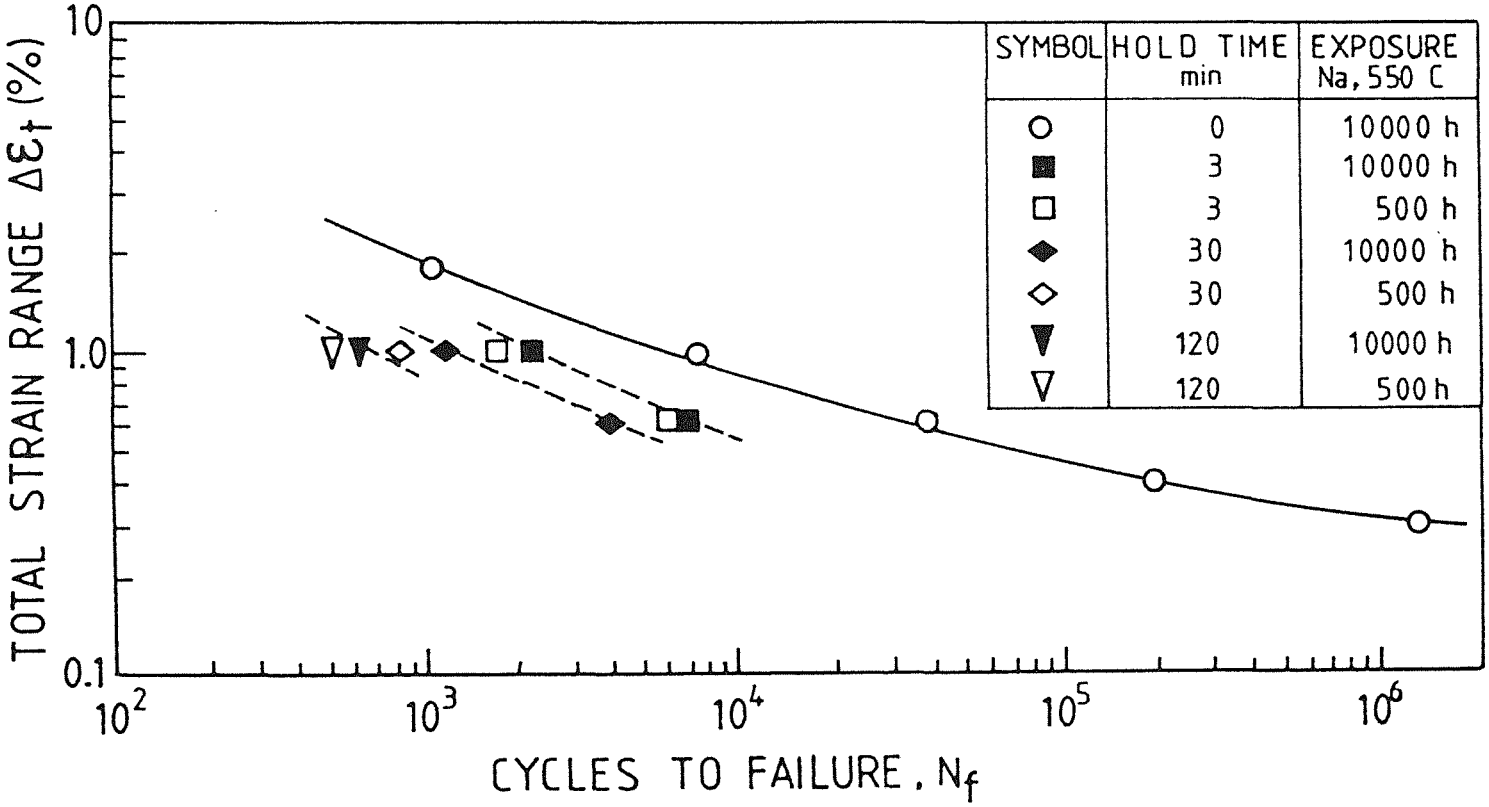

Fig. 4 LCF behaviour of Type 304 SS at 550 °C in flowing sodium

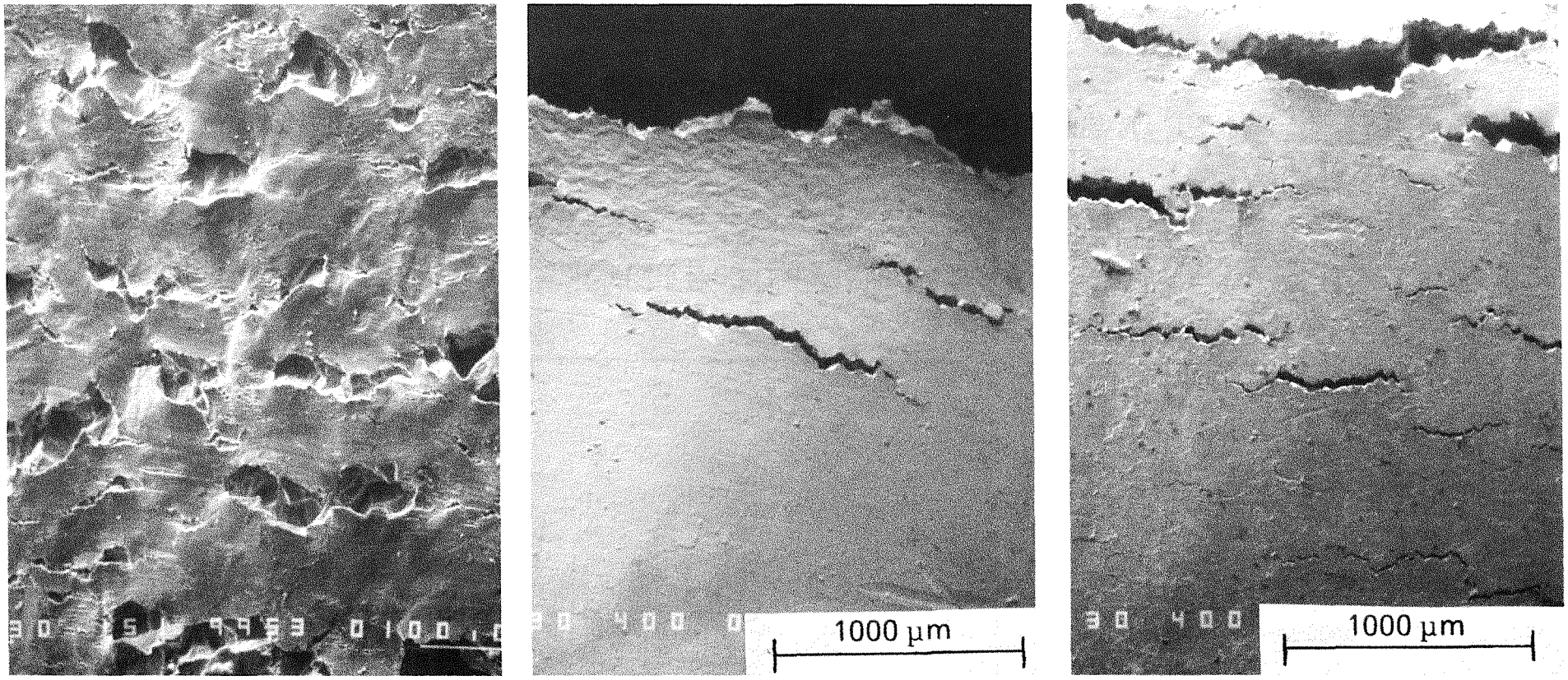

a) Aged 500 h
t_h = 3 min

b) Aged 500 h
t_h = 120 min

c) Aged 10.000 h
t_h = 120 min

Fig. 5 Surface cracks on LCF specimens tested in sodium at 550 °C

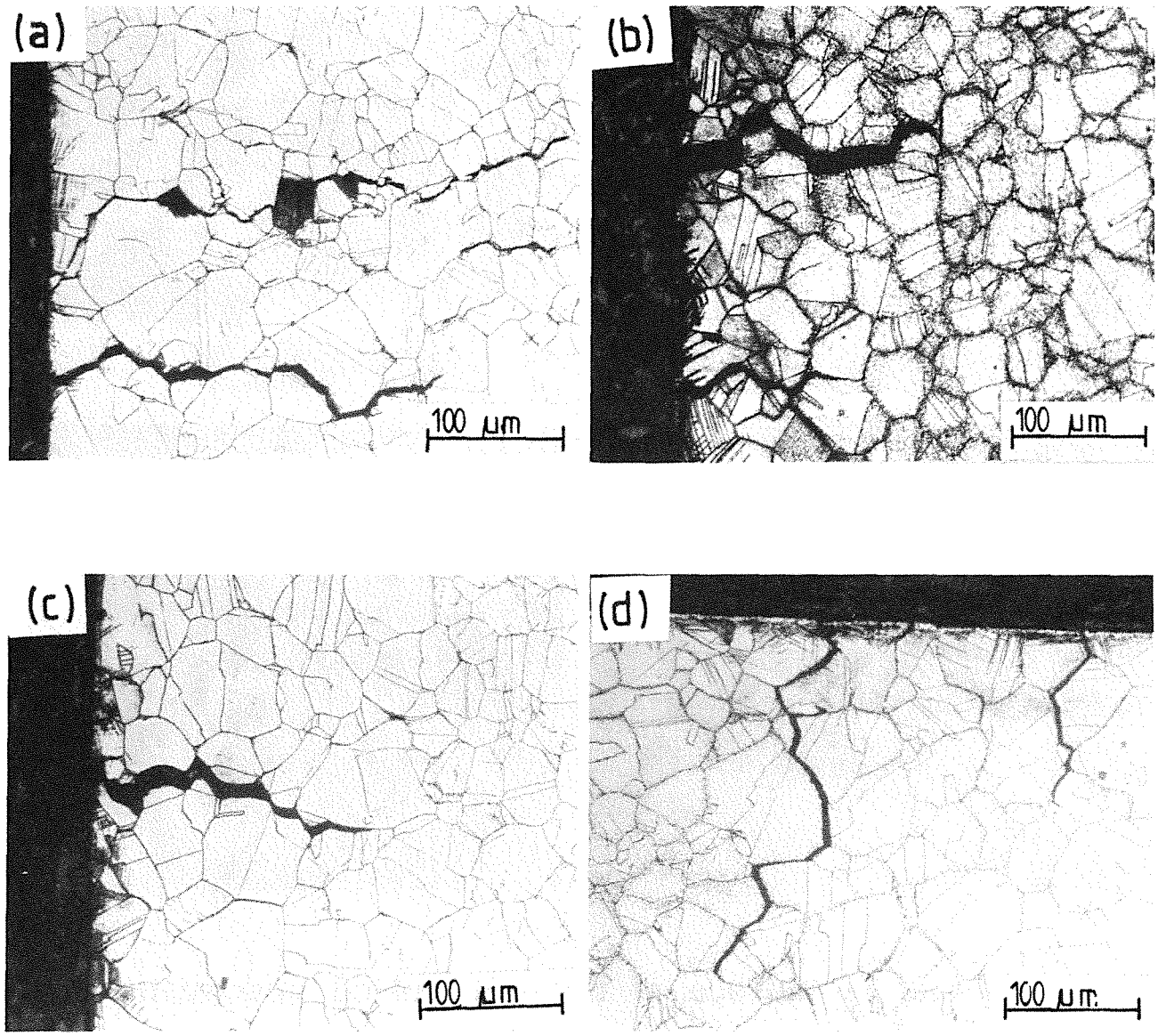

Fig.6 Micrographs of surface cracks formed after LCF testing in sodium (550 ºC, $\Delta\varepsilon_t$= 1.0 %) as a function of pre-exposure and hold time:

a) pre-exposure 500 h, t_h = 3 min
b) pre-exposure 10.000 h, t_h = 3 min
c) pre-exposure 500 h, t_h = 120 min
d) pre-exposure 10.000 h, t_h = 120 min

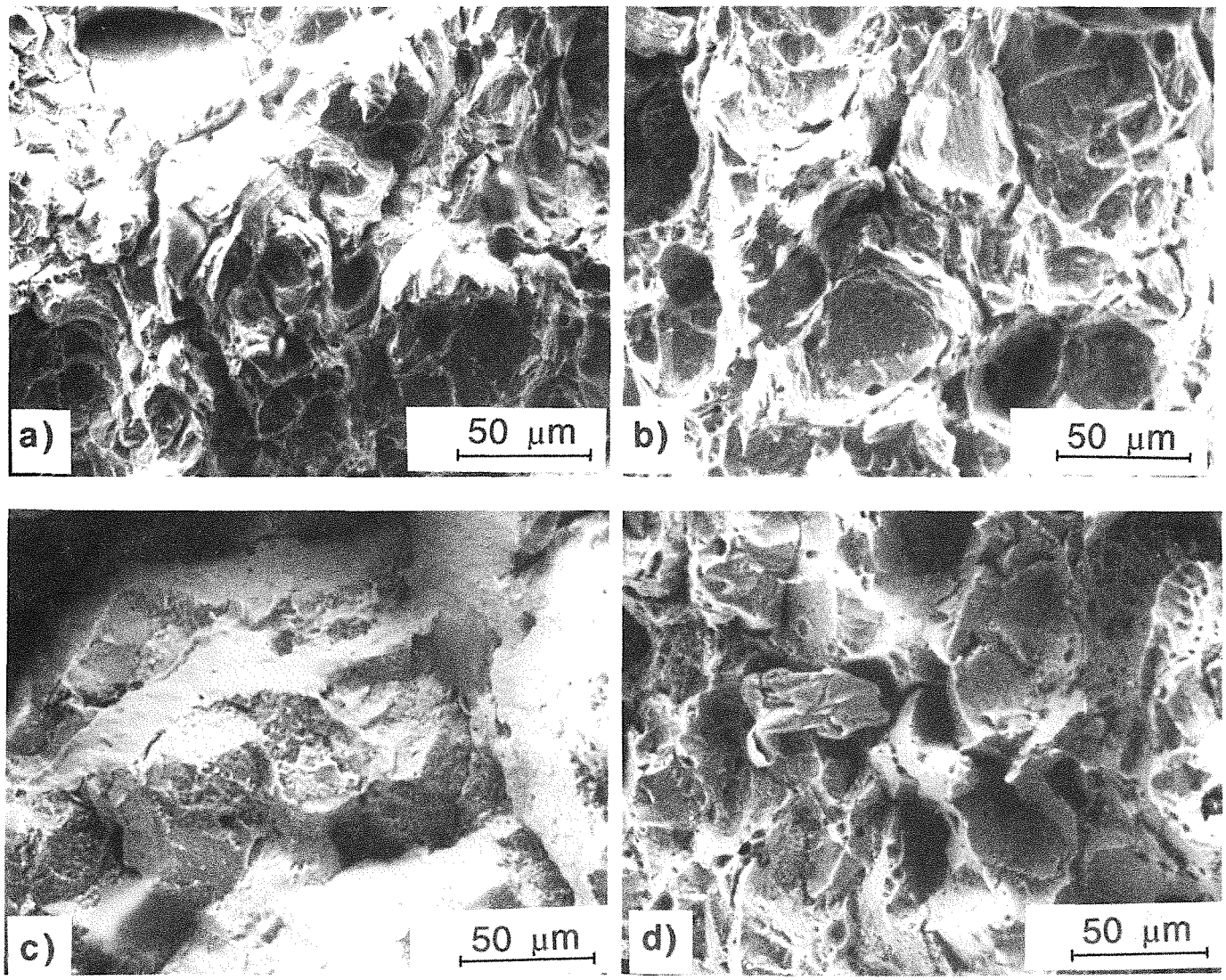

Fig.7 Fracture surface of the LCF tested specimens in sodium (550 ºC, $\Delta\varepsilon_t$= 1.0 %) as a function of pre-exposure and hold time:

a) pre-exposure 500 h, t_h = 3 min
b) pre-exposure 10.000 h, t_h = 3 min
c) pre-exposure 500 h, t_h = 120 min
d) pre-exposure 10.000 h, t_h = 120 min

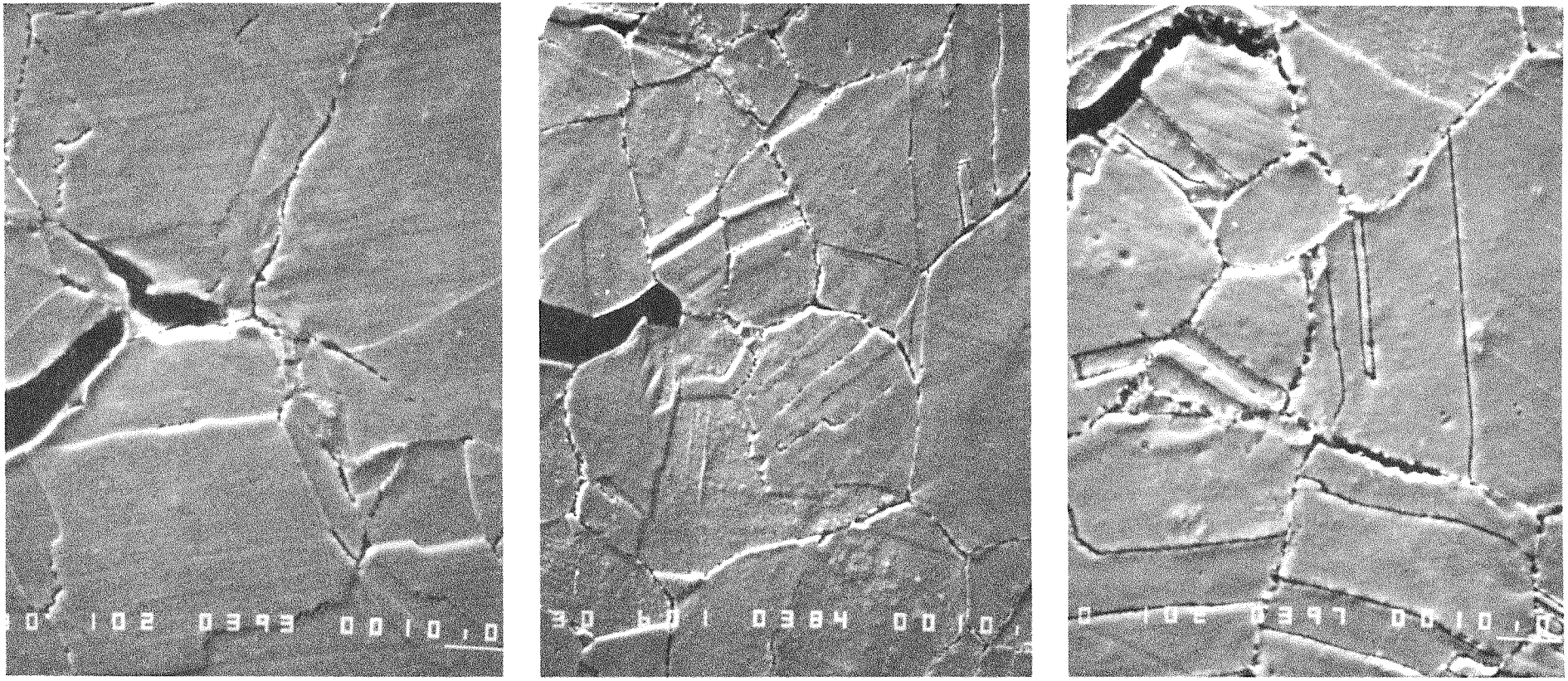

a) Aged 500 h
t_h= 3 min

b) Aged 500 h
t_h = 120 min

c) Aged 10.000 h
t_h = 120 min

Fig. 8 Features ahead of a growing crack during LCF-testing in sodium at 550 °C

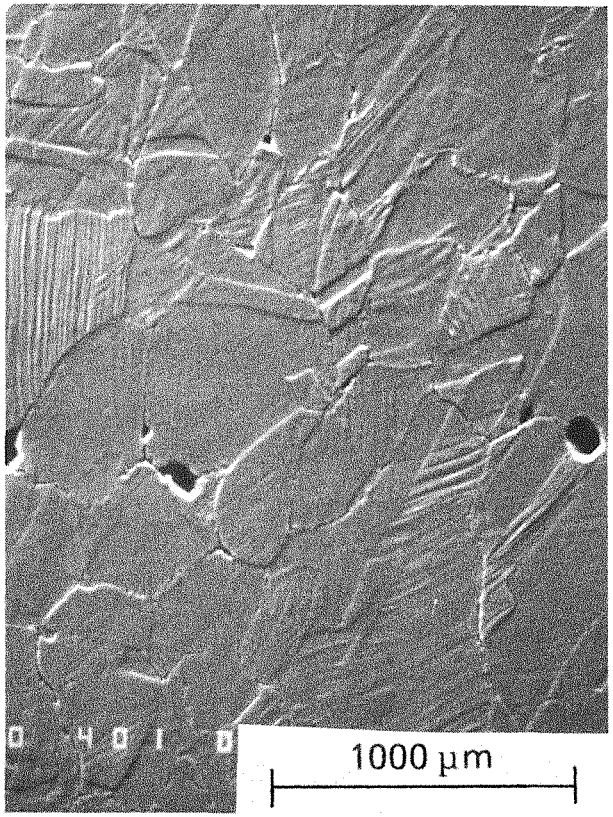

a) Aged 500 h
t_h = 3 min

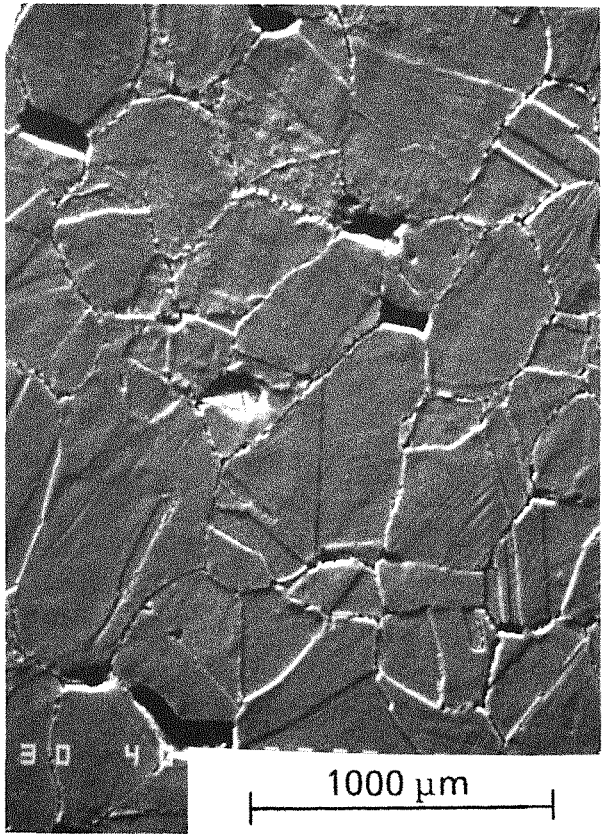

b) Aged 500 h
t_h = 120 min

Fig. 9 Damage near the fracture surface of LCF-specimens tested in sodium at 550 °C

c) Aged 10.000 h
t_h = 3 min

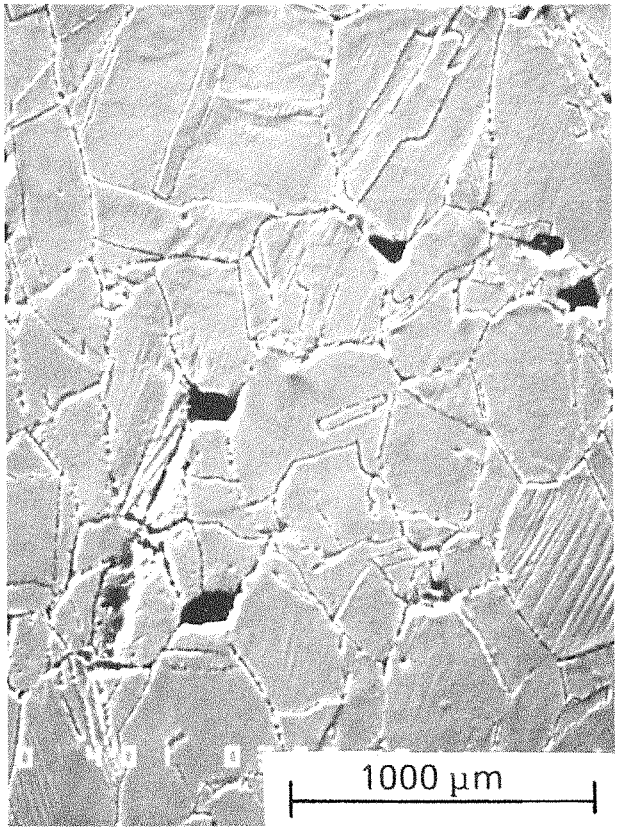

d) Aged 10.000 h
t_h= 120 min

Fig.9 continued
Damage near the fracture surface of LCF-specimens tested in sodium at 550 °C

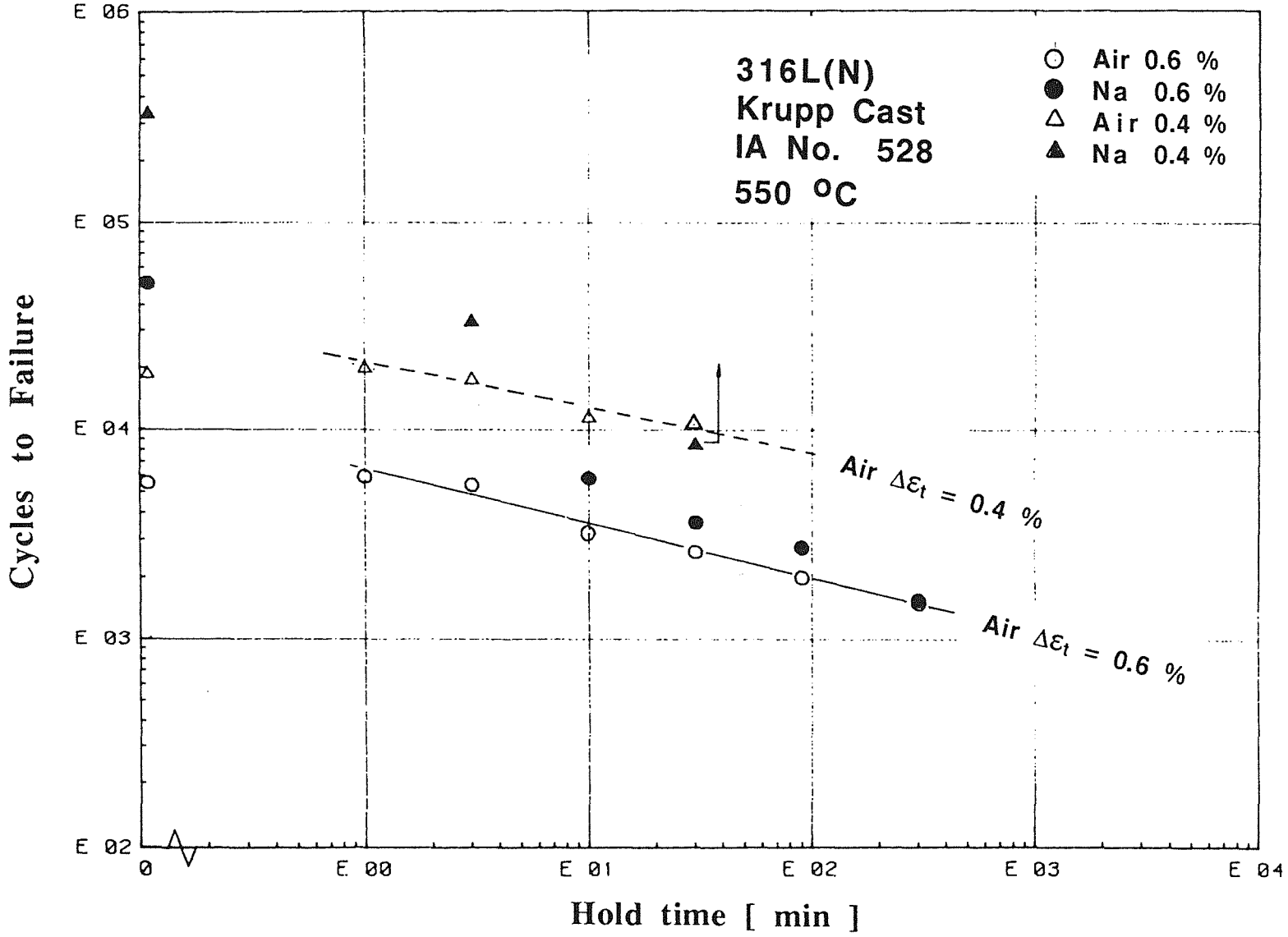

Fig. 10 Influence of hold times on the LCF-behaviour of 316L(N) at 550 °C in air and flowing sodium

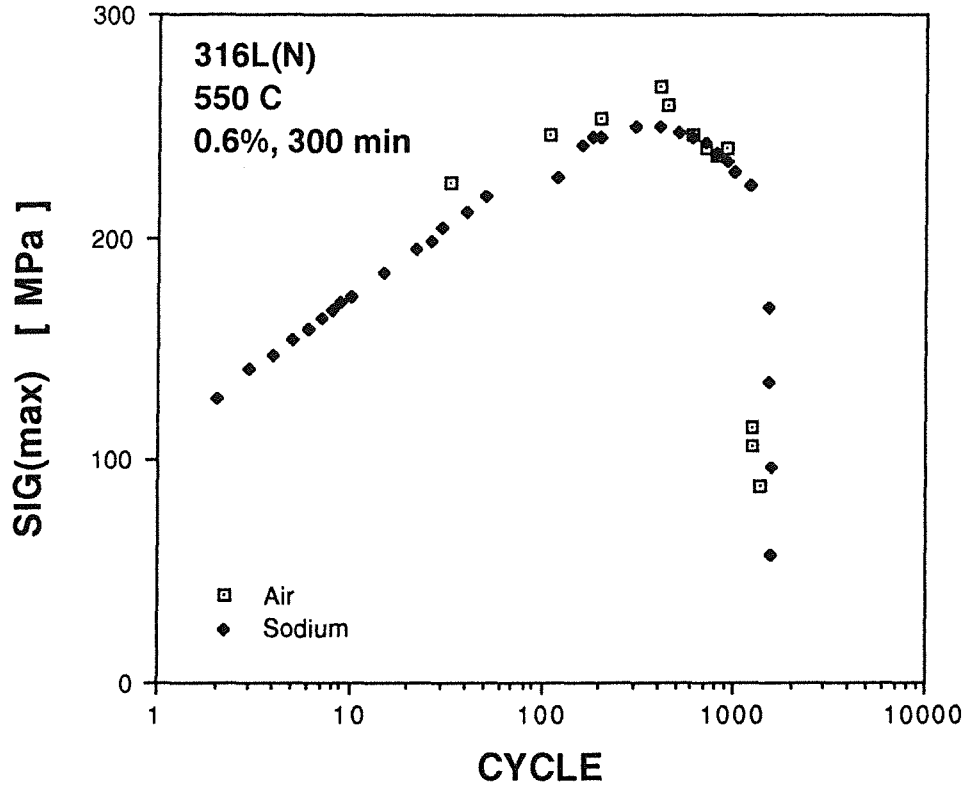

Fig.11 Cyclic hardening in LCF-tests of 316 L(N) at 550 °C with $\Delta\varepsilon_t$= 0.6% and t_h=300 min

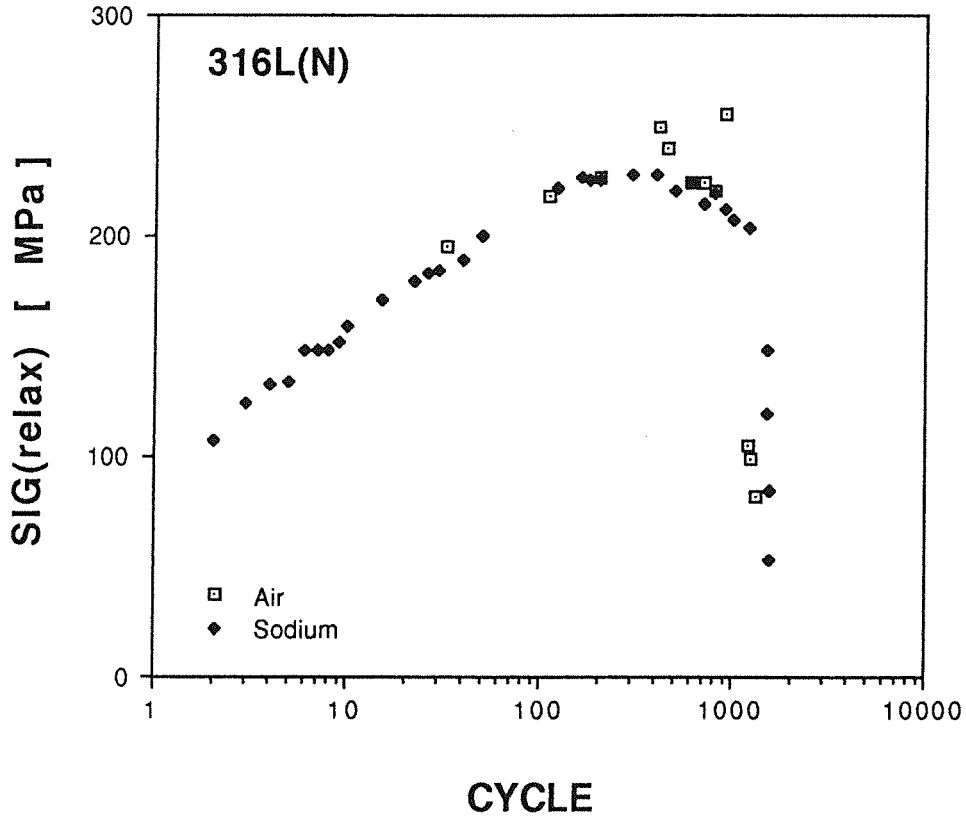

Fig.12 Relaxation behaviour in LCF-tests of 316 L(N) at 550 °C with $\Delta\varepsilon_t$= 0.6% and t_h=300 min

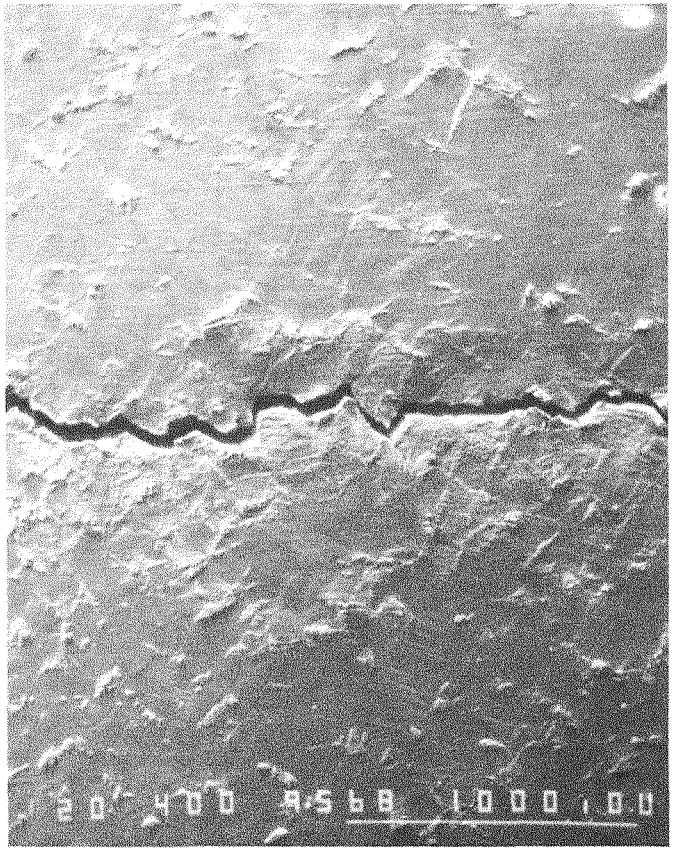

a) Air 550 °C

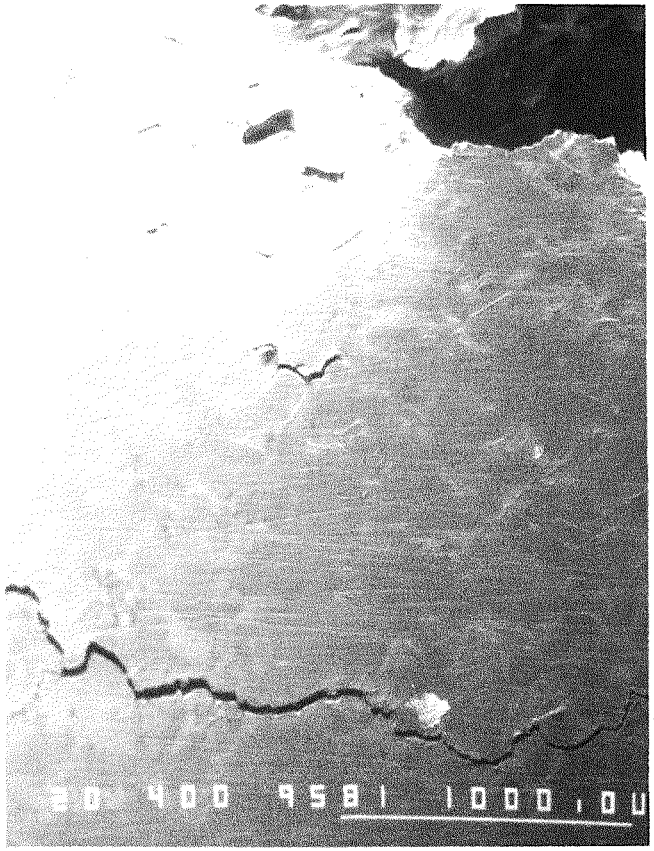

b) Sodium 550 °C

Fig.13 SEM-photographs of surface cracks on LCF-specimens tested at $\Delta\varepsilon_t$= 0.6% and t_h=300 min.

a) Air 550 °C

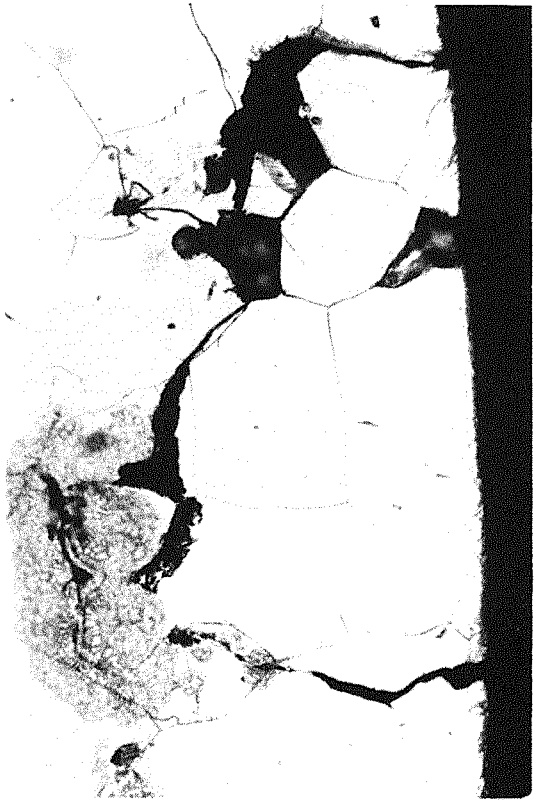

b) Sodium 550 °C

FIG.14 Optical photographs of longitudinal section of LCF-specimens tested at $\Delta\varepsilon_t$=0.6 %, t_h=300 min

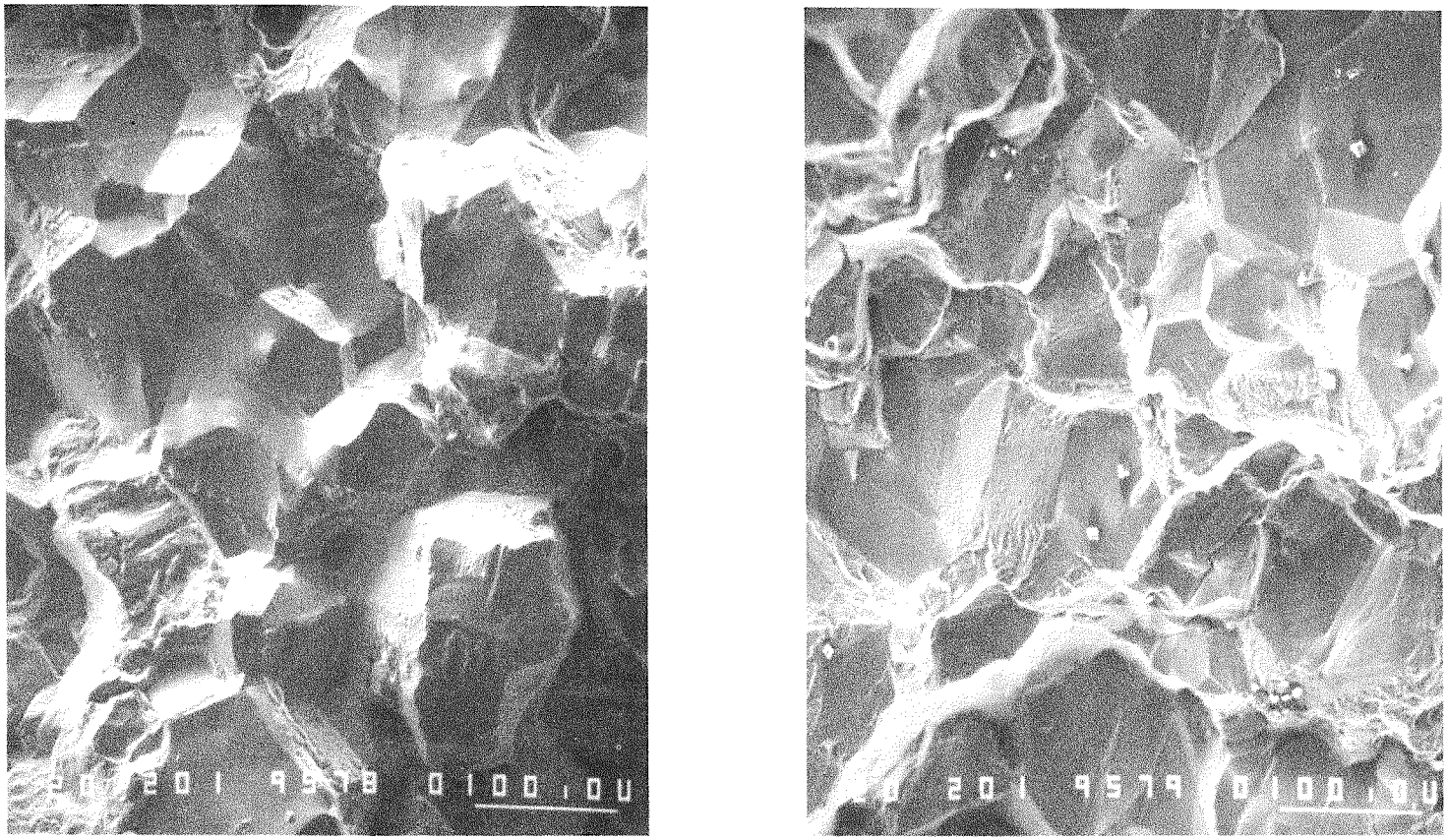

Fig.15 SEM-photograph of fracture surface of LCF-specimen tested in sodium at 550 °C and $\Delta\varepsilon_t$=0.6 %, t_h=300 min

The Measurement of Crack Propagation in CT Specimens of Stainless Steel in a Sodium Environment

H.U. Borgstedt, G. Frees, M.P. Mishra, Z. Peric, B. Seith
Kernforschungszentrum Karlsruhe GmbH.
Institut für Materialforschung III
P.O. Box 3640, D-7500 Karlsruhe 1

ABSTRACT

A test section for fracture mechanic testing of CT specimens was connected to the hot leg of the FARINA sodium loop at KfK. The crack opening displacement (COD) of the specimens was directly measured by means of an encapsulated clip-on-gage which could be used in liquid sodium environment up to the temperature limit of 823 K. The processor calculates the crack length and the factor and the exponent of the "Paris law" on the basis of the measured COD values.

Initially the equipment was used for measuring the fatigue crack growth behaviour of pre-cracked CT specimens of Type 304 stainless steel. More recently, the test section was used for the determination of the threshold fatigue crack growth behaviour of Type 316 LN stainless steel on such CT specimens at 813 K under stress ratio (R) values greater than 0.6. The results obtained so far do not indicate any significant sodium effects on the near threshold fatigue crack growth behaviour of modified Type 316 LN austenitic stainless steel. Modified Type 316 LN base metal had better resistance to fatigue crack growth than Type 316 base metal and Type 16-8-2 weld metal in a sodium environment at 813 K.

1.0 INTRODUCTION

The work on liquid alkali metals particularly compatibility studies of the sodium with structural materials was started in early sixties at the Nuclear Research Centre, Karlsruhe (KfK) [1-3]. However, the major mechanical testing in flowing liquid sodium environment started with the setting up of the two in-sodium test facilities viz. the FARINA and the CREVONA, designed and built at Institut für Materialforschung III, in the late seventies as part of a programme designed to investigate the mechanical behaviour of materials subjected to conditions typical of a liquid metal fast breeder reactor (LMFBR). The aim of these investigations was to use constant sodium purity and flow conditions to test a range of candidate fast reactor materials particularly steels in various metallurgical states. The creep, fatigue, creep - fatigue interaction and the crack growth studies have already been completed on base and weld metals of austenitic, ferritic and martensitic steels and alloy 800. The parameters which affect mechanical properties of the material in sodium environment were studied such as environmental effects of sodium itself both in static and dynamic conditions, corrosion and mass transfer, thermal aging including pre-corrosion for which references can be found in the literature [4-10].

Earlier work had suggested that sodium was most likely to have an effect when degradation processes particularly creep and crack growth are concentrated at grain boundaries. Creep - rupture tests of Type 304 stainless steel in a sodium loop have shown earlier onset of the tertiary creep and subsequently time to rupture is reduced in the liquid sodium environment [4-5]. These observations have led to evolve a materials testing programme on a range of candidate FBR structural materials in liquid sodium environment. Since last years services of these testing facilities have been extended further and efforts have mainly been directed towards testing candidate materials for planned European Fast Reactor (EFR). As part of the EFR material development programme, the creep, fatigue, creep - fatigue interaction and crack growth studies on modified Type 316 LN austenitic stainless steel and modified Type 9Cr-1Mo ferritic steel are in progress in various metallurgical states.

There have been a few published reports concerning the influence of sodium on creep and fatigue crack growths [11-13]. However, most of the crack growth test results show significant variations because of the restrictions on testing machines, differing purity of the sodium environment, heat to heat variations in the composition of the test material itself, varying metallurgical state of the material tested etc. and therefore, test results lack reliability. Furthermore, almost no data exists on fatigue crack growth behaviour of modified Type 316 LN stainless steel for service type of loadings for which near threshold fatigue crack growth data in sodium environment is important. The present study has therefore, been taken to characterize the effects of sodium on the threshold fatigue crack growth behaviour of modified Type 316 LN stainless steel base material in as received condition, in order to aid in the evaluation of the test results in sodium. However, to avoid closure and simulate service type of loading, the testing was carried out at the stress ratio "R" values greater than 0.60. The test results obtained earlier in air and argon environments on this steel at KfK and Interatom [14-16] and in-sodium fatigue crack growth data on Types 304 [11] and 316 stainless steel base material and 16-8-2 weld metal [12] are also reviewed and compared.

2.0 EXPERIMENTAL PROCEDURE

2.1 Material and Testing Details

The test material was as received (solution annealed) modified Type 316 LN stainless steel plate 40 mm thick manufactured and supplied by M/s Creusot Marrel, France (heat no. 11477) for application to FBR components fabrication. The chemical composition and the mechanical properties of the tested material are shown in Tables 1 and 2 respectively. The threshold fatigue crack growth tests were performed on compact tension (CT) specimens conforming to ASTM-E 399-83 specification as shown in Fig. 1. The thickness of the CT specimen used, however, was half the value recommended in the ASTM specification due to experimental limitations in sodium testing facility. The rolling direction was parallel to the chevron - notch (T-L orientation). All specimens were pre-cracked in fatigue at load levels lower than the load levels employed in the tests. The starting crack length "a" prior to insertion into the test chamber was approximately 10 mm. The crack length (total length of the crack starter configuration plus the fatigue crack) was in the range of $0.20 < a/W < 0.60$.

The threshold fatigue crack growth tests were carried out in a servo - hydraulic computer controlled 100 kN material testing machine of MTS Systems. The load was used as the control parameter. Sinusoidal loading waveforms were employed as shown in Fig. 2. The stress ratios ($R = F_{min.}/F_{max.}$) used were 0.60 and 0.80. The R constant test was started by stress intensity factor range ΔK decreasing conditions until the threshold stress intensity factor range ΔK_{th} was achieved. Then the test was continued under ΔK increasing conditions till the crack length reaches the upper limit of the a/W (~30 mm in the case of present study). The R constant ΔK decreasing tests involve the stepping down of the maximum stress intensity factor ($K_{max.}$) as well as minimum stress intensity factor ($K_{min.}$) for a given R value. The cyclic frequency for all tests was 5 Hz. The crack lengths were measured by using a fully encapsulated "Micro - Epsilon Messtechnik" made "Clip-on-gage". Its application in liquid sodium is limited to a temperature of 823 K.

The fatigue crack propagation rate was characterized as a function of the applied stress intensity factor range ΔK, using the power law of Paris and Erdogan [18] :

$$da/dN = C\,(\Delta K)^n \qquad (1)$$

Where
da/dN = fatigue crack growth rate mm/cycle
C, n = constants for a given material and environment
ΔK = stress intensity factor range = $K_{max.}(1-R)$ MPa $m^{1/2}$
R = stress ratio = $K_{min.}/K_{max.} = P_{min.}/P_{max.}$

The stress intensity factor range ΔK was calculated using the ASTM-E 399-83 standard expression as given below:

$$\Delta K = \frac{F}{B \cdot W^{1/2}} \cdot \frac{(2+\alpha)(0.886+4.64\alpha-13.32\alpha^2+14.72\alpha^3-5.6\alpha^4)}{(1-\alpha)^{3/2}} \qquad (2)$$

Where F is the load on the CT specimen in kN, B is the specimen thickness in cm, W is the width of the specimen in cm and , α = a/W, where "a" is the crack length in cm. The above equation is considered to be accurate within ± 0.5 % over the range of a/W from 0.2 to 1.

The growth of the fatigue crack is determined by means of crack opening displacement (COD). Crack opening displacements felt by a "Clip-on-gage" on the front of the CT specimen are printed out by the processor. The processor calculates the relationship between crack growth rate da/dN and the stress intensity factor range ΔK.

Since it is necessary to evaluate the fatigue crack growth results at the two different stress ratios, the effective stress intensity factor $K_{eff.}$ was calculated using the following expression:

$$K_{eff.} = K_{max.}\,(1 - R)^m \qquad (3)$$

Where R is stress ratio as defined in equation (1). The value of the exponent m was taken as 0.5 at 811 K (538°C) as given by James et.al. [12]. $K_{max.}$ is the peak load stress intensity factor for the load cycle.

2.2 Sodium Loop and Test Facility

The tests in sodium were carried out in a specially designed chamber that allowed a continuous flow of sodium around the CT specimen in "FARINA" loop at KfK. Fig. 3 shows the schematic of the test section for fatigue crack growth measurements. Although the detailed descriptions of the test facility is given earlier [19,20], for the sake of completion main characteristic parameters of the loop used for this study are listed in Table 3.

The flowing sodium was continuously purified by means of cold trapping. Oxygen was kept at a concentration level < 2 ppm by maintaining the cold trap temperature at 398 ± 5 K. Chemical activities of carbon and nitrogen in sodium were measured by means of equilibration of 50 μm thick, Type 316 stainless foils exposed to liquid sodium for 420 hours at 973 K. The carbon and the nitrogen contents in the foil after exposure to sodium were reduced to 0.045 and 0.005 wt % from the initial values of 0.095 and 0.045 wt % respectively. Thus the analysis of foils revealed slightly decarburizing and denitriding conditions in the loop for modified Type 316 LN stainless steel. The chemical activities of carbon and nitrogen in steel at 973 K are shown in Table 3.

3.0 RESULTS

The in sodium test results conducted in the present study at 813 K are shown in Figs. 4 - 6. A typical R constant (0.80) fatigue crack growth data in liquid sodium environment is shown in Table 4. Tests had previously been conducted on the same material of different heat at the same temperature in air and argon environments at Interatom and KfK. These results are shown in Fig. 7, which can be used as a basis of reference for comparing the effects of sodium and argon environments. The following observations have been made:

- The crack growth rates in sodium and argon are considerably lower than the crack growth rate in air environment at the same temperature (Fig. 7).

-The sodium tests curves are essentially parallel to the argon tests curves but are below them. The scatter bands for sodium and argon tests seems to overlap for the entire da/dN values. There is a larger scatter band for the argon tests than in sodium at higher da/dN values (Fig. 7).

-There seems to be a large gap between 0.80 and 0.60 R curves near the threshold regions in all the environments tested and the curves are generally parallel, but at higher da/dN values this gap is reduced (Fig. 7).

The fatigue crack growth behaviour of stainless steel Types 304, 316 and modified 316 LN base materials and 16-8-2 weld metals in sodium environment are compared in Fig. 8. It is evident from Fig. 8 that stainless steel Types 304 and modified 316 LN lie in the lower regions of da/dN curve, whereas Type 316 lies at the top, at the same temperature conditions in sodium. The fatigue crack growth curve for 16-8-2 weld metal lies in between 316 and 316 LN base materials. As can be seen from Figs. 4 - 6 there is a wider scatter band for all R constant crack growth data, single line drawn through the middle of each scatter bands are shown for the comparative studies in Figs. 7 and 8 for the sake of convenience and ease graphical representation.

4.0 DISCUSSION

The lower crack growth rates observed in sodium tests than that in air are in agreement with the earlier observations of James et.al [11], Yuen et.al [12], Huthmann et.al [13] and Borgstedt et.al [10]. Nuclear grade sodium is thought to act as an essentially inert environment in so for as crack extension is concerned. Generally crack growth rates are much less in inert environments like argon, vacuum and sodium than in more aggressive environments like air, oxygen etc. This has already been verified by previous observers [11-12]. The effect of sodium environment on the rate of crack propagation is most pronounced at the lower values of ΔK, where the crack extension (Δa) is less for each cycle. Thus, there is more disparity between the air and the argon and sodium results at lower ΔK values . Curves for the sodium and air environments tend to converge at the higher values of ΔK. However, this convergence is less in sodium than in air. This is because at the higher crack growth rates associated with the higher values of ΔK, new crack surfaces are being created at a faster rate than the environmental attack. From this it seems that environmental attack is more in air than in sodium on the crack tip. Higher crack growth rates observed in air than in sodium are attributed to the oxidizing environment present in the former than in the latter.

The results of James et.al. [11], Yuen et.al. [12] and Shahinian et.al. [21] offer the best opportunity for comparison with the present results. James et.al. [11] studied the fatigue crack propagation behaviour of solution annealed Type 304 stainless steel base material in low oxygen (1-3 ppm) and high oxygen (20-40 ppm) sodium environment at 700 and 811 K and reported considerably lower fatigue crack growths in sodium and in vacuum than that in air environment at the same test temperature. James et.al [11] concluded that this is due to a lack of oxygen at the crack tip. Fatigue crack growth is dependent on the carburizing or decarburizing nature of the sodium environment and amount of oxygen present [12]. Significantly higher fatigue crack growth rates in both carburizing and decarburizing sodium environments are expected to occur on stainless steel than those in neutral carbon activity sodium. However, with a few limited studies on Types 304 [11] and 316 [12] stainless steels, the effect of high carbon liquid sodium on the rate of fatigue crack growth was insignificant.

This is due to the fact that the available carbon diffuses through the sodium toward the crack tip but diffuses into the crevice surfaces prior to reaching the crack tip. To verify that carburization would not be expected to occur at the crack tip Yuen et.al. [12] had conducted a test on 316 stainless steel specimen with 1.4 mm fatigue pre-crack and crack extension (Δa) of about 0.25 to 0.76 mm. It has been observed that the 1000 hour pre-exposure plus the approximately 330 hour test time is not sufficient to allow crack tip carburization, which hold good for decarburization as well. In fact in this study slower crack growth rates were observed than conventional tests. Although liquid sodium at elevated temperature is known to act as a slightly embrittling environment in creep rupture tests, it does not affect the crack growth under static load and cyclic load as well [10]. Sodium causes the formation of small cracks in the surface layers of highly strained specimens, while it does not affect the processes at the crack tip, if load does not cause large plastic deformation. Also it is not the total amount of

oxygen present in liquid sodium which is responsible for enhanced fatigue crack growth rates in some observations, but the amount of oxygen available as a free oxygen to attack the crack tip is important [11-12].

Corrosion and mass transport associated with non-isothermal experimental sodium loops and in actual reactor operating conditions, where large temperature difference exists between hot and cold legs, is well known phenomena. A somewhat similar argument applies to the kinetics of corrosion and mass transport in the crack tip. This could be either from the external action of the sodium such as corrosion and leaching of substitutional and interstitial alloying elements or due to the internal migration of defects, within the plastic zone surrounding the crack tip. Hydraulic considerations indicate that the sodium will be essentially static for a crack length "a" greater than three times the opening at the mouth of crack [20]. The earlier findings show that in spite of high diffusivity in the liquid state, crack tip carburization / decarburization is severely limited by the gettering action of the crack faces which prevent carbon from reaching / escaping the crack tip [20]. The same analogy may be applied to the diffusion of other interstitial and substitutional elements to the crack tip. In fact, the sharper and deeper a crack, the less likely is the environment to affect the tip since the sink or supply area of crack face will be large in relation to the volume of sodium within the crack. The situation with respect to fatigue loading is somewhat more complex, where relative displacement of the crack faces cause sodium to be pumped into and out of the cracks. There always exists the possibility of wetting the crack tip with a potentially damaging environment, which reduces the protective gettering action of the crack tip. Except in some cases notably when the load is applied occasionally such as reactor start up, which give rise to very high "R" (ripple loads), the fluid within the crack may be considered as relatively stagnant otherwise, and fatigue crack growth may be treated as analogous environmentally to creep cracks.

A diffusion model has also been developed by Yuen et.al. [12] to explain the above results, which substantiate the experimental results that the crack tip carburization / decarburization would not occur. It is obvious due to the fact that the diffusion of carbon is much faster in sodium than in stainless steel and carbon profiles in sodium achieve a pseudo - equilibrium with respect to the stainless steel surface. It appears that the geometry of a crack as well as the condition of loading (frequency, stress ratio "R", stress etc.) are crucial in determining whether or not crack tip will be wetted and carburized / decarburized in a particular situation. However, if the carburization / decarburization rate of crevice is always slower than the crack growth rate, the crack propagation behaviour of the plant components will not be affected for the life of the plant. However the rate at which crevice carburizes / decarburizes (beyond 1000 hour) remain unanswered. Long time tests with low stress intensity values and low frequency loading would be required to qualify this behaviour of da/dN. Long term crevice exposure results would supplement such testing .

Even given the pumping mechanism, it is inconceivable that this effect could produce a crack tip structure substantially more detrimental than that produced at a free surface, unless their is enhanced diffusivity in this region. As already noted, such enhancement has not been observed either in substitutional element transfer or in the sodium carburization / decarburization

of stressed notched specimens [12,20]. Thus this study on modified Type 316 LN stainless steel on fatigue crack growth suggests that crack growth behaviours of this steel are unlikely to be degraded by the sodium environment.

The fatigue crack growth behaviour of Types 304, 316 and 316 LN base materials and 16-8-2 weld metal in sodium environment are compared in Fig. 8. It is evident from Fig. 8 that the crack growth behaviour of modified Type 316 LN stainless steel base material is superior to Type 316 stainless steel in a sodium environment. Lower fatigue crack growth rates observed in modified Type 316 LN than that in Type 316 is mainly attributed to higher yield and ultimate strengths of the farmer than that of the latter. Strengthening, particularly the yield strength has sometimes been observed to influence elevated temperature crack growth behaviour [11]. The superior fatigue crack growth resistance of 16-8-2 weld metal relative to that of Type 316 base material appears to be related to microstructural difference. At elevated temperatures the fine duplex delta ferrite - austenite microstructure of the weld metal with its many phase boundaries apparently produces better resistance to crack growth than the larger grain, fully austenitic structure of the base metal. It is evident from Fig. 8 that the modified Type 316 LN base metal offers even superior fatigue crack growth resistance than that to 16-8-2 weld metal despite fully austenitic coarse structure. Lower fatigue crack growth rates observed in Type 304 base metal than that of Type 316 base metal and 16-8-2 weld metal are in agreement with the findings of Shahinian et.al. [21] and Yuen et.al. [12].

Although there is a very large amount of crack growth information still required to allow satisfactory design, especially in relation to combined creep and fatigue and to end of life microstructural conditions particularly the effects of irradiation and aging, it appears that their are good grounds for believing that a sodium environment may be beneficial. Post fracture metallurgical examinations of sodium exposed, failed fatigue crack growth test specimens are in progress, findings of which will be reported in subsequent reports. Further tests are also in progress with welded specimens of the same stainless steel. Although, carburization / decarburization effects are more in Type 304 than that in Type 316 stainless Steel but these effects are limited to the face of the crack and do not affect the crack tip carburization / decarburization. This is mainly due to the fact that Type 316 stainless steel does not get carburized / decarburized in liquid sodium to the extent Type 304 does. Although in fatigue crack growth resistance Type 316 base metal is poorer than Type 304 base metal in sodium as well as in air, the relative merits of the latter should not be expected to reflect the relative merits of the former on other mechanical properties in long time at elevated temperature because of the differences in composition and microstructure.

5.0 CONCLUSIONS

1. The threshold fatigue crack-growth rate of modified Type 316 LN stainless steel in sodium environment at 813 K is considerably lower than in air environment at the same test temperature.

2. The threshold fatigue crack growth rate in argon environment is slightly higher than sodium environment, however the scatter bands for both the environments overlap. This could be attributed to the higher oxygen content in argon environment, which is known to have resulted in little higher crack growth rates and higher scatter band in argon environment.

3. The available experimental results show that the modified Type 316 LN stainless steel is compatible with liquid sodium environment and its mechanical behaviours particularly fatigue crack growth resistance is superior to those of Type 316 base metal and 16-8-2 weld metal and slightly lower than that of Type 304 base metal. There is no indication that unstable fracture will occur at operating conditions. The critical crack lengths are so large, compared to the wall thickness generally used in LMFBR pipings and structures that the failures will manifest themselves always by leaking rather than by fracture.

4. Although there is no direct evidence of possible effects of carburization or decarburization in above studies on fatigue crack growth rates, since present studies have been carried out in an essentially neutral carbon activity sodium environment. However hydraulic and diffusion models developed by Charnock et.al. [20] and Yuen et.al. [12] respectively and further crack growth studies carried out by them on stainless steel show that the transfer of carbon or indeed other alloying elements to and from the tip of cracks in components, operating in sodium is likely to be severely limited. Thus increase in crack propagation rates from this cause are very unlikely. Indeed the sharper and deeper a crack (i.e. mechanically more damaging), the less likely are environmental effects to operate.

5. Further studies are needed on threshold fatigue crack growth rates, particularly on sodium pre-exposed samples and welded joints to assess the possible effects of aging, environment and welding respectively.

ACKNOWLEDGEMENTS

Authors gratefully acknowledge the efforts of Messrs E. Wollensack and K.H. Kleiber in operation of sodium loops during the above studies.

REFERENCES

[1] H.U. Borgstedt and E.D. Grosser,
Proc. Conf. on Liquid Alkali Metals , BNES, Nottingham, UK, 1973, p. 275.

[2] H.U. Borgstedt, G. Frees and H. Schneider,
Journal of Nuclear Technology Vol. 34, 1977, p. 290.

[3] H.U. Borgstedt, G. Frees and H. Schneider,
Proc. Conf. on Liquid Alkali Metals, BNES, Nottingham, UK, 1973, p. 239.

[4] H. Huthmann, G. Menken, H.U. Borgstedt and H. Tas,
Proc. Sec. Int. Conf. on Liquid Metal Technology in Energy Production,
Richland, Washington, 1980, Vol. 2, p. 19.33.

[5] H. Huthmann and H.U. Borgstedt,
IWGFR Specialists Meeting on Mechanical Properties of Structural Materials Including Environment Effects, Chester, UK, 1983.

[6] M. de la Torre, R.R. Solano, I. Melches, S. Barosso, J. Arroyo, H.U. Borgstedt, M. Schirra and G. Frees,
Proc. Conf. on Liquid Metal Engineering and Technology, BNES, London, 1984, p. 467.

[7] H. Huthmann and H.U. Borgstedt,
Proc. Conf. on Liquid Metal Engineering and Technology, Avignon, France, 1988, p. 510.1. (Accepted for publication in Journal of Nuclear Materials).

[8] C. Phaniraj, B. Seith and H.U. Borgstedt,
Internal KfK report 1987.

[9] H.U. Borgstedt and H. Huthmann,
Proc. Conf. on Liquid Metal Engineering and Technology, Avignon, France, 1988, p. 509.1.

[10] H.U. Borgstedt, G. Drechsler, G. Frees, H.S. Khatak, Z. Peric and B. Seith
Int. Journal of Fracture, Vol. 32, 1986, p. R23.

[11] L.A. James and R.L. Knecht,
Met. Trans. 6A, 1975, p. 109.

[12] J.L. Yuen and J.F. Copeland,
Trans. of ASME, Journal of Engg. Mat. and Tech., Vol-101, 1979, p. 214.

[13] H. Huthmann and O. Gossmann,
Proc. Conf. on Liquid Metal Engineering & Technology, BNES, London, 1984, p. 453.

[14] H. Huthmann,
Internal report of Interatom, Bergisch Gladbach, 1988.

[15] G. Balzer and S. Müller,
Internal KfK report, 1987.

[16] S. Müller und M. Brandle,
Internal KfK report, 1989.

[17] P. Paris and F. Erdogan,
ASME Journal of Basic Engineering, Vol. 85, 1963, p. 528.

[18] G. Frees, G. Drechsler, and E. Wollensack,
Internal KfK report, 1983

[19] H.U. Borgstedt, G. Drechsler, G. Frees and E. Wollensack,
Proc. Conf. on Material Behaviour and Physical Chemistry in Liquid Metal System, Ed. H.U. Borgstedt, Plenum Press, New York, 1982, p. 185.

[20] W. Charnock and P. Marshall,
"An Assessment of the Performance of U.K. CDFR Candidate Structural Materials," BNL Report RD/B/N - 4184, 1977.

[21] P. Shahinian, H.H. Smith and J.R. Hawthorne,
Welding Research Supplement, 1972, p. 527-$_{s}$.

Table 1: Chemical composition of modified Type 316 LN stainless steel (Wt -%)

C	Mn	Si	P	S	Cr	Ni
.02	1.80	.32	.020	.0006	17.34	12.50
Mo	Cu	B	N	Co	Nb/Ta	Ti
2.40	.12	.0014	.08	0.3	.042	.008

Table 2: Mechanical properties of modified Type 316 LN stainless steel (Solution annealed condition)

Heat No.	Temp. (K)	0.2 Y.S. (Mpa)	U.T.S. (Mpa)	Elong. %	R.A. %	Grain Size (ASTM 112)
11477 (Creusot)	293	210	580	82	81	4
-	823	150	420	58	70	-

Table 3: Sodium loop used for fatigue crack growth studies

Facility	FARINA
Location	KfK
Material of construction	Type 304 stainless steel (German specification 1.4301)
Inventory of sodium	400 kg.
Flow of sodium in the test section	0.130 - 0.150 m^3/hr.
Sodium velocity at the specimen	3 m/sec.
Temperatures: Test section Main loop Cold leg Cold trap	 823 and 873 K (as desired) 773 K 673 K 398 ± 5 K
Sodium chemistry: Oxygen concentration (Oxygen meter) Carbon activity at 973 K (Foil equilibration) Nitrogen activity at 973 K (Foil equilibration)	 < 2 ppm (at cold trap temperature 398 ± 5 K) 1.067 X 10^{-2} (decarburizing) 8.46 X 10^{-3} (denitriding)

Table 4: Fatigue crack growth test results for R = 0.80 at 813 K

P max MPa	crack length "a" mm	Δ K MPa $m^{1/2}$	Δ a mm	Δ N cycles	da/dN mm/cycle
8.0	11.50	4.30	-	-	-
8.0	11.80	4.50	0.30	653100	$4.6 \cdot 10^{-7}$
8.0	12.00	4.60	0.20	450000	$4.0 \cdot 10^{-7}$
7.0	12.30	4.10	0.30	1320500	$2 \cdot 10^{-7}$
7.0	12.60	4.15	0.30	1120400	$2 \cdot 10^{-7}$
7.0	12.70	4.20	0.20	1550800	$1 \cdot 10^{-7}$
7.0	12.70	4.20	0.00	3010500	Nil
9.0	12.93	5.30	0.23	33100	$7 \cdot 10^{-6}$
9.0	13.10	5.40	0.17	28550	$6 \cdot 10^{-6}$
10.0	13.30	6.10	0.20	40200	$5 \cdot 10^{-6}$
10.0	13.46	6.20	0.16	28500	$6 \cdot 10^{-6}$
10.0	13.60	6.30	0.14	18000	$8 \cdot 10^{-6}$
10.0	14.00	6.50	0.40	81200	$5 \cdot 10^{-6}$
11.0	14.20	7.00	0.20	25000	$8 \cdot 10^{-6}$
11.0	14.50	7.10	0.30	28600	$1 \cdot 10^{-5}$
11.0	14.72	7.20	0.22	15500	$2 \cdot 10^{-5}$
10.0	15.00	6.60	0.28	44100	$6 \cdot 10^{-6}$
10.0	15.60	6.80	0.60	51000	$1 \cdot 10^{-5}$
10.0	15.93	7.00	0.33	33100	$1 \cdot 10^{-5}$
9.0	16.40	6.40	0.47	105000	$5 \cdot 10^{-6}$
9.0	16.98	6.60	0.58	100800	$6 \cdot 10^{-6}$
9.0	17.55	6.80	0.57	80500	$7 \cdot 10^{-6}$
8.0	18.00	6.10	0.45	105100	$4 \cdot 10^{-6}$
8.0	18.60	6.30	0.60	81300	$7 \cdot 10^{-6}$
7.0	18.95	5.60	0.35	110500	$3 \cdot 10^{-6}$
7.0	19.40	5.70	0.45	150600	$3 \cdot 10^{-6}$
7.0	19.85	5.80	0.45	84400	$6 \cdot 10^{-6}$
6.0	20.15	5.00	0.30	240200	$1 \cdot 10^{-6}$
6.0	20.35	5.10	0.20	77000	$3 \cdot 10^{-6}$
6.0	20.68	5.30	0.28	50100	$5 \cdot 10^{-6}$
4.5	21.02	4.10	0.32	860200	$3 \cdot 10^{-7}$
4.5	21.40	4.20	0.38	670800	$5 \cdot 10^{-7}$
4.5	21.70	4.30	0.30	650950	$4 \cdot 10^{-7}$
4.5	22.13	4.40	0.43	1750100	$2 \cdot 10^{-7}$
4.5	22.20	4.40	0.07	2500000	Nil
5.5	22.40	5.50	0.20	281900	$7 \cdot 10^{-7}$
5.5	22.90	5.70	0.50	210100	$2 \cdot 10^{-6}$
5.5	23.60	6.00	0.33	90300	$3.7 \cdot 10^{-6}$
5.5	24.20	6.20	0.60	150000	$4 \cdot 10^{-6}$
5.5	25.05	6.50	0.85	180200	$5 \cdot 10^{-6}$
6.0	26.30	7.60	1.25	195000	$7 \cdot 10^{-6}$
6.0	27.70	8.30	1.40	80300	$3 \cdot 10^{-5}$
6.0	28.65	9.00	0.95	26500	$5 \cdot 10^{-5}$
6.0	29.35	9.50	0.75	12900	$6 \cdot 10^{-5}$
6.0	30.10	10.1	6.85	18500	$6 \cdot 10^{-5}$

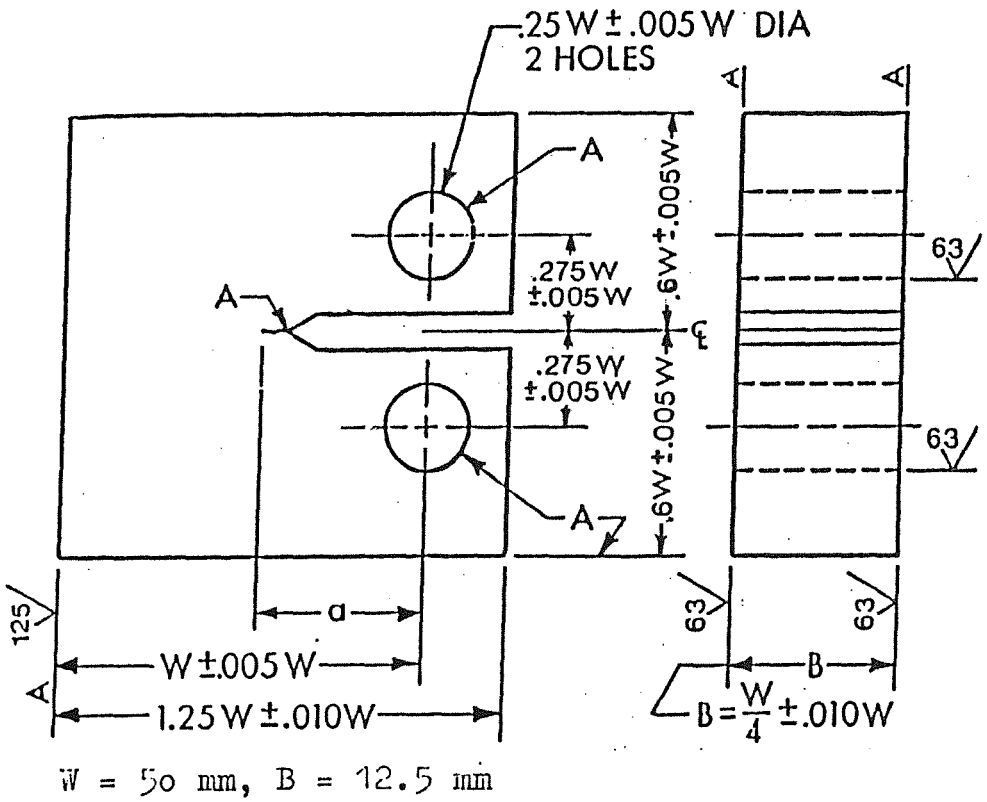

Fig. 1: Fatigue crack growth CT specimen standard dimensions and tolerances

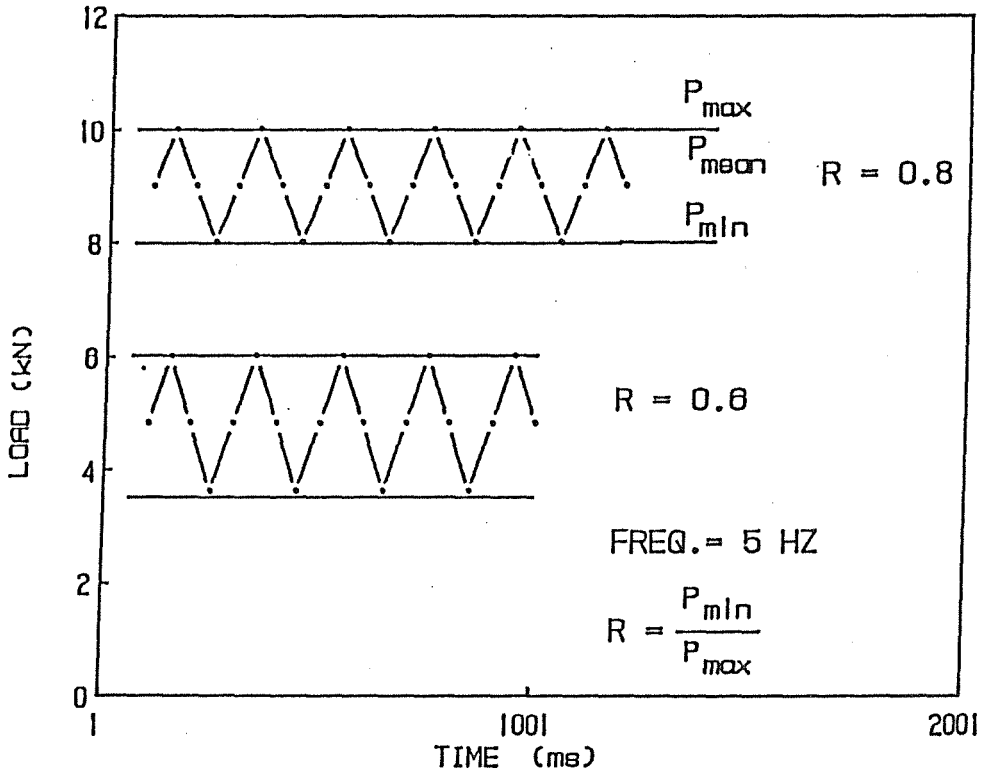

Fig. 2: Schematic representation of wave forms for R = 0.60 and 0.80

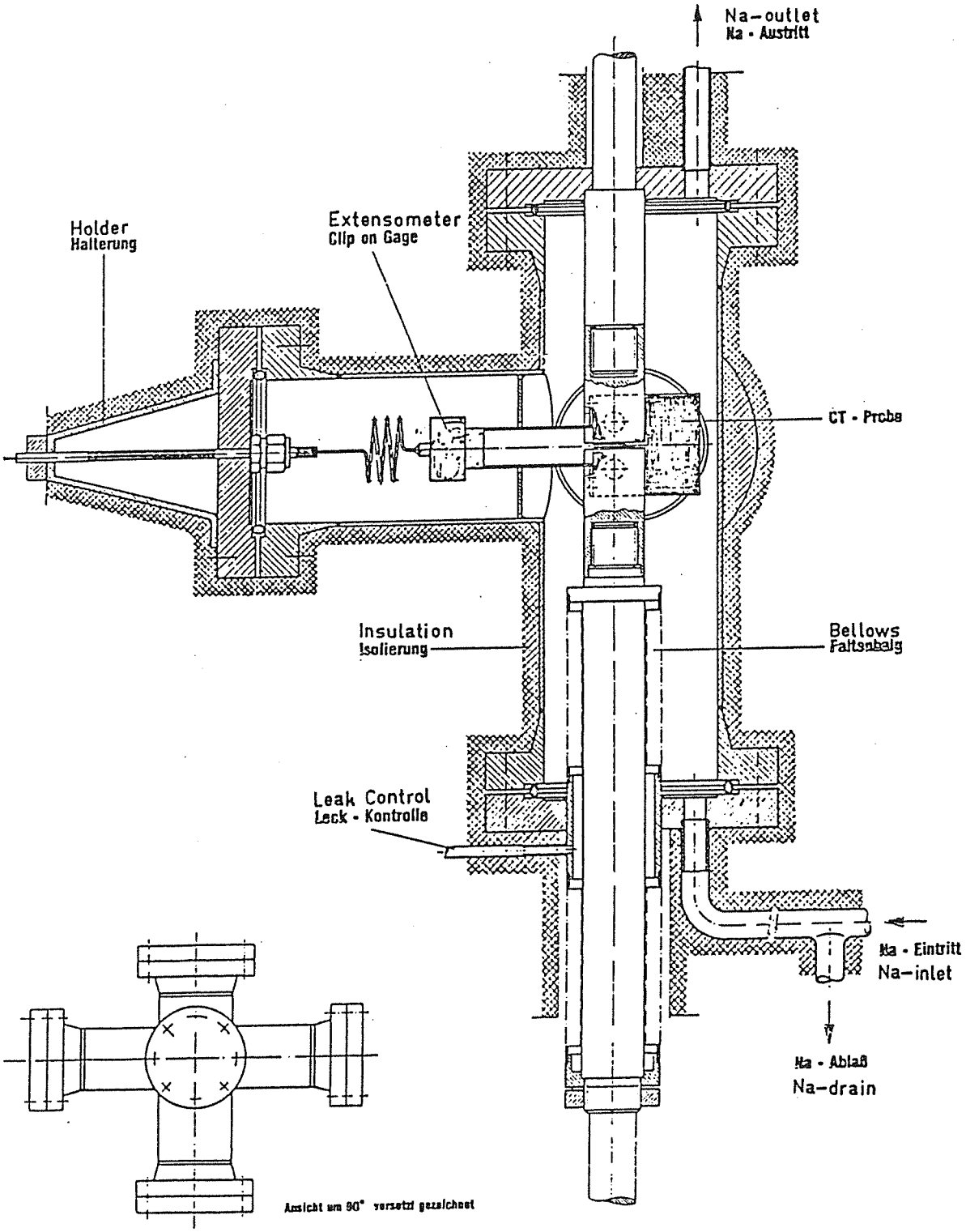

Fig. 3: Schematic illustration of test section for fatigue crack growth studies in sodium

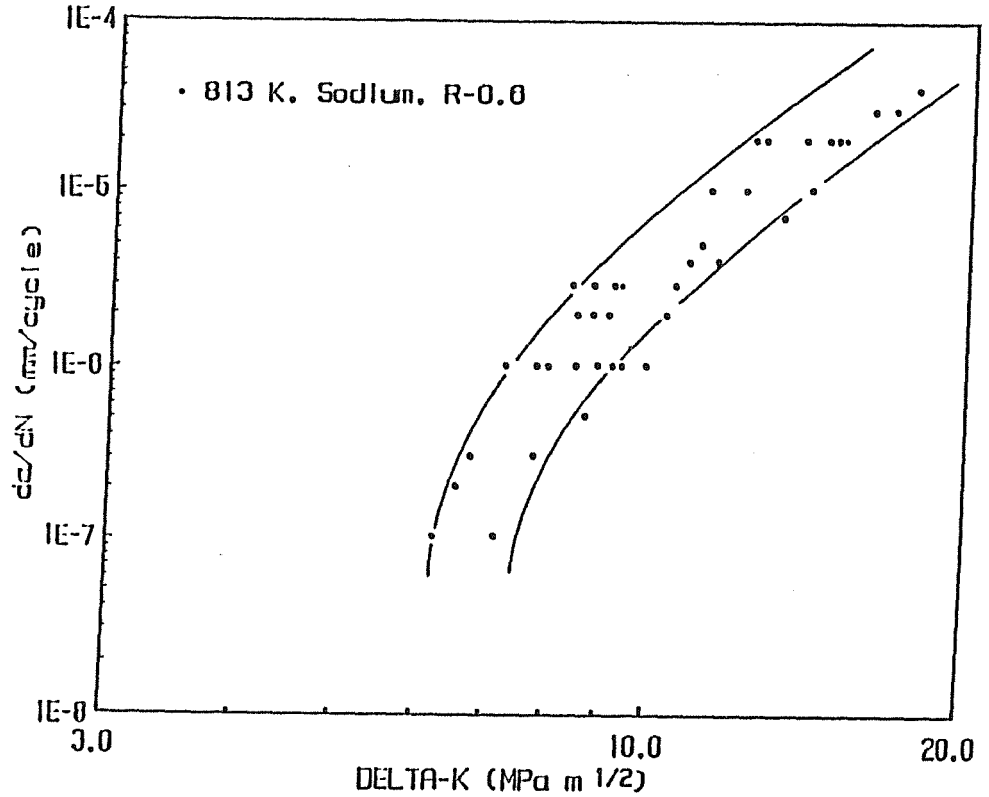

Fig. 4: Fatigue crack growth behaviour of mod. Type 316 LN stainless steel for R = 0.60 in sodium at 813 K

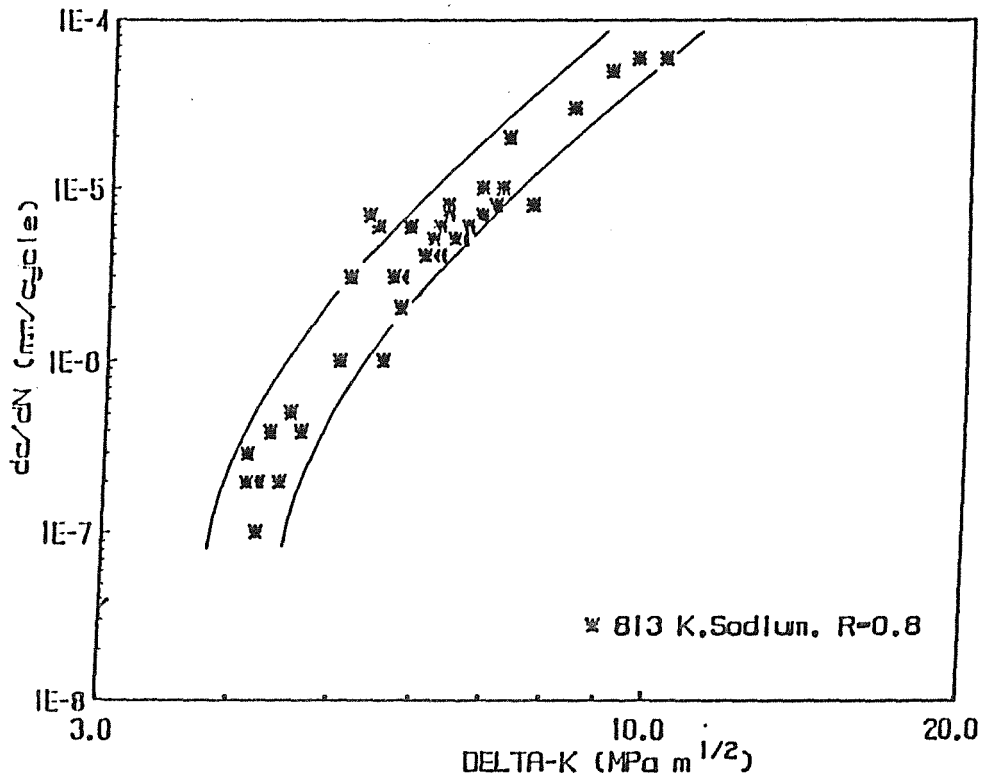

Fig. 5: Fatigue crack growth behaviour of mod. Type 316 LN stainless steel for R = 0.80 in sodium at 813 K

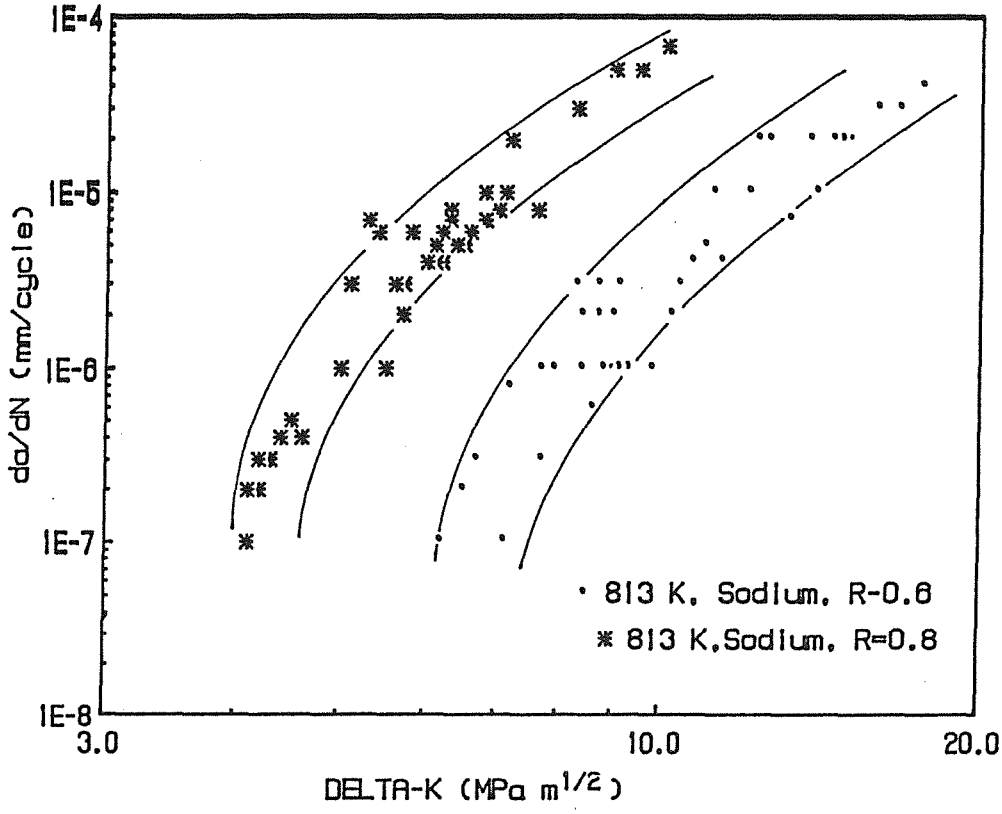

Fig. 6: Fatigue crack growth behaviour of mod. Type 316 LN stainless steel for R = 0.60 and 0.80 in sodium at 813 K

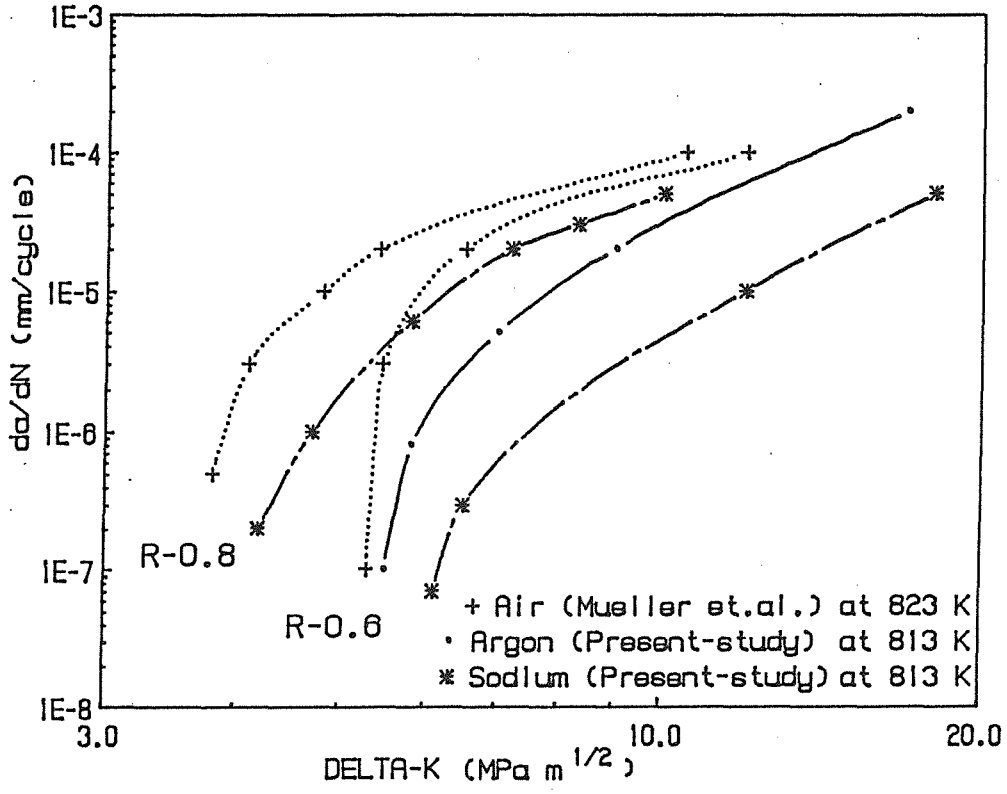

Fig. 7: Comparison of fatigue crack growth behaviour of mod. Type 316 LN stainless steel in air, argon and sodium environments

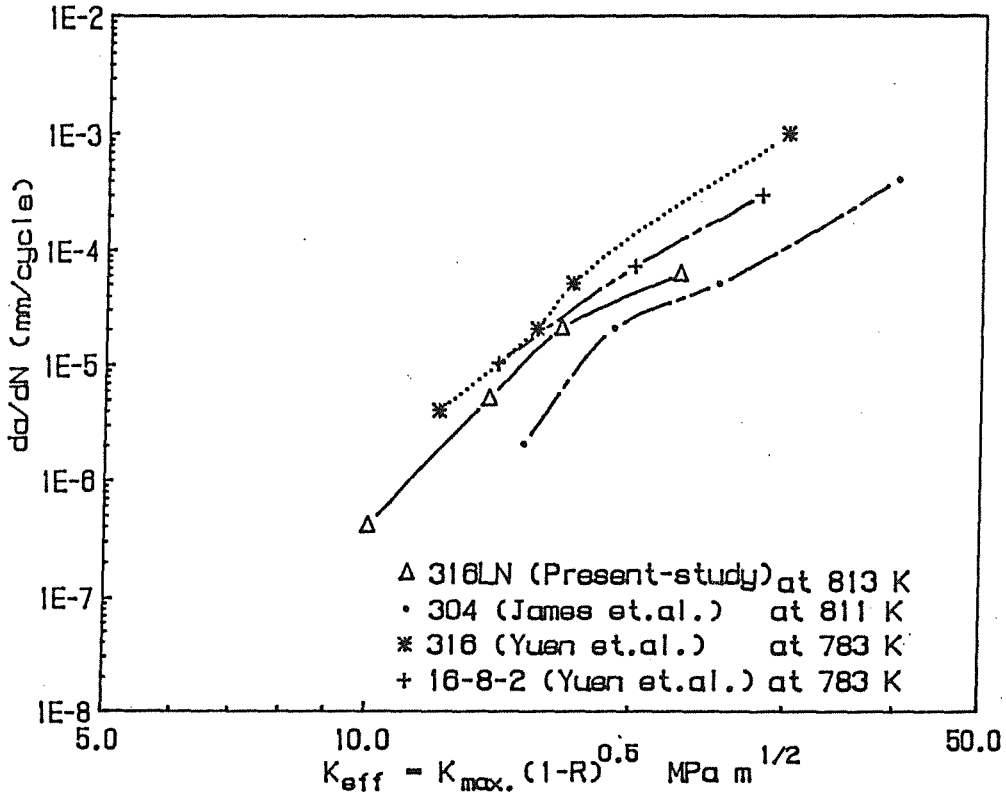

Fig. 8: Comparison of fatigue crack growth behaviour of Types 304, 316, and mod. 316 LN base material and 16-8-2 weld metal in sodium

Crack Initiation (J -Δa curves) in Liquid Sodium on Type 304 SS after Previous Creep Damage

(short contribution)

by

H.Huthmann and O. Gossmann

Interatom GmbH, Bergisch Gladbach,

Germany

Motivation

* Reduced plastification at crack tips, after crack initiation in sodium in creep crack growth tests
* Reduced ductility in tertiary creep

Technique

* Multi specimen technique with compact-tension specimens, side grooved, W = 25.4 mm, B = 12.5 mm, creep pre-loaded specimens were prepared by electron beam welding
* Material: 304 ss, IA-no. 402
  a) base material as received condition
  b) base material with previous creep loading (150 MPa, 3000 h, 550 °C = secondary creep)
  c) base mat with previous creep loading (200 MPa, 3015 h, 550 °C = end of secondary creep)
* Test-chamber for CT-specimens with load point displacement measurement
* Flowing sodium environment 550 °C and some parallel tests in air

Results

* Blunting line is determined by 3 tests, where REM-examinations confirmed that no stable crack extension

* Measured J-Δa curves (Fig.1) show 2 scatterbands:
  - the higher one is due to the as- received condition
  - the lower one is measured for the creep pre-loaded material
  - no difference occurred for different preloading conditions
  - the intersection with the blunting lines delivers for crack initiation:
    750 N/mm for as-rec. material
    300 N/mm for creep pre-loaded material
  - test data in air are in the scatterband of in-sodium data, therefore no influence of sodium is indicated

Table: J-Integral tests in flowing sodium and in air at 550 ºC on Type 304 SS with and without previous creep damage

Test No.	Material condition	Environ-ment	a_0/W	Δa [mm]	J [N/mm]
J 002	A	Na	0.54	3.80	1083
J003	A	Na	0.56	3.83	1001
J004	A	Na	0.58	1.66	791
J005	A	Na	0.53	0.80	493
J006	A	Na	0.54	0.53	351
J318	B	Air	0.55	2.29	514
J012	B	Na	0.54	3.92	597
J013	B	Na	0.52	2.03	485
J014	B	Na	0.52	0.39	222
J015	B	Na	0.56	2.62	524
J016	B	Na	0.52	1.10	281
J017	B	Na	0.55	4.57	586
J317	C	Air	0.52	2.49	562
J319	C	Air	0.52	3.07	549
J001	C	Na	0.53	7.99	927
J007	C	Na	0.52	3.30	547
J008	C	Na	0.53	4.01	560
J009	C	Na	0.51	0.84	311
J010	C	Na	0.51	2.52	523
J011	C	Na	0.52	0.74	266

C(T) specimens , side grooved; B_0= 12.5 mm, W=25.4mm, B_{netto}=9.8 mm
Orientation: T-L, Pre-loading in crack growth direction
Displacement rate: 0.016 mm/s (0.0009 in test J002)
Material conditions:

A: sol. annealed
B: previous creep damage: 550 °C, 150 MPa, 3015 h
C: previous creep damage: 550 °C, 200 MPa, 3000 h

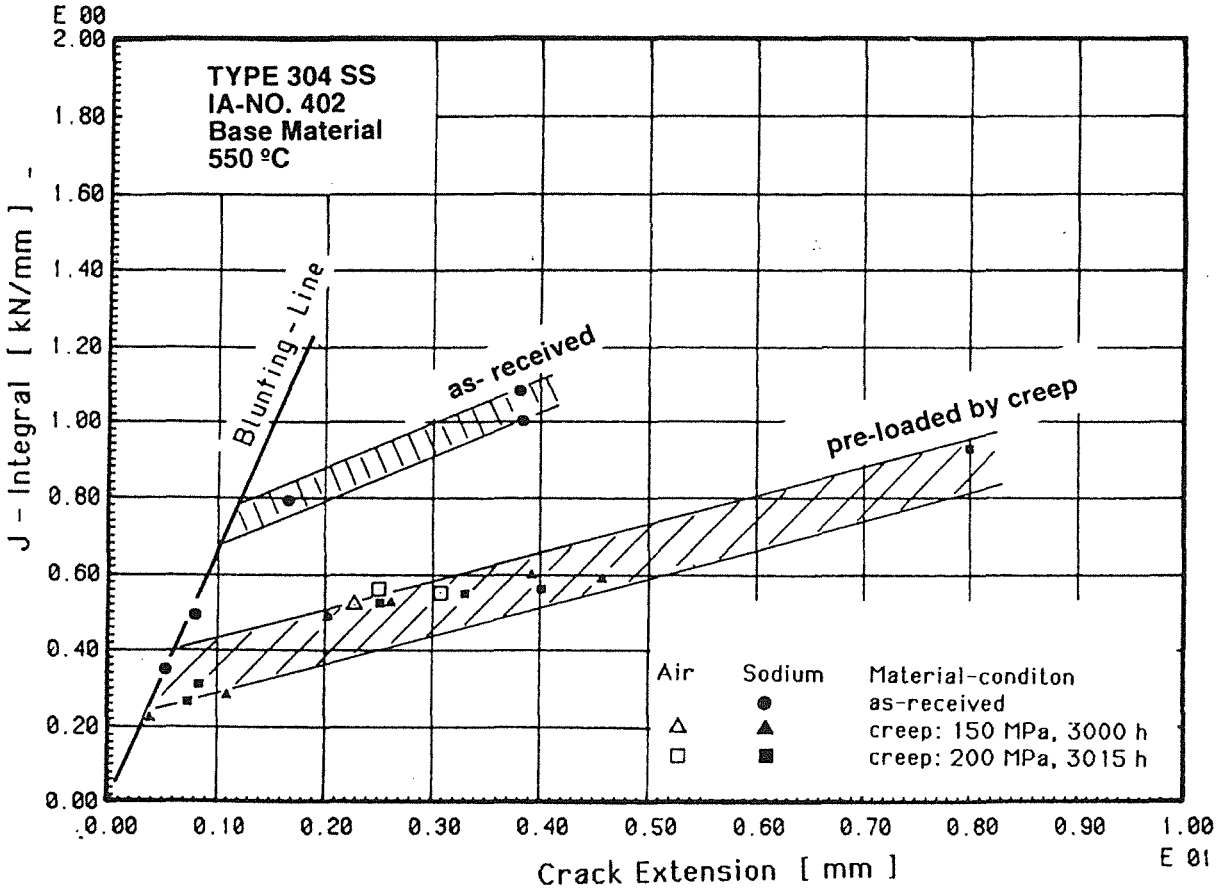

Fig.1 J-Δa values measured in flowing sodium and in air at 550 ºC on Type 304 SS with and without previous creep damage